Book of Abstracts:

BIFD2026
L'AQUILA

11th Bifurcations and Instabilities in Fluid Dynamics
6-10 July 2026

UNIVERSITÀ DEGLI STUDI DELL'AQUILA

GRAN SASSO SCIENCE INSTITUTE
SCHOOL OF ADVANCED STUDIES
Scuola Universitaria Superiore

Under the patronage of:

erc

REGIONE ABRUZZO

COMUNE DELL'AQUILA

IL SEGNO DELLA RINASCITA

L'AQUILA 2026
Capitale italiana della Cultura

DIIIE
Dipartimento di Ingegneria Industriale e dell'Informazione e di Economia

Index

Abstracts - Room 1: Auditorium

Abstracts - Room 2: Ipogea

Suspensions and Particulate Flows

Suspensions and Particulate Flows

Waves and Vortex Dynamics

Abstracts - Room 3: Main lecture hall

Computational Methods

July 9th, 10.00-11.00; Chair: Francesco Duronio

Computational Methods

July 9th, 11.30-12.30; Chair: Francesco De Vita

Programme at a Glance

July 6th

	Room 1: Auditorium	Room 2: Ipogea	Room 3: Main lecture hall
07.30	Registration		
08.30	Tea / Coffee		
09.00	Opening Welcome		
09.45	Plenary: Nicolas Noiray		
10.45	Coffee break	Coffee break	Coffee break
11.15	Geophysical, Astrophysical and MHD Flows	Drops and Bubbles	MS: Rigid Bodies to Elastic Sheets / FSI
12.30	Lunch	Lunch	Lunch
14.00	Classical Hydrodynamic Instabilities	Drops and Bubbles	MS: Rigid Bodies to Elastic Sheets / FSI
15.45	Coffee break	Coffee break	Coffee break
16.15	Classical Hydrodynamic Instabilities	Liquid Films and Interfacial Dynamics	Multiphase Flows
18.30	Welcome Reception	Welcome Reception	Welcome Reception

July 7th

	Room 1: Auditorium	Room 2: Ipogea	Room 3: Main lecture hall
09.00	Plenary: Helen Wilson		
10.00	Classical Hydrodynamic Instabilities	Interfacial and Small-Scale Flows	Fluid-Structure Interaction
11.00	Coffee break	Coffee break	Coffee break
11.30	Classical Hydrodynamic Instabilities	Interfacial and Small-Scale Flows	MS: Asymptotics meets Numerics in non-Newtonian Flows
12.30	Lunch	Lunch	Lunch
14.00	Plenary: Eckart Meiburg		
15.00	Classical Hydrodynamic Instabilities	Multiphase Flows	MS: Asymptotics meets Numerics in non-Newtonian Flows
16.30	Coffee break	Coffee break	Coffee break
17.00	Transition to Turbulence	MS: Metastability and Phase Change	MS: Asymptotics meets Numerics in non-Newtonian Flows

July 8th

	Room 1: Auditorium	Room 2: Ipogea	Room 3: Main lecture hall
09.00	Plenary: Stefania Cherubini		
10.00	BIFD 2028 presentation		
10.15	Coffee break	Coffee break	Coffee break
10.45	MS: Emerging Patterns in Biological Flows	MS: Metastability and Phase Change	Transition to Turbulence
12.45	Lunch	Lunch	Lunch
14.30	Excursion to L'Aquila	Excursion to L'Aquila	Excursion to L'Aquila
20.00	Banquet	Banquet	Banquet

July 9th

	Room 1: Auditorium	Room 2: Ipogea	Room 3: Main lecture hall
09.00	Plenary: Pierre-Thomas Brun		
10.00	MS: Emerging Patterns in Biological Flows	Suspensions and Particulate Flows	Computational Methods
11.00	Coffee break	Coffee break	Coffee break
11.30	Waves and Vortex Dynamics	Suspensions and Particulate Flows	Computational Methods
12.30	Lunch	Lunch	Lunch
14.00	MS: Emerging Patterns in Biological Flows	Waves and Vortex Dynamics	
15.15	Coffee break	Coffee break	Coffee break
15.45	Closing remarks		

BIFD2026 Chairs

Luca Biancofiore
chair
University of L'Aquila

Francesco Viola
chair
Gran Sasso Science Institute

Local Organising Committee

Andrea Di Mascio
University of L'Aquila

Roberto Verzicco
Gran Sasso Science Institute

Francesco Duronio
University of L'Aquila

Davide Modesti
Gran Sasso Science Institute

Conference Secretariat

Emily Catena
Gran Sasso Science Institute

BIFD Advisory Committee

Zvi Pinhas Bar-Yoseph
Technion-Israel Institute of Technology

Morten Brøns
Technical University of Denmark

Alexander Gelfgat
Tel Aviv University

Ranga Narayanan
University of Florida

Alex Oron
Technion-Israel Institute of Technology

Prashant Valluri
University of Edinburgh

Plenary Lectures

Pierre-Thomas Brun

KU Leuven (Belgium)

From Instability-Driven Fabrication to Soft Robotics: A Mechanics-First Approach

Bio. Pierre-Thomas Brun received his bachelor's degree in Mechanical Engineering from École Polytechnique, Palaiseau in 2008, his Master's degree in Advanced Chemical Engineering from the University of Cambridge in 2009, and his PhD in Mechanical Engineering from Sorbonne University in 2012 for work on the dynamics and instability of viscous and elastic threads. He then joined the École Polytechnique Fédérale de Lausanne (EPFL) as a postdoctoral fellow, where he specialized in interfacial fluid mechanics and instabilities. In 2014, he joined the Massachusetts Institute of Technology (MIT) as an instructor in Applied Mathematics. He moved to Princeton University in 2017, joining the Department of Chemical and Biological Engineering, where he was promoted to Associate Professor with tenure in 2024. In 2025, he returned to Europe to join the Department of Chemical Engineering at KU Leuven. His research is curiosity-driven and focuses on the quantitative modeling of nonlinear fluid and elastic processes in complex soft materials, as well as on the mathematical description of structure formation in inert and biological systems. His work is highly interdisciplinary and closely integrates theory, modeling, and experiments.

Abstract. A central theme of our research is that interfacial flows and mechanical instabilities offer powerful and scalable routes for generating structure and function in soft materials. Through studies of viscous–elastic coupling in curable liquids and nonlinear deformation in slender bodies, we have shown how controlled buckling, coiling, and pattern formation can be harnessed as both fabrication tools and mechanisms for complex actuation and motion. I will discuss how these instability-based principles have enabled emerging applications ranging from programmable filaments to deployable architectures and smart elastoactive structures. Advances in modeling, fabrication, and materials characterization have reshaped the landscape of instability engineering, revealing new opportunities and challenges in using mechanics as a design language for robust, adaptive, and scalable soft robotic systems.

Stefania Cherubini

Polytechnic University of Bari (Italy)

The Emergence of Large-Scale Spatial Modulations in Turbulent Channel Flow

Bio. Stefania Cherubini is Full Professor at the Polytechnic University of Bari. In 2010, she obtained a joint Italian PhD in Machinery Engineering from the Polytechnic University of Bari and a French PhD in Mechanics from Arts et Métiers ParisTech. She was finalist for the Leonardo da Vinci Award of ERCOFTAC for her PhD thesis. From 2012, she was Assistant Professor at the DynFluid Laboratory of Arts et Métiers ParisTech, and in 2015 she received the AIMETA Junior Prize for Fluid Mechanics, awarded by the Italian Association of Theoretical and Applied Mechanics. Since 2016, she has been Professor of Fluid Machinery at the Polytechnic University of Bari. Her research focuses on understanding and modeling instabilities and coherent structures in transitional and turbulent flows, with applications including drag reduction through rough surfaces and energy harvesting from fluid flows.

Abstract. Large-scale coherent structures are frequently observed in turbulent channel flows, both at high Reynolds numbers and in transitional regimes preceding laminar–turbulent pattern formation. In both cases, the origin of such spatial modulations remains an open question. In this talk, a possible mechanism for the emergence of large-scale structures is proposed, interpreting them as secondary instabilities of small-scale streaks. The problem is addressed numerically through linear stability analysis, considering a base flow composed of the mean flow and coherent streaks. The results show that this flow becomes unstable to large-scale modulations whose structure, critical Reynolds number, orientation, and wavelength agree well with observations from the literature. The role of eddy viscosity is discussed through an energy budget analysis, and a nonlinear model is proposed to explain the persistence of laminar–turbulent patterns.

Eckart Meiburg

University of California, Santa Barbara (USA)

Fluid Mechanics of the Dead Sea: Rise of the Salt Giants

Bio. Eckart Meiburg received his PhD in Mechanical Engineering from the Technical University of Karlsruhe in Germany in 1986. After a postdoctoral stay at Stanford University and faculty appointments at Brown University and the University of Southern California, he joined the University of California, Santa Barbara in 2000, where he is currently Distinguished Professor of Mechanical Engineering. He is a recipient of the NSF Presidential Young Investigator Award and the Humboldt Senior Research Award, a Fellow of the American Physical Society and the American Society of Mechanical Engineers, a former Chair of the APS Division of Fluid Dynamics, and an Associate Editor of Physical Review Fluids. He has held visiting positions in France, Switzerland, Australia, New Zealand, Germany, and Israel. His research interests lie broadly in fluid dynamics and transport phenomena, with particular emphasis on multiphase and environmental fluid mechanics.

Abstract. The Dead Sea provides a unique environmental setting in which buoyancy-driven flows, phase change, and sedimentation processes interact in ways not observed elsewhere on Earth. As a terminal lake with salinity close to saturation, precipitation and dissolution processes are tightly coupled to fluid motion, leading to continuous halite deposition. During summer, thermohaline stratification produces descending supersaturated salt fingers that precipitate halite, while in winter the well-mixed water column generates salt throughout its depth. Rapid lake-level decline exposes vast new shoreline areas, carved by streams into deeply incised channels. Together, these phenomena offer insight into the formation of ancient salt giants and provide lessons for understanding coastal stability and erosion under changing sea levels.

Nicolas Noiray

ETH Zurich (Switzerland)

Fascinating Aeroacoustic Instabilities in Spinning-Wave Whistles

Bio. Nicolas Noiray is Associate Professor at ETH Zurich, where he founded the Combustion, Acoustics and Flow Physics (CAPS) Laboratory in 2014. He received his PhD from École Centrale Paris in 2007 and subsequently worked in the Gas Turbine Research Division of Alstom. His research combines theoretical, experimental, and computational approaches to study combustion, acoustics, and fluid mechanics, addressing both fundamental and applied problems. He has received several prestigious awards, including the Silver Medal and the Hiroshi Tsuji Early Career Researcher Award of the International Combustion Institute, as well as ERC Consolidator and Synergy Grants. A central theme of his work is the modeling and control of instabilities across a wide range of time and length scales.

Abstract. This talk explores aeroacoustic instabilities in axisymmetric whistles, focusing on spinning acoustic modes rather than the standing-wave oscillations typical of classical wind instruments. Using a combination of experiments, particle image velocimetry, stochastic modeling, large-eddy simulations, and linearized Navier–Stokes analysis, we investigate the coupling between helical hydrodynamic modes and spinning acoustic waves. Different symmetry-breaking mechanisms and bifurcations are discussed, including transitions between intermittently reversing and stable spinning states, as well as the emergence of mean swirl induced by aeroacoustic limit cycles.

Helen Wilson

University College London (United Kingdom)

Instabilities in Viscoelastic Fluids

Bio. Helen Wilson is Professor of Applied Mathematics at University College London and former Head of the UCL Department of Mathematics. She obtained her PhD from the University of Cambridge in 1998 and held positions at the University of Colorado and the University of Leeds before joining UCL. She has published nearly 50 papers on the flow of complex fluids and has played a leading role in the rheology community. She served as President of the British Society of Rheology (2015–2017) and as Vice-President of the Institute for Mathematics and its Applications (2019–2020). She is an editor of the Journal of Non-Newtonian Fluid Mechanics and Proceedings of the Royal Society A, and currently chairs the Nominating Committee for ICMS and the Scientific Steering Committee of the Isaac Newton Institute.

Abstract. Many industrial fluids possess complex microstructures that lead to viscoelastic behavior, allowing them to store and release elastic energy during flow. This can give rise to a wide range of instabilities, often with undesirable consequences. This talk reviews the modeling of viscoelastic fluids, including polymer solutions and melts, and examines how viscoelasticity affects flow stability. After discussing well-understood mechanisms such as curved-streamline instabilities, shear banding, and interfacial instabilities, the focus shifts to flows with straight streamlines, where instability mechanisms remain less understood. Open challenges and directions for future research are highlighted.

Keynote Lectures

Alexander Alexeev

Georgia Institute of Technology (USA)

Undulatory locomotion of elastic propulsors with standing and traveling waves

---

Evgeniy Boyko

Technion–Israel Institute of Technology (Israel)

Understanding the long-standing puzzle of theory–experiment discrepancy in pressure drop of dilute viscoelastic fluids in channel flows

---

Mattia Serra

University of California San Diego (USA)

Instabilities and flow control in living tissues

Shigeru Takata

Kyoto University (Japan)

H theorem of the Enskog–Vlasov equation: kinetic theory approach for phase change

---

José Eduardo Wesfreid

Sorbonne Université / Université Paris Cité (France)

Henri Bénard (1874–1939): experiments and scientific outreach

---

Mini Symposia

Asymptotics meets Numerics in non-Newtonian Flows

Organisers: Gaetano D'Avino and Luca Biancofiore

This mini symposium brings together theoretical, asymptotic, numerical, and experimental perspectives on non-Newtonian flow instabilities. The focus is on dilute polymer solutions, thin-film flows, pressure-driven configurations, extensional dynamics, and the transition mechanisms that emerge at finite elasticity.

From Rigid Bodies to Elastic Sheets: Bifurcations in Fluid-Structure Interaction

Organisers: Yuri Feldman and Oz Oshri

This session explores bifurcations and instabilities across fluid-structure interaction problems, from rigid bodies immersed in viscous flows to deformable sheets and flexible structures. Contributions connect numerical methods, reduced models, and experiments in regimes where elasticity, geometry, and flow feedback shape the observed dynamics.

Metastability and Phase Change

Organisers: Mirko Gallo and Eugene Benilov

This mini symposium focuses on metastable states and phase-change processes, including nucleation, boiling, condensation, evaporation, and related rare-event dynamics. The emphasis is on how hydrodynamics, thermal effects, fluctuations, and material properties interact across scales.

Emerging Patterns in Biological Flows

Organisers: Rajat Mittal and Francesco Viola

This mini symposium highlights instability, pattern formation, and flow organisation in biological and bio-inspired systems. Topics include locomotion, collective motion, active and deformable media, physiological flows, and the fluid-mechanical mechanisms behind robust biological function.

CONVECTION IN A RAPIDLY ROTATING SPHERICAL SHELL: NEWTON'S METHOD USING IMPLICIT CORIOLIS INTEGRATION

Juan Cruz Gonzalez Sembla[1], Camille Rambert[1], Alan Riquier[2], Fred Feudel[3], Laurette S. Tuckerman[1]
[1] *PMMH, CNRS, ESPCI Paris, Univ. PSL, Sorbonne Univ., Univ. de Paris, 75005 Paris, France*
[2] *Department de Mathématiques, Ecole Normale Supérieure, 75005 Paris, France*
[3] *Institut für Physik und Astronomie, Universität Potsdam, 14476 Potsdam, Germany*

Abstract For rapidly rotating geophysical flows, implicit numerical treatment of the Coriolis force allows much larger timesteps to be taken. By modifying a timestepping code to carry out Newton's method, we discover parameter regions in which the solution changes dramatically. We also carry out the first continuations in Ekman number with automatic adjustment of the spatial resolution.

Geophysical and astrophysical flows are characterized by rapid rotation. Simulating these flows requires small timesteps to achieve stability and accuracy. The stability of numerical schemes can be greatly improved by implicit integration of the terms responsible for the numerical instability[1]. We have implemented an implicit treatment of the Coriolis force in a rotating spherical shell driven by a radial thermal gradient[2]. We have modified the resulting time-stepping code to carry out steady-state solving via Newton's method, which has no time-stepping error[3]. The implicit terms effectively precondition the linear systems, which can then be rapidly solved by a matrix-free Krylov method. We compute branches of rotating waves with azimuthal wavenumbers ranging from 4 to 12 for Ekman numbers as low as 10^{-5} ($Ek \equiv \nu/(d^2\Omega)$, where ν is the kinematic viscosity, d is the difference between the outer and inner radii, and Ω is the imposed rotation). As the Ekman number decreases, the flows are increasingly axially independent and localized near the inner cylinder, in keeping with well-known theoretical predictions and previous experimental and numerical results[4]. The implicit method is always much faster than the explicit method, with the advantage growing as Ek decreases, as shown in figure 1 (left). At $Ek = 3.53 \times 10^{-5}$, we find a branch which displays saddle-node bifurcations and plateaus in the drift velocity, as shown in figure 1 (right).

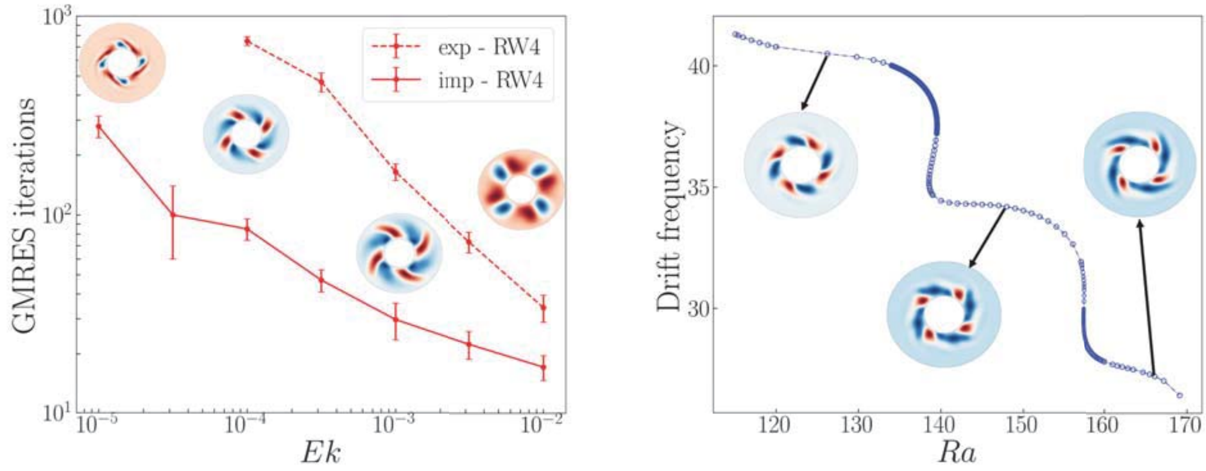

Figure 1. Left: total number of matrix-vector actions (equivalent to a linearized timestep) required by the nested Newton-GMRES algorithm to compute RW_4 as a function of Ek with explicit and implicit implementation of Coriolis force. The average and error bars are computed from 20 values of Ra. The number of actions required by the explicit algorithm is always greater than that required by the implicit algorithm, with the ratio between them increasing from ≈ 2 at $Ek = 10^{-2}$ to ≈ 9 at $Ek = 10^{-4}$. For $Ek < 10^{-4}$, the explicit algorithm requires an unfeasible amount of time. Right: Bifurcation diagram for $Ek = 3.53 \times 10^{-5}$ containing saddle-node bifurcations and plateaus in drift frequency.

[1] Hollerbach, *Int. J. Numer. Methods Fluids* **32**, 773-797 (2000).
[2] Gonzalez Sembla, Rambert, Feudel, Tuckerman, *Mathematics (MDPI)* **13**, 2113 (2025)
[3] Feudel, Bergemann, Tuckerman, Egbers, Futterer, Gellert, Hollerbach, *Phys. Rev. E* **83**, 046304 (2011)
[4] Busse, *J. Fluid Mech.* **44**, 441-460 (1970).

INSIDE THE GEOTHERMAL ENGINE: A NUMERICAL STUDY OF THERMAL AND STRUCTURAL CONTROLS ON HYDROTHERMAL ERUPTIONS

María Cruz Navarro[1], Jesús Saucedo[1] & Damián Castaño[2]
[1] *Departamento de Matemáticas, Facultad de CC. y TT. Químicas, Universidad de Castilla- La Mancha, Spain*
[2]*Departamento de Matemáticas, Escuela de Ingeniería Industrial y Aeroespacial, Universidad de Castilla- La Mancha, Spain*

Abstract Fluid dynamics; hydrothermal eruptions; eruptive cycles; flow patterns.

In this work, we present a numerical study of eruptive activity in fractured, brittle, low- to medium-enthalpy hydrothermal systems composed of a single conduit connected to a geothermal reservoir with an outlet exposed to the atmosphere (Figure 1). The model solves the coupled Navier-Stokes and heat-transfer equations for a simplified hydrothermal fluid represented as a homogeneous equilibrium water-steam mixture.
A sensitivity analysis is performed on geometric parameters (conduit length and diameter) and thermal parameters (reservoir temperature) to evaluate their influence on eruptive behaviour. The results show that temperature variations exert a significant control on eruptive dynamics, enhancing the thermal effusivity of hydrothermal activity. Regarding conduit length, a clear decrease in the number of eruptive cycles is observed as the conduit becomes longer. For conduit diameter, we find that the thermal gradient during the eruptive cycle is greater when the conduit is narrower. Consequently, smaller conduit diameters lead to more violent eruptive events.
Overall, the outcomes of this study qualitatively reproduce the hydrothermal eruptive processes characteristic of fractured systems with low to moderate structural development involving a single conduit [1, 2].

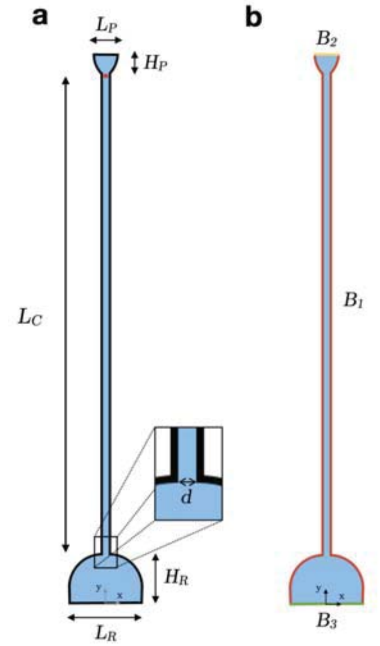

Figure 1. a) Physical domain setup. b) Boundaries of the prototype.

References

[1] A. Tsuge & H. Aoyama, *Numerical experiments of geyser eruption caused by ascent-driven decompression boiling, using the wellbore-reservoir simulator T2Well/ECO2N*, Journal of Volcanology and Geothermal Research **465**, 108366 (2025).
[2] A. Namiki& C. Muñoz-Saez& M. Manga, *El Cobreloa: A geyser with two distinct eruption styles*, Journal of Geophysical Research: Solid Earth. **119**, 6299–6248 (2014).

THERMOHYDRODYNAMIC HYSTERESIS AS A REGULATING MECHANISM OF ERUPTIVE ALTERNATION IN HYDROTHERMAL DOUBLE CONDUIT SYSTEMS: A NUMERICAL STUDY

Jesús Saucedo[1], María Cruz Navarro[1] & Damián Castaño[2]
[1] *Departamento de Matemáticas, Facultad de CC. y TT. Químicas, Universidad de Castilla- La Mancha, Spain*
[2]*Departamento de Matemáticas, Escuela de Ingeniería Industrial y Aeroespacial, Universidad de Castilla- La Mancha, Spain*

Abstract Fluid dynamics; hydrothermal eruptions; hysteresis; drainage; imbibition.

We present a numerical study of eruptive alternation in a brittle fractured hydrothermal double conduit system with two atmospheric outlets, in which an inclined conduit is coupled to a main conduit connected to a geothermal reservoir (Fig. 1), and analyze the role of thermohydrodynamic hysteresis as a physical regulatory mechanism controlling the eruptive styles generated during the alternation between conduits. The study combines: (i) a simulation model that solves the coupled Navier-Stokes and heat-transfer equations for a simplified thermofluid treated as a homogeneous-equilibrium water-vapor mixture; and (ii) a deterministic hysteresis model (Jiles-Atherton/Duhem type) which maps the competition between the vapor pressure $p_{\text{sat}}(T)$ and the confining hydraulic load p into an internal response expressed through the void fraction α and the velocity ratio $|\frac{u_y}{u_x}|$, without explicitly having to resolve the process microscopically.

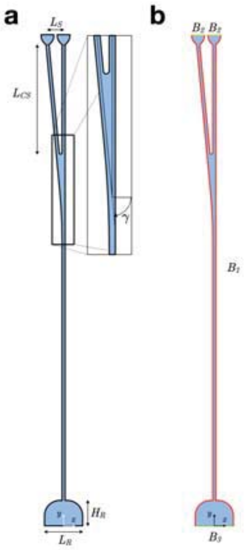

Figure 1. (a) Physical domain setup. (b) Boundaries of the prototype.

A Horner-type petrophysical methodology for recharge/discharge (drainage/imbibition) reveals delays and trajectory dependence, consistent with a deterministic hysteretic coupling between outlet thermodynamics and reservoir hydrodynamics. A sensitivity study is performed by varying (L_S, L_{CS}, γ) and tracking $(T_{\text{sat}}, p_{\text{sat}}(T), p, \alpha, |\frac{u_y}{u_x}|)$. Deeper connections L_{CS} enhance the basal pressurization/thermal buildup and intensify the response, while larger pool spacing L_S modifies communication between outlets, shifting recurrence and persistence. Geometry dominates: high γ sustains alternation, whereas low γ weakens coupling and can extinguish the inclined branch. In this regime, the trajectory-dependent α and $|\frac{u_y}{u_x}|$ indicate a non single-valued output for the same outlet thermodynamic forcing (tracked in (T_{sat}, p)), with distinct recharge versus discharge paths. This behavior is consistent with a deterministic internal regulator with memory (thermohydrodynamic hysteresis) controlling alternation phases [2].

References

[1] A. Namiki& C. Muñoz-Saez& M. Manga, El Cobreloa: A geyser with two distinct eruption styles, Journal of Geophysical Research: Solid Earth. 119, 6299-6248 (2014).
[2] S. Gharari & S. Razavi, A review and synthesis of hysteresis in hydrology and hydrological modeling: Memory, path-dependency, or missing physics?, Journal of Hydrology 566, 500-519 (2018).

IDENTIFICATION OF FLOW STATES FOR THE DRESDYN PRECESSION EXPERIMENT USING ULTRASOUND DOPPLER VELOCIMETRY

Kunal K Jani[1], André Giesecke[1], Thomas Gundrum[1] & Frank Stefani[1]
[1]*Magnetohydrodynamics in Geophysics and Astropyhsics,*
Institute of Fluid Dynamics, Helmholtz-Zentrum Dresden-Rossendorf, Germany

Keywords: Axial Precession, Inertial Modes, Ultrasound Doppler Velocimetry (UDV), Hysteresis.

Abstract
Precession-driven flows in rapidly rotating cylinders are promising drivers of laboratory dynamos. However, the flow transitions that precede magnetic field generation are highly sensitive to control parameters and difficult to detect in real time. The present work focuses on the identification of flow states for the DREsden Sodium DYNamo (DRESDYN) precession experiment, with a preliminary focus on using a distributed network of UDV transducers deployed in a 1:6 downscaled water model (radius R = 163 *mm*, height H = 326 *mm*). Figure 1 shows the layout of this experiment, where Ω_p and Ω_c denote the axis of precession and rotation, respectively, and α is the angle of nutation between them. The identification of the flow states is done using UDV with ultrasound transducers that are located at various radial positions on one end cap of the cylinder. Measurements are performed sequentially, with only one transducer active at a time. The red arrows (the cones schematically show the exaggerated widening of the beam) in Figure 1 show how the axial velocity field is obtained using the ultrasound transducer at a particular radial location.

Building on prior characterisations [1,2] of inertial modes and their dependence on the Poincaré number (precession ratio = Ω_p/Ω_c) and rotation Reynolds number ($Re = 2\pi R^2\Omega_c/\nu$, ν being the kinematic viscosity), this work targets the transition regimes, associated hysteresis and the emergence of large-scale structures. Particular focus is given to the axisymmetric double-roll mode (azimuthal wave number m = 0, axial wave number k = 2), which can be linked to the onset of dynamo action [3]. The upper and lower transition thresholds in Poincaré number for different Reynolds numbers remained insufficiently constrained in previous investigations, yet are essential for the forthcoming DRESDYN experiment. A key aim of this study is therefore to establish these thresholds accurately and to identify the most effective strategy for reliably accessing and sustaining the double-roll mode flow state, achieved by approaching the transition regime using multiple complementary methodologies. These methodologies include systematic upward and downward sweeps of the Poincaré number using step sizes of varying magnitude, as well as sustained measurements at fixed Poincaré numbers over extended durations to obtain statistically converged axial velocity profiles. Additional simultaneous data acquisition from pressure transducers on the end caps and power measurements also help in qualitatively identifying the flow transitions by correlation with the UDV data. This method will be particularly valuable at higher Reynolds numbers where UDV data alone becomes less reliable for flow state characterisation.

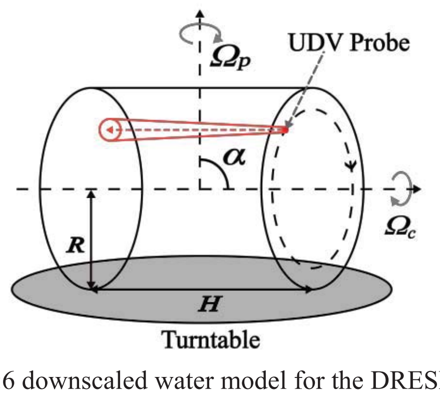

Figure 1: Schematic of the 1:6 downscaled water model for the DRESDYN precession experiment.

References

[1] A. Giesecke, T. Vogt, F. Pizzi, V. Kumar, F. Garcia Gonzalez, T. Gundrum & F. Stefani, The global flow state in a precessing cylinder, J. Fluid Mech. **998**, A30 (2024).
[2] V. Kumar, F. Pizzi, A. Giesecke, J. Šimkanin, T. Gundrum, M. Ratajczak & F. Stefani, The effect of nutation angle on the flow inside a precessing cylinder and its dynamo action, Phys. Fluids **35**, 014114 (2023).
[3] A. Giesecke, T. Vogt, T. Gundrum & F. Stefani, Nonlinear large scale flow in a precessing cylinder and its ability to drive dynamo action, Phys. Rev. Lett. **120**, 024502 (2018).

This project has received funding from Deutsche Forschungsgemeinschaft (DFG) under the research project 532905681 "Real-time identification of flow states in the DRESDYN precession experiment using distributed ultrasound sensors".

REDUCED-ORDER MODEL FOR MAGNETIC FIELD REVERSALS IN SIMULATIONS OF THE VON KÁRMÁN SODIUM EXPERIMENT

Caroline Nore[1], Rémi Bousquet[1] & Victor Botez[1]
[1] *Université Paris-Saclay, CNRS, Laboratoire Interdisciplinaire des Sciences du Numérique (LISN), F-91405 Orsay, France*

Abstract We perform numerical simulations of magnetic field reversals in the Von Kármán Sodium experiment and derive a reduced-order model providing a foundation for predicting behavior in turbulent magnetic fields (Magnetohydrodynamics).

Understanding how magnetic fields reverse in electrically conducting fluids is important in planetary and stellar physics. This study investigates magnetic field reversals in the Von Kármán Sodium (VKS) experiment using numerical simulations with the SFEMANS code [1]. The reversal process is identified as a five-stage sequence, transitioning from a strong dipolar state to a temporary quadrupolar state before reforming a dipole of opposite polarity (see Fig. 1). This is seen as the interaction of global magnetic dipole and quadrupole, influenced by localized dipoles near the impellers. A time lag in flipping these dipoles causes a temporary weakening of the global field. Proper Orthogonal Decomposition (POD) is used to analyze the most energetic modes of the magnetic and velocity fields, following up on a recent study on VKS simulations [2]. Four axisymmetric POD modes dominate the dynamics: a magnetic dipole D and quadrupole Q, alongside a zonal velocity mode V and a mean-field velocity mode U. A reduced-order DQVU Galerkin model captures the key processes involved in these reversals, highlighting the role of ferromagnetic impellers and creating a foundation for future research in dynamo behavior and symmetry breaking in turbulent flows [3].

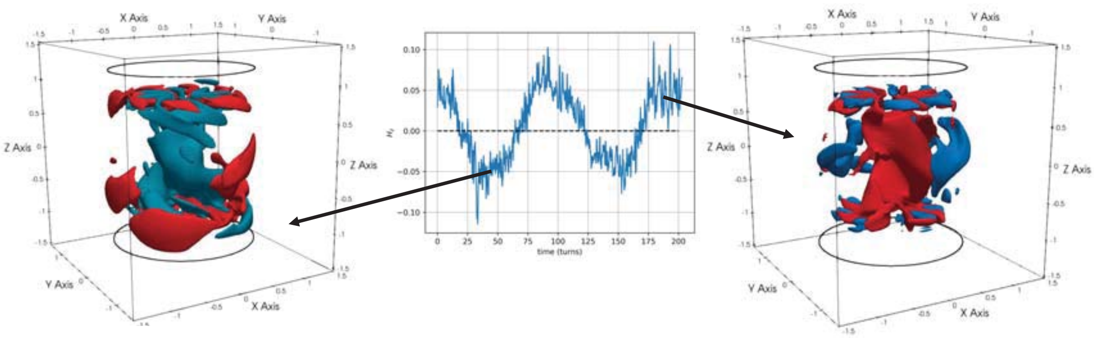

Figure 1. Reversals of magnetic field in the von Kármán Sodium dynamo experiment obtained numerically: isosurfaces of the vertical magnetic field (blue for negative B_z, red for positive B_z) and time evolution of B_z at the cylinder center. Note that B_z is dominated by a **dipole** D, aligned with the vertical axis of the cylinder, that **reverses** in time.

References

[1] C. Nore, D. Castanon Quiroz, L. Cappanera, and J.-L. Guermond, *Numerical simulation of the von Kármán sodium dynamo experiment*, Journal of Fluid Mechanics, **854**, 164–195 (2018).
[2] V. Botez, R. Bousquet, and C. Nore, *Large scale analysis of the von Kármán sodium experiment using proper orthogonal decomposition*, Magnetohydrodynamics, **61**, 13–24 (2025).
[3] R. Bousquet, Y. Ponty, V. Botez, N. Plihon, and C. Nore, *Magnetic Field Reversals in Numerical Simulations of the Von Kármán Sodium Experiment*, submitted to Physical Review Letters (2026).

HENRI BENARD (1874–1939) : EXPERIMENTS AND SCIENTIFIC OUTREACH

José Eduardo Wesfreid
PMMH, ESPCI-CNRS-Sorbonne Université-Université Paris Cité, Paris, France

Keywords:

Thermal and hydrodynamic instabilities; history of science

Abstract

The French physicist Henri Bénard (1874–1939) pioneered the experimental investigation of two significant topics in fluid dynamics. His research focused on thermal convection in fluids heated from below (Rayleigh–Bénard and Bénard–Marangoni convection) as well as on the periodic vortex shedding that occurs behind bluff bodies in a flow (Bénard–Kármán vortex street). At the beginning of the 20th century, Bénard was the first to conduct rigorous experiments on these two canonical fluid systems. These experiments opened a large research field, especially in the last 50 years, and left many open questions to explain his experiments for many years.
This talk presents a brief review of his work and in particular the description of his use of cinema, a new technique at the time. In 1907, with the help of the Lumière brothers, he used cinematography as a scientific instrument to measure the periodic properties of vortex shedding [3]. In 1913, he produced seven movies [4] documenting convection patterns, with the Gaumont company and destinated to public outreach [5]. A summary of these films will be presented at this conference.

Figure 1: Example of the title, booklet, and images from the 1913 films.

References

[1] J.E. Wesfreid, Scientific biography of Henri Bénard (1874–1939). In *Dynamics of spatio-temporal cellular structures: Henri Bénard centenary review*, New York, NY: Springer New York, 9-37 (2006).
[2] J.E. Wesfreid, Henri Bénard: Thermal convection and vortex shedding, CR Mec. 345.7, 446 (2017).
[3] H. Bénard, Etude cinématographique des remous et des rides produits par la translation d'un obstacle, C.R. Acad. Sci., 147, 970 (1908).
[4] *Les tourbillons cellulaires: Particules solides et méthodes optiques* (8'28''); *Les tourbillons cellulaires du spermacéti: Leur régularisation progressive enregistrée par les méthodes optiques* (3'46''); *Les chaînes de tourbillons cellulaires de l'éther* (11'45''); *Les tourbillons cellulaires de l'éther: Relief de la surface libre* (5'49''); *Tourbillons cellulaires isolés: Observation par la méthode optique en lumière réfractée* (4'40''); *Les deux espèces de tourbillons cellulaires* (4'2''); *Solidification cellulaire* (4'48'').
[5] H. Bénard and M. C. Dauzère, "Les tourbillons cellulaires, notice sur une série de films obtenus dans les laboratoires Gaumont, juillet–octobre 1913." Société des Établissements Gaumont (1914).

MINIMAL ABSORBING ZONES IN PLANAR FLOWS

Péter Tamás Nagy[1]
[1]*Department of Hydrodynamic Systems, Faculty of Mechanical Engineering, Budapest University of Technology and Economics, Budapest, Hungary*

Keywords:absorbing zone, Couette flow, Poiseuille flow, variation, energy method, stability

Abstract

Absorbing sets [1] play a fundamental organizing role in the long-time analysis of dissipative partial differential equations, particularly those arising in fluid mechanic [2]. Utilizing the Reynolds-Orr identity, it can be shown that there exists a region in the infinite-dimensional state space of incompressible fluids such that any solution initialized outside this region will eventually enter and remain there. Consequently, this zone contains all possible chaotic and non-chaotic attractors. In the simplest cases, such a region is a hypersphere characterized by its center and radius. The center of this zone is referred to as the background flow, while the radius is quantified by the perturbation kinetic energy (e_β). A simplified representation of the state space is depicted in Figure 1 (a).

The method is applied to plane Couette and Poiseuille flows. It was hypothesized that, because a chaotic turbulent trajectory wanders quasi-randomly and uniformly within its admissible region, the geometric center of the smallest absorbing zone (the optimal backgroundt flow) would approximate the turbulent mean profile. Instead, excessively sharp near-wall gradients are obtained, and quantitative discrepancies with direct numerical simulations and canonical laws of the wall are observed. Nevertheless, novel insight into shear-flow dynamics is provided, and a route to improved global stability estimates is suggested. The energy levels in the case of optimal background flows for Couette a Poseuille flow is depicted in Figure 1 (b) and (c), respectively.

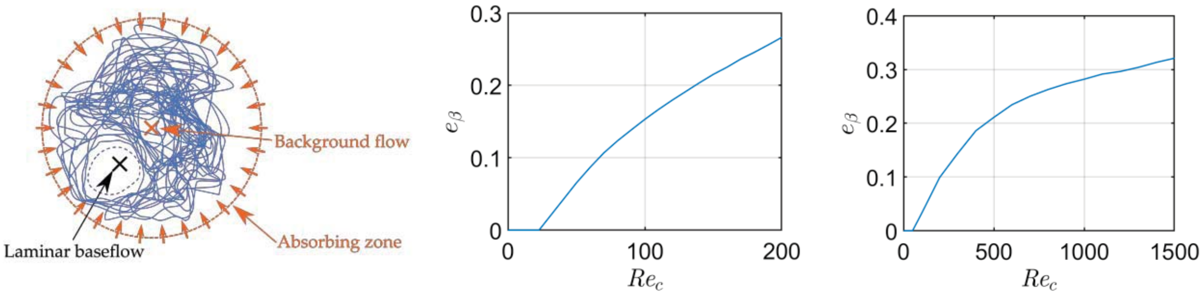

(a) (b) (c)

Figure 1. (a) Simplified state space representation of shear flows. The perturbation kinetic energy threshold as a function of Reynolds number is shown for (b) Couette flow and (c) Poiseuille flow.

Acknowledgements
The research was supported by the János Bolyai Research Scholarship of the Hungarian Academy of Sciences and the National Research Development and Innovation Office of Hungary under Grant Agreement no. K142675.

References

[1] Temam, Roger M. Infinite-Dimensional Dynamical Systems in Mechanics and Physics, Applied Mathematical Sciences, vol. 68. New York, NY: Springer New York (2013)
[2] O. Dauchot & P. Manneville (1997) Local *ver sus* global concepts in hydrodynamic stability theory. J. Phys. II France 7 (2), 371–389. (1997).
[3] , G. Fantuzzi, A. Arslan & A. Wynn The background method: theory and computations. Philos. Trans. R. Soc. A 380 (2225), 20210038 (2022)

WEAKLY NONLINEAR ANALYSIS OF UNSTABLE PERIODIC FLOWS

Marco Carini[1], Alessandro Chiarini[2], Edouard Boujo[3] & Franco Auteri[2]
[1] *DAAA, ONERA, Paris Saclay University, F-92190 Meudon, France* [2] *Dipartimento di Scienze e Tecnologie Aerospaziali, Politecnico di Milano, via La Masa 34, 20156*
[3] *Laboratory of Fluid Mechanics and Instabilities, École Polytechnique Fédérale de Lausanne, CH 1015 Lausanne, Switzerland*

Abstract We present a weakly nonlinear stability analysis of unstable time-periodic flows. Building on classical weakly nonlinear theory and centre-manifold reduction, we extend existing methodologies to periodic base states. (WNL; centre manifold; multiple scales).

The understanding of turbulence, and of the mechanisms through which turbulence emerges from laminar flow, remains one of the most intriguing and challenging problems in contemporary science. Over the past decades, this problem has been addressed using a variety of theoretical and numerical approaches, leading to significant progress in our understanding of flow transition and turbulence. As a result, the tools available to fluid dynamicists have become increasingly sophisticated.

Despite these advances, linear stability analysis, while often successful in predicting the onset of instabilities and some of their basic properties, is insufficient to address deeper questions, particularly those related to the nonlinear evolution of disturbances and the transition process itself. As already emphasised by Stuart in his seminal work on nonlinear hydrodynamic stability [1], "the stability problem in its general form must be considered to be non-linear". Following this insight, nonlinear approaches to flow stability, and in particular the weakly nonlinear, have been extensively developed. Although mathematically demanding, nonlinear stability analysis provides access to phenomena that are inherently beyond the scope of linear theory. A paradigmatic example is the weakly nonlinear analysis of the Couette–Taylor flow based on centre-manifold theory, as carried out by Ioss & Chossat [2].

In recent years, several studies have applied weakly nonlinear analysis to bifurcating *steady* base flows, using both multiple-scale techniques [3] and centre-manifold reduction [4]. In the present work, we extend these approaches to periodic flows and perform a weakly nonlinear analysis of unstable *time-periodic* base states. At the conference, we will introduce the proposed methodology from both the multiple-scale and centre-manifold perspectives, and present a formalism for the weakly nonlinear analysis of unstable periodic flows. We will discuss illustrative examples including both low-dimensional dynamical systems and flows governed by the Navier-Stokes equations.

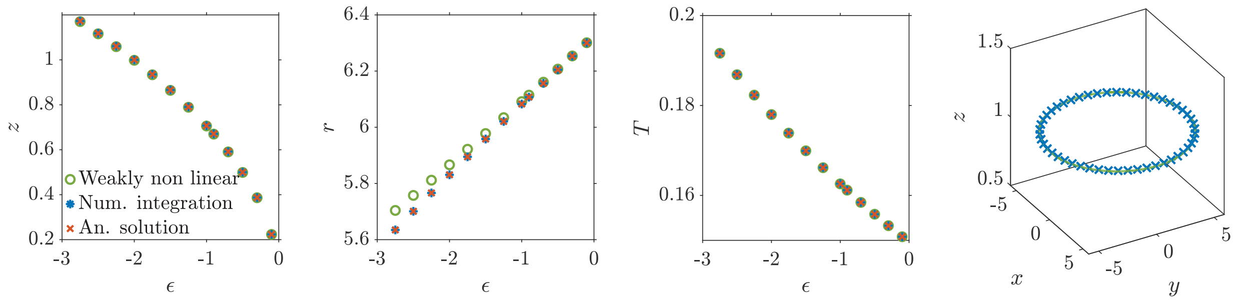

Figure 1. Weakly nonlinear analysis of a simple low-dimensional dynamical system with three degrees of freedom (x, y, z). For $\epsilon > 0$, the system converges to a limit cycle, whereas for $\epsilon < 0$ the limit cycle undergoes a pitchfork bifurcation. The panels compare with the results obtained from direct numerical integration of the system and the analytical solution. Here, $r = \sqrt{x^2 + y^2}$ and T denotes the period of the oscillation. The right panel is for $\epsilon = -2$.

References

[1] J. T. Stuart, *On the non-linear mechanics of hydrodynamic stability*, J. Fluid Mech. **4**, 1–21 (1958).
[2] G. Ioss & P. Chossat, *The Couette–Taylor Problem*, Applied Mathematical Sciences **102**, New York: Springer-Verlag (1990).
[3] D. Sipp & A. Lebedev, *Global stability of base and mean flows: a general approach and its applications to cylinder and open cavity flows*, J. Fluid Mech. **593**, 333–358 (2007).
[4] M. Carini, F. Auteri & F. Giannetti, *Centre-manifold reduction of bifurcating flows*, J. Fluid Mech. **767**, 109–145 (2015).

NONLINEAR DYNAMICS IN THE BÖDEWADT LAYER OF A ROTOR-STATOR CAVITY

Yohann Duguet[1], Artur Gesla[2] & Laurent Martin Witkowski[3] and Patrick Le Quéré[1]
[1] *LISN-CNRS, Université Paris Saclay, Orsay, France*
[2] *HEAD Laboratory, EPFL Lausanne, Switzerland*
[3] *Universite Claude Bernard Lyon 1, LMFA, UMR5509, CNRS, Ecole Centrale de Lyon, INSA Lyon, 69622 Villeurbanne France*

Abstract Numerical investigation of the onset of unsteadiness inside a closed rotor-stator geometry.

We investigate numerically the onset and origin of unsteadiness inside an elongated rotor-stator geometry, with or without central hub. In the absence of hub, concentric axisymmetric rolls propagating inside the Bödewadt layer can be excited by unsteady external disturbances and amplified by non-normal effects [1]. Subcritical instabilities leading to axisymmetric unsteady flow have also been recently identified [2]. In the presence of a wide enough hub, they can turn into supercritical linear instabilities [3]. In that regime we propose a new explanation for the merging as the result of a nonlinear forcing-free mechanism. We begin by computing, depending on the hub ratio, the eigenmodes of the Navier-Stokes operator linearised around the base flow. We demonstrate that, for the eigenmodes contained in the Bödewadt layer, their radial support is localised, and its location varies linearly with the imaginary part of the corresponding eigenvalue. We then show how roll merging, as is frequently observed in the nonlinear regime (see figure), can be interpreted as a sequence of resonances involving such eigenmodes. These results appear specific to circular geometries because of the space-dependent convective radial velocity.

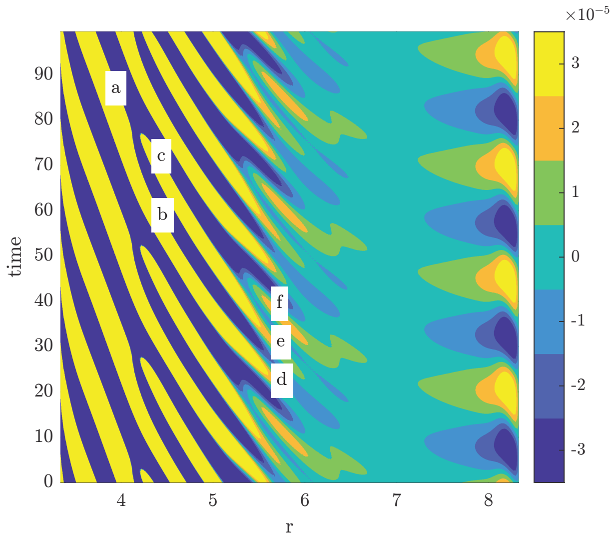

Figure 1. Space–time diagram of the azimuthal velocity fluctuation in an axisymmetric rotor-stator flow, inside the Bödewadt layer located close to the stator. Going downstream the Bödewadt layer (from right to left) towards the hub located at $r \approx 3$, three structures (d,e,f) merge into two (b,c) at $r \approx 5.5$ while two structures (b,c) merge into one (a) at $r \approx 4$.

References

[1] A. Gesla *et al.*, *On the origin of circular rolls in rotor-stator flow.*, J. Fluid Mech. **1000**, A47 (2024).
[2] A. Gesla *et al.*, *Subcritical axisymmetric solutions in rotor-stator flow*, Phys. Rev. Fluids **9**(8), 9(8), 083903 (2024).
[3] A. Gesla *et al.*, *From annular cavity to rotor-stator flow: Nonlinear dynamics of axisymmetric rolls*, Phys. Rev. Fluids **10**(7), 073904 (2025).

TRANSIENT REGIME OF A TWO PHASE ROTATING FLOW IN A CYLINDER : WAVES CHARACTERISATION

Félix Picot, Hélène Scolan, Nathalie Grosjean, Jean-Philippe Matas & Laurent Martin Witkowski
[1] *Universite Claude Bernard Lyon 1, LMFA, UMR5509, CNRS, Ecole Centrale de Lyon, INSA Lyon, 69622 Villeurbanne France*

Abstract Rotating flow, transient regime, interfacial waves

The dynamics of a cylindrical air-water interface in a horizontally rotating cylinder is studied experimentally. A cylinder partially filled with water is rotating at sufficiently large rotation rate so that centrifugal acceleration dominates gravity. In this configuration, the water is driven toward the cylinder wall, forming an annular layer around a cylindrical air bubble. In the limits of large rotation rate, the annular layer and the bubble become coaxial and align with the rotation axis, while the flow velocity field follows a solid-body rotation. This steady-state flow is known as 'rimming flow' and can be achieved with any two non-miscible fluids of different density [2].

Centrifugal waves can be observed along the interface in this large Reynolds number flow. In our experiments, these waves are triggered either by a continuous forcing—such as time harmonic oscillations of the rotation rate (or inherent system vibrations), —or by a sudden change in rotation rate. In the former case, waves are sustained, while in the latter, they eventually vanish.

The periodicity in the azimuthal direction restricts the wave number to integer values, denoted as m. Waves develop with phase velocities, either faster (leading waves) or slower (lagging waves) than the angular velocity of the cylinder [1].

For various triggering mechanisms, we have experimentally characterised the waves, separating each m by spatial Fourier transform and monitoring the dynamic of the phase velocities using short-time Fourier transform.

A typical example for $m = 3$ is shown in figure 1, where both leading and lagging waves (i.e. normalised phase velocity greater or lesser than 1) are observed. Here the triggering mechanism corresponds to a sudden increase in the rotation rate. The transient regime observed for the phase velocities of the waves is coherent with the typical 'spin-up' timescale of the flow.

(a) Front view of the rotating cylinder with an interface showing an azimuthal mode $m = 3$

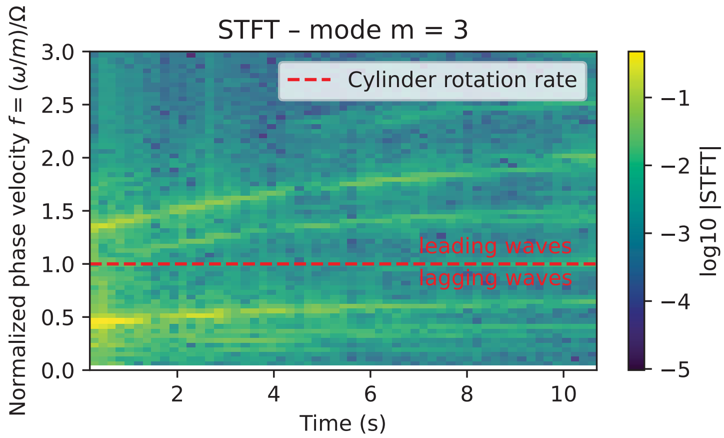

(b) Short time Fourier transform of the azimuthal mode $m = 3$, phase velocities are normalized by the final cylinder rotation rate

Figure 1: 'Spin-up' of the phase velocities of centrifugal waves for azimuthal mode $m = 3$, measured after a sudden change of the rotation rate of the cylinder from 8Hz to 20Hz. The ratio of the volume of water to the total volume of the cylinder is 0.92.

A systematic study has been carried out by varying the ratio of water volume to the total cylinder volume showing a rich variety of the dynamics of the waves, not only in the azimuthal direction but also in the axial direction.

References

[1] O.M Phillips , *Centrifugal waves*, J. Fluid Mech. **7(3)**, 340-352 (1960).
[2] N.V. Kozlov, A.N. Kozlova & D.A. Shuvalova, *Dynamics of immiscible liquids in a rotating horizontal cylinder*, Physics of Fluids, **28(11)**, 112102 (2016).

GLOBAL BIFURCATION STRUCTURE OF QUANTUM WAKES PAST OBSTACLES OF GENERAL SHAPE

Niccoló Geracitano[1], Francesco Viola[1], Paolo Luchini[2] & Vincenzo Citro[2,3]
[1] *Gran Sasso Science Institute, Viale Francesco Crispi 7,67100, L'Aquila, Italy*
[2]*DIIN, Università di Salerno, Via Giovanni Paolo II 132, 84084, Fisciano, Italy*
[3]*CNR - Nanotec, Unità di Roma, P.le Aldo Moro 5, 00185 Rome, Italy.*

Abstract Quantum fluids, vortex shedding, global bifurcation theory

The dynamics of vortex formation and release is fundamental to describing the physics of quantum fluids, such as zero-temperature superfluid helium and atomic Bose-Einstein condensates (BECs), as it dictates how an otherwise dissipationless flow gives way to instability, energy transfer, and turbulence [1]. In the context of Newtonian fluids, the prototypical setup used to study vortex shedding is the uniform flow past a circular cylinder. In this configuration, the flow remains steady and symmetric up to a Reynolds number of approximately $Re \approx 47$, beyond which periodic vortex shedding, commonly known as the von Kármán vortex street, emerges via a Hopf bifurcation. Quantum fluids, on the contrary, have no intrinsic viscosity, making a direct application of the classical Reynolds number impossible, and support vorticity exclusively through quantized vortices, each carrying a fixed circulation quantum h/m. However, both experiments and numerical simulations [3] reveal that a laser-induced obstacle moving through a Bose–Einstein condensate at speeds exceeding a critical velocity k_c generates long-lived vortex wakes, with the resulting quantized vortices often arranging into coherent wake patterns reminiscent of classical von Kármán streets.

In this talk, we will describe the bifurcation scenario governing the onset of vortex emission in quantum fluids past obstacles of general shape and strengths, showing how quantized vorticity fundamentally alters the dynamics with respect to the viscous counterpart. Combining phase portraits, eigenvalue analysis, and time-dependent simulations, we identify a bottleneck trajectory near a saddle-node equilibrium, indicating a global saddle-node on invariant cycle (SNIC) bifurcation [2]. This classification is confirmed by a normal form reduction, which recovers the universal square-root divergence of the shedding period with critical exponent $-1/2$. Modal analysis, performed using the Bogoliubov–de Gennes equations, further shows that the marginally stable direct and adjoint eigenmodes at the critical velocity localize near the obstacle boundary, coinciding with the region of vortex nucleation in the supercritical regime.

The same critical behavior is observed across a broad class of laser profiles, including circular, elongated, square, and airfoil-like obstacles, and for different values of the obstacle potential strength. In this sense, the obstacle geometry and intensity change the quantitative realization of the wake, such as the critical velocity, the nucleation region, and the force response, but not the underlying route to vortex emission. The persistence of the inverse square-root scaling near threshold therefore points to a universal global bifurcation mechanism for quantum wakes, providing a unified interpretation of vortex shedding beyond the specific details of the obstacle shape and strength.

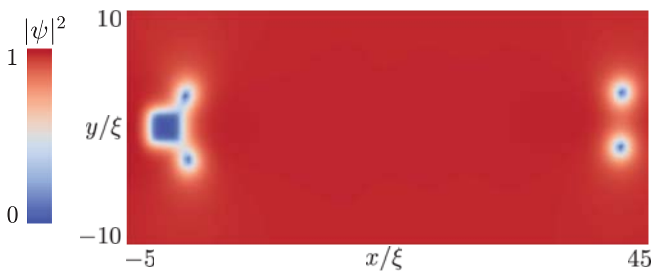

Figure 1. Quantum vortices shedding from a square-shaped obstacle.

References

[1] R. J. DONNELLY, *Quantized vortices in helium II*, vol. 2, Cambridge University Press, 1991.
[2] Y. A. KUZNETSOV, *Elements of Applied Bifurcation Theory (2nd ed.)*, Springer-Verlag, Berlin, Heidelberg, 1998.
[3] K. SASAKI, N. SUZUKI, AND H. SAITO, *Bénard-Von Kármán Vortex Street in a Bose-Einstein Condensate*, Phys. Rev. Lett., 104 (2010), p. 150404.

DIMENSION REDUCED MODEL FOR A TWO-LAYER SYSTEM

Michael Bestehorn
Institut für Physik, Brandenburgische Technische Universität Cottbus-Senftenberg, Germany

Abstract Keywords: Two-layer system, reduced model, Rayleigh-Taylor and Kelvin-Helmholtz instability, numerical solutions.

As an extension of a dimension-reduced model derived earlier [1] for an infinitely deep, inviscid, and irrotional layer, a two-layer system is examined in the present paper. The second layer has a finite depth and is located on top of the layer with infinite depth. The setup is a combination of a long-wave approximation (upper layer) and a deep water approximation (lower layer). It consists of four coupled 1+1 dimensional (space+time) nonlinear partial differential equations for the interface profile and the horizontal velocity component of each layer.

Linear stability analysis provides the conditions for Rayleigh-Taylor and Kelvin-Helmholtz instabilities. Finally, we present numerical solutions of the model showing spatial and temporal pattern formation in the weakly nonlinear regime of both instabilities (Fig. 1).

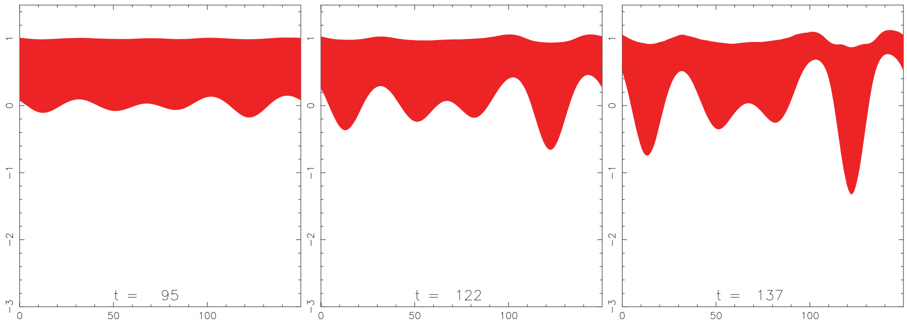

Figure 1. Rayleigh-Taylor instability of a two-layer fluid setup.

References

[1] M. Bestehorn, P. A. Tyvand, T. M. Michelitsch, *Dimension-reduced model for deep-water waves*, JAMP **7**, 72–92 (2019).
P. A. Tyvand, C. Mulstad, M. Bestehorn, *A nonlinear impulsive Cauchy-Poisson problem. Part 1. Eulerian description*, J. Fluid Mech. **906**, A24-1–32 (2020).

LOCAL AND GLOBAL LINEAR KARREN INSTABILITY

Simeon Djambov[1,2] & François Gallaire[1]
[1] *Laboratory of Fluid Mechanics and Instabilities, EPFL, 1015 Lausanne, Switzerland*
[2] *LadHyX, CNRS, Ecole Polytechnique, Institut Polytechnique de Paris, 91128 Palaiseau, France*

Abstract thin films, morphological instability.

Linear karren are dissolution patterns, carved into inclined limestone slabs (fig. 1a). They appear as arrays of regularly spaced rills, oriented along the slope and present wavelengths, ranging from millimetres to several metres [1]. While their hydrodynamical origin is undisputed, the mechanics at play behind their formation remain elusive. The pattern's wavelength selection and streamwise extent are two questions of particular interest.

One point of view on their origin involves the destabilisation of a run-off film flow over a soluble substrate. Indeed, it was experimentally observed that uniform film flows over inclined gypsum substrates carve streamwise streaks [2]. An instability mechanism in the coupling between the flow velocity and the dissolution rate was proposed: over a range of transverse wavenumbers, the flow is accelerated in the perturbation's troughs compared to the crests, causing a thinning of the solutal boundary layer and enhancing the dissolution. Soon after, a local linear instability analysis on the laminar film flow over a soluble substrate was performed, confirming the mechanism [3].

On one hand, the obtained local dispersion relations present a plateau of almost equally unstable modes (fig. 1b), which hinders the predictive power of the analysis. On the other hand, interpreting the resulting locally varying temporal growth rates is challenging. We thus perform a global, two-dimensional, linear instability analysis. We exploit the separation between the geological time scale of the dissolution process and the hydrodynamical time scale of the flow, in order to formulate a quasi-stationary eigenvalue problem, in which the flow and concentration fields adapt instantaneously; the eigenmodes are then contained only in the substrate topography perturbation. While the local instability mechanism remains pertinent, the resulting global dispersion relation has a far more peaked dominant wavenumber region, holding promise for future validation.

(a) (b)

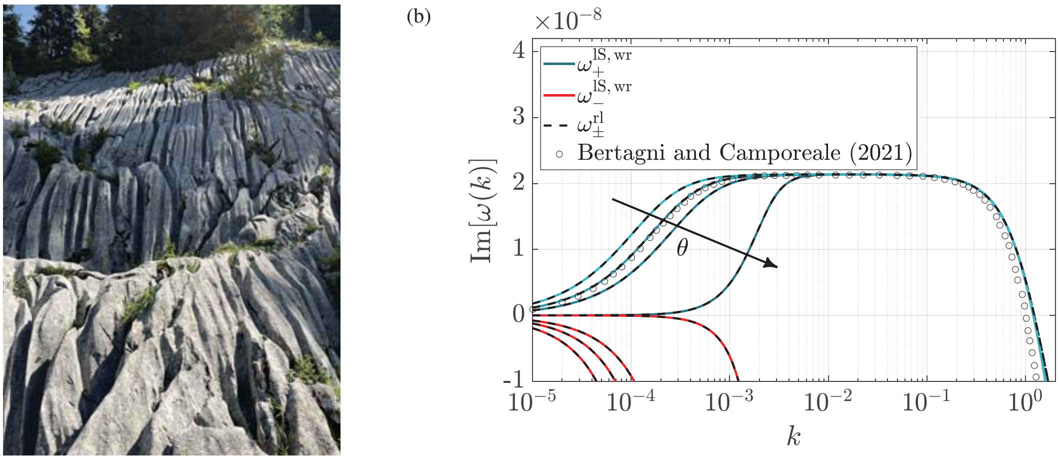

Figure 1: (a) Linear karren near Stockhorn in the Bernese Alps. (b) Sample local dispersion relations for varying inclination angle with respect to the horizontal $\theta = \{\pi/8, \pi/4, 3\pi/8, \pi/2\}$: dimensionless growth rate $\mathrm{Im}[\omega]$ as a function of the dimensionless wavenumber k. The circles represent Bertagni & Camporeale's (2021) result [3], while the lines follow several explicit dispersion relations obtained through boundary-layer models [4].

References

[1] A. Ginés, M. Knez, T. Slabe & W. Dreybrodt, *Karst Rock Features. Karren Sculpturing*, Vol. 9 of Carsologica, Založba ZRC, Ljubljana (2009).
[2] A. Guérin, J. Derr, S. Courrech du Pont & M. Berhanu, *Streamwise dissolution patterns created by a flowing water film*, Phys. Rev. Lett. **125**, 194502 (2020).
[3] M. B. Bertagni & C. Camporeale, *The hydrodynamic genesis of linear karren patterns*, J. Fluid Mech. **913**, A14 (2021).
[4] S. Djambov & F. Gallaire , *Boundary-layer approach to the linear karren instability*, J. Fluid Mech. **977**, R3 (2023).

STABILITY OF A SWIRLING FLOW IN A TURBINE DRAFT TUBE

Lester C. Toledo, Artur Gesla & Eunok Yim
Hydro Energy and Applied fluid Dynamics (HEAD) Laboratory, École Polytechnique Fédérale de Lausanne (EPFL), 1015 Lausanne, Switzerland

Abstract swirling jet, linear stability analysis, adjoint sensitivity analysis

Hydraulic turbines suffer from performance degradation when operated away from their design condition due to flow instabilities. To better understand this instability, we perform a local linear stability and adjoint-based sensitivity analysis of the turbulent swirling flow at the outlet of a Francis turbine using the experimentally validated velocity and turbulence profiles from Susan Resiga et al. [1, 2] at several operating conditions (below, at, and above the best efficiency point (BEP) flow rate). Three eddy viscosity ν_t (constant, mixing-length, and measured $k-\varepsilon$-based) are compared with the laminar case $\nu_t = 0$. Results show that turbine outlet flow is unstable to centrifugal instability and reveal that eddy viscosity strongly damps inviscid growth rates and restricts instability to low azimuthal modes $m \in [-1, 2]$, more consistent with experiments. The three models yield similar spectra, with close agreement between mixing-length and measured models, and identify the partial load (0.92 BEP) as the most unstable regime as shown in Figure 1. Sensitivity results show that axial velocity modifications primarily control growth rates, while azimuthal velocity changes mainly shift frequencies. We also derive the sensitivity kernel for turbulent viscosity modifications and find that spatial variations of eddy viscosity are essential to predict the unstable mode range. The predictions accurately estimate stability changes for small operating-point variations. We further analyze the flow using classical inviscid swirling jet instability criteria (the generalized Rayleigh discriminant) and Wentzel-Kramers-Brillouin (WKB) analysis to predict the stability to broader operating points and reconcile these results to the stability and sensitivity analyses. The approach used in this study is fast and interpretable, but neglects draft tube geometry (non-parallel effects), motivating future global stability and sensitivity analyses, as well as sensitivity-based flow control.

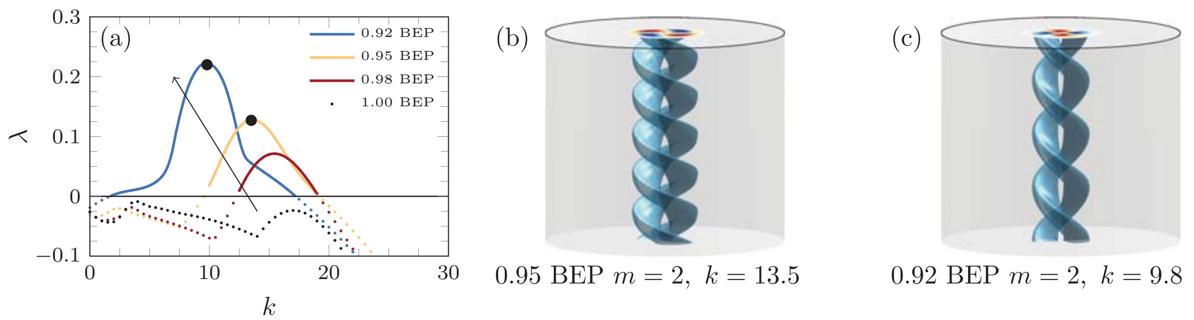

Figure 1. (a) Growth rate λ curves of the $m = 2$ mode under different flow rate conditions using the experimentally measured $k-\varepsilon$ viscosity model as a function of the axial wavenumber k. Solid lines indicate positive growth rates, while dotted markers indicate negative growth rates. Three-dimensional expansion of the most unstable modes in vorticity (b) 0.95 BEP and (c) 0.92 BEP.

References

[1] Susan-Resiga, R. and Ciocan, D. and Anton, I. and Avellan, F., *Analysis of the swirling flow downstream a Francis turbine runner*, J. Fluids Eng. **128**, 1 (2006).

[2] Susan-Resiga, R. and Muntean, S. and Hasmatuchi, V. and Anton, I. and Avellan, F., *Analysis and Prevention of Vortex Breakdown in the Simplified Discharge Cone of a Francis Turbine*, J. Fluids Eng. **32**, 5, 051102 (2010).

BISTABLE FLOW DYNAMICS OF AIRFOIL STALL UNDER VARYING ANGLE OF ATTACK: A STOCHASTIC MODEL WITH MULTIPLICATIVE NOISE

Edouard Boujo[1], Ivan Kharsansky Atallah[2,3] & Luc R. Pastur[3]
[1]École Polytechnique Fédérale de Lausanne, CH-1015 Lausanne, Switzerland
[2]EM2C Laboratory, CNRS, CentraleSupelec, Université Paris-Saclay, F-91190 Gif-sur-Yvette, France
[3]Fluid Mechanics Department, ENSTA Paris, Institut Polytechnique de Paris, F-91120 Palaiseau, France

Abstract Aerodynamics, Bifurcations, Low-dimensional models, Noise-induced transitions, Stochastic dynamical systems

We model the intermittent, bistable stall dynamics of an airfoil under varying angle of attack α. Experiments at $Re \approx 10^5$ show random transitions between two flow states, high-lift attached state A and low-lift detached state D, with very long residence times [1]. We propose a one-dimensional Langevin equation using the lift coefficient $C_L(t)$ as a scalar observable. The deterministic potential depends continuously on α and, crucially, the stochastic forcing is multiplicative, i.e. depends on the flow state (A or D). The model, identified based on the flow statistics and dynamics [2], reproduces the S-shaped lift curve $C_L(\alpha)$ as well as the flow dynamics. It also predicts that the bistable region is delimited by two saddle-node bifurcations and yields their normal form.

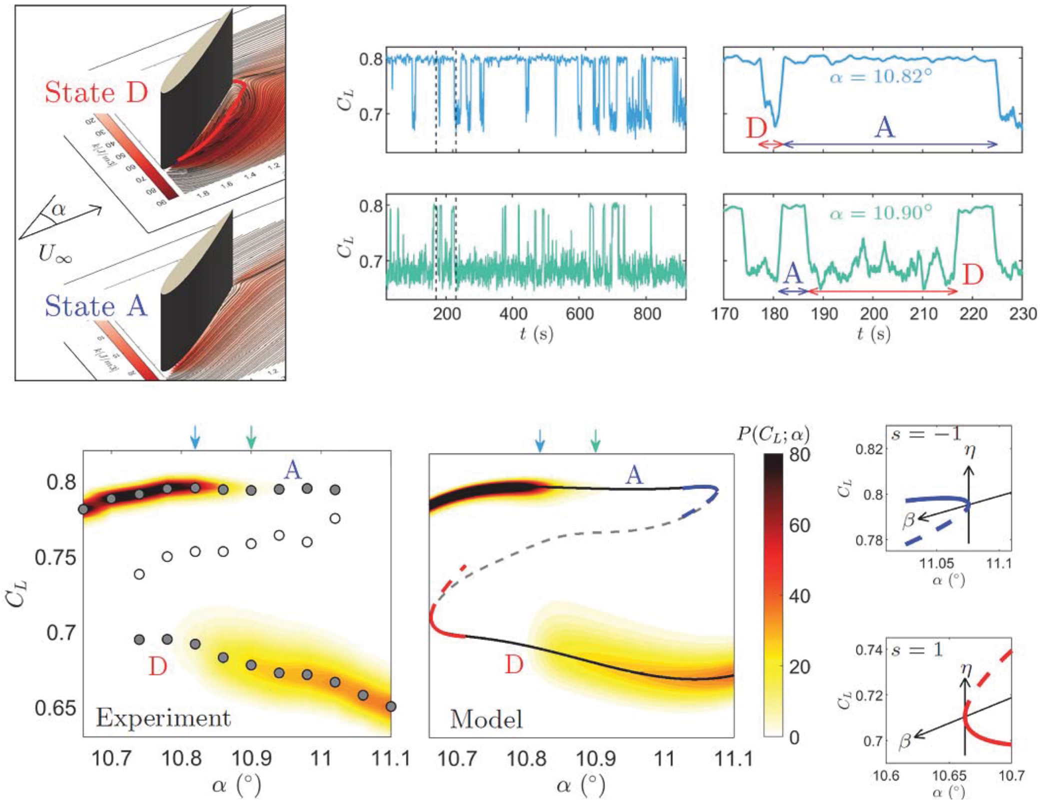

Figure 1. Top left: bistable states A (high-lift attached flow) and D (low-lift detached flow; red: backflow region boundary) from conditional PIV. **Top right:** transitions between states A and D in the experimental lift coefficient signals $C_L(t)$, for two different angles of attack α. Left: 15 min window; right: 1 min window. **Bottom left and middle:** experimental and identified lift coefficient as a function of α in the bistable range. Contours: PDF $P(C_L;\alpha)$. Gray circles: maxima of the PDF in states A and D; white circles: minimum of the PDF. Solid black lines: stable states A and D; dashed grey line: unstable branch of the double saddle-node bifurcation. **Bottom right:** zoom on the two local saddle-node bifurcations described by the identified normal forms.

References

[1] I. Kharsansky Atallah, L. Pastur, R.Monchaux & L. Zimmer, *From low-frequency oscillations to Markovian bistable stall dynamics*, Phys. Rev. Fluids **9**, 063902 (2024).
[2] E. Boujo & N. Noiray, *Robust identification in thermo-acoustic systems with the adjoint Fokker-Planck equation*, Proc. R. Soc. A **473**: 20160894 (2017).

STABILITY OF BLUFF BODY WAKES: EFFECT OF MISALIGNMENT AND GROUND

A. Lagwankar[1], A.Chiarini[2], F. Gallaire[1] & E. Boujo[1]
[1] *École Polytechnique Fédérale de Lausanne, CH-1015 Lausanne, Switzerland*
[2]*Politecnico di Milano, 20156 Milano, Italy*

Abstract Imperfect bifurcation, Instability, Bluff body wake, Misalignment, Ground effect

The laminar wake of a perfectly aligned Ahmed body undergoes pitchfork bifurcations, leading to a static symmetry-breaking deflection, either vertical or horizontal [1]. At slightly larger Re, the deflected wake undergoes a secondary Hopf bifurcation, leading to vortex shedding. When the body is misaligned with the incoming flow, the bifurcation scenario becomes richer. Here, using 3D linear and weakly nonlinear stability analysis, as well as DNS, we investigate how pitch and yaw affect these bifurcations, thus complementing existing turbulent studies [2, 3].

As typically observed for imperfect pitchfork bifurcations, at low Re a small misalignment selects one of the steady states: vertical deflection under pitch (Fig. 1a), and horizontal deflection under yaw. Interestingly, pitch reduces the critical Re of the vertical Hopf bifurcation but also increases the critical Re at which the vertically deflected state loses stability (Fig. 1b), resulting in a cross-over of the two bifurcations. For small angles, the effect of combined yaw and pitch is studied efficiently via a weakly nonlinear analysis, unveiling intricate bifurcation diagrams.

We also study the effect of a moving ground, a more realistic situation for a ground vehicle, on the bifurcation sequence. Depending on the ground clearance, different modes are expected to compete or new ones may even appear, as suggested by studies of simple bluff bodies in ground proximity [4].

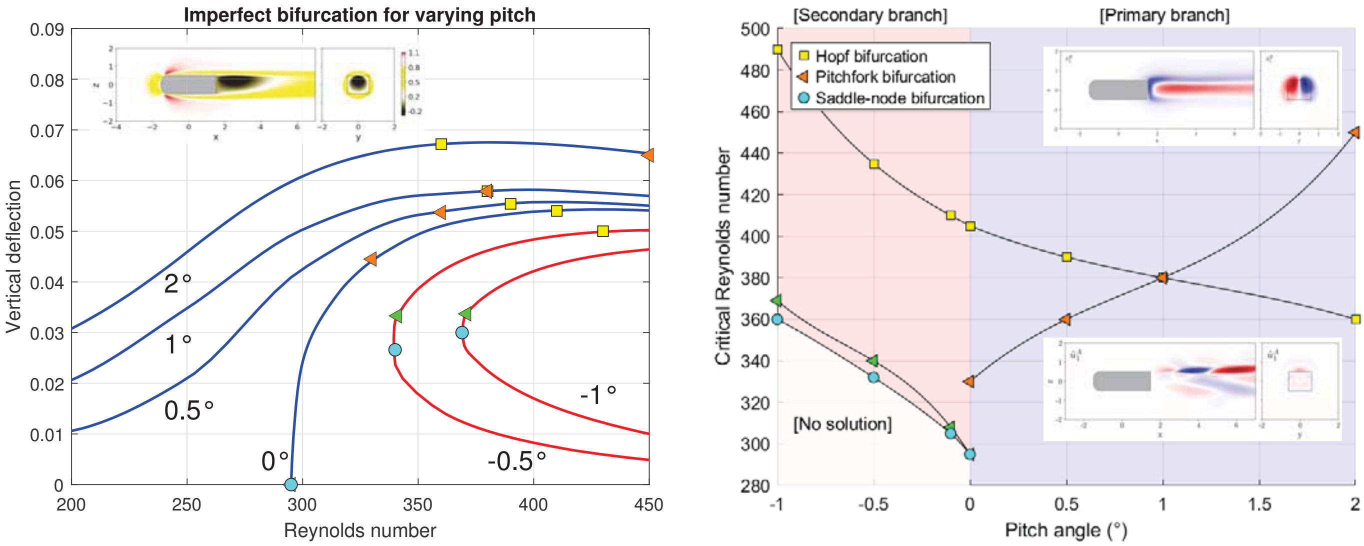

Figure 1: (a) Nonlinear base states (vertical velocity w measured in the wake on the axis $y = z = 0$). Inset: streamwise velocity (side and rear view) for $\alpha = 2°$ at $Re = 340$ (b) Critical Reynolds numbers for different pitch angles. Insets: stationary ($Re = 440$) and oscillatory ($Re = 360$) eigenmodes (side and rear view) for $\alpha = 2°$ on the primary branch. The blue and red zones correspond to the primary and secondary branches respectively.

References

[1] G. Zampogna and E. Boujo, *From thin plates to Ahmed bodies: linear and weakly nonlinear stability of rectangular prisms,* J. Fluid Mech. **966**, A19 (2023).

[2] M. Grandemange, M. Gohlke, and O. Cadot, *Turbulent wake past a three-dimensional blunt body. part 1. global modes and bi-stability,* J. Fluid Mech. **722**, 51–84 (2013).

[3] Y. Fan, V. Parezanović, and O. Cadot, *Wake Transitions and Steady z-Instability of an Ahmed Body in Varying Flow Conditions,* J. Fluid Mech. **942**, A22 (2022).

[4] M.C. Thompson, T. Leweke, and K. Hourigan, *Bluff bodies and wake–wall interactions,* Ann. Rev. Fluid Mech. **53**, 347-376 (2021).

VORTEX BREAKDOWN IN A HYDROTURBINE DRAFT TUBE SWIRLING JET

Artur Gesla & Eunok Yim

Hydro Energy and Applied fluid Dynamics (HEAD) Laboratory, École Polytechnique Fédérale de Lausanne (EPFL), ME A2 464, Station 9, 1015 Lausanne, Switzerland

Abstract swirling jet dynamics, hydropower, vortex breakdown, Hopf bifurcation, transcritical bifurcation, subcritical states

The swirling flow in a Francis type hydropower turbine is known to be susceptible to the formation of a large helical structure known as a vortex rope. This vortex rope can be seen as an unstable mode of the vortex breakdown phenomenon. This perspective is adopted here for a simplified case of laminar flow to isolate bifurcation scenarios. We perform DNS and linear stability analysis using two wall models: no-slip and free-slip (shear-free) boundary conditions. An axisymmetric draft tube geometry is adopted from [1] and the inflow velocity profile is based on the experimental measurement reported therein. The helical vortex rope mode is shown to bifurcate supercritically from an axisymmetric flow inside a turbine draft tube when a no-slip boundary condition is used. When friction effects on solid walls are neglected, the formation of a large recirculation region on the axis can be obtained and a region of subcritical solutions is identified for a flow regime that corresponds to a partial load of the turbine. The existence of subcritical solutions promotes the existence of a hysteresis loop. A regular dynamics of formation of the recirculation bubble at the axis and its destruction due to a helical vortex rope forming at its periphery is described (selected snapshots are presented in figure 1). Increasing the axial discharge towards the regime corresponding to full turbine load is shown to cause unfolding of the branch of steady solutions in a transcritical bifurcation, a scenario similar to the one proposed by [2] for unfolding of a pitchfork bifurcation is a swirling jet. This bifurcation takes place at a finite Reynolds number and complements the existing evidence of the transcritical bifurcation of swirling jet flows that has been shown to exist only in an inviscid limit [3].

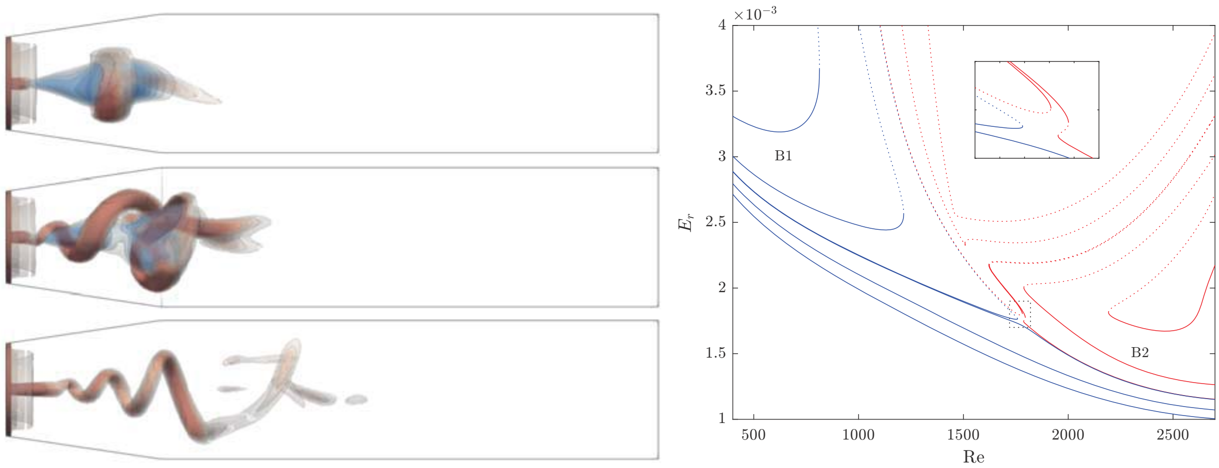

Figure 1. Left: snapshots of the recirculation bubble formation (negative axial velocity shown in blue isosurface) and its destruction due to formation of a helical vortex rope (visualised with positive Q-criterion isosurfaces in red). Right: collision of two families of branches of steady solutions plotted for a series of turbine operating points leading to a transcritical bifurcation, zoom on which is shown in the inset. Stability to axisymmetric modes is marked with solid (stable) and dotted (unstable) lines.

References

[1] Susan-Resiga, R., Muntean, S., Hasmatuchi, V., Anton, I., and Avellan, F. (2010). Analysis and prevention of vortex breakdown in the simplified discharge cone of a Francis turbine. *J. Fluids Eng.*, 132(5).
[2] Lopez, J. M. (1994). On the bifurcation structure of axisymmetric vortex breakdown in a constricted pipe. *Phys. Fluids*, 6(11):3683–3693.
[3] Wang, S. and Rusak, Z. (1997). The effect of slight viscosity on a near-critical swirling flow in a pipe. *Phys. Fluids*, 9(7):1914–1927.

INSTABILITY OF THE BOUNDARY LAYER AROUND THIN POROUS AIRFOILS: A WEAKLY NONPARALLEL APPROACH

Mahbod Mohammadrashidi[1] & François Gallaire[1]
[1] *Laboratory of Fluid Mechanics and Instabilities, École Polytechnique Fédérale de Lausanne, CH-1015 Lausanne, Switzerland*

Abstract nonparallel stability analysis, interactive boundary layer, porous airfoil.

Porous airfoils, which are reminiscent of many natural flyers, have great potential for exploitation in nature-inspired engineering. However, these porous airfoils are mostly efficient when operating at moderate Reynolds numbers, where the flow is neither trivially laminar nor turbulent. Therefore, an effective yet simple model for the instability and transition behavior of the boundary layer around such airfoils is a prerequisite for their accurate aerodynamic modelling.
In this study, using an interactive boundary-layer model [1] coupled with a homogenized model for flow through thin porous surfaces [2], we compute the laminar boundary layer over a thin porous airfoil. This base flow is then subjected to two-dimensional linear instability analysis combined with the e^N method to identify the transition to turbulence. Due to the intrinsically non-parallel nature of these boundary layers, particularly on the suction side of the airfoils, the parabolized stability equations (PSE) are employed as a weakly nonparallel tool [3]. The results are compared with those obtained from a multiple-scale (WKBJ) model and locally parallel analysis, i.e., solutions of the Orr–Sommerfeld equation.
Subsequently, we discuss the dual effect of porosity on boundary-layer instability and the conditions under which permeability either stabilizes or destabilizes the flow. We demonstrate that, on one hand, permeability stabilizes the boundary layer by suppressing flow separation through regulation of the adverse pressure gradient. On the other hand, it can destabilize the boundary layer, as seepage velocity on the suction side of the airfoil tends to thicken the boundary layer.

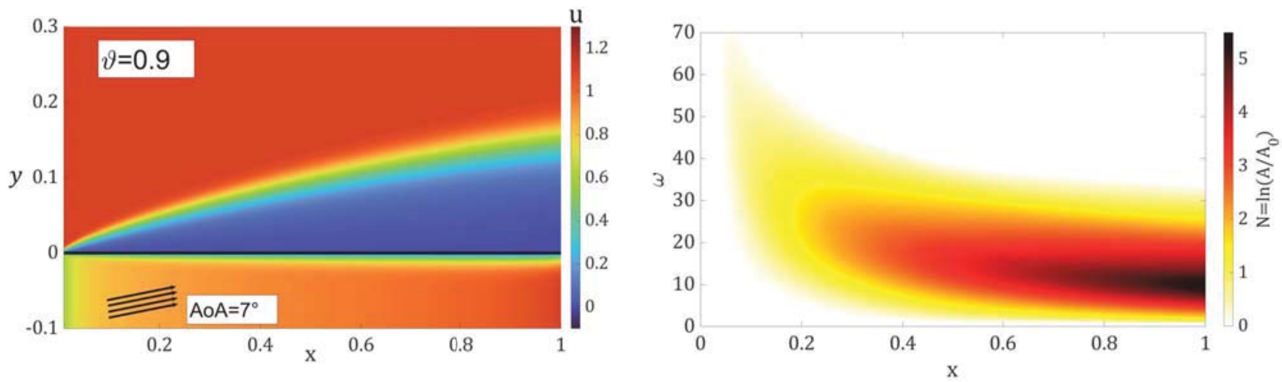

Figure 1. Flow field around a thin porous airfoil with a porosity (void space ratio) of 0.9 and an angle of attack of 7° and a Reynolds number of 5000, obtained by the interactive boundary layer model (left panel). Corresponding amplification contour for boundary layer on the suction side of the airfoil, obtained by parabolized stability equation (right panel).

References

[1] P.Y. Lagrée, *Interactive boundary layer (IBL)*, In Asymptotic methods in fluid mechanics: survey and recent advances. Vienna: Springer Vienna. 247–286 (2010).
[2] G. A. Zampogna & F. Gallaire, *Effective stress jump across membranes*, Journal of Fluid Mechanics. **892**, A9 (2020).
[3] T. Herbert, *Parabolized stability equations*, Annual Review of Fluid Mechanics. **29(1)**, 245–283 (1997).

FINITE-AMPLITUDE BISTABILITY AND BIFURCATION TOPOLOGY IN TRANSONIC BUFFET

Giulio Soldati[1], Hang Song[2], Alessandro Ceci[3], Sergio Pirozzoli[1] & Sanjiva Lele[2]
[1]*Sapienza Università di Roma, Dipartimento di Ingegneria Meccanica e Aerospaziale, Roma, Italy*
[2]*Center for Turbulence Research, Stanford University, Stanford, CA, USA*
[3]*Gran Sasso Science Institute, Mathematics, L'Aquila, Italy*

Keywords: Transonic Buffet, Bistability, Hysteresis, Hopf Bifurcation, Finite-Amplitude Stability.

Abstract

This work investigates the non-linear stability characteristics of turbulent transonic buffet on a V2C supercritical airfoil. We perform Unsteady Reynolds-Averaged Navier–Stokes (URANS) simulations using the Spalart-Allmaras turbulence model – validated against DNS data – at Mach number 0.7 and Reynolds numbers of 300,000 and 3 million. While transonic buffet is often modeled as a global supercritical Hopf bifurcation [1], our results suggest a richer bifurcation structure. By performing quasi-steady pitch-up and pitch-down manœuvres at three different values of pitch rate, we identify a distinct hysteresis loop in the onset and extinction of shock oscillations, as shown in Fig. 1. To disentangle dynamic lag effects from genuine topological features, we perform numerous additional simulations at a fixed angle of attack, initialized from both the stable branch (pitch-up) and the fully-developed limit-cycle branch (pitch-down). We reveal a narrow range of angles of attack near the critical onset where two distinct attractors coexist, namely a steady flow solution and a high-amplitude limit cycle. The robustness of the steady solution within this bistable region is probed via both impulsive perturbations and low-amplitude broadband forcing. We demonstrate that the steady state exhibits finite-amplitude stability, transitioning to the limit cycle when disturbances exceed a specific threshold. This dependence on perturbation amplitude implies a bifurcation topology more complex than the standard supercritical model, likely involving subcritical characteristics or a fold of cycles. We discuss the implications of reconciling these finite-amplitude bistability results with linear global modes for improved buffet prediction.

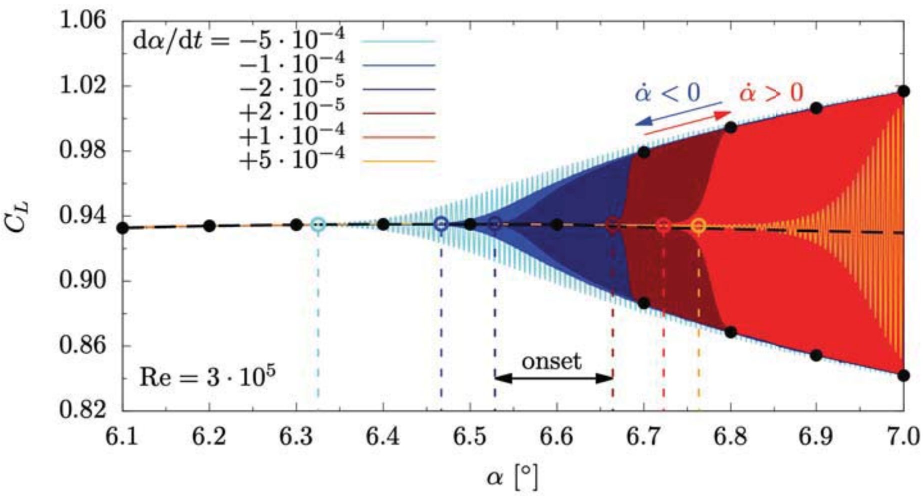

Figure 1. Hysteresis loops of the lift coefficient (C_L) versus angle of attack (α) obtained from quasi-steady pitch-up and pitch-down manoeuvres. Different colours correspond to different non-dimensional pitch rates (° u_0/c, where c is the chord length and u_0 the freestream velocity), as shown in the legend.

References

[1] Crouch, J. D., Ahrabi, B. R., & Kamenetskiy, D. S. (2024). Weakly nonlinear behaviour of transonic buffet on airfoils. *Journal of Fluid Mechanics*, *999*, A8.

STABILITY OF LAMINAR BOUNDARY LAYERS OVER FLAT PLATES WITH SPANWISE-PERIODIC SURFACE MODULATIONS

S. Camarri[1], L. Siconolfi[1], A. Innocenti[1] & J. H. M. Fransson[2]
[1]*Dipartimento di Ingegneria Civile e Industriale, Università di Pisa, I-56122 Pisa, Italy*
[2]*FLOW Dept. Engineering Mechanics, KTH Royal Institute of Technology, Stockholm, Sweden*

Abstract Boundary-layer stability; Tollmien–Schlichting waves; curvature effects; passive transition control.

Spanwise-periodic surface modulations represent a possible approach to passive control of boundary-layer transition and can be regarded as a distributed analogue of discrete roughness elements previously explored in the literature (see for instance [1, 2]). In this context, we investigate the stability of laminar boundary layers developing over a nominally flat plate whose surface is sinusoidally corrugated in the spanwise direction, with an amplitude that grows in the downstream direction proportionally to the Blasius boundary-layer thickness. The steady base flow is computed by combining detailed Navier-Stokes simulations with a dedicated three-dimensional boundary-layer solver, which allows the velocity field to be simulated over a sufficiently long portion of the plate for transition prediction. Local spatial stability analyses are then performed at selected streamwise stations to determine spatial growth rates and construct the corresponding stability maps; for representative cases, the transition point is finally estimated through the e^N method.

The results show that the wavy surface produces competing effects on Tollmien-Schlichting (TS) waves. In particular, within the range of geometric parameters explored, the critical Reynolds number increases, suggesting a stabilising influence close to the lower branch of the stability curve, while larger growth rates are observed further downstream, ultimately leading to an earlier transition with respect to the Blasius boundary layer. This is illustrated in Fig. 1, which reports a representative spatial stability map (left) showing an increase of the critical Reynolds number, and a representative N-factor envelope (right) highlighting an earlier transition for a controlled configuration. This apparently contradictory behaviour

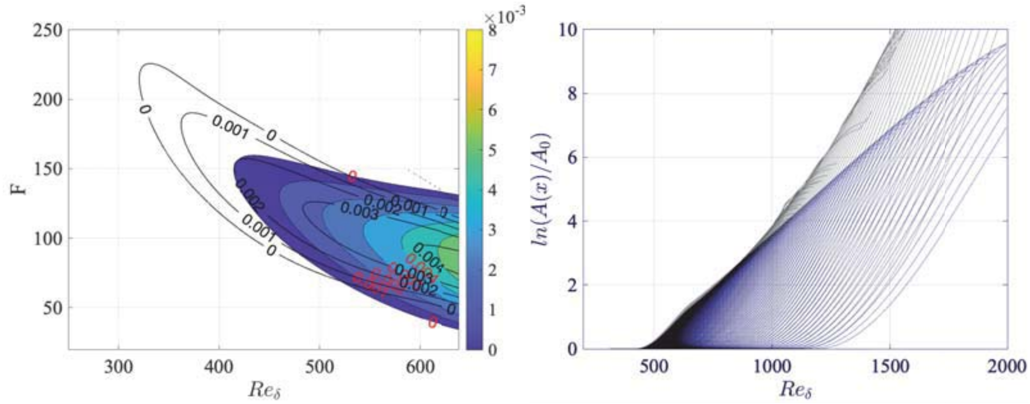

Figure 1. Representative examples of a spatial stability map (left; the colour map refers to a controlled case and black isolines to the Blasius case) and of an N-factor envelope (right; the blue envelope refers to the Blasius case and the black envelope to a controlled configuration).

is traced back to the inflectional streamwise-velocity profiles developing in the valleys of the corrugation due to curvature effects. The regions characterised by inflectional velocity profiles provide a local destabilising mechanism whose impact strengthens as the modulation amplitude increases downstream.

The present contribution discusses these results, highlighting the physical mechanisms governing the evolution of Tollmien-Schlichting waves in the configurations considered and providing quantitative indications relevant to the design of passive transition-control devices. Finally, a framework for the optimisation of the wall shape aimed at minimising the global amplification of TS waves, inspired by [3], is concisely illustrated and may serve as a basis for future investigations.

References

[1] S. Shahinfar, S. S. Sattarzadeh, J. H. M. Fransson & A. Talamelli, *Revival of classical vortex generators now for transition delay*, Phys. Rev. Lett. **109**, 074501 (2012).
[2] R. S. Downs & J. H. M. Fransson, *Tollmien–Schlichting wave growth over spanwise-periodic surface patterns*, J. Fluid Mech. **754**, 39-74 (2014).
[3] F. Viola, E. Pezzica, G. V. Iungo, F. Gallaire & S. Camarri, *Flow control of weakly non-parallel flows: application to trailing vortices*, J. Fluid Mech. **822**, 342-363 (2017).

FLOW STABILITY IN HELICAL PIPES

Riccardo Casali[1], Isa Mammadli[1], Valerio Lupi[2] & Philipp Schlatter[1]
[1] *Institute of Fluid Mechanics (LSTM), Friedrich–Alexander–Universität Erlangen–Nürnberg, Germany*
[2] *Gran Sasso Science Institute (GSSI), L'Aquila, Italy*

Abstract linear stability analysis, transition, helical pipes

Stability, transition, and turbulence are well-studied topics in pipe flows, going back to the seminal studies by Osborne Reynolds (1883). However, for straight pipes, only recently has a fairly complete picture emerged [1], highlighting the subcritical nature of transition to turbulence. Concerning bent pipes, Lupi et al. [2] could show that even (very) low curvatures lead to a modal instability, with a well-defined critical Reynolds number Re_c. Modal stability of helical pipe flows has only been considered in the study by Gelfgat [3]. However, no subcritical routes to turbulence were discussed, and flow structures at transition have not yet been documented.

Given the limited available data for helically bent pipes, also regarding the turbulent regime, we initiated the current research, including a detailed analysis of the laminar flow (see [4] for the corresponding toroidal flows), linear modal and non-modal stability, and turbulent flows. A helical pipe is characterised by two non-dimensional geometrical parameters, *i.e.* curvature $\varepsilon = R_c R_p/(R_c^2 + p_s^2)$ and torsion $\tau = p_s R_p/(R_c^2 + p_s^2)$, where R_p, R_c, and p_s are the pipe radius, the curvature radius, and the pitch, respectively. The torsion-to-curvature ratio $\lambda = \tau/\varepsilon$ is commonly defined. The flow is further characterised by the mass-flow-based bulk Reynolds number $Re = 2U_b R_p/\nu$.

Our study uses two numerical methods. Stability calculations are performed using a newly implemented 2D solver for both the non-linear, steady base flow and the linear disturbances, formulated in orthogonal helical coordinates [6]. The fully spectral Fourier–Chebyshev discretisation is described in detail by Lupi et al. [2]. The tracking of the eigenvalues along the neutral curve is achieved using a pseudo–arclength continuation algorithm [5]. A volume force $\mathbf{f}$ is applied in the streamwise/axial direction ($\mathbf{e}_s$) to drive the base flow, $\mathbf{f} = F/h_s \mathbf{e}_s$. The resolution is dynamically adjusted according to the local residuals. In this way, we significantly improve the accuracy of the neutral curves compared to [3].

Nonlinear simulations are performed using the spectral-element method [7], including a validation of the 2D base flow against a setup with inflow–outflow boundary conditions. The errors are of the same order of magnitude as the solver tolerances. Based on these base flows, we compute the critical Re for various geometrical parameters (see Fig. 1). The comparison with the results by Gelfgat [3] is, in general, good. However, our method shows more accurate data in critical places. A detailed analysis of the modal instabilities, including mode shapes and non-linear saturated states, is also performed. We will further study, for the first time, also non-linear saturation and eventual transition to turbulence in helical flows. Similarly, the importance of transient amplification and potential subcritical transition will be studied using our combination of linear and nonlinear methods.

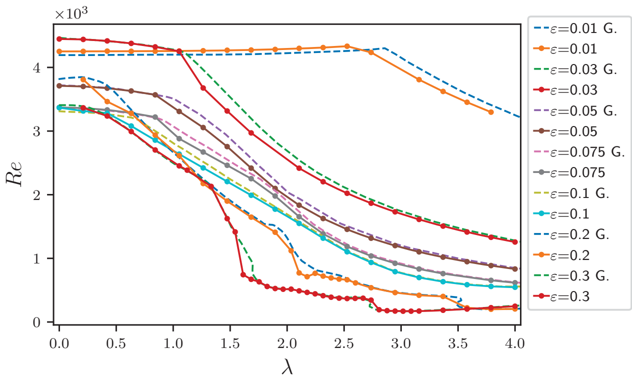

Figure 1. Critical Reynolds number for linear stability in helical pipe flow (filled circles) compared to literature results by Gelfgat [3] (G). Different curvatures ε and torsion-to-curvature ratios λ are considered.

References

[1] M. Avila, D. Barkley & B. Hof, *Transition to turbulence in pipe flow*, Annu. Rev. Fluid Mech. **55**, 575–602 (2023).
[2] V. Lupi, J. Canton, E. Rinaldi, R. Örlü, & P. Schlatter, *Modal stability analysis of toroidal pipe flow approaching zero curvature*, J. Fluid Mech. **987**, A40 (2024).
[3] A. Gelfgat, *Instability of steady flows in helical pipes*, Phys. Rev. Fluids **5** (10), 103904 (2020).
[4] J. Canton, R. Örlü & P. Schlatter, *Characterisation of the steady, laminar incompressible flow in toroidal pipes covering the entire curvature range*, Int. J. Heat Fluid Flow **66**, 95–107 (2017).
[5] R. Casali, *Laminar flow and linear stability in helical pipes*, MSc thesis, Università di Bologna (2025).
[6] M. Germano, *On the effect of torsion on a helical pipe flow*, J. Fluid Mech. **125**, 1–8 (1982).
[7] N. Jansson, M. Karp, A. Podobas, S. Markidis, and P. Schlatter, *Neko: A modern, portable, and scalable framework for high-fidelity computational fluid dynamics*, Computer & Fluids **275**, 106243 (2024).

MULTISTABLITY AND QUANTISATION IN TRIADIC RESONANCES OF INTERNAL WAVE MODES

Ilias Sibgatullin[1], Julie Deleuze[21] & Sylvain Joubaud[1]
[1]*Laboratoire de Physique (UMR CNRS 5672), École normale supérieure de Lyon, 46, allée d'Italie, Lyon, France*
[2]*Institut de Recherche sur les Phénomènes Hors Équilibre IRPHE – UMR7342, 49, rue Frédéric Joliot-Curie BP146 13384 Marseille Cedex 13, France*

Keywords: internal waves, inertial waves

Abstract

Internal and inertial waves can show unique behaviour that challenges conventional modal descriptions. In typical closed hydrodynamical systems, the dynamics are often described in terms of global modes - solutions that satisfy boundary conditions and oscillate harmonically in time, such as Fourier modes in rectangular domains. However, internal and inertial waves defy this framework.
These waves preserve a constant angle with respect to gravity (for internal waves) or the rotation axis (for inertial waves) upon reflection at boundaries. This constraint leads to striking consequences for both their linear and nonlinear dynamics. In stratified or rotating fluids, wave beams tend to focus and form persistent patterns known as wave attractors, rather than standing global modes. Such wave attractors may dominate energy pathways, particularly in complex geometries with pronounced slopes to the anisotropy direction.
The dynamical impact of internal and inertial waves is far from negligible: they are capable of transporting significant kinetic energy over vast distances in the ocean interior. In the deep ocean, their vertical amplitudes can reach several hundred metres, underscoring their crucial role in large-scale oceanic processes. Rectangular tanks aligned with gravity and/or rotation therefore represent an exceptional, yet highly important, case.
Our work focuses on two aspects of internal wave dynamics in this context. First, we investigate the influence of the aspect ratio on the transition to turbulence and mixing for structurally stable wave attractors. Second, we examine the interplay between wave-attractor regimes and modal structures in the vicinity of rectangular geometries. Surprisingly, a conventional rectangular geometry may exhibit much more complex regimes with multistability, than those observed for simple wave attractors. We demonstrate competition between different triadic instability pairs, leading to multistability and a nearly uniform picket-fence spectrum, which is markedly different from the spectrum resulting from cascades of triadic instabilities driven by large-aspect-ratio wave attractors.

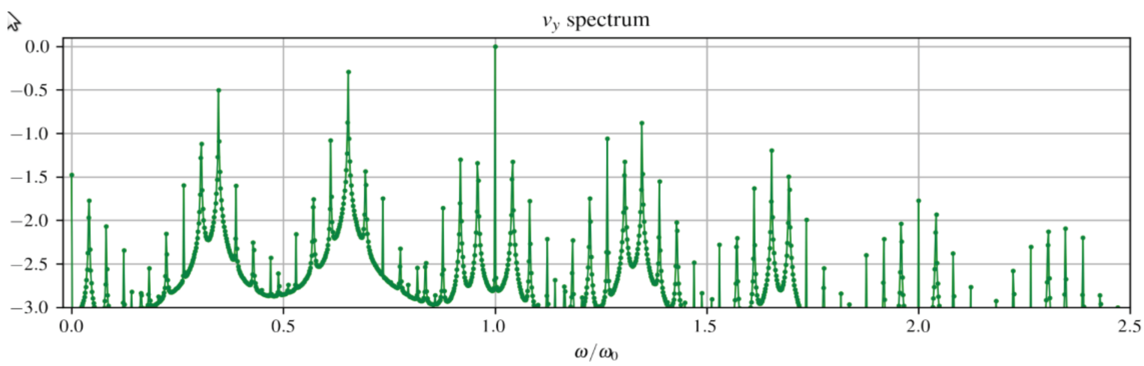

Figure 1. Picket-fence spectrum of the vertical velocity

References

[1] 8. J. Deleuze, I. Sibgatullin, P. Odier, and S. Joubaud, "Triadic instabilities of internal wave standing modes," Phys. Rev. Fluids, vol. 10, pp. 124803, 2025. doi: 10.1103/2pvv-wkc4.

BIFURCATIONS IN RAPIDLY ROTATING SPHERICAL SHELL CONVECTION

Fred Feudel[1], Juan Cruz Gonzalez Sembla[2] & Mathis Flouquet[2] & Laurette S. Tuckerman[2]
[1] *Institut für Physik und Astronomie, Universität Potsdam, 14476 Potsdam, Germany*
[2]*PMMH, CNRS, ESPCI Paris, Université PSL, Sorbonne Université, Université de Paris, 75005 Paris, France*

Abstract Bifurcations, convection in spherical shells, low Ekman numbers, continuation techniques.

We study rotating spherical shell convection in the incompressible Boussinesq approximation by heating the inner sphere under the action of an externally applied central force field. This configuration serves as a model for various geophysical applications, notably convection in the outer cores of earth-like planets. For an electrically conducting fluid, this model is also of interest for dynamo theory. The question there is which of the convective flows has the ability to generate and to maintain a magnetic field, i.e. the dynamo effect.

Due to the spherical geometry, the velocity and temperature fields are expanded in spherical harmonics with respect to the longitude and latitude, and in Chebyshev polynomials along the radial direction. In order to study the flow and temperature after onset of convection, numerical bifurcation techniques have been developed in order to compute both stable and unstable solution branches depending on the Rayleigh, Prandtl and Ekman numbers and the aspect ratio. Special attention has been devoted to computing bifurcation diagrams for Ekman numbers lower than $\mathrm{Ek} = 10^{-5}$. The dominant Coriolis is treated implicitly in a timestepping code. This timestepping solver forms in turn the core of an associated pathfollowing code which can be used to compute rotating wave (RW) branches via Newton method; details are given in [1].

An example of a bifurcation diagram computed at Ekman number, $\mathrm{Ek} = 10^{-5}$, Prandl number, $\mathrm{Pr} = 1$, and for an earth-like radius aspect ratio of $\eta = 0.35$ with the Rayleigh number as bifurcation parameter is presented in Fig. 1. The first primary bifurcation breaks the longitudinal rotational symmetry, leading to a RW with a cyclic symmetry Z_{15}. The left panel in the figure shows the amplitude $\sqrt{E_{\mathrm{kin}}}$ of this and the subsequent unstable primary RW branches, which are stabilised by secondary bifurcations. The stars in the figure mark the results of long-term simulations illustrating the good agreement between simulations and the Newton method. On the right panel are drawn the critical Rayleigh numbers as a function of azimuthal wavenumber m. The minimum of the parabola is at $(m_c, Ra_c) = (15.35, 105.65)$, but the possible wavenumbers are required to be integers. The prediction and computation of secondary bifurcations in the form of modulated rotating waves (MRWs) and and their relationship to the Eckhaus scenario [2] is in progress.

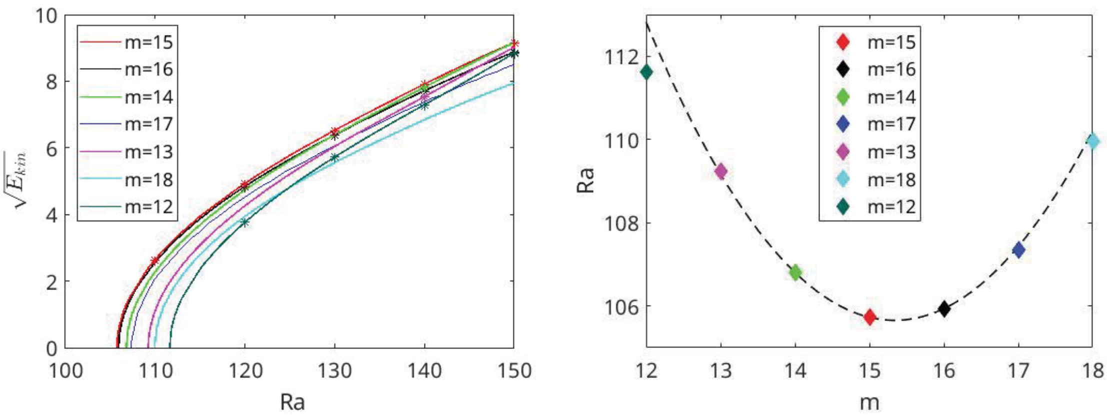

Figure 1. Left: bifurcating RWs with cyclic symmetry Z_m. Right: Critical Rayleigh numbers of the bifurcating branches as a function of wavenumber m lie almost exactly on the neutral parabolic stability curve.

References

[1] J.C. Gonzalez Sembla, C. Rambert, F. Feudel & L.S. Tuckerman, *Convection in a Rapidly Rotating Spherical Shell: Newton's Method Using Implicit Coriolis Integration*, Mathematics (MDPI) **13**, 2113 (2025).
[2] L.S. Tuckerman & D. Barkley, *Bifurcation analysis of the Eckhaus instability*, Physica D **46**, 57–86 (1990).

WEAKLY NONLINEAR RESOLVENT ANALYSIS IN AN AXISYMMETRIC SUDDEN EXPANSION

T. Salamon[1], E. Boujo[1], Y.-M. Ducimetière[2] and F. Gallaire[1]
[1] *LFMI, EPFL, Route Cantonale 1, 1015, Lausanne, CH*
[2] *Courant Institute of Mathematical Sciences, New York University, New York, NY 10012, USA,*

Abstract Sudden expansion flow, Linear resolvent analysis, Weakly non-linear analysis.

Flows in sudden symmetric planar expansion are known to undergo a symmetry-breaking bifurcation at low Reynolds numbers ($\leq$ 300 for expansion ratios greater than 2), which are well predicted by linear stability analysis[1]. In its axisymmetric counterpart, early experimental studies show a periodic time-breaking bifurcation for Re between 600-1600 for a 1:2 outlet to inlet ratio, prior to the transition to turbulence[2]. More recent work suggests the existence of a low-Re steady symmetry breaking[3]. Classical linear stability analysis, however, seems to fail to capture both of these bifurcations and predicts a critical Re of 3600 for a periodic symmetry-breaking perturbation [4]. Evidence of large transient growth has been brought to light for Re ≤ 1200, showing the sensitivity of this system to experimental noise and imperfections due to its non-normality[5].

In order to reconcile these observations, we propose to investigate the axisymmetric expansion by means of a resolvent analysis. Using the optimal frequency response and forcing for different azimuthal wavenumbers, we derive a weakly-nonlinear equation to predict the saturated state in the presence of external volume or inlet forcing as well as in the presence of geometry imperfection. This provides useful insights on the impact of experimental imperfections in this system, as well as a better physical understanding of its dynamics.

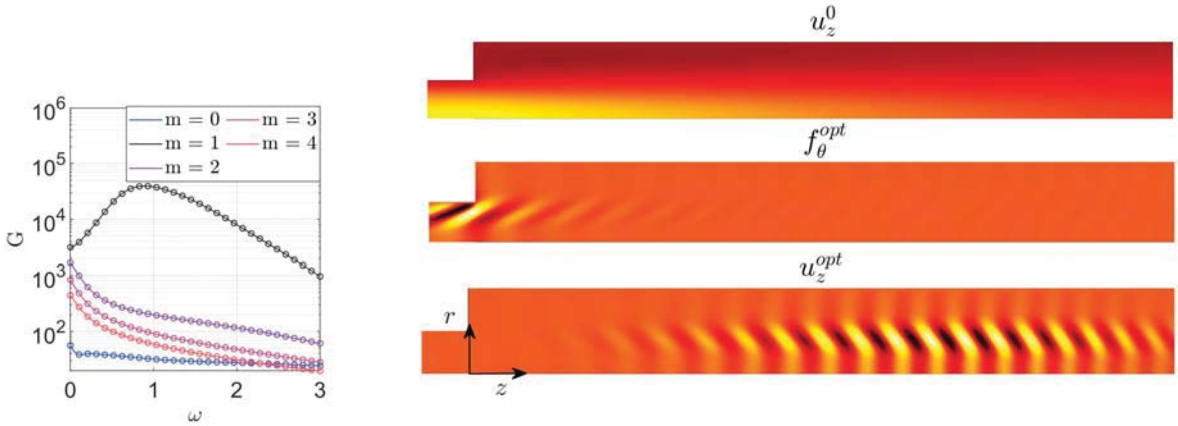

Figure 1. Linear resolvent analysis at $Re = 1200$. a) Harmonic optimal gain for azimuthal numbers $m \in [0, 4]$. b) top: streamwise velocity of the base flow, middle and bottom: azimuthal component of the optimal forcing and response for $\omega = 0.94$, $m = 1$.

References

[1] T. Hawa, and Z. Rusak. Viscous flow in a slightly asymmetric channel with a sudden expansion. *Phys. Fluids*, 12:2257–2267, 2000.
[2] K. R. Sreenivasan, and P. J. Strykowski. An instability associated with a sudden expansion in a pipe flow. *Phys. Fluids*, 26:2766-2768, 1983.
[3] T. Mullin, and J. R. T. Seddon, and M. D. Mantle, and A. J. Sederman. Bifurcation phenomena in the flow through a sudden expansion in a circular pipe. *Phys. Fluids*, 21:014110, 2009.
[4] E. Sanmiguel-Rojas, and C. del Pino, and C. Gutiérrez-Montes. Global mode analysis of a pipe flow through a 1:2 axisymmetric sudden expansion. *Phys. Fluids*, 22:071702, 2010.
[5] C. D. Cantwell, and D. Barkley, and H. M. Blackburn. *Transient growth analysis of flow through a sudden expansion in a circular pipe*. *Phys. Fluids*, 22:034101, 2010.

INFLUENCE OF FREE-SURFACE DEFORMATION ON THE STABILITY OF A FLOW DRIVEN BY A ROTATING DISK

Wen YANG[1], Congle XU[1], Yann FRAIGNEAU[2] & Laurent MARTIN WITKOWSKI[3]
[1] *Sino-European Institute of Aviation Engineering, Civil Aviation University of China, Tianjin 300300, China*
[2] *LISN-CNRS, Université Paris Saclay, F-91400 Orsay, France*
[3] *Universite Claude Bernard Lyon 1, LMFA, UMR5509, CNRS, Ecole Centrale de Lyon, INSA Lyon, 69622 Villeurbanne France*

Abstract Rotating flow, interface, instabilities

Figure 1. Artist view of the experimental setup.

The instabilities arising in a flow driven by a rotating disk located at the bottom of a partially filled, stationary cylindrical cavity are known to be highly sensitive to free-surface contamination [1]. An illustration of the experimental setup is shown in figure 1. The system is governed by at least three dimensionless parameters: (i) the aspect ratio $G = H/R$, where H is the filling height and R the cylinder radius; (ii) the Reynolds number $Re = \Omega R^2/\nu$, where Ω is the angular rotation rate and ν the kinematic viscosity; and (iii) the Froude number $Fr = \Omega^2 R/g$, where g denotes gravitational acceleration.

When water or glycerol–water mixtures are used as working fluids, instability thresholds are significantly shifted—by up to a factor of five in the critical Reynolds number—and modal selection may differ from numerical simulations employing the classical free-slip boundary condition [2]. These discrepancies are observed at low Froude number, where the free surface remains flat and parallel to the rotating disk.

In the present study, we focus primarily on the aspect ratio $G = 0.25$. Experiments were conducted using silicone oil, a fluid known for its low sensitivity to surface contamination. For low Froude numbers, we recover both the critical Reynolds number (~ 3500) and the instability patterns predicted by numerical simulations.

In a second stage, we investigate regimes in which the rotation rate is sufficiently high for centrifugal acceleration to become comparable to gravity (typically $Fr \sim 1$). Under these conditions, the free surface deforms, significantly increasing the complexity of numerical simulations [3]. Two complementary numerical approaches are employed: linear stability analysis (LSA) formulated in body-fitted coordinates, and fully nonlinear simulations using the in-house code *Sunfluidh*, which relies on a level-set method to capture surface deformation. Both approaches predict the same critical Reynolds number (~ 3500) for the transition from axisymmetric to azimuthal modes, in excellent agreement with experimental observations. The transition appears to be nearly independent of the Froude number. However, beyond a threshold value of Fr, discrepancies between simulations and experiments emerge, revealing a regime that is currently under investigation.

References

[1] A. Faugaret, Y. Duguet, Y. Fraigneau & L. Martin Witkowski, *A simple model for arbitrary pollution effects on rotating free-surface flows.* J. Fluid Mech. **935**, A2 (2022).
[2] A. Faugaret, Y. Duguet, Y. Fraigneau & L. Martin Witkowski, *Influence of interface pollution on the linear stability of a rotating fluid.* J. Fluid Mech. **900**, A42 (2020).
[3] W. Yang, I. Delbende, Y. Fraigneau, & L. Martin Witkowski, *Large axisymmetric surface deformation and dewetting in the flow above a rotating disk in a cylindrical tank: Spin-up and permanent regimes.* Phys. Rev. Fluids, **5**, 044801, (2020).

LOW FREQUENCY PHENOMENA IN SHEAR FLOWS: AN EXPERIMENTAL APPROACH

Juan Pimienta[1,2] & Jean-Luc Aider[2]
[1] *Laboratoire PMMH, ESPCI-PSL, CNRS, 7-9 Quai Saint Bernard, Paris, 75005, France.*
[2] *Photon Lines, 10 avenue des Touches, Pacé, 35740, France.*

Abstract Mean-flow descriptions of separated shear flows typically assume that, after a short transient, the dynamics are statistically stationary and dominated by "classical" instability frequencies. Here we show that this assumption can fail at very long (hours) time scales. Using Live Optical Flow Velocimetry (L–OFV) [1, 2] continuous velocity-field measurements are carried out in two canonical separated flows: the backward-facing step (BFS) flow and the wake of a cylinder. Using both local and global observables measured over very long times, ultra-low frequencies (down to $O(10^{-5})$ Hz) could be found.

Fig. 1 shows a 15 hours-long acquisition with an acquisition frequency $f_{ac} = 40$ Hz (2.16×10^6 samples) of two quantities measured in the BFS flow at $Re_h = U_\infty h/\nu = 380$: the space–averaged streamwise velocity $\langle u \rangle_{x,y}(t)$ and a global separation metric, the instantaneous recirculation area $RA(t)$, defined as the area of the region of reverse flow in the measurement plane. The raw signals (blue) are complemented by a rolling mean (red) computed over 1000 samples (25 s), which filters fast fluctuations while preserving slow evolution. Both observables reveal a remarkably long establishment time of approximately 5 hours before reaching a statistically stationary regime before exhibiting persistent slow modulation/drift thereafter. Such measurements, based on very long recordings of quantities derived from 2D instantaneous velocity fields, were made possible by L-OFV [3]. These results imply that mean-flow quantities based on shorter acquisitions may be ill-estimated not only because of sampling variability, but because of nonstationarity on time scales comparable to or exceeding the duration of standard experimental runs. It means that the convergence of mean states and associated uncertainties must account for the low-frequency content only accessible through block statistics over hour-scale acquisitions. Beyond the example of the BFS flow, we will present companion measurements and analysis of the cylinder wake to further characterize these very-low-frequencies and discuss how they couple to the more familiar instability signatures of separated shear flows.

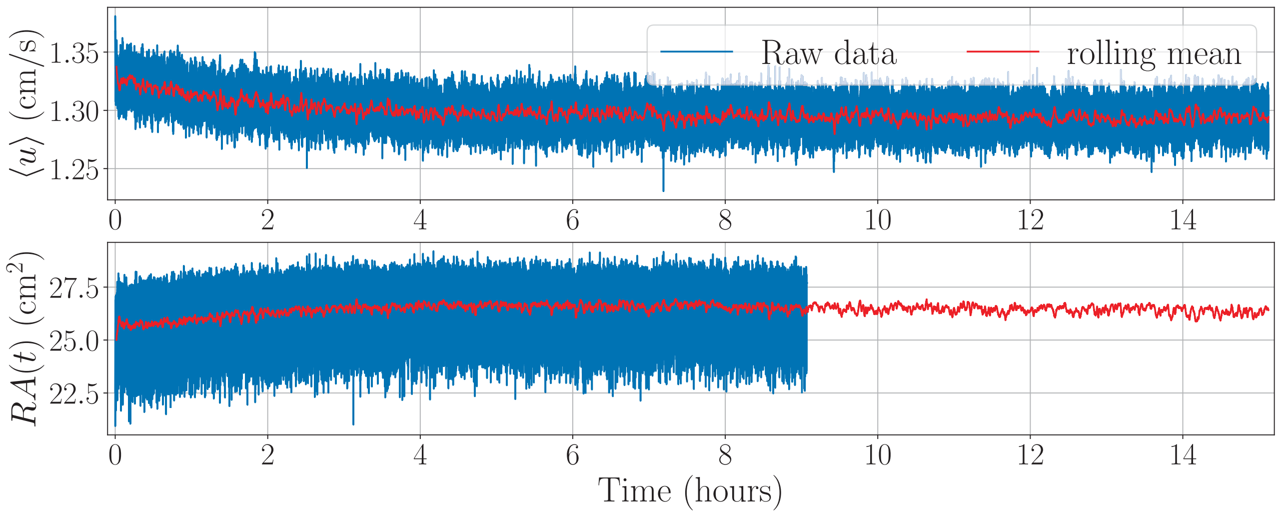

Figure 1. Time series of the space–averaged streamwise velocity component (upper panel) and of the recirculation area of a BFS flow at $Re_h = 380$. These scalars were extracted in real–time with L–OFV for 15 hours with an acquisition frequency $f_{ac} = 40$ Hz. Blue curves represent the raw signal, while red curves represent a rolling mean with 1000 samples of the signal (25 seconds).

References

[1] Nicolas Gautier and JL Aider. "Real-time planar flow velocity measurements using an optical flow algorithm implemented on GPU". In: *Journal of Visualization* 18.2 (2015), pp. 277–286.

[2] Juan Pimienta and J. L. Aider. "Towards High-Speed And High-Resolution Real-Time Optical Flow Particle Image Velocimetry". In: *Proceedings of the International Symposium on the Application of Laser and Imaging Techniques to Fluid Mechanics* (2024).

[3] Juan Pimienta and Jean-Luc Aider. "High Resolution and High-Speed Live Optical Flow Velocimetry". In: *arXiv preprint arXiv:2509.25924* (2025).

NEIMARK–SACKER BIFURCATIONS IN VISCOELASTIC TIME-MODULATED TAYLOR–COUETTE FLOW

Mehdi Riahi[1,2], Mohamed Hayani Choujaa[2], and Said Aniss[2]
[1] *Department of Mechanics, Royal Air School, Marrakech, Morocco*
[2]*Laboratory of Mechanics, B.P 5366, University Hassan II Casablanca, Morocco.*

Abstract Modulated Couette flow, Flow reversal, Boger fluid, First normal stress difference, nonlinear elasticity.

Time-periodically forced systems can lose their stability via three generic ways: a synchronous bifurcation, a period doubling bifurcation or a Neimark–Sacker bifurcation where a pair of complex-conjugate Floquet multipliers cross the unit circle. In the latter case, we are dealing with the occurrence of quasi-periodic states in viscoelastic time-modulated Taylor–Couette flow, one of the generic examples that can exhibit such bifurcations at the onset of the instability. However, for a Newtonian fluid in a Taylor-Couette flow generated by oscillating the inner cylinder in the azimuthal direction with a stationary outer cylinder, Avila et al.[1] showed that this system loses its stability only via synchronous bifurcations. Neither subharmonic nor quasi-periodic solutions were observed. In this study, the focus is on this family of flows, especially when the inner and outer cylinders co-oscillate and the fluid obeys the Oldroyd-B model characterized by a constant kinematic viscosity and a single relaxation time. The linear stability of the basic state is considered when the elastic and inertial mechanisms are of the same order of magnitude corresponding to an elasticity number $E = 1$ defined as a ratio between the elastic effects, measured by the Weseinberg number, and the inertial ones, measured by the Reynolds number. Using Floquet theory, it is shown that the presence of the first normal stress difference in the destabilization mechanism leads to the apparition of new quasi-periodic flows characterized by two incommensurate frequencies. In addition, it turns out that the fluid elasicity significantly alters the flow reversal of the system by completely suppressing the non-reversing instability mode observed in the Newtonian case [1, 2]. The dimensionless linearized equations governing the stability of the system in the narrow gap approximation are retained and it takes the following form:

$$\mathbf{A}^* \frac{d\mathbf{x}^*}{dt^*} = \mathbf{B}^* \mathbf{x}^* \tag{1}$$

where $\mathbf{x}^*$ represents the vector of the unknown physical quantities. The components of the two operators $\mathbf{A}^*$ and $\mathbf{B}^*$ are given in [3]. In Figure (1) the time series of the radial velocity at a fixed point of the geometrical space related to the quasi-periodic state and its corresponding power spectra are shown over 58 oscillation periods. As it can be seen, we are dealing with a quasi-periodic state oscillating with four fundamental frequencies written as linear combinations of ω_s and ω_f denoting respectively the Neimark-Sacker and forcing frequencies. This multiplicity of oscillation frequencies could be attributed to the presence of the subsequent bifurcations that occur very close to the primary instability.

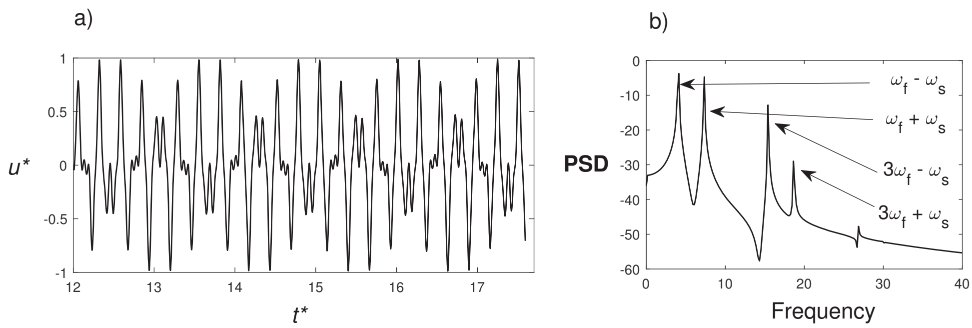

Figure 1. a) Time series of the radial velocity $u^*(t^*)$ for the quasiperiodic instability mode over 58 oscillation period and b) the corresponding power spectra at the first critical onset of instability : $Ta_c = 20.4198$, $q_c = 9.7$ and $\gamma = 4.225778$. Her, the dimensionless quantities Ta_c, q_c and γ represent respectively the critical Taylor number, the critical axial wave number and the frequency number. The radial, azimuthal and axial coordinates are denoted by x, θ and z respectively.

References

[1] M. Avila, M. J. Belisle, J. M. Lopez, F. Marques & W. S. Saric, J. Fluid Mech. 601, 381-406 (2008).
[2] M. Riahi , S. Aniss, and M. Ouazzani Touhami, Phys. Fluids 31, 014101 (2019).
[3] Hayani Choujaa M., Riahi M. and Aniss S., J. of Non-Newtonian fluid Mechanics 325 (2024) 105202.

LINEAR INSTABILITY OF MODULATED TAYLOR–COUETTE FLOW

Harvansh Dandelia[1], Benoît Pier[2], Frédéric Alizard[2] & Vinod Narayanan[1]
[1] *Department of Mechanical Engineering — Indian Institute of Technology Gandhinagar — India.*
[2] *Laboratoire de mécanique des fluides et d'acoustique — CNRS, École centrale de Lyon, Université Claude-Bernard Lyon 1, INSA Lyon — France.*

Abstract Taylor–Couette flow, time-periodic flow, linear instability, Floquet analysis, harmonic–subharmonic bifurcation.

The modulated Taylor–Couette flow takes place in the annular gap between two concentric cylinders, assumed of infinite extent in the axial direction. Inner and outer cylinders rotate about their common axis with two independent rotation rates that are periodically modulated in time. While there exists a significant literature on the time-periodic Taylor–Couette configuration (*e.g.* [1, 2, 3, 4, 5]), many investigations have addressed purely oscillating situations, and the dynamics of the general problem where steady and oscillating flow components cooperate is not yet fully understood.

The radius ratio (η) fixes the geometry and the Womersley number (Wo) characterizes the modulation frequency. Assuming harmonic modulation of the cylinders' rotation rates, the flow dynamics is further governed by four Reynolds numbers accounting for the steady (Re_i^0, Re_o^0) and oscillating (Re_i^1, Re_o^1) velocities of inner and outer cylinders.

The unperturbed base flow is obtained as an exact solution of the Navier–Stokes equations that is temporally periodic and consists of a velocity field purely in the azimuthal direction that only depends on the radial coordinate.

In this study we investigate the dynamics of small-amplitude perturbations, the governing equations are therefore linearized about the base flow, and perturbations are written as spatial normal modes of the form $\mathbf{u}(r,t)\exp \mathrm{i}(\alpha z + \beta\theta)$, where α is a real axial wavenumber and β an integer azimuthal mode number.

Linear instability features such as complex growth rates and Floquet multipliers are computed with two different methods: generalized eigenvalue problems using Floquet theory and direct numerical simulations of the linearized Navier–Stokes equations. Neutral stability boundaries in the multi-dimensional parameter space are obtained with continuation methods.

Our study systematically explores the effects of varying all non-dimensional control parameters. For narrow-gap configurations ($\eta = 0.9$), low Wo and increasing oscillation amplitudes initially show destabilizing effects, and eventually lead to the emergence of multiple neutral curves, demarcated by harmonic and subharmonic instability transitions. At higher Wo, these transitions shift to significantly larger oscillation amplitudes. Wider-gap systems ($\eta = 0.75$ and $\eta = 0.50$) display harmonic–subharmonic bifurcations at even lower values of oscillation amplitude and a wider range of Wo, indicating enhanced sensitivity of the flow to temporal modulation and large curvature effects. Our findings analyse the fine mechanisms of the harmonic–subharmonic bifurcations, provide a comprehensive map of the stability boundaries in modulated Taylor–Couette systems and reveal the critical role of geometry and modulation parameters in shaping the onset of instabilities.

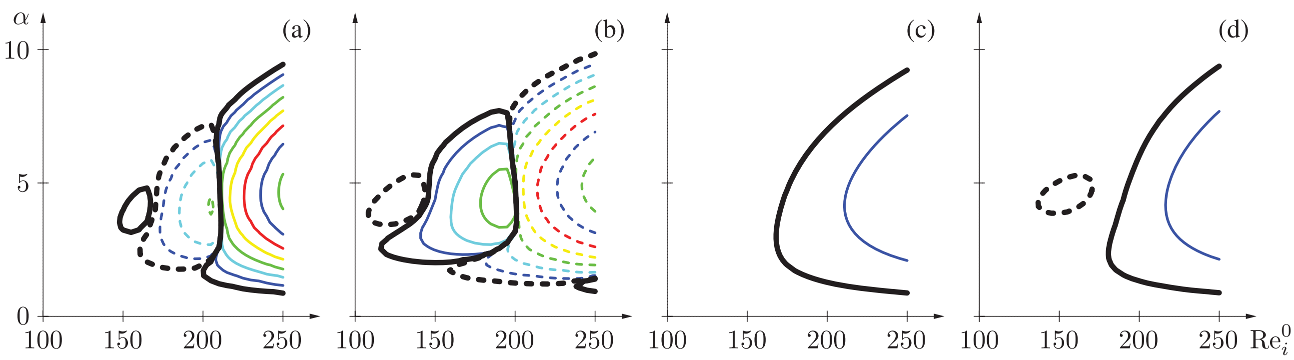

Figure 1. Isolines of Floquet multipliers for $\eta = 0.75$, $\beta = 0$, $\mathrm{Re}_o^0 = 100$, $\mathrm{Re}_o^1 = 0$ and (a) $\mathrm{Re}_i^1 = 60$, Wo $= 2$, (b) $\mathrm{Re}_i^1 = 100$, Wo $= 2$, (c) $\mathrm{Re}_i^1 = 60$, Wo $= 4$, (d) $\mathrm{Re}_i^1 = 100$, Wo $= 4$. Neutral curves ($|\mu| = 1$) in black, unstable regions ($|\mu| = 10$, 10^2, $10^3, \ldots$) in color. Continuous lines indicate harmonic perturbations ($\mu > 0$), dashed lines indicate subharmonic perturbations ($\mu < 0$).

References

[1] Barenghi & Jones, Modulated Taylor–Couette flow, *J. Fluid Mech.* **208**, 127–160 (1989).
[2] Ern & Wesfreid, Flow between time-periodically co-rotating cylinders, *J. Fluid Mech.* **397**, 73–98 (1999).
[3] Lopez & Marques, Modulated Taylor–Couette flow: Onset of spiral modes, *Theoret. Comput. Fluid Dynamics* **16**, 59–69 (2002).
[4] Avila, Belisle, Lopez, Marques & Saric, Mode competition in modulated Taylor–Couette flow, *J. Fluid Mech.* **601**, 381–406 (2008).
[5] Riahi, Choujaa & Aniss, Reversing and non-reversing Taylor vortex flows in modulated Taylor–Couette flow with counter-oscillating cylinders, *Eur. J. Mech. B/Fluids* **95**, 148–159 (2022).

SPONTANEOUS SYMMETRY BREAKING IN A TRIPLE INLET CHANNEL.

T. Salamon[1], R. Debuysschère[2], A. Chafaï[2], B. Scheid[2], F. Gallaire[1].
[1]LFMI, EPFL, Route Cantonale 1, 1015, Lausanne, CH
[2] TIPs lab, ULB, Avenue F.D. Roosevelt, 1050, Bruxelles, BE

Abstract Microfluidic experiment, Linear Stability and Weakly Non-Linear Analysis.

Flows in planar sudden expansions are known to bifurcate spontaneously at a low Reynolds number Re to an asymmetric steady state [1]. Linear stability analysis has proven its capability to accurately predict this critical Reynolds number Re_c, matching experimental data [2, 3]. Kim & al. (2012) [4] took inspiration from the planar sudden expansion by adding two lateral inlets and confinement in the third direction to produce lipid-polymer hybrid nanoparticles of controlled size distribution by injecting polymers in the central inlet and lipids in the lateral ones. We want to investigate this system considering a central inlet with a controlled flow rate Q_c by adding lateral inlets at each side-wall with a controlled flow rate $Q_e/2$ (see fig.1 inset). Fixing the height-to-width ratio $h/W = 0.2$ and the inlet-to-outlet ratio $w/W = 0.1$, we study the influence of the flow rate ratio $\Gamma = Q_e/Q_c$ on the transition threshold Re_c to an asymmetric state, where the Reynolds number $Re = \bar{U}D_h/\nu$ is constructed with the mean flow velocity in the main chamber $\bar{U} = Q_{out}/(hW)$, the hydraulic radius D_h and ν the kinematic viscosity of the fluid. Experimental results using time-averaged measurements show the existence, at low Reynolds number, of a steady bifurcation to an asymmetric case that breaks lateral symmetry. It also shows the disappearance of such a bifurcation in an intermediate region of Γ.

We perform a global stability analysis to get better insights into the flow as well as the nature of bifurcation. The linear stability analysis shows good agreement with the experimental Re_c on a range $\Gamma \in [0, 0.2] \cup [0.9, 3]$. In the intermediate range of $\Gamma \in [0.2, 0.9]$, no evidence of bifurcation is found. To rationalize this behaviour, a weakly nonlinear analysis is performed, confirming stabilisation in this range.

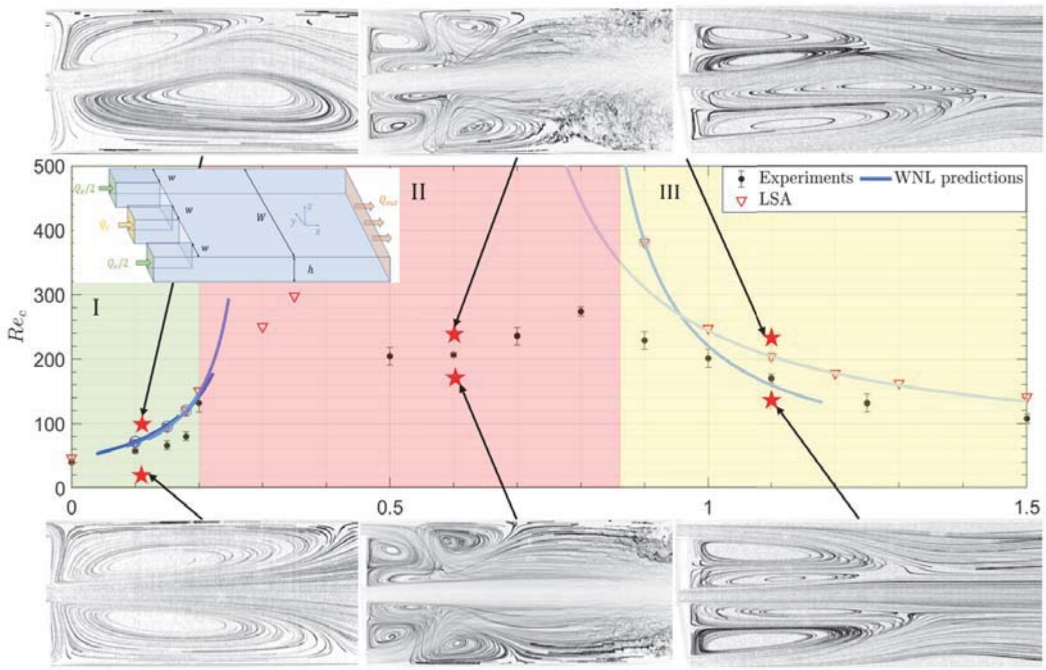

Figure 1. Sketch of the triple inlet channel and critical Reynolds number Re_c as a function of the flow rate ratio Γ. Experimental thresholds are depicted with black filled circles, and the linear stability predicted thresholds (LSA) are in red empty triangles. The weakly nonlinear (WNL) predictions of the neutral curves $Re_c(\Gamma)$ obtained at different nominal (Re_c,Γ_c) are depicted with blue lines. For each region (I-II-III) depicted in green/red/yellow, two experimental images are shown below and above the experimental Re_c.

References

[1] Durst, Pereira & Tropea, *The plane Symmetric sudden-expansion flow at low Reynolds numbers*, JFM **248**, 567–581 (1993).
[2] Battaglia & al., *Bifurcation of Low Reynolds Number Flows in Symmetric Channels*, AIAA Journal **35**, 1533-385X (1997).
[3] Lanzerstorfer & Kuhlmann, *Global Stability of Multiple Solutions in Plane Sudden-Expansion Flow*, JFM **702**, 378–402 (2012).
[4] Kim, & al., *Mass production and size control of lipid–polymer hybrid nanoparticles through controlled micro vortices*, Nano letters **12(7)**, 3587–3591 (2012).

DEPLETION LAYERS, APPARENT SLIP, AND THE POLYMER DIFFUSIVE INSTABILITY

Shruti Pandey[1] & V. Shankar[1]
[1] *Department of Chemical Engineering, Indian Institute of Technology, Kanpur 208016, India.*

Abstract polymer migration, diffusive instability, apparent slip.

The recent discovery of polymer diffusive instability (PDI) [1] in the plane Couette flow of an Oldroyd-B fluid challenges the use of artificial conformation diffusion (ACD) in simulating transitional viscoelastic wall-shear flows. Another study [2] shows that PDI can be eliminated by modifying the conformation boundary conditions imposed in the ACD formulation. The present work focusses on the roles of apparent slip and depletion layers on the PDI using two models: depletion layer model and slip model. The two sets of boundary conditions that are commonly used in the diffusive models are the no-flux of stresses and implying no-diffusion at the boundaries (i.e. apply classical Oldroyd-B stress equations).

The experimental observations [3] and theoretical analysis support the formation of depletion layers adjacent to the rigid boundaries due to the cross-streamline polymer migration into the bulk-fluid. This migration results in the concentration gradients near the boundaries, while concentration being uniform in bulk of the channel. Consequently, the bulk fluid appears to slip along the tube wall, allowing the use of slip boundary conditions in our slip model.

Our numerical results reveal that the depletion layer model suppresses the PDI for no-flux boundary conditions to some extent but destabilizes the flow for the no-diffusion case. Overall, it fails to achieve the complete stabilization for any parameter space considered in this study. The slip model, using no-flux boundary conditions for the dilute polymer solutions, results in the shrinking of the unstable region and shifting towards the lower wavenumbers. Interestingly, at higher polymer concentrations, PDI is completely suppressed with increasing thickness of the depletion layer (l_d), as shown in Fig.1. Conversely, no-diffusion boundary conditions cause the flow to destabilize, irrespective of the polymer concentration. The present work therefore suggests the need for a more detailed modelling to obtain physically consistent results, either in stability calculations or in direct numerical simulations involving polymer stress diffusion.

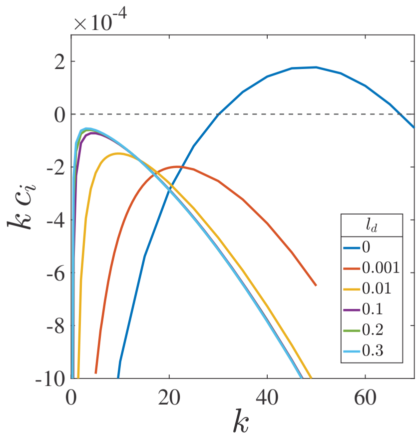

Figure 1. Effect of depletion layer thickness l_d on the growth rate for the slip model using no-flux boundary conditions for $\beta = 0.7$, Wi = 150, $\mathcal{D} = 10^{-5}$. (β is solvent to solution viscosity ratio, Wi is Weissenberg number and $\mathcal{D}$ is dimensionless diffusivity.)

References

[1] M. Beneitez, J. Page, & R. R. Kerswell , *Polymer diffusive instability leading to elastic turbulence in plane couette flow*, Phys. Rev. Fluids **8**, L101901 (2023).
[2] M. Dong & D. Wan, *Asymptotic-analysis-inspired boundary conditions aiming at eliminating polymer diffusive instability*, J. Fluid Mech., 1020 (2025).
[3] D. Ausserre, H. Hervet, & F. Rondelez , *Concentration profile of polymer solutions near a solid wall*, Phys. Rev. Lett. **54**, 1948 (1986).

TRANSITION IN ELASTIC DEAN FLOW: THE CENTRE-MODE VERSUS HOOP-STRESS PATHWAYS

P. S. D. Surya Phani Tej[1], Ganesh Subramanian[2] & V. Shankar[1]
[1] *Department of Chemical Engineering, Indian Institute of Technology, Kanpur-208016, India*
[2] *Engineering Mechanics Unit, Jawaharlal Nehru centre for Advanced Scientific Research, Bangalore - 560064, India*

Abstract We analyse the stability of viscoelastic Dean flow (flow of an elastic fluid through a curved two-dimensional channel, driven by an azimuthal pressure gradient) in the absence of fluid inertia. This configuration is well known to exhibit a hoop-stress-driven 'purely elastic' instability (referred to henceforth as the hoop-stress mode – 'HSM') on account of the base-flow streamline curvature. The objective of this study is to demonstrate the existence and importance of a distinct elastic instability in this flow configuration, which is not driven by hoop-stresses, but instead is a continuation of a novel 'centre-mode' (CM) instability recently identified in rectilinear shear flows. On account of its origins, the CM instability in Dean flow is expected for two-dimensional (azimuthally varying) disturbances with no axial variation, but continues to exist for three-dimensional disturbances. In contrast, the HSM instability is expected primarily in the axisymmetric limit, and again continues to exist for three-dimensional disturbances.

We use both the Oldroyd-B and FENE-P models to map out parameter regimes in the Wi–ϵ–β space where the aforementioned instabilities are present. Here, Wi is a suitably defined Weissenberg number that characterizes fluid elasticity, β is the ratio of solvent to total solution viscosity, and ϵ is the ratio of the gap (channel) width to the radius of curvature. While its origin in rectilinear shearing flows might lead one to expect the CM instability to only be present for small ϵ's (the 'narrow-gap' limit), we show that it exists even for $O(1)$ values of ϵ, and over a larger range of Wi. Nevertheless, within the Oldroyd-B framework, the HSM determines the stability threshold for experimentally relevant gap-width ratios, corresponding to $0.1 \leq \epsilon \leq 1$, with the CM becoming the most unstable mode only for $\epsilon < 0.001$. For the more accurate FENE-P model, however, decreasing the finite extensibility parameter L has opposing effects on the HSM and CM instabilities – stabilising the former, but destabilising the latter. In the dilute solution regime ($\beta > 0.95$), and for realistic values of $L \sim O(100)$, corresponding to polymer molecular weights of $O(10^{5-6})$g/mol, the CM remains the most unstable mode for $\epsilon \leq 0.25$, rendering it potentially relevant to the onset of elastic turbulence in the flow of such polymer solutions through curved channels..

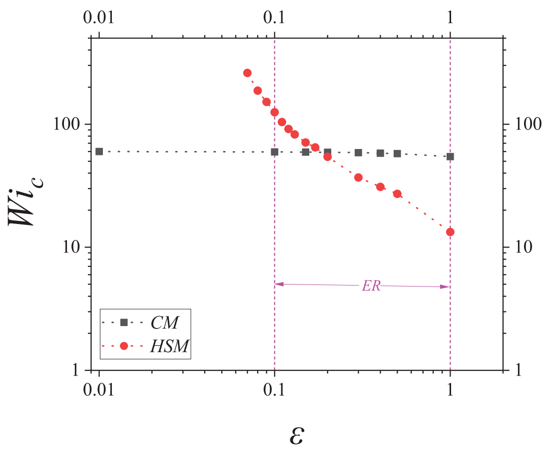

Figure 1. Data showing Wi_c vs ϵ at $\beta = 0.98$, $Re = 0$. The range indicated by 'ER' denotes the ϵ's typically used in experiments.

References

[1] Khalid, M., Shankar, V., & Subramanian, G. (2021). Continuous pathway between the elasto-inertial and elastic turbulent states in viscoelastic channel flow. Physical Review Letters, 127(13), 134502.
[2] Joo, Y. L., & Shaqfeh, E. S. (1992). A purely elastic instability in Dean and Taylor–Dean flow. Physics of Fluids A: Fluid Dynamics, 4(3), 524-543.
[3] Joo, Y. L., & Shaqfeh, E. S. (1991). Viscoelastic Poiseuille flow through a curved channel: A new elastic instability. Physics of Fluids A: Fluid Dynamics, 3(9), 2043-2046.
[4] R. G. Larson, E. S. G. Shaqfeh, and S. J. Muller, "A purely elastic instabilitv in Tavlor-Couette flow," J. Fluid Mech. 218, 573 (1990).

INSTABILITY AND BIFURCATION CHARACTERISTICS OF SLIP CHANNEL FLOW IN THE FLUID-POROUS INTERFACIAL SYSTEM

Ajay Sharma[1, 2] & P. Bera[2]
[1] *Department of Chemical Engineering, Indian Institute of Technology Kanpur, Uttar Pradesh, India-208016*
[2]*Department of Mathematics, Indian Institute of Technology Roorkee, Uttarakhand, India-247667*

Abstract This study examines the linear and weakly non-linear stability analyses to understand the influence of anisotropic slip on the instability and bifurcation characteristics of pressure-driven parallel flow in the fluid overlying a porous medium. The investigation is made by imposing Navier slip on the upper plate which is dominating in the streamwise direction. A cubic-Stuart Landau approach is used to investigate the bifurcation about the critical instability point (CIP) chosen in accordance with the linear stability theory, and as a function of Reynolds number away from the CIP.

Key words: Bifurcation theory; Porous medium; Shear flows

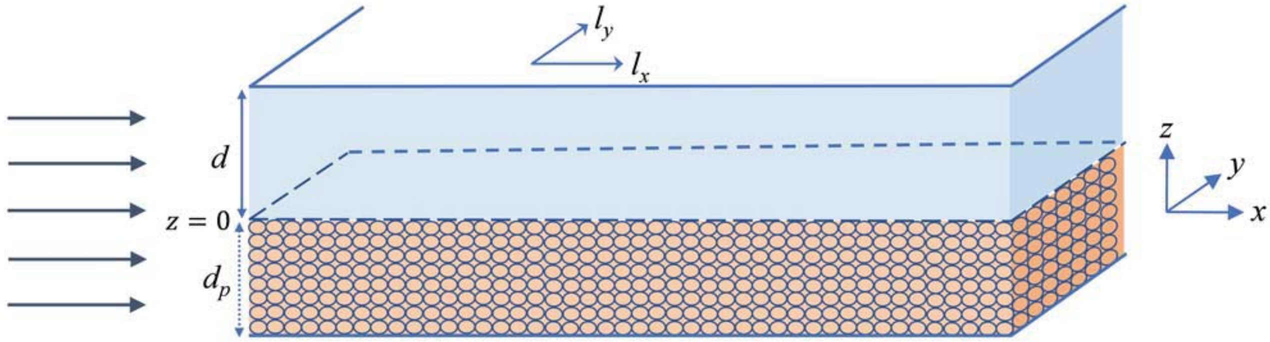

Figure 1. Physical and mathematical description of the flow domain

The system under consideration, as shown in figure 1, consists of pressure-driven flow inside a porous region of depth d_m lying under a fluid region of depth d, which is covered by an anisotropically slippery upper plate. These flows are primarily relevant to microelectronic devices, where the porous medium acts as a thermal conductor, and the slippery channel wall ensures a significant drag reduction and noise attenuation. The governing equations follows from the classical model considered in Aleria, Khan & Bera [1]. The instability and bifurcation characteristics of steady, unidirectional and fully-developed laminar base state are analysed using linear and weakly non-linear stability analyses, respectively.

The linear stability shows that Squire's theorem does not hold for anisotropic slip, and the mode of instability along the neutral curve is sensitive to slip length. The streamwise slip stabilises (destabilises) the porous mode (odd-fluid mode), whereas in the even-fluid mode, the same can play a dual role of stabilization or destabilization. When the porous mode or odd-fluid mode dominates the flow instability, only supercritical bifurcation exists at and away from the CIP. For each value of the depth ratio ($\hat{d} = \frac{d}{d_m}$), there exists a finite interval of slip length where the oblique disturbances are least stable, and the critical mode is even-fluid mode. Both the subcritical and supercritical bifurcations are possible for the even-fluid mode, and the supercritical bifurcation at CIP always shifts to subcritical bifurcation away from the CIP. The non-linear kinetic energy analysis reveals that modifications due to gradient production and viscous dissipation are mainly responsible for inducing the subcritical instability. The role of spanwise slip, Darcy number, and Beavers-Joseph coefficient is also investigated. The results demonstrate a stabilising (destabilising) impact of spanwise slip (Beavers-Joseph coefficient), and instability as well as bifurcation characteristics are function of $\frac{\sqrt{Da}}{\hat{d}}$, rather than individual Darcy number (Da) and depth ratio. Overall, the study finds a significant relationship among the critical modes of instability, dimension of the least stable disturbances and bifurcation phenomena. The present results also witness good experimental support for stability of flow in the fluid overlying a porous medium [2] and slippery flow in a single-fluid layer configuration [3].

References

[1] A. Aleria, A. Khan and P. Bera, *Finite Amplitude Analysis of Poiseuille Flow in Fluid Overlying Porous Domain*, SIAM J. App. Math. **84**, 433–463 (2024).
[2] G. S. Beavers, E. M. Sparrow & R. A. Magnuson, *Experiments on coupled parallel flows in a channel and a bounding porous medium*, J. Basic Engg. **92**, 843–848 (1970).
[3] R. J. Daniello, N. E. Waterhouse & J. P. Rothstein, *Drag reduction in turbulent flows over superhydrophobic surfaces*, Phys. Fluids **21**, 085103 (2009).

MACH-NUMBER SENSITIVITY OF PARTICLE DYNAMICS IN COMPRESSIBLE TURBULENT CHANNEL FLOW

Hamood Ur Rahman[1] & Cristian Marchioli[2]
[1-2]*Dipartimento Politecnico di Ingegneria e Architettura*
Università degli Studi di Udine, Italy

Keywords: Compressible Turbulent Flows, Particle-Laden Flow, Turbophoresis

Abstract

Particle-laden flows are ubiquitous in nature and in engineering applications, such as erosive flows, aerosol transport, and rocket engine exhaust, where gas-solid multiphase flow occurs at supersonic speeds. These types of multiphase flows are wall-bounded exhibiting turbuphoresis, and as a consequence, there is preferential concentration of particles towards the wall.

In this study, direct numerical simulations of a compressible turbulent channel ($4\pi h \times 2h \times 2\pi h$) flows are performed using STREAmS [1] at shear Reynolds numbers $Re_\tau = 215$ and 395, with Mach numbers $Ma = 0.1, 0.5$ and 1.5. Inertial particles with Stokes numbers $St = 1, 5$ and 25 are tracked using a Lagrangian point-particle approach under one-way coupling. Statistics are collected after the flow and particle fields reach statistical stationarity, with particular emphasis on near-wall concentration and slip-velocity dynamics.

From the results, it is established that there is an inverse relationship between the Mach number and the preferential particle concentration at the wall. This is consistent over the range of Stokes numbers under consideration, suggesting that compressibility systematically damps the turbophoritic mechanisms. For a given Mach number, the increasing shear Reynolds number enhances the particle accumulation at the wall, affirming improved turbophoresis with a higher shear Reynolds number. The slip velocity statistics further reveal the compressibility effects. At higher Mach numbers, the maximum streamwise slip increases and spatially shifts towards the channel centre, suggesting a relocation in the point of maximum slip interaction. On the other hand, the maximum wall-normal slip velocity also spatially shifts towards the wall, resulting in higher wall-normal excursions and consequently re-entrainment of particles in the bulk flow. To further deepen understanding of particle dynamics, a quadrant analysis of particle-fluid velocity correlation is performed, quantifying the relative contributions of sweep and ejection phenomena near the wall and how the Mach number affects particle dynamics.

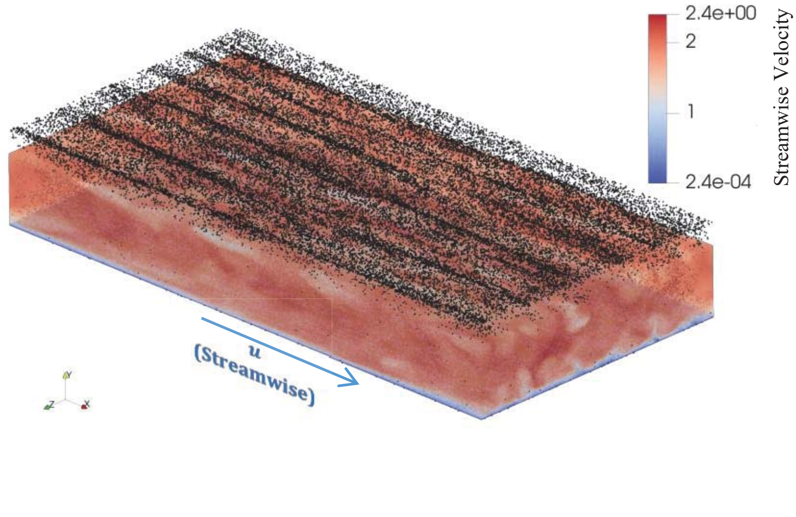

Figure 1. Streaks formation at the wall in particle-laden compressible flow at $Ma = 1.5$

References

[1] Bernardini, M., Modesti, D., Salvadore, F., & Pirozzoli, S. (2021). STREAmS: a high-fidelity accelerated solver for direct numerical simulation of compressible turbulent flows. Computer Physics Communications, 263, 107906.

SMALL-SCALE SECONDARY INSTABILITY OF NONLINEARLY DISTORTED FLOW IN THE PIPE ENTRANCE REGION

Bo Yuan[1], Elena Marensi[1] & Pierre Ricco[1]
[1]*School of Mechanical, Aerospace and Civil Engineering, The University of Sheffield, United Kingdom*

Keywords: secondary instability, mode crossing, temporal-spatial transformation

Abstract

This study investigates small-scale secondary instability of nonlinearly distorted pipe-entrance flows. The nonlinear distortion is induced by a pair of low-frequency vortical modes entrained through the pipe inlet [1]. Relative to this distortion, the secondary instability modes possess high frequency and short wavelengths, allowing them to be formulated as bi-global instability problems. First, we calculate the temporal instability modes by solving linear generalised eigenvalue problems. Figure 1 presents the growth rates of the distorted flow at 26 radii downstream of the inlet. Rather than being dominated by a single continuous mode, the maximal growth rate curve is composed of segments from distinct modes. This suggests that multi-family modes coexist with the "mode crossing" phenomenon. Parametric studies indicate that increasing the Reynolds number and disturbance amplitude both enhances the growth rates and widens the unstable frequency range. Next, we compute the spatial instability modes by solving nonlinear eigenvalue problems. Initial guesses are obtained via a second-order temporal-spatial transformation [2]. Comparisons between the transformed and calculated eigenvalues show strong agreement. Finally, we account for non-parallel effects, arising from the developing base flow and the streamwise variation of the instability modes, using the non-perturbative approach [3] in the secondary instability analysis. The small-scale secondary instability drives the distorted flow toward breakdown. This framework provides accurate initial profiles for subsequent direct numerical simulations (DNS) of disturbed pipe flows.

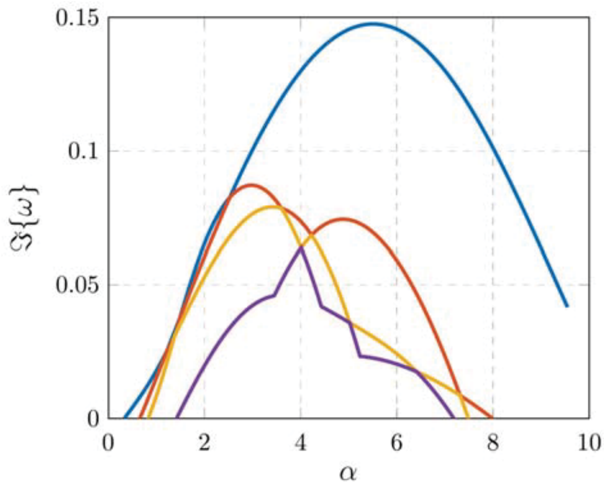

Figure 1. Growth rates of temporal secondary instability for an entrained vortical disturbance at $Re = 2000$ (based on the pipe radius) and amplitude 0.05. Results are calculated at 26 pipe radii downstream of the inlet. The first several modes are plotted and colored according to their growth rate ranking.

References

[1] K. Zhu & P. Ricco, Nonlinear evolution of vortical disturbances entrained in the entrance region of a circular pipe, J. Fluid Mech. 998, A19 (2024).
[2] J. Xu, J. Liu, Z. Zhang & X. Wu, Spatial-temporal transformation for primary and secondary instabilities in weakly non-parallel shear flows, J. Fluid Mech. 959, A21 (2023).
[3] Z. Huang & X. Wu, A non-perturbative approach to spatial instability of weakly non-parallel shear flows, Phys. Fluids, 27(5): 054104 (2015).

OPTIMIZATION OF FLOW COEFFICIENTS IN STABILIZED TURBULENT FLOW PAST A ROTATING CYLINDER FOR FLETTNER ROTOR MARINE APPLICATIONS

Marios E. Mastrokalos[1]& Christos I Papadopoulos[2]
[1]*Merchant Marine Academy of Aspropyrgos, Paralia Aspropyrgou, GR - 193 00 Aspropyrgos Attikis, Greece*
[2]*National Technical University of Athens, School of Naval Architecture and Marine Engineering, 9 Heroon Polytechniou Str., Zografos 15710, Athens, Greece*

Keywords: Flettner Rotor applications, Turbulent Flow, Computational Fluid Dynamics, 2- D and 3-D Flow

Abstract
In 2023, the International Maritime Organization (IMO) Strategy on the Reduction of Greenhouse Gas (GHG) Emissions from Ships set a goal of achieving net zero emissions from ships by 2050. This can be achieved through the adoption of energy-saving technologies such as Wind-Assisted Propulsion Systems (WAPS). The Flettner Rotor (FR) is the most promising WAPS, whose thrust maximization is critical. This strongly depends on the significantly high values of the Lift Coefficient (C_L), caused by the well-known Magnus Effect from cylinder rotation applications, as well as the Drag Coefficient (C_D). For ship applications, the latter coefficients depend on ship velocity, wind velocity, and direction, corresponding to combinations of Reynolds number (Re) and Velocity Ratio (VR) k, where VR is defined as the ratio between the rotor's circumferential speed and the free stream velocity.
FR applications operate effectively for Re values between 5×10^4 and 5×10^6 and VR k values between 1 and 3. C_L is a strongly increasing function of k in this region. Regarding the Reynolds number range, FR operate in the drag crisis region, suggesting that small changes in k significantly affect C_D. On the other hand, for k values below 1, flow is not yet stabilized, whereas for $k > 3$, C_L does not increase further, and the flow becomes destabilized again.
Force coefficients for FR applications are traditionally calculated using the well-known Prandtl relationship, which accounts only for their dependency on k. Recent studies have demonstrated that force coefficients are also strongly influenced by: (a) Reynolds number value, (b) the rotor's Aspect Ratio (AR), defined as the ratio between rotor height (H) and cylinder diameter (D), (c) the addition of end plates of proper diameter (known as Thom Discs), and (d) flow destabilizing effects for k values outside the stabilized regime.
The goal of the present computational study is: (i) first, to define force coefficients as a function of Re and k using 2D calculations, and (ii) second, to incorporate AR effects through 3D calculations, addressing the dependence of force coefficients on AR. Furthermore, for all Reynolds number values considered, the maximum C_L in the stabilized flow region ($k < 3$) will be calculated.
Here, the ANSYS Fluent solver is utilized to solve the non-dimensional Reynolds-Averaged Navier-Stokes (RANS) equations for incompressible Newtonian flow, using the k-ω SST turbulence model. For 2D flow, a mesh of 150,000 finite volumes is used in the x-y plane, with a y^+ value of 1 imposed on the cylinder surface. For 3D flow, 80 elements are used in the span-wise direction for different ARs; a non-dimensional time-step value of 0.01 is applied for all simulations.
Validation of the model is performed by comparing the predicted results with experimental data, where the mean values of the Lift Coefficient, $\langle C_L \rangle$, show excellent agreement.
The results of the present study demonstrate that, for all Reynolds number values considered, the stabilized flow region corresponds to $1.5 < k < 2.5$. The dependence of force coefficients on AR is further analyzed, with AR defined as H/D. The final relationships for the force coefficients are expressed as functions of: (a) Velocity Ratio (k), (b) Reynolds number (Re), and (c) Aspect Ratio (AR = H/D).

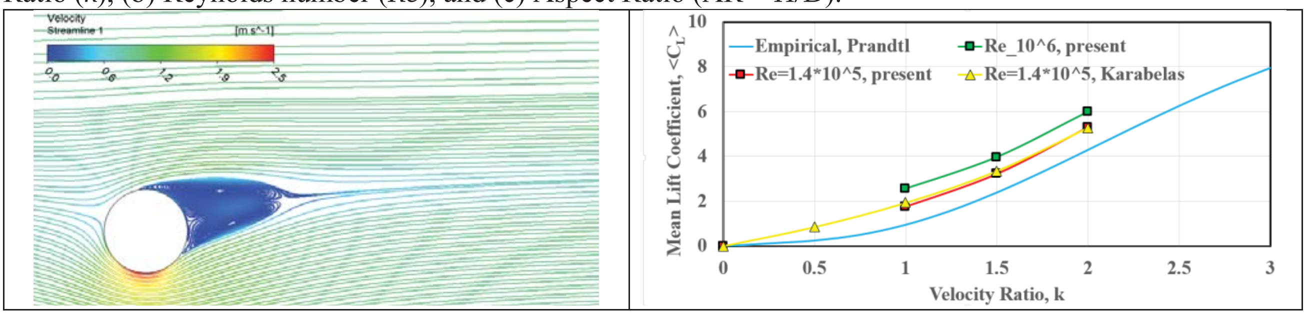

Figure 1. (a) Streamlines for stabilized flow at Re=140000 & k=2 and (b) Lift Coefficient mean value vs. Velocity ratio k

References

[1] S.J. Karabelas, B.C. Koumroglou, C.D. Argyropoulos, N.C. Markatos, High Reynolds number flow past a rotating cylinder, App. Math. Mod. 36, 379–398 (2012).

Instabilities and Flow Control in Living Tissues

Mattia Serra,
University of California San Diego, Department of Physics, California, USA

Keywords: Active Matter, Morphogenesis, Mathematical Modeling, Tissue Flows Control

Abstract

Living Active Matter, such as multicellular tissues in early embryonic development, displays complex tissue flows driven by self-organizing patterns of active forces. I will present a nonlinear continuum model—a system of coupled PDEs for tissue velocity and mechanosensitive myosin—that explains the motion of thousands of cells during early chick embryo development. Linear stability analysis reveals an active-stress instability as the primary driver of tissue flows, confirmed experimentally. Guided by the model, we demonstrate experimental control of tissue flows *in vivo*, generating drastically distinct flow topologies, their associated Lagrangian attractors and repellers, and the overall embryo geometry.

References

[1] Serrano Nájera, Guillermo, Alex M. Plum, Ben Steventon, Cornelis J. Weijer, and Mattia Serra. "Control of tissue flows and embryo geometry in avian gastrulation." *Nature Communications* 16, no. 1 (2025): 5174.

CONFINEMENT DENSITY DRIVES STATE TRANSITIONS IN SCHOOLING FISH

R. Godoy-Diana, B. Lafoux, P. Bernard & B. Thiria
Physique et Mécanique des Milieux Hétérogènes (PMMH), CNRS, ESPCI Paris–Université PSL, Sorbonne Université, Université Paris Cité, F-75005 Paris, France

Abstract We quantify how the behavior of fish swimming in groups is modulated by population density. We observed that fish alternate between two primary locomotor patterns: coordinated unidirectional movement and circular, vortex-like motion. The spatial constraints imposed by available area directly influence the duration of each behavioral state and the frequency of transitions between them.

Keywords: collective dynamics | fish swimming | collective behavior | experiments

We present quantitative insights into the collective dynamics of rummy-nose tetra fish (*Hemigrammus rhodostomus*) under controlled laboratory conditions, focusing on how confinement density—defined as the number of fish per unit tank area—governs a continuous behavioral transition. We demonstrate that increasing confinement induces a bistable regime in which the school alternates stochastically between polarized (aligned) and milling (circular) states, with bout durations and transition statistics directly modulated by density. Our findings reveal that physical boundaries and group size exert similarly influential roles in shaping emergent collective behavior, offering a simplified yet robust framework for understanding how environmental constraints drive complex group dynamics in schooling fish. These results have been published in [1].

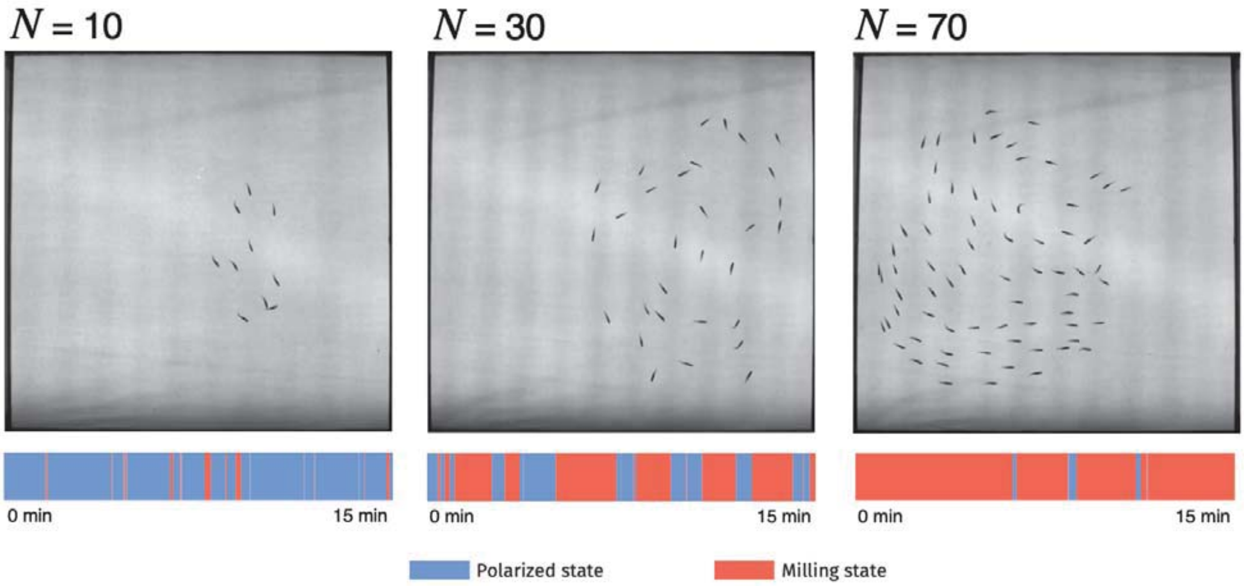

Figure 1. Example of experimental results for $N = 10$, 30, and 70 fish schooling in a square tank of swimming area $S = 1\mathrm{m}^2$. The colored bars below each experimental snapshot represent the statistics of state transitions between milling and polarization over 15 min experiments.

References

[1] B. Lafoux, P. Bernard, B. Thiria, & R. Godoy-Diana, Physical Review E, **110**(3), 034613 (2024). doi: 10.1103/PhysRevE.110.034613

STRUCTURAL ANISOTROPY STABILISES ASYMMETRIC BEATING IN INSTABILITY DRIVEN FILAMENTS

Eric E Keaveny[1], Bethany J Clarke[1] & Yongyun Hwang[2]
[1] *Department of Mathematics, Imperial College London, UK*
[2] *Department of Aeronautics, Imperial College London, UK*

Abstract Cilia dynamics, fluid-structure interactions, Stokes flow, biofluiddynamics, instability, nonlinear dynamics (Key words).
Asymmetries and anisotropies are prevalent in biological systems, including in the structure and dynamics of cilia and eukaryotic flagella used by cells to move surrounding fluids. These microscopic, hair-like appendages possess internal structural anisotropies and exhibit asymmetric beating patterns needed to enable fluid transport at low Reynolds numbers. In this talk, we will study in detail how asymmetry (intrinsic filament curvature) and structural anisotropy (direction-dependent bending-stiffness) affect the dynamics of a filament driven by a compressional follower force, a toy mathematical model for cilia dynamics [1]. Using numerical simulation and bifurcation analysis, we show that the three-dimensional whirling solution that arises for isotropic filaments can be suppressed entirely. In addition, we demonstrate that for bending-stiffness ratios as low as 2, asymmetric beating can be stabilised, highlighting the crucial role of anisotropy in ciliary dynamics.

References

[1] Bethany J Clarke, Yongyun Hwang & Eric E Keaveny, *Structural Anisotropy Stabilises Asymmetric Beating in Instability Driven Filaments*, J. Fluid Mech. **1023**, A24 (2025).

DIMENSIONALITY REDUCTION OF A MULTISTABLE, STOCHASTICALLY DRIVEN ACTIVE FLUID MODEL: A WEAKLY NONLINEAR APPROACH.

Yves-Marie Ducimetière[1] & Michael J. Shelley[1,2]
[1] *Courant Institute of Mathematical Sciences, New York University, New York, NY 10012*
[2] *Center for Computational Biology, Flatiron Institute, Simons Foundation, New York, NY 10010*

Abstract Noise-induced transitions can be efficiently predicted by projecting an active fluid model onto its dominant slow manifold.

This talk will focus on the Saintillan-Shelley model for dilute suspensions of self-propelled, rigid particles in a Stokes flow [1]. In a certain regime, two stable periodic orbits coexist, each corresponding to a distinct collective motion of the particles. Subjecting this model to a weak stochastic forcing thus enables possibly extremely rare noise-induced transitions between these two orbits. We aim to compute the associated mean transition rates and trajectories.
Within the framework of equilibrium statistical mechanics, steady states of the system would minimise a potential, and probability laws could be derived for the mean passage time between distinct attractors. However, the constant injection and dissipation of energy at the particle scale here make the dynamics out-of-equilibrium. No potential then exists, which, together with the very large number of degrees of freedom involved, makes the characterization of rare transition events a challenging task.
The proposed paradigm is as follows: first, we generalize the weakly nonlinear expansion technique used in [1] to reduce the stochastically forced original model to a minimal-order one for the amplitudes along the dominant (slow) manifold, valid in the vicinity of a bifurcation point. The low dimensionality of the reduced system (eight degrees of freedom) then enables mean transition paths and rates to be computed at an extremely low numerical cost with standard techniques from statistical mechanics.
In a second part, a rare event algorithm [2] will be applied to the fully dimensional/fully nonlinear system. An ensemble of trajectories are simulated and subjected to a succession of selections, cloning or killing, and dynamical mutation steps. This permits to generate a very large number of reactive trajectories (i.e., transitioning from one stable state to another) and to compute the associated transition rates. The two approaches are found to be in excellent agreement (fig. 1).

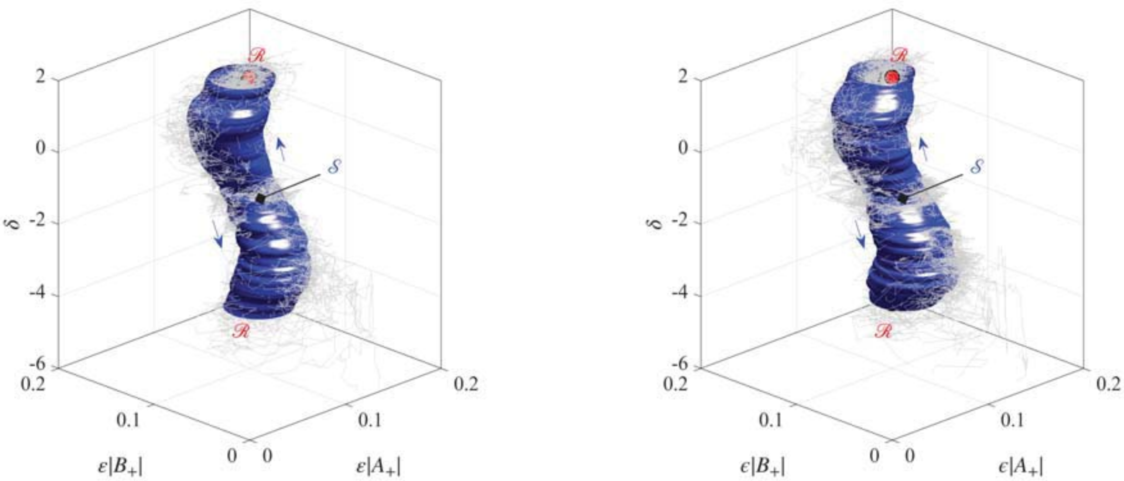

(a) Weakly nonlinear   (b) Fully nonlinear

Figure 1. 80% percentile probability tube of the reactive trajectories from one stable periodic orbit ("$\mathcal{S}$") to the other ("$\mathcal{R}$"), shown in a projected phase space. These trajectories were obtained by using the AMS algorithm with both (a) the fully nonlinear and (b) weakly nonlinear approaches. One hundred of these trajectories are shown as the thin gray lines.

References

[1] L. Ohm & M. J. Shelley, *Weakly nonlinear analysis of pattern formation in active suspensions*, J. Fluid Mech. **942**, A53 (2022).
[2] Bouchet, F. and Rolland, J. and Simonnet, E., *Rare Event Algorithm Links Transitions in Turbulent Flows with Activated Nucleations*, Phys. Rev. Lett. **122**, 074502 (2019).

FLOW INSTABILITIES IN A RECORDER'S MOUTHPIECE

R. Ostilla-Mónico[1], A. Tassawar[1], M. Fosas de Pando[1]
[1]*School of Engineering, University of Cadiz, Cadiz, Spain*

Abstract We analyze the different types of instabilities in a recorder's mouthpiece.

The recorder is one of the simplest woodwind instruments, yet despite its 700-year history, a comprehensive understanding of the interplay between hydrodynamic processes and sound generation at the mouthpiece remains incomplete. This study investigates these mechanisms using simplified simulations and hydrodynamic stability theory. We develop a computational model of the recorder, parameterized by key geometric features of the mouthpiece, specifically focusing on the transverse offset between the mouth channel and the labium. Linear stability analysis is performed to identify the onset of hydrodynamic instabilities, with results validated against fully unsteady flow simulations. Notably, our analysis reveals distinct flow regimes dictated by the labium geometry: we identify parameters that produce stable, steady oscillations, as well as regimes characterized by intermittent behavior. Finally, we discuss how these regime transitions influence instrument design and playability, providing a theoretical framework for optimizing the recorder's acoustic response.

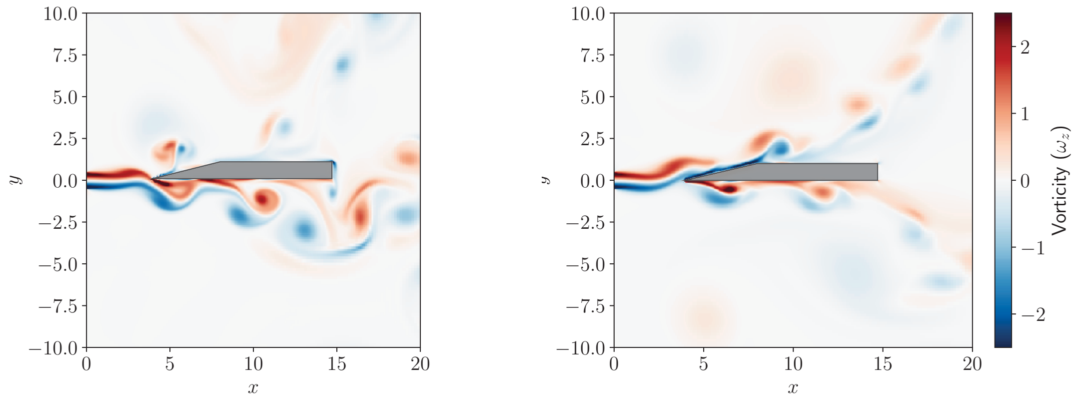

Figure 1. Vorticity for two different offset settings. Left: if the labium is alligned with the top of the channel, the flow is predominantly deflected downwards, generating a force which gives rise to large-scale vortices which cause intermittency. Right: if the labium is slightly shifted, the jet now breaks symmetrically, and no net downforce is generated on the labium.

IMPROVING INFUSION CANNULAS DESIGN FOR SAFER VITREOUS SURGERY WITH REDUCED TRANSPORT AND BIOLOGICAL STRESS

P.G. Ledda[1], T. Rossi[2], M.G. Badas[1] & G. Querzoli[1]
[1]*Department of Civil, Environmental Engineering and Architecture, University of Cagliari, Italy*
[2]*IRCCS Fondazione G.B. Bietti ONLUS, Rome, Italy*

Keywords : pars plana vitrectomy, impinging jet, flow bifurcation, numerical simulation, PIV

Abstract

We present a combined numerical, experimental and biological analysis to assess and improve infusion-driven fluid dynamics in the vitreous chamber during pars plana vitrectomy, with particular focus on the flow bifurcations and the subsequent modified retinal stresses and dye transport during the procedures involving staining. Ophthalmic surgery requires continuous infusion to maintain intraocular pressure. However, the small diameter of infusion cannulas generates high-velocity jets that may directly impinge on the retina, affecting both tissue safety and surgical visibility (Fig. 1a).

We numerically analyse the transient flow within a realistic vitreous chamber geometry over clinically relevant flow rates using the finite-volume solver OpenFOAM. Simulations show that standard cylindrical end-opening cannulas generate a laminar impinging jet, producing high wall stresses and a vortex ring at the retinal impact site. As the Reynolds number increases, the vortex ring destabilises and ejects hairpin vortices that extend toward the anterior chamber, enhancing mixing and dispersing injected substances within the whole chamber (Fig. 1b). Specifically, we identify the transition from an ordered transport, confined to the posterior chamber, to a disordered regime characterised by overall mixing, which is detrimental to visibility and increases surgical time. These flow structures are associated with highly localised retinal pressure peaks, comparable to or exceeding reference physiological thresholds.

Motivated by these findings, a biological analysis on ex vivo pig retinal tissue, exposed to controlled infusion conditions, showed that even short-duration jet impingement induces a measurable molecular response, with upregulation of markers associated with inflammation, oxidative stress, and apoptosis, supporting the biological relevance and potential harmfulness of localised hydrodynamic loads [1].

These results highlighted the need to explore alternative infusion cannula designs to effectively suppress these flow regimes and bifurcations (Fig. 1c). To this end, we developed a scaled-up experimental model of the vitreous chamber. A constant-head reservoir imposes a prescribed flow rate, monitored via a flow meter. Particle image velocimetry measurements, performed on the symmetry plane containing the cannula and jet axis, are first used to faithfully compare the numerical predictions for standard cylindrical cannulas. The same setup is then employed to characterise newly designed infusion cannulas featuring lateral side openings. In this configuration, the impinging jet is suppressed, retinal pressure peaks are effectively eliminated, and dye transport occurs predominantly through surface-parallel sweeping, markedly improving staining efficiency while minimising unwanted dispersion within the vitreous chamber (Fig. 1d). In summary, the modification of the inflow topology emerges as a promising strategy to effectively suppress undesired flow regimes and mitigate retinal stress while improving the safety and controllability of staining procedures in vitreoretinal surgery.

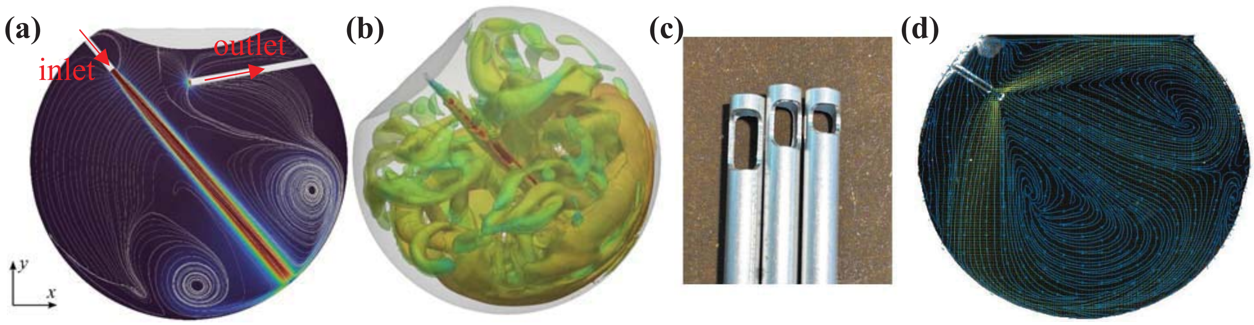

Figure 1. (a) Sketch of the configuration together with the colormaps and streamlines of the ordered jet flow that develops at low flow rate, in the section that contains the jet and cannula axis. (b) Disordered flow within the vitreous chamber at high flow rate, visualized through selected isosurfaces of the Q-Criterion. (c) Experimental design of alternative infusion cannulas. (d) Experimental velocity field, in the same section that contains the jet and cannula axis, for an alternative infusion cannula.

References

[1] T. Rossi, G. Querzoli, P.G. Ledda at al, Is the Laminar Flow From the Vitrectomy Infusion Cannula Potentially Harmful? Trans. Vis. Sci. Tech.14(11):29 (2025).

THE INFLUENCE OF CORNEAL TOPOGRAPHY ON TEAR FILM RUPTURE

Deepak Kumar[1], Subramaniam Pushpavanam[1]
[1] *Indian Institute of Technology Madras, India, 600036*

Abstract We investigate the effect of corneal roughness on tear film dynamics (Tear Film, Human Eye, Floquet Theory, Fourier Spectral).

The instability of tear film is a central cause of dry eye syndrome, a condition that affects millions worldwide. In this work, we analyze tear film rupture over experimentally observed rough corneal structures [1, 2]. A detailed mathematical framework is developed to describe the influence of surface roughness, interfacial slip, van der Waals interactions, and lipid layers at the film-air surface. To predict film rupture, we employ linear stability using Floquet theory alongside non-linear simulations using Fourier spectral method, for physiologically relevant values of slip and roughness. Our findings demonstrate that, unlike a smooth cornea where rupture initiates symmetrically at the centre of the cornea, rough surfaces induce asymmetry shifting the rupture site laterally depending on wall topography and the nature of initial disturbances. Our model provides a mechanistic explanation for the enhanced breakup rate associated with corneal irregularities. The results emphasize that surface roughness have a pronounced influence on both the dynamics and spatiotemporal patterns of rupture. Pathological disruption of mucins often increases slip, thereby lowering viscous resistance and accelerating film thinning which is consistent with earlier studies [3, 4]. Consequently, tear film instability in infected eyes occurs early, where elevated slip coefficients and roughness amplitudes are present. As these factors are explicitly included in our model, the study underscores their importance in understanding dry eye syndrome. Clinically, this suggests that therapeutic approaches should not limit to chemical stabilization of the tear film but should also target restoration of corneal smoothness. Our results reveal that tear film rupture is not solely dictated by evaporation or surfactant effects, but also strongly modulated by interfacial slip and the physical features of corneal surface. Contact lens failure and ocular discomfort are likely linked to incomplete understanding of tear film behaviour under realistic conditions. Our study closes this gap providing a more realistic description of tear film dynamics.

References

[1] Gipson, I.K., Argüeso, P. (2003). Role of mucins in the function of the corneal and conjunctival epithelia. *International Review of Cytology* 231(1): 1–49.
[2] King-Smith, P.E., Kimball, S.H., Nichols, J.J. (2014). Tear film interferometry and corneal surface roughness. *Investigative Ophthalmology & Visual Science* 55(4): 2614–2618.
[3] Zhang, Y.L., Craster, R.V., Matar, O.K. (2003). Surfactant driven flows overlying a hydrophobic epithelium: film rupture in the presence of slip. *Journal of Colloid and Interface Science* 264(1): 160–175.
[4] Dey, M., Vivek, A.S., Dixit, H.N., Richhariya, A., Feng, J.J. (2019). A model of tear-film breakup with continuous mucin concentration and viscosity profiles. *Journal of Fluid Mechanics* 858: 352–376.

VORTICES WRITE THE BLUEPRINT: HOW VORTEX DYNAMICS REVEAL THE EVOLVED DESIGN OF SWIMMING FISH

Rajat Mittal, Jung Hee Seo & Ji Zhou
Mechanical Engineering, Johns Hopkins University, Balitmore, Maryland, USA

Abstract Biolocomotion; Vortex Dynamics; Body-Caudal Fin Swimming.

Body–caudal fin (BCF) propulsion is used by many swimming fish and is increasingly adopted in biorobotic underwater vehicles (BUVs). In this mode, a traveling body wave culminates in large-amplitude caudal-fin oscillations that generate thrust through the formation and shedding of organized vortical structures. This paper develops a vortex-dynamics-centered framework that links swimmer anatomy (morphology), prescribed kinematics, and hydrodynamic performance for a mackerel-inspired carangiform swimmer.

We employ high-fidelity, three-dimensional simulations over a broad range of Reynolds numbers and swimming kinematics (including wide variations in Strouhal number) to quantify how changes in midline motion and caudal-fin actuation affect thrust, power, and energetics. Central to the analysis is a leading-edge vortex (LEV) on the caudal fin. Using force partitioning analysis, the study identifies this LEV as the dominant contributor to caudal-fin thrust. Building on this mechanistic insight, an LEV-based model is derived and used to obtain scaling laws for thrust, power expenditure, Froude efficiency, cost of transport, and swimming speed. These scaling relations are grounded in the physics of vortex formation and are parameterized using the simulation database, enabling direct mapping from measurable kinematic and morphometric quantities to force and energetic outcomes.

The paper also characterizes the wake as an evolving chain of vortical structures whose organization depends strongly on Strouhal number and whose persistence and breakdown are influenced by Reynolds number through dissipation and instability to smaller-scale eddies. Wake descriptors, including wavelength and near-wake spreading angle, are related to the kinematics through Strouhal-number-based relationships, providing a compact description of how body/fin motion imprints on wake geometry. In addition, the analysis highlights key non-dimensional groups, most notably the slip ratio (equivalently the inverse of the wavelength-based Strouhal number), that govern efficiency trends and serve as interpretable links between kinematics and propulsive performance.

Finally, the proposed scaling laws are validated against published simulation and experimental data. The validation supports the LEV-centric interpretation of thrust generation and reveals kinematic and morphometric parameters that significantly influence hydrodynamic performance. Overall, the results show how vortex dynamics—specifically LEV formation on the caudal fin and its downstream wake organization—provides a mechanistic route to interpreting the role of anatomy and kinematics in BCF swimming, with direct implications for performance prediction and bioinspired design.

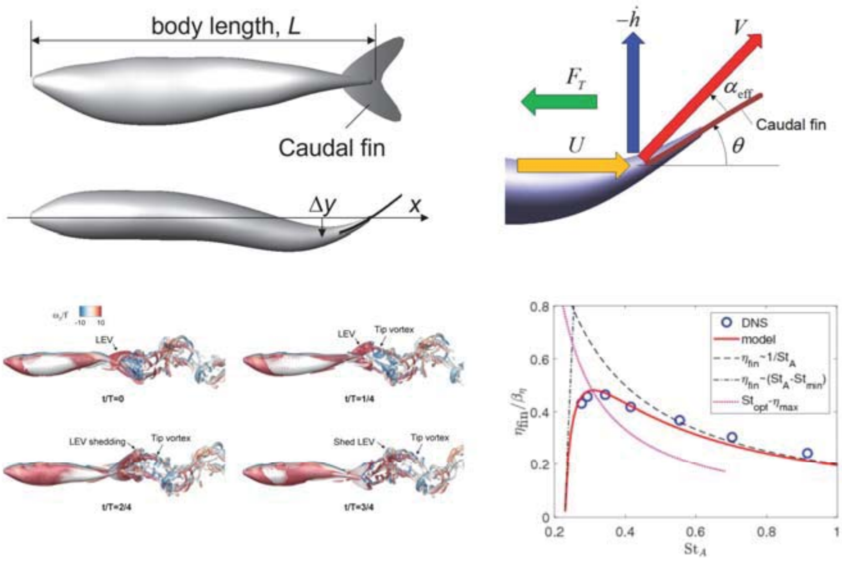

Figure 1. Anatomy and kinematics of a body-caudal fin swimmer along with simulation-based results and scaling laws.

KEY FEATURES OF BATOID LOCOMOTION: A NUMERICAL STUDY

Roberta Santoriello[1], Giovanni Vagnoli[2], Francesco Viola[2], & Vincenzo Citro[1]
[1] *Department of Industrial Engineering (DIIN), University of Salerno, Fisciano 84084, Italy*
[2] *Gran Sasso Science Institute (GSSI), Viale F. Crispi 7, 67100 L'Aquila, Italy*

Abstract biological flows, propulsion, swimming, vortex dynamics, bioinspired design

The different swimming modes of aquatic animals provide a rich resource for bio-inspired and bio-hybrid swimming robots [1]. Among these animals, batoid fishes [2] are particularly attractive for designing fast, efficient, and maneuverable platforms [3] due to their unique disk-shaped bodies with expanded pectoral fins. This anatomical hallmark, ranging from circular to rhomboid geometries, is correlated with their propulsive strategy and ecological niches: rhomboid-shaped oscillators are typically benthopelagic, whereas circular-shaped undulators are primarily benthic [4]. However, the extent to which these morphological variations influence swimming dynamics, in both near-ground and free-stream conditions [5], remains to be fully explored. Furthermore, the influence of kinematic parameters, such as oscillation frequency and tip-to-tip amplitude, on swimming performance still defies a complete understanding.

In this study, we perform large-eddy simulations [6], combined with an immersed boundary method [7], to elucidate the key principles of batoid locomotion. Swimming kinematics are prescribed based on experimental data [8, 9], allowing for a comprehensive characterization of propulsive performance across distinct flow regimes, using kinematic variables, hydrodynamic loads, and energetic metrics. As a representative example, the three-dimensional wake development of a cownose ray model (*Rhinoptera bonasus* [2]), is illustrated in Figure 1. The wake topology features primary vortical structures, including pairs of leading-edge, trailing-edge, and tip vortices that are connected to form a vortex loop [8]. Through a systematic investigation of various species – encompassing different body shapes and swimming strategies [8, 9] in both near-ground and free-stream scenarios – we aim to uncover the key principles governing the swimming dynamics of batoid fishes, offering useful design principles that can guide the development of bio-inspired and bio-hybrid swimming vehicles.

Figure 1. Wake structures around a cownose ray, visualized via isosurfaces of the Q-criterion, colored by vorticity magnitude.

References

[1] X. Li *et al.*, *Magnetic field–enhanced vertical induction of soft actuators for high-performance aquatic robots*, Nat. Commun. **16**, 123–135 (2025).
[2] J. D. McEachran *et al.*, *Batoid fishes*, Living Mar. Resour. West. Cent. Atl. **1**, 507–589 (2002).
[3] H. Qing *et al.*, *Spontaneous snapping-induced jet flows for fast, maneuverable surface and underwater soft flapping swimmer*, Sci. Adv. **10**, eadq4222 (2024).
[4] L. J. Rosenberger, *Pectoral fin locomotion in batoid fishes: undulation versus oscillation*, J. Exp. Biol. **204**, 379–394 (2001).
[5] Y. Zhu *et al.*, *Wavenumber affects the lift of ray-inspired fins near a substrate*, J. R. Soc. Interface **22**, 231 (2025).
[6] F. Nicoud & F. Ducros, *Subgrid-scale stress modelling based on the square of the velocity gradient tensor*, Flow, Turbul. Combust. **62**, 183–200 (1999).
[7] F. Viola *et al.*, *High-fidelity model of the human heart: an immersed boundary implementation*, Phys. Rev. Fluids **8**, 100502 (2023).
[8] D. Zhang *et al.*, *Vortex dynamics and hydrodynamic performance enhancement mechanism in batoid fish oscillatory swimming*, J. Fluid Mech. **930**, A28 (2022).
[9] R. G. Bottom II *et al.*, *Hydrodynamics of swimming in stingrays: numerical simulations and the role of the leading-edge vortex*, J. Fluid Mech. **788**, 407–443 (2016).

WHY JELLYFISH NEED STOPPING VORTICES: HYDRODYNAMIC CONSEQUENCES OF BELL PERFORATION

Eric Segalerba[1], Roberta Santoriello[1], Alexander P. Hoover[2] & Vincenzo Citro[1]
[1]*Department of Industrial Engineering (DIIN), University of Salerno, Fisciano 84084, Italy*
[2]*Department of Mathematics, Cleveland State University, Euclid Avenue, 2121, 44115, Cleveland, Ohio*

Abstract Fluid–structure interaction, Vortex dynamics, Bio-inspired propulsion, Evolutionary morphology
Jellyfish are among the most efficient swimmers [1] in the animal kingdom and have therefore been extensively studied as model organisms for pulse-jet propulsion [2]. Their high efficiency is typically associated with the formation of stopping vortices during the relaxation phase of a pulsation cycle. While these structures are known to facilitate passive energy recapture [3], the extent to which their efficacy depends on the morphological integrity of the bell remains to be fully explored. The central idea of this work is inspired by a recent study [4] which interprets jellyfish morphology as a mechanical balance and explore the functional consequences of structural perturbations to the bell geometry. Building on this perspective, we present a geometric modification to the jellyfish bell that is designed to suppress the formation of stopping vortices in a controlled manner. This approach allows us to investigate how these vortical structures contribute to thrust generation, swimming performance and flow organization. We use three-dimensional immersed boundary numerical simulations [5] to solve the fluid-structure interaction of an oblate jellyfish (Figure 1a) and a family of perforated bell geometries, with increasing central aperture size (Figure 1b), while maintaining identical actuation protocols, material properties and kinematics across all configurations. By isolating geometry as the only control parameter, we can establish a direct link between changes in swimming performance and alterations in vortex dynamics. Our results reveal a monotonic degradation of propulsion efficiency with increasing perforation, with negligible or reversed motion occurring for the largest apertures. This loss of performance is not associated with changes in bell kinematics, but instead arises from a profound reorganization of the surrounding flow field. Specifically, the suppression of stopping vortices weakens vortex coherence, disrupts passive energy recapture and introduces an adverse jet through the aperture that counteracts forward motion. Overall, these findings provide direct evidence that stopping vortices play a central role in medusan swimming. By clarifying their contribution, this study offers a mechanistic explanation for the evolutionary robustness of the intact jellyfish bell and highlights key design principles for bio-inspired and biomimetic swimming vehicles [6].

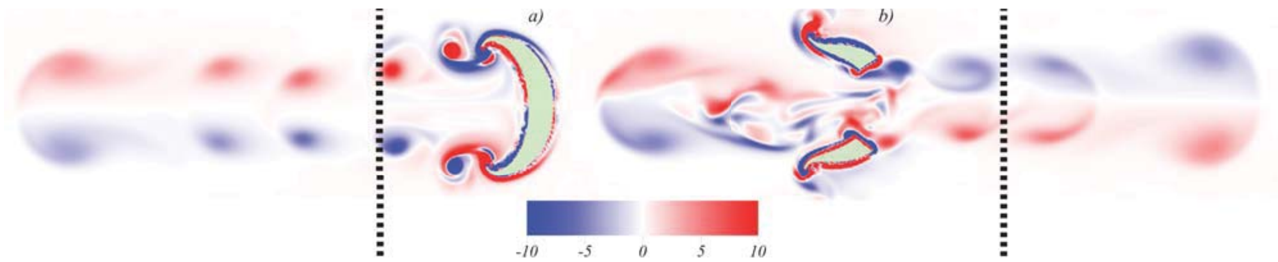

Figure 1. Normalized vorticity field $\hat{\omega}$ around the unmodified jellyfish (a) and the jellyfish with a central perforation (b), shown after the fifth swimming cycle. The dotted line indicates the initial bell position, highlighting the differences in wake structure and vortex organization between the two configurations.

References

[1] J. H. Costello, S. P. Colin, J. O. Dabiri, B. J. Gemmell, K. N. Lucas, and K. R. Sutherland. The hydrodynamics of jellyfish swimming. *Annual Review of Marine Science*, 13(Volume 13, 2021):375–396, 2021.
[2] J. Dabiri, S. Colin, J. Costello, and M. Gharib. Flow patterns generated by oblate medusan jellyfish: Field measurements and laboratory analyses. *The Journal of experimental biology*, 208:1257–65, 05 2005.
[3] B. J. Gemmell, J. H. Costello, S. P. Colin, C. J. Stewart, J. O. Dabiri, D. Tafti, and S. Priya. Passive energy recapture in jellyfish contributes to propulsive advantage over other metazoans. *Proceedings of the National Academy of Sciences of the United States of America*, 110(44):17904–17909, Oct. 2013. Epub 2013 Oct 7.
[4] M. Gong, M. Ashok, A. Helou, and L. Goentoro. Jellyfish shape as a mechanical balance. *Proceedings of the National Academy of Sciences*, 122(13):e2412082122, 2025.
[5] A. P. Hoover, A. J. Porras, and L. A. Miller. Pump or coast: the role of resonance and passive energy recapture in medusan swimming performance. *Journal of Fluid Mechanics*, 863:1031–1061, 2019.
[6] J. C. Nawroth, H. Lee, A. W. Feinberg, C. M. Ripplinger, M. L. McCain, A. Grosberg, J. O. Dabiri, and K. K. Parker. A tissue-engineered jellyfish with biomimetic propulsion. *Nature Biotechnology*, 30(8):792–797, Aug. 2012.

GEOMETRY-DEPENDENT OPTICAL TRAPPING AND DYNAMICAL STABILITY OF DEFORMED RED BLOOD CELLS

Emir Erdem[1], Gökberk Kabacaoğlu[2], Agnese Callegari[3], Giovanni Volpe[3], Luca Biancofiore[4]
[1]*M.Sc. Simulation Sciences, RWTH Aachen University, Aachen, Germany*
[2]*Department of Computer Science, Durham University, Durham, England*
[3]*Department of Physics, University of Gothenburg, Gothenburg, Sweden*
[4]*Department of Industrial and Information Engineering and Economics, University of L'Aquila, L'Aquila,Italy*

Abstract Red blood cells (RBCs) undergo pronounced shape transformations when subjected to shear flows, Poiseuille flows, and constricted microvascular environments [1, 2]. These deformations alter their symmetry, curvature distribution, and hydrodynamic response. Understanding how such morphology changes affect mechanical stability under external forcing is relevant both to rheology and to optical manipulation techniques.

We develop a computational framework to investigate the static and dynamic trappability of deformed RBC morphologies under a single-beam optical trap. The geometries considered (Fig. 1) represent flow-induced or physiologically relevant states: dumbbell (rouleaux-like aggregation), four- and eight-bumped shapes (echinocyte-like spiculation), necked configurations (strong constriction), and oblate forms (elliptocytic or shear-elongated cells). Optical forces and torques are computed within the geometrical-optics approximation using the OTGO toolbox, where a focused Gaussian beam is represented as a discrete ray bundle and momentum exchange is evaluated at each ray–surface interaction [3].

A systematic static analysis is performed by displacing and rotating each morphology about its principal axes. Near equilibrium, restoring forces and torques exhibit approximately linear behavior, indicating locally stable trapping configurations for all investigated shapes. However, geometric symmetry and anisotropy strongly influence the strength and directional character of confinement. Highly anisotropic morphologies generate pronounced restoring responses along selected directions, whereas near-spherical geometries exhibit weak orientational confinement due to reduced torque generation.

Dynamical stability is assessed through overdamped Brownian simulations incorporating geometry-dependent diffusion tensors [4]. Thermal fluctuations, viscous resistance, and optical restoring forces jointly determine motion. Time evolution of the center–trap distance, mean-squared displacement, and orientation autocorrelation functions demonstrate sustained confinement over physiologically relevant timescales. Importantly, dynamical relaxation behavior mirrors the symmetry properties identified in the static analysis.

From a dynamical-systems perspective, morphology effectively reshapes the local optical potential landscape, modifying translational and rotational restoring modes and thereby altering the stability characteristics of the trapped state. These results show that even strongly deformed RBCs can be both statically and dynamically trapped, while their confinement properties depend sensitively on geometric anisotropy and symmetry, features that are directly linked to flow-induced shape transformations in complex fluids.

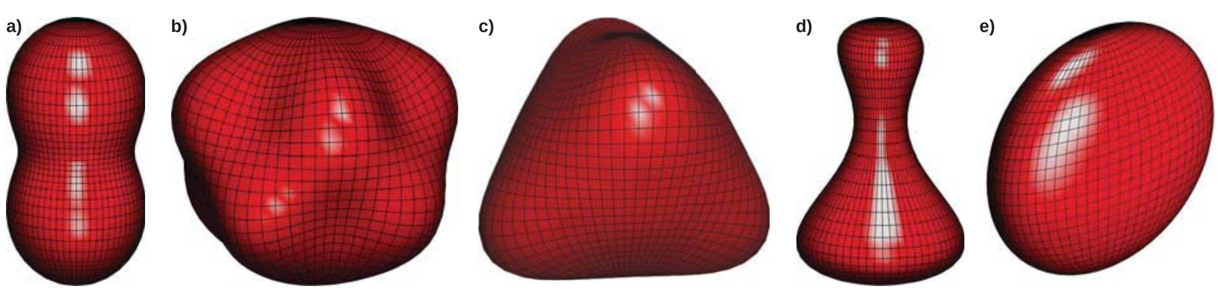

Figure 1. Representative red blood cell morphologies analyzed in this study: (a) dumbbell, (b) eight-bumped, (c) four-bumped, (d) necked, and (e) oblate configurations.

References

[1] R. Skalak and P. I. Branemark, Deformation of red blood cells in capillaries, Science, 1969.
[2] M. Diez-Silva et al., Shape and biomechanical characteristics of human red blood cells, MRS Bulletin, 2010.
[3] A. Callegari et al., Optical Tweezers in Geometrical Optics (OTGO), JOSA B, 2015.
[4] P. H. Jones et al., Optical Tweezers: Principles and Applications, Cambridge University Press, 2015.

TWO-PARAMETER BIFURCATIONS OF CRITICAL POINTS OF VORTICITY

Ilteber R. Ozdemir[1], Morten Brøns[2]
[1] *Department of Mathematics, Imperial College London, SW7 2AZ London, United Kingdom*
[2] *Department of Applied Mathematics and Computer Science, Technical University of Denmark, 2800 Lyngby, Denmark*

Abstract Two-dimensional incompressible flow, vorticity, bifurcation, vortex interactions, vortex merging

In a two-dimensional incompressible flow the critical points of vorticity, that is, the points where $\boldsymbol{\nabla}\omega = \mathbf{0}$, organize the topology of the vorticity field. Local extrema of vorticity can be identified as centers of vortices, and tracing their motion provides an overview of the vortex dynamics of the flow. This has been extensively used to describe vortex merging [1, 2]. In [1] we have developed a fundamental bifurcation theory for critical points of vorticity with time as the parameter. We show that the basic bifurcation phenomenon is a cusp or saddle-center bifurcation as shown in Figure 1. A vortex can disappear through the merging with a vorticity saddle as time progresses ((a) $\to$ (c)), or be created out of nowhere together with a saddle in the reverse process.

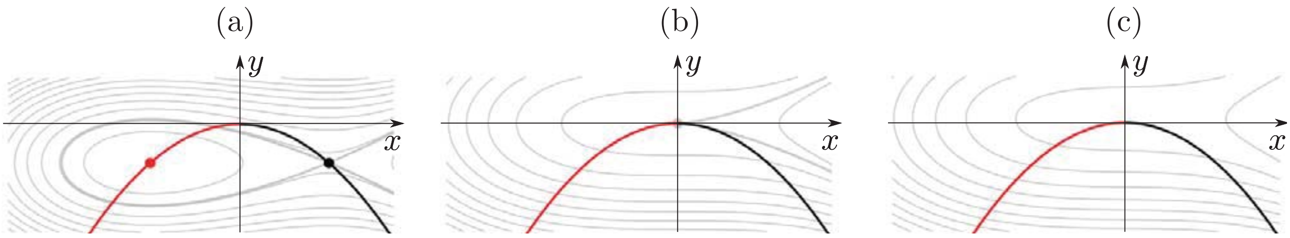

Figure 1. Time sequence of the vorticity field during the destruction of a vortex in a cusp bifurcation. A vortex (red) and a vorticity saddle (black) move along a locally parabolic trajectory and merge and disappear. Reproduced from [1].

The cusp bifurcation occurs when, at the origin in a suitable coordinate system, we have

$$\partial_x\omega = \partial_y\omega = 0, \quad \partial_{xx}\omega = \partial_{xy}\omega = 0, \quad \partial_{yy}\omega \neq 0, \quad \partial_{xt}\omega \neq 0, \quad \partial_{xxx}\omega \neq 0. \tag{1}$$

In the present paper we consider the effect of replacing one of the two latter inequalities in (1) with an equality. Such a situation may arise at some specific value of an auxiliary parameter such as the Reynolds number or a geometric parameter. We will derive the two-parameter bifurcation diagrams that result close to such higher-order degeneracies. The main types of temporal bifurcations which ensue are the *isola*, where a vortex is created and soon disappears again, an *inverse isola*, where a vortex disappears for a short time and then reappears, and *hysteresis*, where the saddle created in one cusp bifurcation interacts and destroys a vortex created in another cusp bifurcation. We will illustrate the theory with numerical examples of flows close to walls and bluff bodies.

References

[1] M. Brøns, I. R. Ozdemir, M. Heil, M. Andersen, and J. S. Hansen. Dynamics and bifurcations of critical points of vorticity, with application to vortex merging. *Journal of Fluid Mechanics*, 1010:A64, 2025.

[2] C. Cerretelli and C. H. K. Williamson. The physical mechanism for vortex merging. *Journal of Fluid Mechanics*, 475:41–77, 2003.

RANS CLOSURE-DRIVEN STABILITY OF THE DRAFT TUBE VORTEX ROPE

Ahmet Cagdas Kalayci, Artur Gesla, Eunok Yim

Hydro Energy and Applied Fluid Dynamics (HEAD) Laboratory, École Polytechnique Fédérale de Lausanne (EPFL), ME A2 464, Station 9, 1015 Lausanne, Switzerland

Abstract swirling flows, RANS modelling, vortex rope, linear stability, adjoint analysis

The operation of Francis turbines under part-load conditions is characterized by the formation of a precessing helical structure known as the vortex rope. This phenomenon resulting from strong residual swirl and flow deceleration leads to severe pressure fluctuations, structural vibrations, and reduced hydraulic efficiency. Therefore, understanding the mechanisms governing the emergence and stability of this structure is critical. In this study, we perform a systematic numerical investigation of a simplified Francis turbine draft tube geometry adopted from [1]. Various Reynolds-Averaged Navier-Stokes (RANS) turbulence models are considered, including Spalart–Allmaras (SA), standard and realizable k–ϵ, k–ω, k–ω SST, and the Reynolds stress model (RSM), using the open-source computational fluid dynamics framework OpenFOAM. The inlet velocity and turbulent viscosity are prescribed based on measurement data [1] and are used for all models. Significantly different convergence behaviors are observed among the models. While standard and realizable k–ϵ and k–ω SST models converge to steady axisymmetric solutions (figure 1a,b), other closures (SA and RSM) do not reach a steady state and instead resulted in persistent residual oscillations together with a self-excited precessing vortex rope within the time integration (figure 1c). To better characterize the role of eddy viscosity on the formation of vortex rope, a global stability and resolvent analyses are conducted on some selected RANS solutions using finite element code FreeFEM++. The leading eigenvalues and direct global modes associated with the vortex rope instability were compared across the different eddy viscosity models, using a frozen eddy-viscosity approach. Finally, an adjoint-based sensitivity analysis of spectrum to turbulent viscosity modifications is performed to assess the sensitivity of the vortex rope to perturbations in the eddy viscosity field.

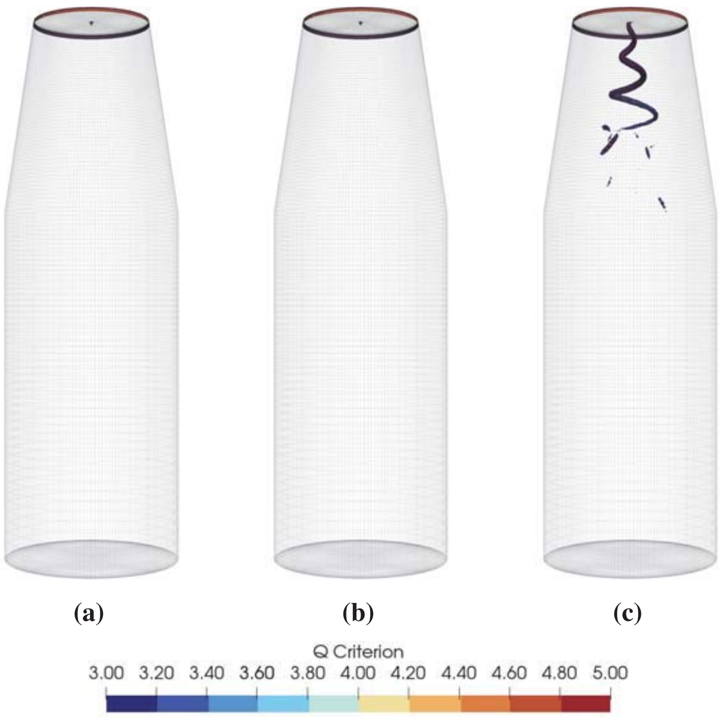

Figure 1: Q-criterion isosurfaces obtained from unsteady RANS simulations: (a) standard k–ϵ, (b) k–ω SST, (c) Spalart–Allmaras models. While the k–ϵ and k–ω solutions yield axisymmetric flow, the Spalart–Allmaras model shows the formation of a helical vortex rope.

References

[1] Susan-Resiga, R., Muntean, S., Hasmatuchi, V., Anton, I., and Avellan, F. (2010). Analysis and prevention of vortex breakdown in the simplified discharge cone of a Francis turbine. *J. Fluids Eng.*, 132(5).

ON THE CHANGE IN FLOW TOPOLOGY FROM DIFFERENT WING TIP GEOMETRIES IN GROUND EFFECT

Tristan Favre[1] & Flavio Noca[2]
[1] *Laboratory of Fluid Mechanics and Instabilities, Ecole Polytechnique Fédérale de Lausanne, Switzerland*
[2] *Département de génie aérospatial, Ecole de Technologie Supérieure de Montréal, Canada*

Abstract Ground-effect, Wing-tip Vortices, Aerodynamics, Vortex Dynamics.

When a wing is moved close to the ground, at a distance of one chord-length or less, an increase of its efficiency is observed due to the so-called ground-effect. Gliding birds especially are known to exploit this phenomenon [1], as well as some human-made aircrafts [2]. Finite wings produce vortices at their tips, and the presence of a ground alters their downwash and reduces the corresponding induced drag. This, in turns, contributes to the increase of the wing efficiency. When these Wing-tip vortices maintain high vorticity in close vicinity of the ground, boundary layer eruption [3, 4] is seen, which leads to the production of new vortices that eventually interact with the original tip vortices.

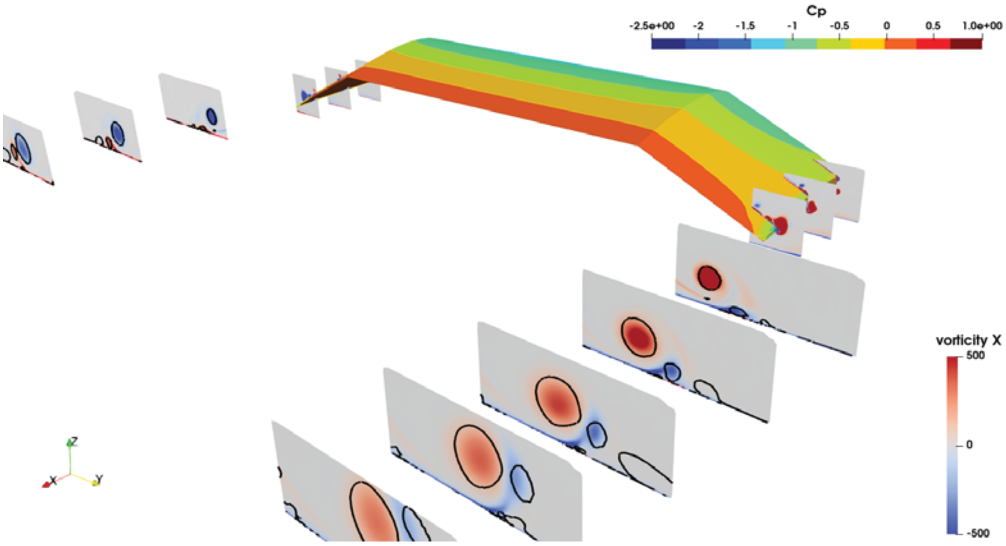

Figure 1. A Wing-tip vortex interacting with the ground provokes a boundary layer eruption that creates a secondary vortex. In this figure, streamwise vorticity is shown on each plane, with red and blue indicating, respectively, a positive and a negative rotation. The thick black lines on the planes are contours of $Q = 0$ (Q is the second invariant of the velocity tensor). The static pressure coefficient Cp (the static pressure normalized by the dynamic pressure) is shown on the surface of the wing.

In this numerical study, various wing geometries (as used in [5], i.e. straight planform and wing with an anhedral incline shape outboard, see an example in Figure 1) of low aspect-ratio (≈ 4) and with two types of wing tips (square tip and Hoerner tip [6]) are evaluated in moderate ground-effect at $Re = 240000$. The open-source finite-volume code OpenFoam [7] is used for performing Reynolds-Averaged Navier-Stokes simulations as well as Detached-Eddy Simulations of these geometries. Integrated quantities and flow topology are studied to assess the impact of the Wing-tip vortex - ground vortex interaction on the reduction of induced drag, and to understand the mechanisms involved.

Acknowledgement The authors are thankful to the Swiss National Science Foundation for the fundings of this work (grants "515 356" and "515 341").

References

[1] Hainsworth, F. R., *Induced Drag Savings From Ground Effect and Formation Flight in Brown Pelicans*, J. of Exp. Biol., **135 (1)**, 431–444 (1988).
[2] Rozhdestvensky K. V., *Wing-in-ground effect vehicles*, Prog. Aerosp. Sci., **42**, 211-283 (2006).
[3] Kudela H. & Malecha Z. M., *Eruption of a boundary layer induced by a 2D vortex patch*, Fluid Dyn. Res., **41**, 055502 (2009)
[4] Nielsen, A. R., Heil, M., Andersen, M., & Brøns, M., *Bifurcation theory for vortices with application to boundary layer eruption*, J. of Fluid Mech., **865**, 831–849 (2019).
[5] de Sepibus, C., Ground effect aerodynamics for fixed-wing drones, Master Thesis, EPFL, (2022)
[6] Hoerner, S., *Aerodynamic Shape of the Wing Tips*, Report No **AMC-AF-TR-5752**, (1952).
[7] OpenFOAM (Version 2012), OpenCFD Ltd.

FROM MILES TO HOLMBOE TO KH: INSTABILITY TRANSITIONS IN TWO-PHASE SHEAR FLOW

Anil Kumar[1], S. Ravichandran[2] & Ratul Dasgupta[1]
[1]*Department of Chemical Engineering, Indian Institute of Technology Bombay, India 400 076*
[2]*Centre for Climate Studies, Indian Institute of Technology Bombay, India 400 076*

Abstract Shear-driven interfacial instabilities and mode transition in two-phase flows.
Key words: Shear instability; wind-waves; capillary-gravity waves; KH instability; Holmboe instability; critical layer; ocean waves.

We investigate the generation of interfacial waves between two immiscible fluids driven by shear-induced, inviscid instabilities. The base flow is the classical exponential velocity profile of Morland & Saffman (1993), together with a sharp, stably stratified density interface. For low Froude number ($\sim O(1)$) and high Bond number ($\sim O(100)$), as motivated by geophysical and astrophysical settings, we identify a smooth transition of the fastest-growing mode: from Kelvin–Helmholtz (KH) instability at density ratio $\delta = 0.9$ (upper-to-lower density ratio), to Holmboe (H) instability as $\delta \to 0.5$, and onwards to the Miles (Miles, 1957) critical-layer instability as $\delta \to 0.001$ (air–water). Remarkably, the fastest-growing Miles mode, characterized by a sharp jump in the inviscid Reynolds stress (τ) at the critical level, persists up to $\delta = 0.01$, i.e. an order of magnitude larger than the air–water value.

The vertical (z) structure of the Reynolds stress for the fastest mode changes qualitatively with increasing δ: it transitions from exhibiting a sharp jump at the critical level for $\delta \ll 1$ (Miles) to varying smoothly through that location for $\delta \geq 0.5$ (Holmboe). We provide a theoretical explanation for this behaviour. In the higher density-ratio range $(0.5 \leq \delta \leq 0.9)$, comparison with stability results for the corresponding piecewise-linear (PL) velocity profile shows that both H and KH instabilities can occur for the exponential model.

We also report simulations of the incompressible Euler equations including gravity and surface tension. In the Miles regime ($\delta = 0.01$), we observe excellent agreement with linear theory for up to five wave periods; upon saturation, small surface ripples emerge. At $\delta = 0.1$, the resulting finite-amplitude waves develop larger ripples reminiscent of capillary-modified Stokes waves. For $\delta = 0.5$, the exponentially growing waves enter a nonlinear regime with a sheared cusp at the crest, emitting spume droplets and resembling the asymmetric Holmboe waves reported by Lawrence et al. (1998). At $\delta = 0.9$, the growing interfacial waves rapidly roll up into classical KH spirals within five wave periods. Comparisons between the PL and exponential profiles elucidate the role of base-flow curvature and the critical level. To the best of our knowledge, this is the first demonstration of three canonical instabilities in these background states without invoking the Boussinesq approximation.

References

Morland, L. C. & Saffman, P. G. (1993). Effect of wind profile on the instability of wind blowing over water. *Journal of Fluid Mechanics*, *252*, 383–398.

Miles, J. W. (1957). On the generation of surface waves by shear flows. *Journal of Fluid Mechanics*, *3*(2), 185–204.

Lawrence, G. A., Haigh, S. P. & Zhu, Z. (1998). In search of Holmboe's instability. *Physical Processes in Lakes and Oceans*, *54*, 295–304.

ANOMALY OF DARCY-BÉNARD INSTABILITY WITH ANOMALOUS DIFFUSION

Antonio Barletta
Department of Industrial Engineering, Alma Mater Studiorum Università di Bologna, Italy

Abstract The interplay between anomalous mass diffusion and instability in a fluid saturated porous layer is investigated. (Rayleigh-Bénard instability; Porous medium; Anomalous diffusion).

Anomalous diffusion is the departure from the standard picture of mass transfer in a fluid saturated porous layer where, at a microscopic level, the mean-squared displacement of the diffusing molecules grows linearly in time [1, 2]. A possible model of the anomalous mass diffusion is through a time-dependent mass diffusivity coefficient, $\mathscr{D}(t)$ [1], while other models are based on the use of fractional time-derivative or Laplacian [2]. If one focusses on a time-dependent mass diffusivity, one may have subdiffusive, standard or superdiffusive molecular transport, depending on the functional form of $\mathscr{D}(t)$ at large times

$$\lim_{t\to+\infty} \frac{1}{t} \int_0^t \mathscr{D}(t')\,\mathrm{d}t' = \begin{cases} +\infty & \text{superdiffusion,} \\ \mathscr{D}_\infty > 0 & \text{normal diffusion,} \\ 0 & \text{subdiffusion.} \end{cases}$$

Physics behind superdiffusion or subdiffusion is based on such phenomena as Levy flights, responsible for superdiffusive statistics, or particle trapping, responsible for subdiffusive statistics of random walk [1, 2].

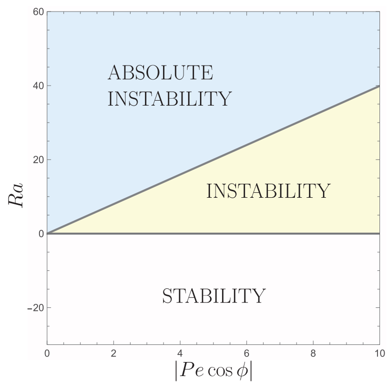

Figure 1. A sketch of the stability diagram for subdiffusion in the $(|Pe\,\cos\phi|, Ra)$ parametric plane, where Pe is Péclet number, Ra is Rayleigh number and ϕ is the angle between the basic flow and the perturbation wave directions [3]

The aim of this study is the analysis of the linear instability, either convective or absolute, for the stationary through-flow in a horizontal porous layer subject to a destabilising solute concentration gradient and to Darcy's law for momentum transfer. The type of instability is the variant Rayleigh-Bénard for Darcy's flows in porous media where the destabilising agent is mass transfer instead of heat transfer in the fluid.

The presented study features first an analysis of the modal instability to arbitrary waves propagating along a direction inclined an angle ϕ to the through-flow direction. Differences in the convective stability/instability of superdiffusive, normal or subdiffusive transport are discussed. It is shown that superdiffusion always means a linearly stable condition, while convective instability may arise for subdiffusion. The transition to absolute instability is possible for normal diffusion [4] as well as for subdiffusion. A stability diagram for the case of subdiffusion is sketched in Fig. 1.

References

[1] B. I. Henry, T. A. M. Langlands & P. Straka, *An introduction to fractional diffusion*, In "Complex Physical, Biophysical and Econophysical Systems." 37–89 World Scientific (2010).
[2] R. Metzler & J. Klafter, *The random walk's guide to anomalous diffusion: a fractional dynamics approach*, Phys. Reports **339**, 1–77 (2000).
[3] A. Barletta, *On Prats' problem with anomalous diffusion*, arXiv preprint 2512.24769, https://arxiv.org/abs/2512.24769.
[4] A. Barletta, *Routes to Absolute Instebility in Porous Media*, Springer, New York (2019).

DETECTING SEIZURES THROUGH BIFURCATION IN NEURON DYNAMICS

Niteen Kumar, Stefano Pagani & Paola F. Antonietti
MOX, Department of Mathematics, Politecnico di Milano, Milan, 601-8501, Italy

Abstract Epileptic seizures, Bursting activity, Multistability, Bifurcation analysis

Neuronal activity unfolds across two distinct physiological time scales: a fast scale on the order of 10^{-3} seconds, associated with action potentials and channel gating, and a slow scale on the order of 10 seconds, governed by ionic concentration dynamics [1, 2, 3]. Interactions between these fast electrical processes and slower homeostatic mechanisms can produce abnormal rhythmic activity characteristic of epileptic seizures. In this study, we investigate how slow ionic processes contribute to seizure generation by performing a detailed bifurcation analysis of the underlying neuronal dynamics. Nullclines analysis shows that increasing the strength of ionic pumps (ρ) can lead to the coexistence of multiple stable and unstable equilibria and these equilibria may collide or disappear through saddle-node bifurcations, whereas for lower ρ only a single equilibrium exists [5]. These finding emphasize the importance of pump-mediated ion regulation in shaping neuronal excitability and motivate further exploration of neuronal behavior. In addition, potassium currents are known to strongly modulate neuronal firing and network excitability [4], making it essential to understand how pump strength interacts with potassium regulation, as captured by the parameter extracellular potassium concentration (K_{bath}). Bifurcation analysis with respect to pump strength ρ and K_{bath} reveals critical transitions, including the emergence and disappearance of rhythmic firing through Hopf bifurcations and changes in firing patterns mediated by limit points of cycles. Extending this analysis to the (K_{bath}-ρ) parameter space reveals higher-order bifurcations, such as cusp and generalized Hopf points, which delineate the regions of multistability, bursting activity, and transitions between normal and seizure-like states [5]. Together, these results provide biological insight into how impaired potassium homeostasis and pump function can promote seizure dynamics and help define parameter regimes associated with stable, non-pathological neuronal behavior.

References

[1] J. Cressman, G. Ullah, J. Ziburkus, S. Schiff and E. Barreto, *The influence of sodium and potassium dynamics on excitability, seizures, and the stability of persistent states: I. Single neuron dynamics*, Journal Computational Neuroscience, Vol. **26**, pp. 159-170, Year 2009.

[2] A. Erhardt, K. Mardal, J. Schreiner, *Dynamics of a neuron-glia system: the occurrence of seizures and the influence of electroconvulsive stimuli: A mathematical and numerical study*, Journal Computational Neuroscience, Vol. **48**, pp. 229-251, Year 2020.

[3] E. Barreto, J. Cressman, *ion concentration dynamics as a mechanism for neuronal brusting*, Journal of biological physics, Vol. **37**, pp 361-373, Year 2011

[4] X. Wu, J. Shuai, *Multistability in a neuron model with extracellular potassium dynamics*, Physical Review E, Vol. **85**, Year 2012

[5] N. Kumar, S. Pagani, S. Singh, P. Antonietti, *From Excitability to Multistability: A Detailed Bifurcation Analysis of the Unified Barreto-Cressman Neural Model*, In preparation.

HEMODYNAMIC CONSEQUENCES OF VENTRICULAR TACHYCARDIA

Filippo Caruso Lombardi[1], Francesco De Vita[1], Anna Crispino[2], Roberto Verzicco[1,3], Alessio Gizzi[2] & Francesco Viola[1]
[1] *Gran Sasso Science Institute, L'Aquila, Italy*
[2] *University of Rome Campus Bio-Medico, Rome, Italy*
[3] *POF Group, University of Twente, AE Enschede, The Netherlands*

Abstract Fluid-Structure Electrophysiology Interaction, Ventricular Tachycardia, Myocardial Infarction, Electroanatomical Mapping.

Cardiac contraction during each heartbeat results from the synchronized response of the myocardium to the propagation of nonlinear electrophysiological waves. This coordinated process can be severely disrupted under pathological conditions such as ventricular tachycardia (VT) and ventricular fibrillation (VF). These arrhythmias are associated with abnormal impulse propagation patterns within the myocardial tissue, including spiral and scroll waves, often facilitated by structural heterogeneities introduced by myocardial infarction. In particular, the initiation and stabilization of scroll waves can be promoted by pronounced conductivity contrast and electrophysiological heterogeneities between healthy, remodeled and fibrotic tissue. Although the mechanisms underlying the formation and dynamics of arrhythmogenic patterns have been extensively investigated in both in silico and experimental studies [1, 2], their impact on cardiac hemodynamics remains insufficiently explored. In this work, we investigate the effects of ventricular tachycardia on clinically relevant hemodynamic biomarkers, with the objective of identifying which pathological electrophysiological patterns most significantly impair physiological blood flow dynamics in the left heart. Ultimately, we aim to provide insights toward optimizing therapeutic interventions. Patient-specific tissue activation data acquired using the CARTO® 3 electroanatomical mapping system were employed to calibrate the spatial heterogeneities of the electrophysiological substrate and induce reentrant dynamics within the myocardium. Electrical activity was modeled using a monodomain formulation coupled with appropriate cellular models to represent the electrophysiological heterogeneity of healthy tissue, peri-infarct regions, and scar tissue. The resulting activation patterns were coupled to a hemodynamic model governed by the incompressible Navier–Stokes equations, discretized using a staggered finite-difference scheme combined with immersed boundary techniques. The resulting multiphysics framework provides a predictive computational framework to reproduce ventricular arrhythmias and assess their impact on cardiac function, supporting the identification of optimal therapeutic strategies aimed at restoring physiological hemodynamics.

References

[1] H. J. Arevalo et al., Arrhythmia Risk Stratification of Patients After Myocardial Infarction Using Personalized Heart Models, Nature Communications, **7**, 11437, (2016)
[2] E. J. Ciaccio et al., Correlation relationships of the reentrant ventricular tachycardia circuit, Computer Methods and Programs in Biomedicine, **241**, 107764, (2023)

INTRA- VERSUS SUPRA-ANNULAR DEPLOYMENT OF THE MECHANICAL AORTIC VALVE: A FLUID-STRUCTURE INTERACTION INVESTIGATION

Gianlorenzo Granata[1], Martino Andrea Scarpolini[1,2], Roberto Verzicco[1,3] & Francesco Viola[1]
[1] *Gran Sasso Science Institute (GSSI), L'Aquila, Italy*
[2]*INFN Tor Vergata, Rome, Italy*
[3]*Tor Vergata University of Rome, Rome, Italy*

Abstract **Keywords**: Aortic valve replacement; bileaflet mechanical valve; supra-annular vs intra-annular implantation; hemodynamics; fluid–structure interaction; hemolysis.

Surgical aortic valve replacement is a life-saving intervention and remains the only definitive treatment for a range of pathological conditions, such as severe stenosis and valve regurgitation.

Artificial valves can be either mechanical or bioprosthetic. In patients younger than 60 years, bileaflet mechanical prostheses are generally preferred due to their durability, according to the European guidelines [1]. However, these valves generate a non-physiological tripartite flow pattern and require lifelong anticoagulation therapy. In this context, understanding valve hemodynamics in relation to implantation strategies is crucial to optimize postoperative performance and to guide future valve design.

In this work, we investigate the influence of deployment strategy by comparing traditional intra-annular and supra-annular implantation of a bileaflet mechanical aortic valve, focusing on the resulting hemodynamics and commonly used clinical parameters. To this end, we employed high-fidelity fluid–structure interaction simulations integrated within a realistic left-heart model, allowing us to overcome the intrinsic limitations of clinical measurements and simplified numerical approaches previously reported in the literature. The valve leaflets were modeled as rigid bodies, enabling accurate reproduction of their fast dynamics throughout the cardiac cycle.

The hemodynamic analysis reveals a consistent superiority of the supra-annular configuration. Compared with intra-annular placement, supra-annular deployment is associated with a larger effective orifice area, reduced transvalvular pressure drop, lower wall shear stress levels, and decreased hemolysis. Moreover, we compare our findings with those of a previous study on a biological valve by Scarpolini *et al.* [2].

References

[1] Alec Vahanian, Friedhelm Beyersdorf, Fabien Praz, Milan Milojevic, Stephan Baldus, Johann Bauersachs, Davide Capodanno, Lenard Conradi, Michele De Bonis, Ruggero De Paulis, Victoria Delgado, Nick Freemantle, Martine Gilard, Kristina H Haugaa, Anders Jeppsson, Peter Jüni, Luc Pierard, Bernard D Prendergast, J Rafael Sádaba, Christophe Tribouilloy, Wojtek Wojakowski, ESC/EACTS Scientific Document Group , ESC National Cardiac Societies , *2021 ESC/EACTS Guidelines for the management of valvular heart disease: Developed by the Task Force for the management of valvular heart disease of the European Society of Cardiology (ESC) and the European Association for Cardio-Thoracic Surgery (EACTS)*, European Heart Journal, Volume 43, Issue 7, 14 February 2022, Pages 561–632, https://doi.org/10.1093/eurheartj/ehab395

[2] Scarpolini, Martino Andrea, Giovanni Vagnoli, Fabio Guglietta, Roberto Verzicco, and Francesco Viola. *Hemodynamic effects of intra-and supra-deployment locations for a bioprosthetic aortic valve.* Physical Review Fluids 10, no. 9 (2025): 090501.

ON THE LINK BETWEEN HYDRODYNAMIC INSTABILITIES AND FLOW-INDUCED THROMBOSIS IN EXTRACORPOREAL MEDICAL DEVICES

Valerio Lupi[1], Roberto Verzicco[1,2] & Francesco Viola[1]
[1] *Gran Sasso Science Institute (GSSI), L'Aquila, 67100, Italy*
[2] *Physics of Fluids Group, University of Twente, Enschede, 7500AE, The Netherlands*

Abstract Flow-induced thrombosis, hydrodynamic instability

During extracorporeal membrane oxygenation (ECMO) and haemodialysis, blood is drained out of the patient and flows through a circuit consisting of several tubes joined by various connectors. The flow rate in this system is typically high enough for transition to turbulence to occur. Furthermore, since blood experiences non-physiological conditions within the tubing system, thrombotic events can arise [1]. Despite these complications being major clinical concerns, the role of hydrodynamic instabilities and laminar-turbulent transition in promoting thrombogenesis has not been systematically investigated. In the present work, we couple incompressible Navier–Stokes equations with the model developed by Yang et al. [2] and carry out direct numerical simulations (DNS) of blood flow through the connectors used in extracorporeal medical devices. In this way, we identify the transitional regime and assess the effect of the Reynolds number on the formation and evolution of thrombi. To investigate the onset of transition, we perform linear modal stability analysis of the steady base flow [3]. By establishing a correlation between the most unstable eigenmodes, the *wavemaker*, and the spatial locations where clot formation is promoted, we can then provide a physical explanation of how hydrodynamic instabilities affect thrombosis in connectors for extracorporeal blood circulation. These results will also aid in the design of devices that reduce clot formation, thereby improving the health and comfort of patients.

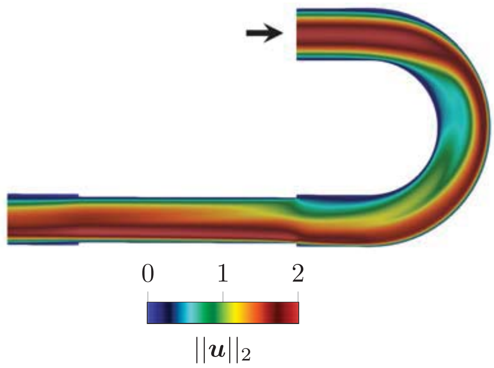

Figure 1. Velocity magnitude on the equatorial plane of the system consisting of a curved tube and a connector.

References

[1] S. M. Hastings, D. N. Ku, S. Wagoner, K. O. Maher & S. Deshpande, *Sources of circuit thrombosis in pediatric extracorporeal membrane oxygenation*, ASAIO J. **63** (1), 86–92 (2017).
[2] L. Yang, N. Tobin & K. B. Manning, *Refining a numerical model for device-induced thrombosis and investigating the effects of non-Newtonian blood models*, J. Biomech. **120**, 110393 (2021).
[3] M. P. Juniper, A. Hanifi, & V. Theofilis, *Modal Stability Theory: Lecture notes from the FLOW-NORDITA Summer School on Advanced Instability Methods for Complex Flows, Stockholm, Sweden, 2013*, Appl. Mech. Rev. **66** (2), 024804 (2014).

DROPLET VAPORIZATION DYNAMICS OF A SINGLE BUBBLE IN AN UNBOUNDED LIQUID UNDER AN ACOUSTIC FIELD

H. Yagız Yahsi[1] & Ilke Kaykanat[1] & A. Kerem Uguz[1]
[1]*Department of Chemical Engineering, Boğaziçi University, Istanbul, Turkey*

Keywords: Microbubble, Acoustic Droplet Vaporization, Ultrasound, Targeted Drug Delivery, Acoustic Field

Abstract

Targeted drug delivery in cancer treatment aims to deliver drug-cargo into the tumour effectively while reducing the toxicity of healthy tissue. Conventional microbubbles were utilized for imaging and therapeutic response. However, their clinical applications are hindered due to the instability and short circulation times in the bloodstream. Acoustic irradiation causes microbubble oscillations, which must be controlled to prevent irreversible damage to healthy tissues. This study focuses on modelling the acoustic droplet vaporization process of microbubbles surrounded by unbounded liquid under an acoustic field. The system involves a microbubble with a volatile perfluorocarbon (PFC) core, surrounded by an incompressible Newtonian liquid undergoing droplet vaporization under acoustic excitation. The system is depicted in Figure 1. It consists of three media: vapor, liquid, and surrounding liquid. The radius of the bubble is denoted as $R_b(t)$, and the radius of the droplet is $R_d(t)$. The time-dependent acoustic field is $p_\infty(t)$. At the droplet/bubble interface, mass transfer occurs between media 1 and 2 due to phase change. This study examines the effects of the initial bubble radius and acoustic parameters, including amplitude and frequency, on the bubble radius $R_b(t)$ and the temperature field. The coupled partial differential equations are solved using the Chebyshev spectral method in space and a finite difference scheme in time.

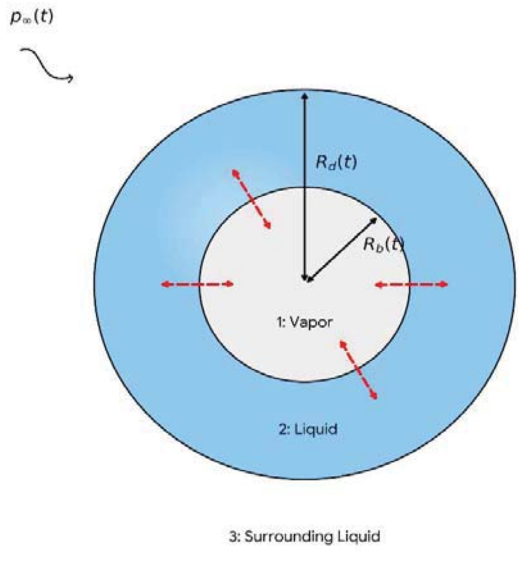

Figure 1. Schematic of acoustic microdroplet vaporization in an infinite liquid

INTERFACE DEFORMATION AND OSCILLATION OF A SESSILE DROPLET UNDER A UNIFORM DC ELECTRIC FIELD

Debabrat Biswal, Arvind Kumar & Rajneesh Bhardwaj
Department of Mechanical Engineering, IIT Bombay, Mumbai-400076, Maharashtra, India.
Email: debabrat.iitb@iitb.ac.in

Abstract

Electric-field-driven droplet manipulation has a wide range of applications such as electro-spraying, inkjet printing, and surface cleaning. A sessile droplet subjected to an electric field may undergo oscillatory motion, conical deformation [1], or jet formation [2]. These various drop dynamics depend on the surface wettability, electric field strength, and the electrochemical properties of the liquid. However, the sustained cyclic motion of sessile droplet and meniscus jet formation in quiescent air under a uniform electric field have not been investigated much in the literature. In the present study, we experimentally investigated the dynamics and deformation of a millimeter-sized sessile droplet resting on surfaces of varying wettability under a uniform DC electric field. We utilized a high-voltage DC power supply, two parallel copper discs with fixed separation for charging the drop and maintaining uniform electric field as illustrated in Fig.1 (a). A high-speed imaging technique was used to visualize and capture droplet dynamics and deformations. A sessile water droplet of 7 μl on superhydrophobic surface elongates and detaches upon the application of critical electric field of 9 kV/cm as shown in Fig.1 (b) at t = 515 ms. After detachment, the drop moves towards top electrode and impacts on the superhydrophobic surface at t = 529 ms. During impaction, the charged droplet reverses direction due to charge induction and returns toward the lower plate, resulting in continuous oscillatory motion. This cyclic motion continues for long time till the electric field is on. This phenomenon occurs due to low surface energy between superhydrophobic surface (160$\pm$5° contact angle) and high electric field between the electrodes. The droplet oscillation dynamics was further validated using a theoretical model which quantitatively matches the experimentally measured oscillation frequency and droplet trajectory. We also observed that with increasing the electric field, a binary droplet with 25% isopropyl alcohol and 75% water on copper surface (60$\pm$5° contact angle) elongates into a conical shape as shown in Fig.1 (c) at t = 589 ms. When the electric field goes beyond the critical threshold, interfacial instability leads to jet emission through breakup of the droplet interface at t = 590 ms. The findings of this study further reveal that both the oscillation frequency and the jet ejection rate scale strongly with the applied voltage and droplet size.

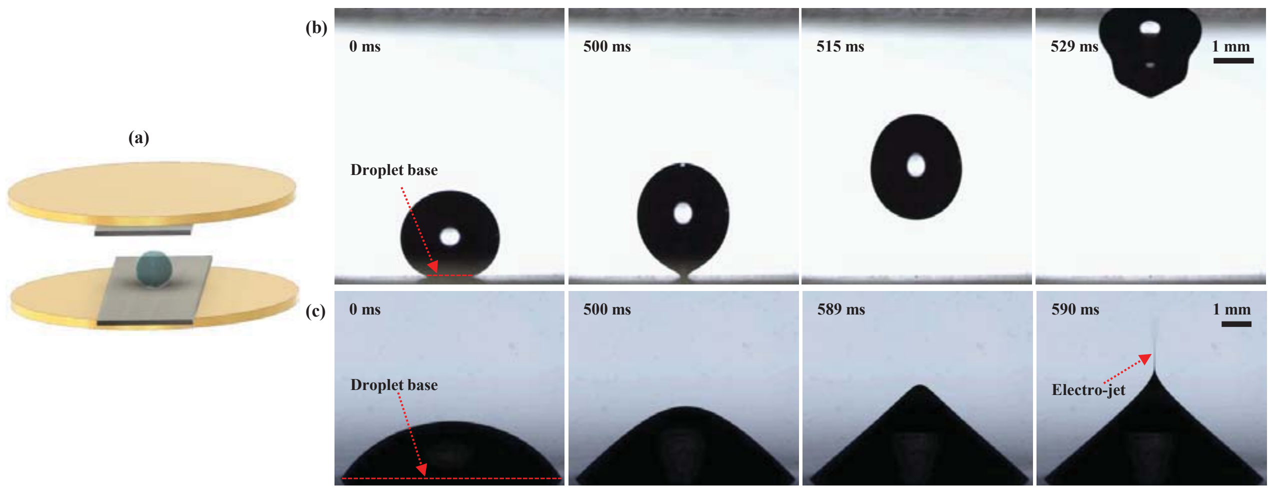

Figure 1. (a) Experimental setup showing a droplet placed between two parallel copper discs. Time-sequence images of a 7 μl droplet under a uniform electric field at 6.5 kV: (b) oscillatory motion of a water droplet on a superhydrophobic surface captured at 1000 fps; and (c) deformation and jet formation of a binary droplet on a copper surface captured at 1500 fps.

References

[1] J. Beroz, A. J. Hart, & J.W. M. Bush, *Stability limit of electrified droplets*, Physical Review Letters, **122**, 244501(2019).
[2] Xiaoye Ren , Wan-Yuan Shi * , Lang Liu , & Meng Li, *Dynamic behaviors and stability limit of sessile droplet on dielectric surface under external electric field*, International Journal of Heat and Mass Transfer, **255**, 127804 (2026).

ULTRASOUND-INDUCED FARADAY INSTABILITY ON WALL-ATTACHED MICROBUBBLES

Louan Presse[1], Daniel W. Meyer[1], Marco Cattaneo[1] & Outi Supponen[1]
[1] *Institute of Fluid Dynamics, ETH Zürich, Zürich, Switzerland*

Abstract Microbubbles, Faraday instability, Ultrasound, Capillary waves, Jetting

When a microbubble resting on a surface is excited with an ultrasound pulse around its resonance frequency, the volumetric oscillations of the interface trigger Faraday waves. Consequently, the bubble exhibits intense shape deformations which eventually focus into jets directed at the surface. Notably, this phenomenon generates strong stresses on and around the surface at driving pressure amplitudes much below the usual threshold for inertial collapse. Harnessing this capillarity-driven cavitation regime at low pressure amplitudes would drastically improve the efficiency of ultrasound-mediated technologies in challenging environments such as targeted drug delivery or cleaning of sensitive surfaces. Our findings provide a quantitative understanding of the underlying dynamics, leveraging ultrafast experiments, numerical simulations, and physical modelling.

We investigate insonified bubble dynamics experimentally using high-speed video-microscopy techniques. In particular, we leverage simultaneous dual-view imaging to uncover the three-dimensional shape deformations of a single wall-attached microbubble. We find that insonified microbubbles follow a predictable sequence of oscillations. First, only volumetric oscillations take place and grow in amplitude. The limited mobility of the contact line formed by the bubble interface on the solid substrate enforces harmonic axisymmetric oscillations identifiable as meniscus waves. Past a volumetric oscillation amplitude threshold, the Faraday instability is triggered and half-harmonic axisymmetric shape oscillations develop. When the amplitude of these shape oscillations is above a specific threshold, jetting occurs on the centre lobe and daughter bubbles are ejected. The bubble usually jets a couple of times before losing symmetry. Finally, the Faraday waves stabilise in a homogeneous lattice pattern.

We compare our experimental results with Boundary Element Method (BEM) simulations. The implementation of accurate models for the gas thermodynamics and the contact line mobility, along with the inherent simplicity and stability of the BEM scheme, produces simulations of bubble oscillations over a large number of cycles at a low computational cost. We obtain very faithful results which validate the implemented models and demonstrate the value of BEM schemes as simulation tools for insonified bubble dynamics.

We complement our experimental and numerical results with an in-depth modal analysis of wall-attached bubble oscillations. We find that the natural mode spectrum differs from the well-established predictions for free bubbles and is heavily affected by the static and dynamic wetting conditions. This linear approach accurately predicts the triggering thresholds for Faraday instabilities. We also exploit this modal decomposition to bring interpretability to the experimentally and numerically observed phenomena. We explore a combined spatial-spectral interpretation for the singular jetting mechanism. Firstly, self-similar asymptotics inform on the scaling laws of the singularity formation. Secondly, a spectral analysis of the non-linear modal leakage surrounding the singular events gives insights into the underlying energy cascade mechanism.

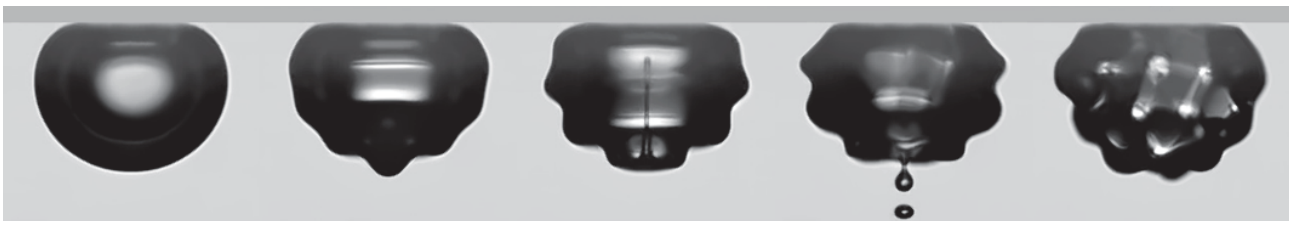

Figure 1. A wall-attached microbubble (95 µm radius) weakly insonified at a frequency of 100 kHz develops shape oscillations as a result of Faraday instability. The five snapshots are taken at successive instants of the 200 µs ultrasound pulse. The Faraday pattern evolves over time and focuses into singularities: inward jets and split ejecta. Adapted from [1].

References

[1] M. Cattaneo, L. Presse, G. Shakya, T. Renggli, B. Lukić, A. Prasanna, D. W. Meyer, A. Rack & O. Supponen, *Shape modes and jet formation on ultrasound-driven wall-attached bubbles*, J. Fluid Mech. **1017**, A9 (2025).

COLLECTIVE DYNAMICS OF GALLOPING BUBBLES

Xinyun Liu[1], Connor W. Magoon[1], Howard A. Stone[2] and Pedro J. Sáenz[1]
[1]*Department of Mathematics, University of North Carolina, Chapel Hill, NC, USA*
[2]*Department of Mechanical & Aerospace Engineering, Princeton University, Princeton, NJ, USA*

Keywords: galloping bubbles, collective dynamics, active matter

Abstract

We study the collective dynamics of galloping bubbles [1]: capillary-size air bubbles held by buoyancy against the top wall of a vertically vibrated fluid chamber that spontaneously break symmetry and self-propel along a horizontal surface. This propulsion arises from the nonlinear coupling of parametrically excited shape oscillation modes that lead to non-reciprocal swimming, allowing bubbles to transform periodic vertical vibrations into sustained horizontal motion without net external forcing in the direction of travel. At the single-bubble level, the galloping mechanism gives rise to a variety of tunable trajectory regimes, including rectilinear, orbital, and chaotic motion.

Building on this foundation, we investigate how galloping bubbles interact and organize collectively across two contrasting limits. In the *dilute* regime, bubbles move without geometric confinement and interact primarily through flow-mediated forces, from which behaviors such as self-assembly, orbiting pairs, promenading motion, and gas-like states emerge. In the *dense* regime, vertical vibration stabilizes a tightly packed layer of bubbles against coalescence, while also transforming it into an active foam where bubbles continuously deform and exchange positions with their neighbors. As the forcing is increased, we observe a two-dimensional melting characterized by transitions from hexagonal order to an intermediate tetratic phase, and finally to active-turbulent states. Special attention is given to characterizing these collective dynamics as functions of bubble size, driving parameters, and packing fraction. Together, our results establish vibrating bubbles as a controllable platform for studying the collective dynamics of deformable active matter, enabling comparisons with crystal melting in condensed matter systems as well as collective motion in biological systems.

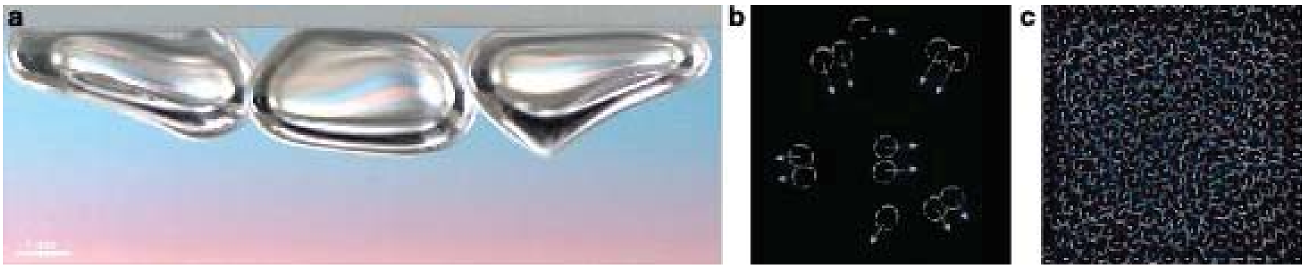

Figure 1. (a) Side view of a galloping bubble self-propelling against the top wall of a vertically vibrating fluid chamber. Representative collective dynamics in the (b) dilute and (c) dense limits, shown in top view.

References

[1] Guan, J. H., Tamim, S. I., Magoon, C. W., Stone, H. A., & Sáenz, P. J. (2025). Galloping Bubbles. Nature Communications, 16(1).

GLOBAL LINEAR STABILITY OF A BUBBLE RISING IN THE PRESENCE OF A SOLUBLE SURFACTANT

M.A. Herrada[1], J.M. López-Herrera[1], D. Fernández-Martínez[2], M. G. Cabezas[2], J. M. Montanero[2]
[1]*Depto. de Ingeniería Aeroespacial y Mecánica de Fluidos, Universidad de Sevilla, E-41092 Sevilla, Spain*
[2]*Departamento de Ingeniería Mecánica, Energética y de los Materiales and Instituto de Computación Científica Avanzada (ICCAEx), Universidad de Extremadura, E-06071 Badajoz, Spain*

Abstract Bubble rising; Path Instability; Soluble surfactant. Global linear stability.

We study the path instability of a bubble rising in the presence of a soluble surfactant both numerically and experimentally. Our numerical study presents the first global stability analysis of a bubble rising in the presence of a surfactant. We consider a fast kinetic-surfactant (Surfynol), so that the surface concentration remains at equilibrium with the volumetric one at the bubble interface. This facilitates the global stability analysis because it hinders the growth of large streamwise gradients and prevents the formation of a thin diffusive surface boundary layer.

Our experiments show significant differences between fast (Surfynol) and non-fast surfactant. Global stability analysis successfully predicts the behavior observed in the experiments without any fitting parameters. The first inestability corresponds to the transition to an oblique path (Fig. 1a) when the Galilei number (the bubble radius) rises above a threshold. This transition is followed by the coexistence of stationary and oscillatory instabilities as the Galilei number increases. This is the same sequence of transitions that occur for a rigid sphere. For the range of surfactant concentrations considered in our simulations, the Marangoni stress almost immobilizes the interface. However, the non-zero surface velocity is crucial to understand the surfactant behavior.

We examine the perturbations responsible for the primary instability. The perturbation produces a bubble deformation (Fig. 1b). The non-axisymmetric The perturbation of the velocity field causes a destabilizing vortex in the rear of the bubble (Fig. 1c), while the perturbed viscous stress produces a torque opposing this vortex. We found that the torque significantly decreases above the critical Galilei number, which may constitute the origin of instability. In particular, the torque produced by the perturbation of the viscous stress at the bubble rear decreases significantly (Fig. 1d). This allows a higher transfer of energy to the recirculation in the rear (Fig. 1c), and can produce the tilting of the main toroidal vortex of the steady flow, leading to the oblique trajectory. A similar mechanism has been described by [1] and [2] for the first bifurcation in the fixed-sphere case.

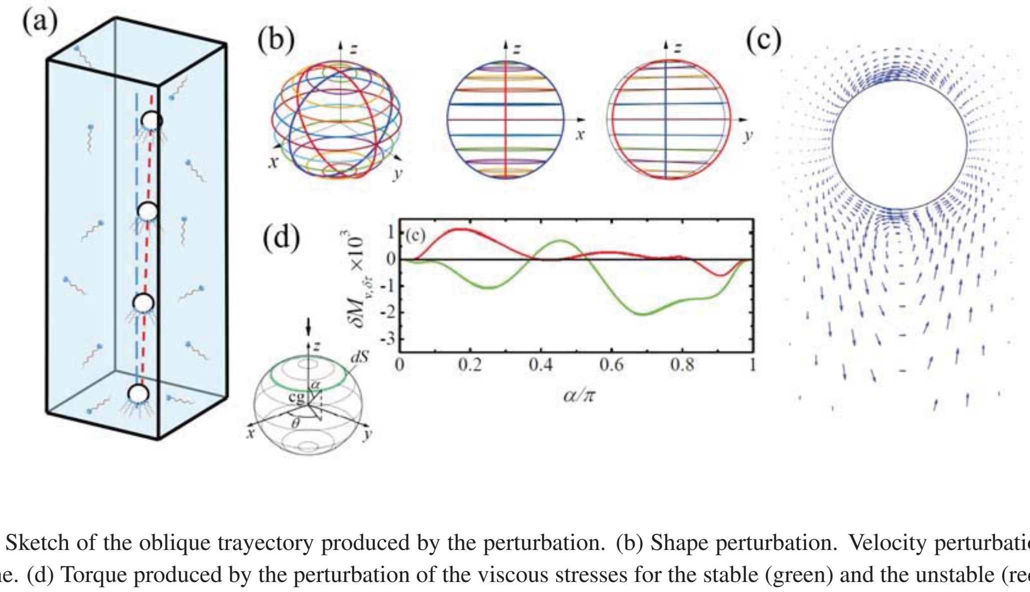

Figure 1. (a) Sketch of the oblique trayectory produced by the perturbation. (b) Shape perturbation. Velocity perturbation projection in the yz plane. (d) Torque produced by the perturbation of the viscous stresses for the stable (green) and the unstable (red) cases.

References

[1] R. Natarajan & A. Acrivos, *The instability of the steady flow past spheres and disks*, J. Fluid Mech. **254**, 323–344 (1993).
[2] P. Ern, F. Risso, D. Fabre & J. Magnaudet, *Wake-induced oscillatory paths of bodies freely rising or falling in fluids*, Annu. Rev. Fluid Mech. **44**, 97–121 (2012).

DEFORMATION AND STABILITY OF A GAS BUBBLE IN A BIAXIAL STRAINING FLOW

Aliénor Rivière[1], David Fabre[2], Jacques Magnaudet[2] & François Gallaire[1]
[1] *Laboratory of Fluid Mechanics and Instabilities, Ecole Polytechnique Fédérale de Lausanne, CH-1015 Lausanne, Switzerland*
[2] *Univ. Toulouse; Toulouse INP, CNRS, IMFT (Institut de Mécanique des Fluides de Toulouse), F-31400 Toulouse, France*

Abstract Bubbles, Deformations, Dynamics, Linear Stability Analysis.

Taking advantage of the recently developed L-ALE framework [1], we characterize the linear dynamics of an incompressible gas bubble immersed in a biaxial straining flow [2], schematized fig. 1a. We show that the system undergoes a saddle-node bifurcation with strongly different equilibrium shapes when varying the Ohnesorge number, Oh, which compares viscous and capillary effects. Equilibrium shapes are found to be oblate for sufficiently large Oh while, counter-intuitively, they are prolate for low-enough Oh, as illustrated fig. 1b. The bifurcation diagram is found to contain also two sets of disconnected branches that cannot be obtained by continuation starting from a spherical shape. One set corresponds to bubble shapes expected to be unstable, while the second set comprises a wide region exhibiting stable shapes that might be observed in practice. We then characterize the linear stability of the various branches. In addition to the unstable axisymmetric mode arising at the saddle-node bifurcation, two non-oscillating drift modes are also identified, together with a new unstable non-oscillating mode with azimuthal wave number $m = 2$. This mode might be responsible for some type of bubble breakup observed in experiments.

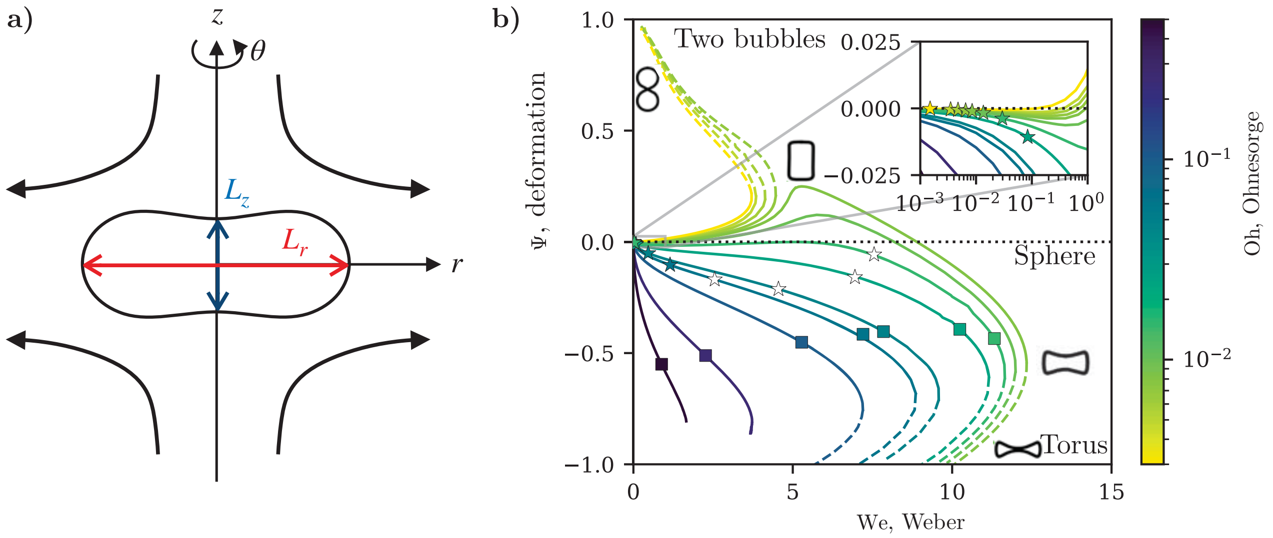

Figure 1. a) Scheme of the numerical configuration of a bubble initially centered at the stagnation point of an axisymmetric biaxial straining flow. b) Shape parameter $\Psi = (L_z - L_r)/(L_z + L_r)$ characterizing the equilibrium bubble shape as a function of the Weber number, We, caracterizing the ratio between inertial and capillary forces, for different Ohnesorge numbers. Typical bubble shapes are also represented. Dashed lines represent branches which are unstable with respect to axisymmetric perturbations. Along solid lines, an unstable drift mode, following the flow exists. In between colored and white stars, another drift mode, which goes along the z-direction, in unstable. Squares denote the appearance of a deformation mode of azimuthal wave number $m = 2$.

Acknowledgment This work is carried out thanks to the financial support of the Swiss National Foundation through the SNSF Swiss Postdoctoral Fellowship, project number 233920.

References

[1] Sierra-Ausin, J., Bonnefis, P., Tirri, A., Fabre, D., & Magnaudet, J. , *A review of fluid dynamics in videogames*, Phys. Rev. Fluids **7**, 113603 (2022).
[2] Rivière, A., Fabre, D., Magnaudet, J., & Gallaire, F., Deformation and stability of a gas bubble in a biaxial straining flow. arXiv preprint *arXiv:2511.18508* (2025).

EFFECT OF ULTRA-FAST SURFACTANTS ON DROP IMPACT ONTO ROUGH SURFACES

Sergio Rodríguez-Aparicio[1], Mario Herreruela-Rosado[1], María Guadalupe Cabezas[1], José María Montanero[4] & Emilio José Vega[1]

[1]*Departamento de Ingeniería Mecánica, Energética y de los Materiales and Instituto de Computación Científica Avanzada (ICCAEx), Universidad de Extremadura, E-06006 Badajoz, Spain*

Keywords: drop impact, rough surface, coverage area, splashing.

Abstract

The improvement of the deposition and coverage area in drop impact over rough surfaces is crucial in many industrial processes such us painting, crop spraying, injet printing, coating, etc [1]. Fast-kinetics surfactants (those with very high adsorption rates) might significantly reduce surface tension during rapid interface creation in phenomena such as jet or drop impact, which occurs on timescales of a few milliseconds [2]. Standard surfactants might fail to act on those timescales, even though they produce a considerable reduction in surface tension at equilibrium. Up to now, the effect of these ultra-fast surfactants has been scarcely assessed in the literature for the mentioned applications. This work investigates the drop impact onto surfaces with different roughness (granulometry) and hydrophobicity by using several types of surfactants in aqueous solutions. Our results show a relevant increase of the coverage area after the drop impact onto rough surfaces when ultra-fast surfactants are used (with a concentration higher than the critical micelle concentration). The change in the drop impact dynamic favors the spreading and inhibits the retraction of the liquid film.

(a) (b) (c)

Footprint

Figure 1. *Final droplet footprint on a rough surface for (a) pure water, (b) water with sodium dodecyl sulfate (SDS), and (c) water with an ultrafast surfactant (Surfynol). The addition of surfactants enhances wetting, with Surfynol yielding the largest final footprint compared to pure water and SDS.*

References

[1] N. Varghese, T. C. Sykes, M.l A. Quetzeri-Santiago, A. A. Castrejón-Pita & J. R. Castrejón-Pita, Effect of Surfactants on the Splashing Dynamics of Drops Impacting Smooth Substrates, Langmuir, 40, 8781−8790 (2024).

[2]A. L. Yarin, "Drop impact dynamics: Splashing, spreading, receding, bouncing..." Annu. Rev. Fluid Mech. 38, 159–192 (2006).

BUBBLE-INDUCED TRANSITION TO DISORDER IN A HELE-SHAW FINGER

Yunshan Jiang[1], Jack Keeler[2], Anne Juel[3] & Andrew L. Hazel[1]
[1]*Department of Mathematics, University of Manchester, Manchester, United Kingdom*
[2]*School of Mathematics, University of Birmingham, Birmingham, United Kingdom*
[3]*Department of Physics and Astronomy, University of Manchester, Manchester, United Kingdom*

Key words Saffman-Taylor instability, Hele-Shaw finger, destabilization, unstable periodic orbit.

In a liquid-filled Hele-Shaw channel operated at a fixed dimensionless flow rate Q, with continuous gas supply at the upstream end, the classical Saffman–Taylor instability induces the formation of a semi-infinite steady Hele-Shaw finger. The thin-gap approximation renders the bulk motion linear, while the nonlinear dynamics arise through the evolution of the free boundary. As the flow rate increases, the Hele-Shaw finger in experiments becomes increasingly sensitive to geometric perturbations and eventually destabilizes with disordered splitting [1]. Under controlled perturbations, the destabilization of the Hele-Shaw finger exhibits more clearly organized structures. In the experiment by Lawless et al. [2], the controlled perturbation of the finger by a small bubble on its tip induces behaviours varying from steady compound propagation, through periodic oscillations to disordered dynamics, depending on bubble size and flow rate. In particular, the disordered behavior shows features of intermittent dwelling and wandering of the system among multiple unstable periodic orbits. It is conjectured that the unstable periodic orbits induced by perturbations persist in the unperturbed chaotic dynamics where locally periodic structures still develop.

In this talk, we explore the depth-averaged modeling of free boundaries in Hele-Shaw channels and present the corresponding bifurcation structure of the finger-bubble system. A qualitative agreement between the simulation and the experiment of Lawless et al. is achieved. Different propagation modes are shown in Fig 1. In particular, effects of residual liquid films and the role of Saffman-Taylor instability in nonlinear boundary dynamics are discussed.

Furthermore, we investigate the evolution of stable orbits at increased flow rates, aiming to decompose the disordered behavior into its constituent periodic components. Recent studies highlighting the importance of unstable periodic orbits as "building blocks" of transitions to turbulence motivates our research, and we aim to confirm the role played by unstable periodic orbits in the transition of the Hele-Shaw finger.

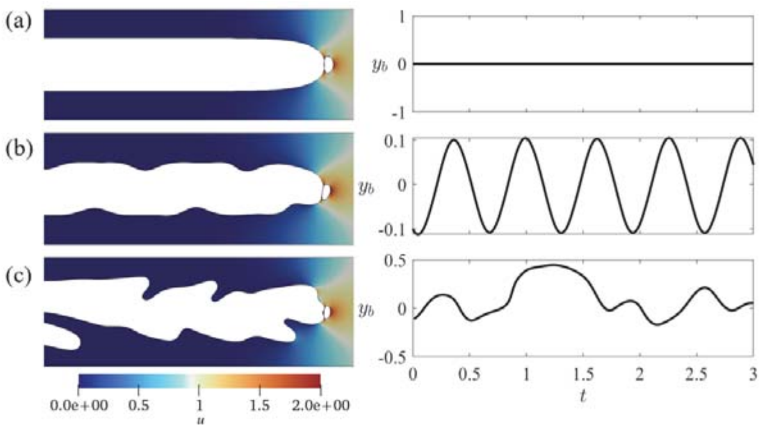

Figure 1. Left column: representative shapes with the color indicating the fluid velocity along the channel direction u. Right column: the corresponding time-evolution of the transverse location of the bubble centroid y_b. Three cases are shown: (a) steady propagation for $r = 0.12, Q = 0.025$, (b) periodic oscillation for $r = 0.1, Q = 0.1$ and (c) disordered propagation for $r = 0.085, Q = 0.28$, with r and Q representing the bubble radius and the flow rate.

References

[1] C. W. Park & G. M. Homsy, Phys. Fluids **28**, (6): 1583–1585, (1985).
[2] J. Lawless, A. L. Hazel, & A. Juel, Journal of Fluid Mechanics **1020**, A39 (2025).

WHAT IS THE EFFECT OF A DOWNSTREAM VERTICAL WALL ON THE RISE REGIME OF AN ISOLATED BUBBLE IN PURE WATER?

Teresa González-Rubio[1], Alejandro Rubio[1], Rocío Bolaños-Jimenez[2] & Emilio J. Vega[1]
[1]*Departamento de Ingeniería Mecánica, Energética y de los Materiales and Instituto de Computación Científica Avanzada (ICCAEx), Universidad de Extremadura, E-06006 Badajoz, Spain*
[2]*Área de Mecánica de Fluidos, Departamento de Ingeniería Mecánica y Minera, Universidad de Jaén and Andalusian Institute for Earth System Research, Campus de las Lagunillas, 23071 Jaén, Spain*

Keywords: bubbles rising, downstream vertical wall, bubble-wall interactions, experimental regimen map.

Abstract

This work experimentally investigates deformable nitrogen bubbles rising in ultrapure water and interacting with a vertical wall, focusing on how this downstream boundary alters their dynamics, an effect critical to many real-world processes. The experiments were conducted with a fixed Morton number, Mo = 2.64×10^{-11}, being Bond, Galilei, and Reynolds numbers in the ranges $0.08 \lesssim \mathrm{Bo} \lesssim 0.33$, $71 \lesssim \mathrm{Ga} \lesssim 194$, and $132 \lesssim \mathrm{Re} \lesssim 565$, respectively. The initial dimensionless horizontal distance between the wall and the bubble centroid was systematically varied, $0.3 \lesssim L \lesssim 5$, and the bubble trajectories from two orthogonal vertical planes were captured using high-speed imaging. While the bubble rising paths were stable without the wall presence for all the cases, the results reveal that wall proximity significantly affects the rising path, depending on Bo (or Ga) and L. A map with four distinct interaction regimes and their transitions is obtained (Figure 1): (i) Rectilinear Path (RP) at low Bo and large L, with negligible wall influence; (ii) Migration Away (MA) at higher Bo and moderate-to-large L, with lateral deviation from the wall; (iii) Collision and Migration Away (C+MA) at high Bo and small L, where bubbles first collide and then migrate away; and (iv) Periodic Collisions (PC) at low Bo, where repeated wall impacts occur due to competing forces. These findings bridge the gap between idealised simulations [1] and practical systems, offering high-quality data to support and refine computational models of bubble-wall interactions in industrial and environmental applications.

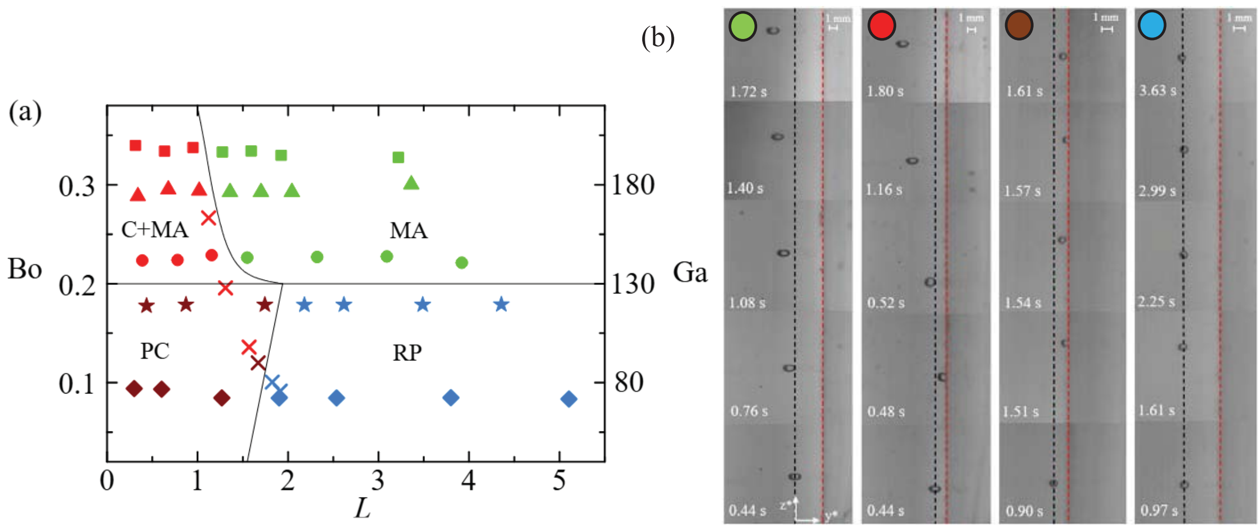

Figure 1. (a) Map of Bond and Galilei number with respect to the initial dimensionless distance between the bubble centroid and the wall L. Green symbols correspond to migration away (MA) region, red to the collision and migration away (C+MA) region, brown to periodic collisions (PC) region, and blue to the rectilinear path (RP) region. Blades are results from [2], in agreement with our experiments. Each symbol shape corresponds to a different gas injector size. The black solid lines are included to guide the eye in the regime transitions. (b) Images of the different map regimes. The circle color indicates the regime according to (a).

References

[1] P. Shi, J. Zhang & J. Magnaudet, Lateral migration and bouncing of a deformable bubble rising near a vertical wall. Part 2. Highly inertial regimes, J. Fluid Mech., 1013, A19 (2025).
[2] A.W.G de Vries, A. Biesheuvel & L. van Wijngaarden, Notes on the path and wake of a gas bubble rising in pure water, Int. J. Multiphase Flow, 28, 1823–1835 (2002).

Rheological Effects on the Axisymmetric Rising of a Single Bubble

Muhammad Yasir, Koorosh Kazemi, Jordi Pallares & Salvatore Cito
Departament d'Enginyeria Mecànica, Universitat Rovira i Virgili, 43007-Tarragona. Spain

Keywords:
Axisymmetric bubble, Galilei number, Bond number, Shear Thinning

Abstract

The dynamics of a single rising bubble in Newtonian and shear-thinning fluids are investigated numerically over a wide range of Galilei (Ga) and Bond (Bo) numbers within the predominantly axisymmetric region of the Ga–Bo phase diagram. The objective is to characterize hydrodynamic regime transitions and rise dynamics, to elucidate the coupled roles of inertia, surface tension, viscosity, and rheology in determining bubble shape, wake structure, drag evolution, and interfacial transport behaviour.

Non-Newtonian effects are modeled using the Carreau constitutive relation, allowing the local viscosity to vary with shear rate and thereby modifying the stress distribution, vorticity generation, and wake structure surrounding the bubble. The simulations are performed using the open-source finite-volume solver Basilisk [1], which combines a geometrical Volume-of-Fluid (VOF) interface-capturing method with adaptive mesh refinement (AMR). These features enable accurate and efficient resolution of coupled interfacial and hydrodynamic phenomena across a wide range of flow conditions.

Two-dimensional axisymmetric coordinates (r,z) are used in a 120 x 120 domain with initial bubble radius R = 0.5, and the bubble shape is defined by Bo = 0.1, 1, 10 and Ga = 5, 10, 20 (all parameters reported in this study are non-dimensional). Initially, the bubble is considered spherical and at rest

To extend the analysis beyond purely hydrodynamic behaviour, bubble shrinkage due to dissolution is incorporated, enabling investigation of the coupling between time- dependent bubble size, evolving hydrodynamic forces, and interfacial mass transfer characterized through Sherwood number scaling. The results reveal how rheology modifies wake structure, drag evolution, and rise velocity, and how dissolution feedback alters drag and mass-transfer characteristics. This study provides new insight into the interplay between flow stability and interfacial mass transfer in multiphase systems, with implications for CO_2 dissolution processes, subsurface gas transport, and polymer-processing applications [2].

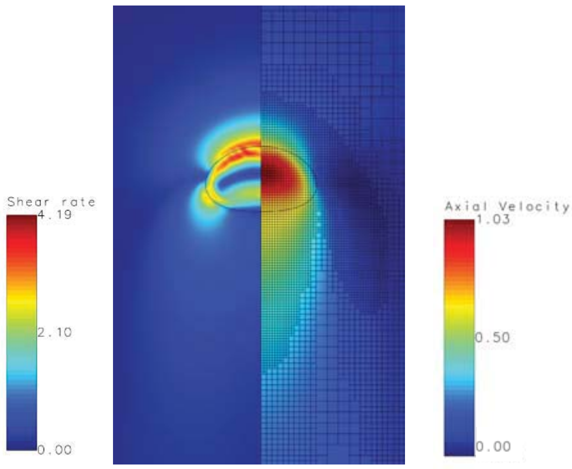

Figure 1. Zoom of the single rising bubble in a Newtonian fluid. The left half shows the shear rate and right half the axial velocity with AMR at Bo=10, Ga=20 and t=10.

References

[1] S. Popinet, see http://basilisk.fr/src/test/beach-ml.c for "Solitary wave run-upon a plane beach" (2019).
[2] Qin, Ya, Yu Chen, Di Bao, Han Zhou, Xiaojin Tang, and Zhenxing Zhu. "Review of Micronano Bubbles: Stability, Mass Transfer Performance, and Application." Industrial & Engineering Chemistry Research 64, no. 37 (2025).

Onset of ligament formation at the free surface of a liquid film on a rotating sphere

Selin Duruk[1], Finn McIntyre[1], Bradley Boyd[2] & Mathieu Sellier[1]

[1]Department of Mechanical Engineering, University of Canterbury, Christchurch 8140, New Zealand
[2]ReGenerateNZ Ltd., Christchurch, New Zealand

Keywords: Thin liquid film, ligament formation and break-up, rotary atomisation, azimuthal instability

Abstract

Rotary atomisers are simple devices that enable the breakup of a fluid stream into a myriad of small droplets. They involve a fluid jet impinging vertically at the centre of a rotating surface. Under the effect of centrifugal forces, the fluid spreads outward and forms a thin film on the surface, which ultimately disintegrates into droplets. Spinning disks are the most common rotary atomiser configuration; however, our recent preliminary experiments have revealed that, as on a disk, instabilities also develop on the surface of a liquid film on rotating spheres. This is illustrated in Fig. 1(a), which shows periodic instability inception along the sphere equator, where the film forms bulges at very regular intervals. These instabilities act as precursors to ligament formation and subsequent droplet breakup, as seen in Fig. 1(b). In the "ligament breakup mode," the number of ligaments is dictated by the most unstable wavenumber, which corresponds to the maximum growth rate of disturbances [1].

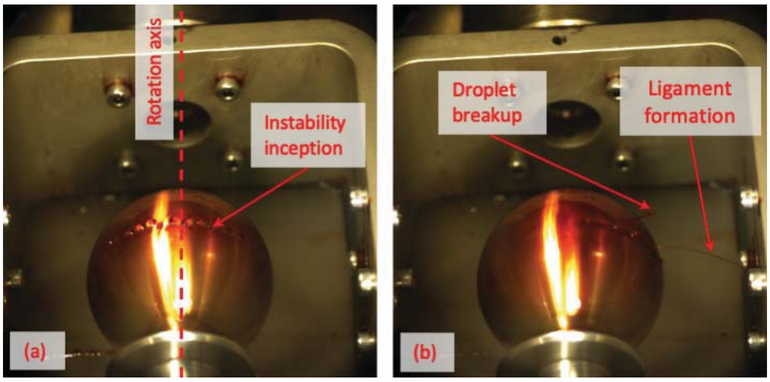

Figure 1. (a) Instability inception at the free surface of a thin liquid film on rotating sphere; (b) Ligament formation and fragmentation into droplets.

We have recently derived a general framework to describe the dynamics of thin liquid films on curved surfaces [2]. Building on this work and that of [3], we investigate the axisymmetric steady states that determine whether and where a liquid band forms on the sphere.
We then perform axisymmetric direct numerical simulations using Basilisk by solving the Navier–Stokes equations for an incompressible, two-phase interfacial flow with surface tension, incorporating the combined effects of gravity and centrifugal forces. These simulations capture the development of free-surface instabilities, the onset and growth of ligaments, and their subsequent breakup into satellite droplets.
Finally, we perform a linear stability analysis of this liquid band, which forms near the equator above a critical rotation rate. At leading order, the band is shown to be linearly stable to all non-axisymmetric perturbations. Higher-order corrections couple the normal body force to the free-surface slope, thereby breaking this structure. Numerical solutions of the linearised eigenvalue problem yield a well-defined most unstable azimuthal wavenumber, which increases monotonically with rotation rate, rising from $m^* = 11$ to $m^* = 29$ over the range considered, in good qualitative agreement with experimental observations.

References

[1] T. Kamiya, Analysis of the ligament-type disintegration of thin liquid film at the edge of a rotating disk, Journal of Chemical Engineering of Japan, *5*(4), 391-396 (1972).
[2] S. Duruk, R.G. Shepherd, E. Boujo & M. Sellier, Three-dimensional nonlinear dynamics of a thin liquid film on a spinning ellipsoid, Physics of Fluids, *35*(7) (2023).
[3] D. Kang, A. Nadim & M. Chugunova, Dynamics and equilibria of thin viscous coating films on a rotating sphere, Journal of Fluid Mechanics, *791*, 495-518 (2016).

DROP PROPULSION ALONG A VIBRATING HETEROGENEOUS RATCHET–STRUCTURED SUBSTRATE

Rodica Borcia[1], Ion Dan Borcia[1] & Michael Bestehorn[1]
[1] *Institut für Physik, Brandenburgische Technische Universität Cottbus–Senftenberg, Germany*

Abstract Keywords: controlled drop motion, computer simulation, ratchet system

We study numerically the propulsion of a microdroplet with applications for microfluidics and microgravity. The investigation will be done via a phase field model earlier developed for describing static and dynamic contact angles [1, 2, 3]. The density field is nearly constant in every bulk region ($\rho = 1$ in the liquid phase, $\rho \approx 0$ in the vapor phase) and varies continuously from one phase to the other with a rapid but smooth variation across the interface. Complicated explicit boundary conditions along the interface are avoided and capturated implicitly by gradient terms of ρ in the hydrodynamic basic equations. The contact angle θ is controlled through the boundary condition for the density at the solid substrate ρ_S, a free parameter varying between 0 and 1. The liquid drop is placed on a heterogeneous ratchet–structured substrate harmonically vibrated either in the lateral x or in the vertical z direction. A heterogeneous ratchet–structured substrate could be experimentally realized through chemical patterning, for example. In our simulation this patterning is obtained by varying ρ_S, resulting thus $\theta(x)$ indicated in Figure 1. Computer simulations are performed and discussed, studying the dependency of the droplet net driven displacement on the excitation parameters (frequency, amplitude) for forcings, respectively, in lateral x and vertical z directions [4].

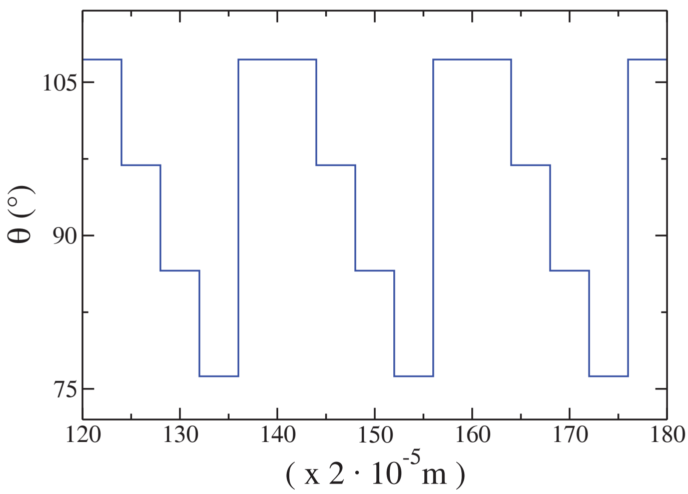

Figure 1. Heterogeneous ratchet–structured substrate realized by varying $\theta(x)$ periodically in lateral direction. Above we show only three periodic structures at the bottom boundary between the mesh points 120 and 180.

References

[1] R. Borcia, I.D. Borcia & M. Bestehorn, *Drops on an arbitrarily wetting substrate: A phase field description*, Phys. Rev. E **78**, 066307 (2008).
[2] R. Borcia, I.D. Borcia & M. Bestehorn, *Can vibrations control drop motion?*, Langmuir **30**, 14113–14117 (2014).
[3] R. Borcia, I.D. Borcia & M. Bestehorn, *Dancing drops over vibrating substrates*, Eur. Phys. J. Special Topics **266**, 1297–1306 (2017).
[4] R. Borcia, I.D. Borcia & M. Bestehorn, *Drop behavior on heterogeneous ratchet–structured substrates harmonically vibrated in lateral direction*, Langmuir **40**, 13709–13715 (2024).

SELF-LUBRICATED SPREADING OF SURFACTANT-LADEN DROPLETS

Yotam Stern[1], Victor Multanen[1] , Rafael Tadmor[1] & Roiy Sayag[1,2,3]
[1] *Dept. of Mechanical Engineering, Ben Gurion University of the Negev, Beer Sheva, Israel*
[2]*Dept. of Physics, Ben Gurion University of the Negev, Beer Sheva, Israel*
[3]*Dept. of Environmental Physics, Blaustein Institutes for Desert Research, Ben Gurion University of the Negev, Sede Boker, Israel*

Abstract Generalized framework and phase portrait for droplet spreading governed by capillarity and interfacial energy gradients.

Surfactants are known to modify fluid–fluid interfaces, yet their dynamic influence on solid–liquid interfaces during droplet spreading remains poorly understood. We investigate the spreading of non-volatile, surfactant-laden droplets using lubrication theory [1] together with experiments spanning thirteen surfactant/solvent/substrate combinations over a wide range of initial concentrations c_0. For nonpolar solvents, where the liquid–vapor surface tension remains effectively constant, we observe classical Tanner spreading [2], $r_B \sim t^{1/10}$, at low c_0. As concentration increases, a transition emerges to a distinct regime $r_B \sim t^{1/7}$, with an explicit $c_0^{1/7}$ dependence and a concentration-dependent temporal crossover between the two regimes [3]. Experiments show that this behavior originates from spatially nonuniform surfactant adsorption at the solid–liquid interface, generating gradients in γ_{SL} that reduce interfacial tangential stress. Incorporating this mechanism into lubrication theory yields a modified evolution equation and a dimensionless group, the Israelachvili number I_J, comparing solid–liquid interfacial energy gradients to capillary stresses; analysis of I_J predicts the observed crossover structure. For polar solvents, surfactants may additionally generate liquid–vapor surface tension gradients, and the ratio $\Upsilon = Ma/I_J$ governs the transition from γ_{SL}-driven spreading to a Marangoni regime. The left panel of Fig. 1 presents the resulting phase portrait unifying these regimes, while the right panel shows an experimentally observed double transition for a polar system, where Marangoni spreading follows $r_B \sim (c_0 t)^{1/4}$ [4]. This framework consolidates previously distinct spreading behaviors into a single predictive description of surfactant-governed droplet dynamics.

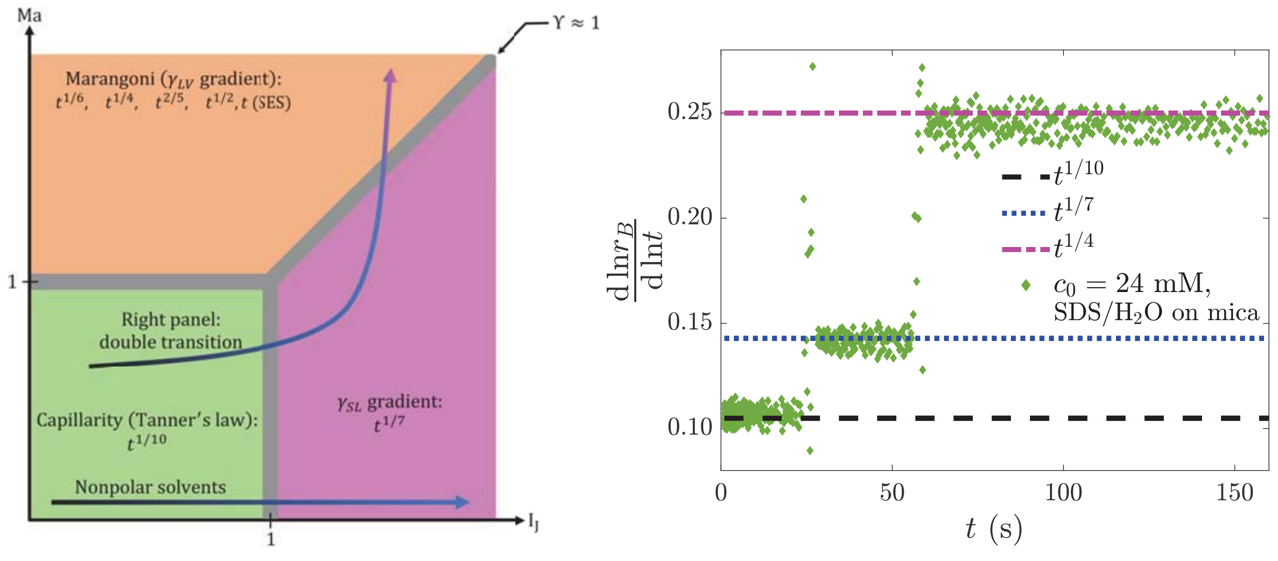

Figure 1. Left: Phase portrait delineating capillary-, γ_{SL}-, and Marangoni-governed spreading regimes. The axes represent I_J and Ma, and the diagonal corresponds to $\Upsilon = Ma/I_J = 1$. Right: Experimental demonstration of a successive double transition between capillary, γ_{SL}-driven, and Marangoni-dominated spreading for a polar solvent.

References

[1] L.M. Hocking & A. D. Rivers , *The spreading of a drop by capillary action*, Journal of Fluid Mechanics **121**, 425–442 (1982).
[2] L. H. Tanner, *The spreading of silicone oil drops on horizontal surfaces*, J. Phys. D: Appl. Phys. **12** (9), 1473 (1979).
[3] Y. Stern, V. Multanen, R. Tadmor, R. Sayag, *Self-lubricated spreading of nonpolar, surfactant-laden droplets*, Under review (2026).
[4] Y. Stern, V. Multanen, R. Tadmor, R. Sayag, *Generalized spreading of surfactant-laden droplets*, In preparation (2026).

SURROGATE MODELLING AND OPTIMIZATION OF DROPLET MOTION ON CHEMICALLY PATTERNED SURFACES VIA AUTOMATIC DIFFERENTIATION

Nikos Savva,[1,2] Anastasios Zeniou,[1] Panayiotis-Yiannis Vrionis[2] & Andreas D. Demou[2]
[1] *Department of Mathematics and Statistics, University of Cyprus, Nicosia, Cyprus*
[2] *Computation-based Science and Technology Research Center, The Cyprus Institute, Nicosia, Cyprus*

Keywords: wetting, droplets, surrogate models, inverse models

<u>*Abstract*</u>

We present a comprehensive framework for modelling and controlling the transport of thin viscous droplets on chemically heterogeneous substrates. The framework integrates two complementary components, both enhanced by automatic differentiation: (i) the development of accurate, reduced-order models for forward droplet dynamics, and (ii) a gradient-based inverse design strategy for optimizing substrate patterns to achieve controlled droplet motion.

For forward modelling, we consider a fourth-order parabolic equation for the droplet thickness, which is derived from the lubrication (long-wave) approximation of the Stokes equations. The model incorporates capillarity, slip at the solid boundary, and gravitational forcing. Building on asymptotic analyses for nearly circular contact lines developed in prior work [1,2], we construct new reduced-order models by systematically matching the bulk flow dynamics to the local dynamics in the contact line region. Automatic differentiation is employed to efficiently solve the boundary value problems arising in this matched asymptotics framework. The resulting formulation yields a lower-dimensional system of evolution equations for the Fourier modes of the contact line, significantly reducing computational cost. Numerical experiments demonstrate that the reduced model is capable of accurately capturing key dynamical features across a range of physical regimes.

For inverse design, we formulate an optimization problem to determine substrate heterogeneity patterns that guide droplets along prescribed trajectories. The objective functional penalizes deviations from target paths, and automatic differentiation enables efficient and exact gradient evaluation with respect to substrate parameters, thus accelerating convergence. This approach establishes a proof-of-concept computational pipeline for designing surface features that guide droplets along predetermined trajectories, as demonstrated through representative numerical experiments.

By leveraging automatic differentiation in both forward modelling and inverse design, this unified framework aims to advance modelling of moving contact line dynamics and to support a principled approach for engineering patterned surfaces to achieve controlled droplet transport in applications.

References

[1] N. Savva, D. Groves & S. Kalliadasis, Droplet dynamics on chemically heterogeneous substrates, J. Fluid Mech. 859, 321-361 (2019).
[2] N. Savva & D. Groves, Droplet motion on chemically heterogeneous substrates with mass transfer. II. Three-dimensional dynamics, Phys. Rev. Fluids 6, 123602 (2021).

THE EVAPORATION OF A SESSILE DROPLET INTO A CONFINED ATMOSPHERE

Caroline L. Purvis[1], Stephen K. Wilson[1] & Jennifer H. Tweedy[1]
[1] *Department of Mathematical Sciences, University of Bath, United Kingdom*

Abstract Sessile droplets, Evaporation, Diffusion

The evaporation of sessile droplets is a challenging and industrially relevant problem that has been the subject of intensive multidisciplinary research. Most previous work in this area considers an isolated droplet in an unbounded atmosphere [1]. Although "shielding effects" in multi-droplet arrays have been successfully captured [2], there has been relatively little work on the related effect of confinement of the atmosphere on the evaporation from a droplet and its consequent evolution. We aim to address this using a range of mathematical techniques to formulate and solve models for the diffusion-limited evaporation of a droplet in different confined geometries, including in particular both open- and closed-ended cylinders. In this talk I will discuss the types of confinement considered and the approaches trialled so far. Our preliminary results indicate that the commonly applied quasi-steady approximation may not be valid for some finite atmospheres, introducing an unexpected subtlety to the problem. We explore different solution methods to investigate the timescales on which this unsteady behaviour appears, and its impact on the overall evolution of the droplet. We also consider the results of varying the extent of the confinement on the lifetime of a droplet evaporating in various different modes, and compare these to the unconfined case.

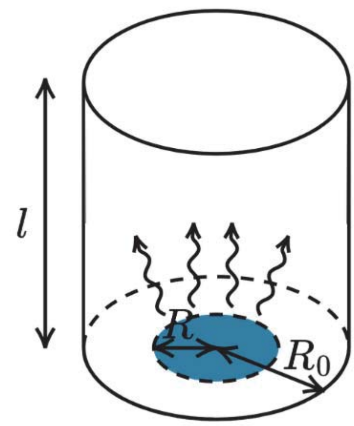

Figure 1. Diffusion-limited evaporation of a droplet in a confined cylindrical geometry

References

[1] S. K. Wilson & H. M. D'Ambrosio, *Evaporation of sessile droplets*, Annu. Rev. Fluid Mech. **55**, 481–509 (2023).
[2] A. W. Wray, B. R. Duffy & S. K. Wilson, *Competitive evaporation of multiple sessile droplets*, J. Fluid Mech. **884**, A45 (2020).

LEIDENFROST LEVITATION OF A DROPLET ABOVE A THIN LIQUID FILM

Gareth Kergoulay[1], Laurent Duchemin[1], Laurette Tuckerman[1] & Christophe Josserand[2]
[1] *PMMH, CNRS, ESPCI Paris, Université PSL, Sorbonne Université, Université de Paris, F-75005 Paris, France*
[2]*Laboratoire d'Hydrodynamique (LadHyX), UMR 7646, CNRS and Ecole Polytechnique, Institut Polytechnique de Paris, 91128 Palaiseau, France*

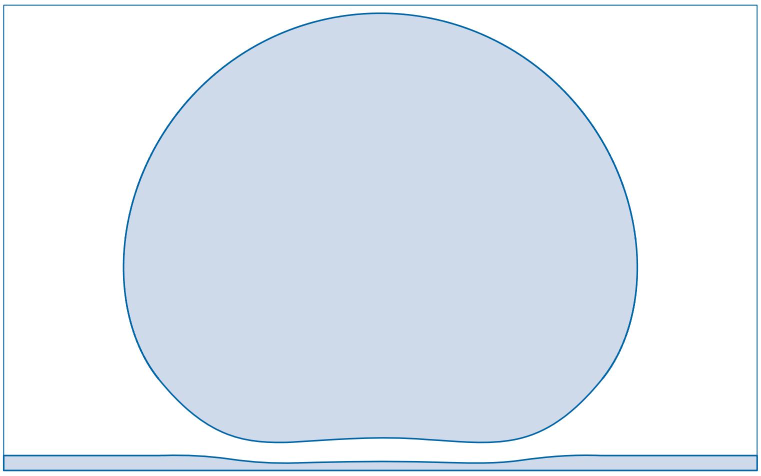

Figure 1. A droplet of radius close to the capillary length ($Bo \simeq 1$) levitating above a thin viscous film.

When a droplet of volume V is put onto a solid surface significantly hotter than the liquid's boiling point, it can levitate on a thin vapor layer. This phenomenon, known as the Leidenfrost effect, has been extensively studied, yet certain aspects remain enigmatic, particularly concerning the stability of the vapor layer and the occurrence of contact between the droplet and the solid surface. The present study aims to elucidate the coupled dynamics of the droplet and a thin liquid film beneath the vapor layer, by varying the Bond number $Bo = V^{2/3}/\ell_c^2$ which compares gravity and surface tension (ℓ_c is the capillary length), and the capillary number $Ca = \eta v/\gamma$, which compares viscous dissipation and surface tension (v is the vapor velocity at the surface of the drop). Utilizing numerical tools, we investigate the dynamics of these droplets, their stability, and the existence of static solutions.

References

[1] L. Duchemin, J. Lister, U. Lange, 2005, Static shapes of levitated viscous drops, *Journal of Fluid Mechanics*, vol. 533, 161–170.
[2] L. Duchemin and C. Josserand, 2020, Dimple drainage before the coalescence of a droplet deposited on a smooth substrate, *Proc. Natl. Acad. Sci. U.S.A.*, vol. 117, 20416–20422.
[3] J.H. Snoeijer, P. Brunet, and J. Eggers, 2009, Maximum size of drops levitated by an air cushion. *Physical Review E—Statistical, Nonlinear, and Soft Matter Physics*, 79(3), 036307.

SHORT-WAVE LINEAR STABILITY OF NON-NEWTONIAN FLUIDS DOWN A SLOPE.

Fabien Depoilly[1], Séverine Millet[1], Simon Dagois-Bohy[1] & Hamda Ben-Hadid[1]
[1] *Universite Claude Bernard Lyon 1, LMFA, UMR5509, CNRS, Ecole Centrale de Lyon, INSA Lyon, 69622 Villeurbanne France*

Abstract film flows, non-Newtonian fluids, rheology, roll waves.

Liquid films flowing down a slope occur in a wide range of industrial, natural and geophysical settings such as coating processes, heat exchangers and debris or mud flows (figure 1a). Despite the diversity of these applications, such flows share two fundamental characteristics: they are driven solely by gravity and possess a deformable free surface on which instabilities may develop as roll waves. In many situations, the fluids involved are non-Newtonian, often exhibiting shear-thinning or viscoplastic behaviour. Existing studies have largely focused on specific constitutive laws, requiring separate stability analyses for each rheology and limiting systematic comparison.
In a recent work by [1], a unified framework for the linear stability of non-Newtonian film flows down an inclined plane was proposed. Using a generalised Newtonian constitutive equation

$$\tau = \eta(\dot{\gamma})\dot{\gamma},$$

where τ denotes the viscous stress, $\dot{\gamma}$ the shear rate, and η is a known viscosity function of the shear rate kept in symbolic form throughout the calculation, a generalised Orr-Sommerfeld formulation was derived. This model was shown to recover existing theoretical results and to accurately predict the long-wave instability onset reported in the literature for various rheologies.
The present study builds upon this framework by investigating the short-wave regime through the numerical resolution of the generalised Orr-Sommerfeld equation, with particular emphasis on viscoplastic rheologies. To address numerical difficulties associated with yield stress fluids, a new regularisation of the rheological law is introduced [2]. The numerically obtained results are compared with new experimental data (figure 1b). The comparison shows encouraging agreement, suggesting that the present approach provides a realistic prediction of instability properties for viscoplastic flows and offers a complementary perspective to earlier results [3, 4] obtained using a reduced Orr-Sommerfeld formulation.

a)

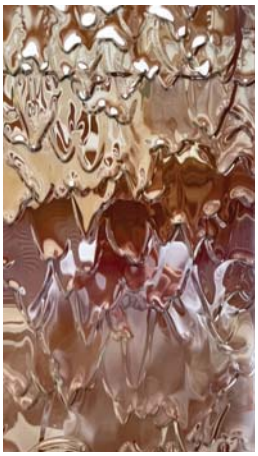

b)

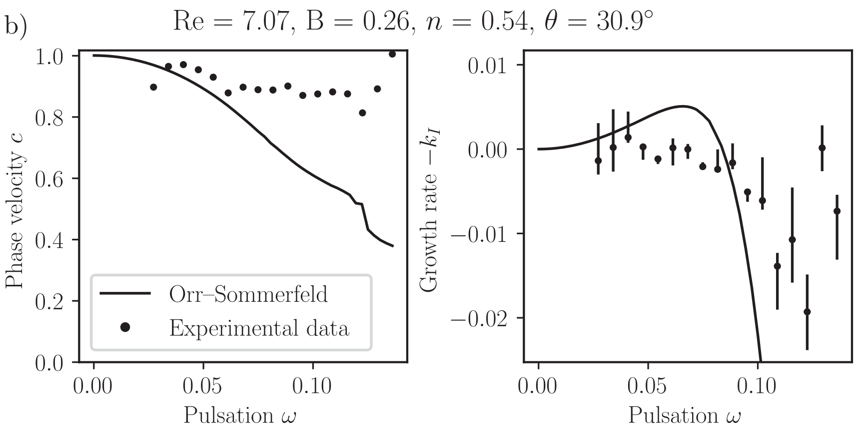

Figure 1. a) Roll waves observed on a chocolate fountain. b) Experimental and numerical dispersion curves of linear disturbances for a viscoplastic fluid flowing at $\mathrm{Re} = 7.07$, $\mathrm{B} = 0.26$, $n = 0.54$, $\theta = 30.9°$. Left: phase velocity as a function of the pulsation. Right: growth rate as a function of the pulsation.

References

[1] Depoilly F, Millet S, Ben Hadid H, Dagois-Bohy S, Rousset F Unifying the roll waves. PLOS ONE 19(11) 2024
[2] Denisenko D, Richard G.L, Chambon G A consistent three-equation shallow-flow model for Bingham fluids Journal of Non-Newtonian Fluid Mechanics 2023
[3] Balmforth NJ, Liu JJ. Roll waves in mud. Journal of Fluid Mechanics. 2004
[4] Mounkaila Noma D, Dagois-Bohy S, Millet S, Botton V, Henry D, Ben Hadid H. Primary instability of a visco-plastic film down an inclined plane: experimental study. Journal of Fluid Mechanics. 2021

Influence of the long-scale substrate topography on interface deformation and Bénard-Marangoni instability of evaporating liquid films

Robin Behle, Peter Stephan & Tatiana Gambaryan-Roisman
Technical University of Darmstadt, Institute for Technical Thermodynamics, Peter-Grünberg-Str. 10, Darmstadt 64287, Germany

Keywords: Marangoni convection, Bénard-Marangoni instability, structured surfaces, evaporation of films, film deformation

Abstract

Evaporation of liquid films from heated surfaces occurs in coating and printing processes, in chemical processing, and in cooling systems. Evaporation of pure liquids into a non-condensable gas may be accompanied by the thermal Marangoni convection, which occurs when the surface tension varies with temperature along the liquid-gas interface. Marangoni convection may arise from an intrinsic instability or be triggered by substrate topography and roughness [1-3].

We experimentally study the influence of the geometric parameters of the long-scale substrate topography on the dynamics of evaporating films of fluorinated HFE-7100 deposited on heated copper substrates. Three substrates with sinusoidal grooves of wavelengths 5 mm, 9 mm, and 18 mm were used. The wall temperature was varied from 25 to 50°C. The transient film thickness was measured along a 4.5 mm-long line using a confocal line sensor. The results of measurements were used to extract the evaporation rate and the evolution of the film deformation. In addition, we visualized the liquid-gas interface shape using Schlieren reflectometry. The long-wave analysis predicts an increase of film deformation with increasing evaporation rate and wavelength of the wall topography [2]. Our experimental findings agree with these trends (Fig. 1). However, we observed that the amplitude of the film deformation was significantly below the predicted values. This discrepancy can be explained by the influence of the short-wave Bénard–Marangoni instability, which generates convection cells that modify the temperature distribution along the liquid–gas interface [3]. Furthermore, the dynamics of interface deformation depends on the wavelength of the substrate. Specifically, the substrate with the largest wavelength exhibited chaotic interface oscillations, whereas no such behavior occurred on the substrate with the smallest wavelength. We analyze the effect of the topography wavelength on the stability properties of the evaporating film.

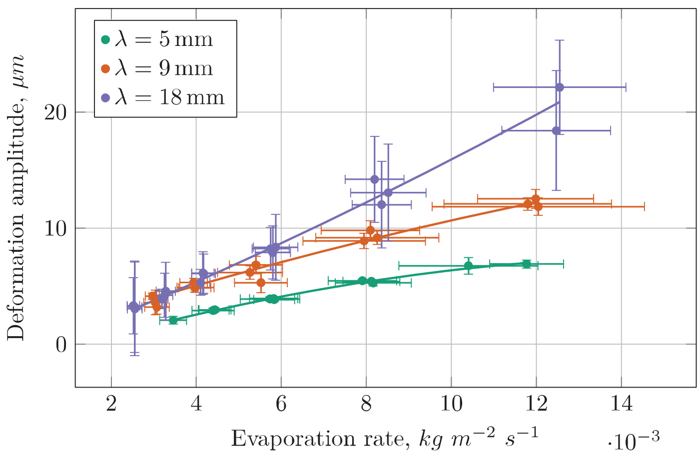

Figure 1. Liquid-gas interface deformation as a function of mean evaporation rate, for substrates with wavelengths (λ) of 5 mm, 9 mm, and 18 mm.

References

[1] T. Gambaryan-Roisman, *Modulation of Marangoni convection in liquid films.* Advances in colloid and interface science 222, 319–331 (2015).

[2] A. Bender, P. Stephan, T. Gambaryan-Roisman, *Numerical investigation of the evolution and breakup of an evaporating liquid film on a structured wall*. International Journal of Heat and Fluid Flow 70, 104–113 (2018).

[3] R. Behle, P. Stephan, T. Gambaryan-Roisman, *Thermocapillary convection and interface deformation in evaporating liquid films on a structured surface*, SSRN, doi: http://dx.doi.org/10.2139/ssrn.5954751 (2025).

FALLING FILMS OVER A PERFORATED PLANE

Supriya Karmakar & C. Ruyer-Quil
Université Savoie Mont Blanc, UMR 5271, LOCIE, 73376 Le Bourget du Lac, France

Abstract structured packing, perforated sheet, thin films, film thickness, liquid curtain, varicose waves

Wet cooling towers are widely used in industrial processes, where structured packings made of thin, vertically oriented corrugated and perforated sheets arranged in parallel promote liquid redistribution. In this study, we consider a simplified yet representative configuration: a thin liquid film flowing on both sides of a vertical plate containing a single perforation. Experiments [2] show that, when liquid fills the perforation, a so-called *curtain mode* develops. This mode is characterized by the formation of a capillary ridge upstream of the perforation, an inertial ridge downstream, and a varicose wave standing on the liquid curtain.

We model the gravity-driven flow of a viscous Newtonian film over a single perforation by representing the geometry as a trench-like profile. The transition from a no-slip boundary condition on the solid plate to a no-shear boundary condition across the perforation is implemented using a Navier-slip boundary condition, with slip length varied continuously to provide a smooth transformation between the two regions. Using a depth-averaged framework, we derive five coupled evolution equations governing the film thickness h, the local flow rate q, and three additional variables quantifying deviations from the classical semi-parabolic Nusselt velocity profile. The mathematical formulation constitutes an extension of the weighted-residual integral boundary-layer (*WRIBL*) method proposed by Ruyer-Quil and Manneville [3]. The model predictions are validated against direct numerical simulations [1] and experiment measurements [2] (see fig. 1). The model accurately captures film-thickness variations and reproduces the key features of the curtain mode. In particular, the curtain mode is found to be highly sensitive to the steepness of the perforation walls. We further analyze the influence of perforation size, imposed flow rate, and liquid properties on the film thickness and on the wavelength of the standing varicose waves.

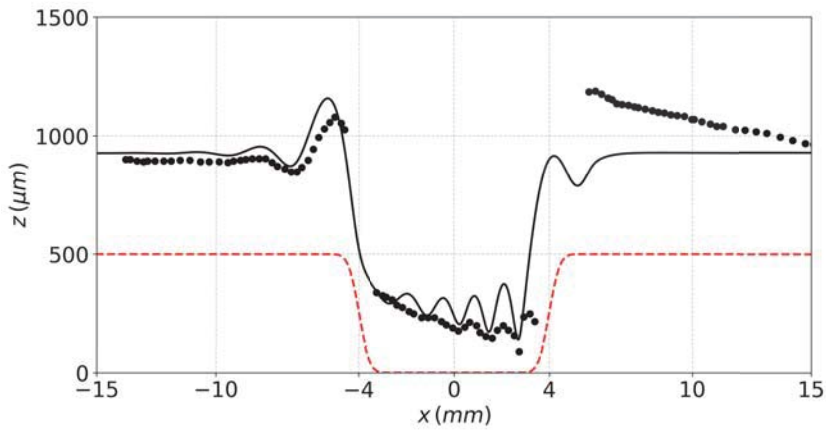

Figure 1. [$Re = 36$, $\Gamma = 348$ (Propan 2-ol)] Free surface profile for plate thickness of 1 mm ($t_p = 0.5$ mm), perforation diameter $d_p = 8$ mm and steepness parameter $w_p = 0.5$. Black dots represent experimental measurements reported in [2]

References

[1] Xie, Hanguang and Hu, Jianguang and Dai, Gance, *Numerical simulation on flow behavior of twin-liquid films over a vertical plate with an open window*, AIChE J. **64**, 1458-1468 (2018)
[2] Periyapattana, Manasa Srinivas Iyer, *Experimental study of liquid films on the structured packing elements of distillation columns*, Theses, Université Paris-Saclay (2021)
[3] Ruyer-Quil, Christian and Manneville, Paul, *Improved modeling of flows down inclined planes*, Eur. Phys. J. B **15(2)**, 357–369 (2000)

REDUCED EQUATIONS FOR A THIN LIQUID FILM SUBJECTED TO SOLAR RADIATION

Omair A. A. Mohamed[1,2], Christian Ruyer-Quil[3], & Luca Biancofiore[4]
[1] *Laboratoire d'hydrodynamique (LadHyX), Ecole Polytechnique, 91120 Palaiseau, France*
[2] *Department of Mechanical Engineering, Bilkent University, 06800, Ankara, Turkiye*
[3] *LOCIE, Université Savoie Mont Blanc,73000 Chambéry, France*
[4] *Department of Industrial and Information Engineering and Economics, University of L'Aquila, 67100 L'Aquila, Italy*

Abstract Thin liquid film, solar radiation, mathematical modeling.

The operating temperature of a photovoltaic (PV) cell can be drastically reduced by the introduction of a thin film of fluid flowing over its surface, which has been shown to result in increased electrical output [1], extended operating lifetime [2], as well as preventing the soiling of its surface. Moreover, studies have indicated that the heat transfer across a wavy liquid film can be up to $10 - 100\%$ larger than that of a flat film [3], and therefore, investigating the complex relationship between the dynamic behavior of the wavy liquid film and the temperature profile across it can yield valuable insights towards optimizing such a system. Typically, dealing with this problem requires the numerical solution of the Fourier heat problem coupled with the Navier-Stokes equations, which is prohibitively expensive for the parametric studies required for a comprehensive understanding of the physical phenomena involved.

Therefore, we tackle this complex problem by employing the Weighted Integral Boundary Layer [4] (WIBL) method to model the hydrodynamics of the film in conjunction with an asymptotic decomposition of the temperature variable [5]. The system of equations governing the temperature field is then truncated consistently in line with the *least-degeneracy principle*, such that all physical effects are retained at leading order. The overall temperature field can be reconstructed by projecting the ansatz chosen for the temperature correction using polynomial functions, allowing parametric studies of this difficult problem. Notably, we also account for the refraction of the incoming solar rays at the liquid interface resulting in a transient distribution of the thermal flux at the solid wall that is coupled to the evolution of the liquid interface.

Our model captures various complex phenomena arising from the intricate interplay between the different heat transfer modes and the physical properties of the liquid and the solid surface, including demonstrating the stabilization of the Marangoni instability due to the concentration of the incoming solar rays under the crests of the liquid interface. This is demonstrated in Fig. 1 which compares the temporal growth rates corresponding to the absence of refraction ($\kappa = 0$) and in its presence ($\kappa = 0.3$).

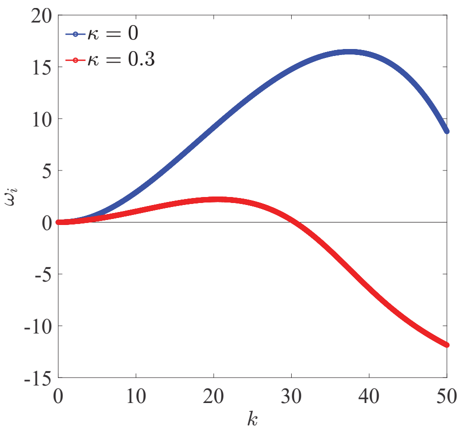

Figure 1. Plot of the temporal growth rate (ω_i) against wavenumber (k) in the absence of refraction ($\kappa = 0$), as well as in its presence ($\kappa = 0.3$). Note the strong stabilization introduced by the refraction effect.

References

[1] S. Krauter, *Solar Energy Materials and Solar Cells*, vol. 82, no. 1, pp. 131–137, 2004. CANCUN 2003.
[2] S. Kurtz, K. Whitfield, D. Miller, J. Joyce, J. Wohlgemuth, M. Kempe, N. Dhere, N. Bosco, and T. Zgonena, *2009 34th IEEE Photovoltaic Specialists Conference (PVSC)*, pp. 002399–002404, 2009.
[3] P. Yoshimura, T. Nosoko, and T. Nagata, *Chemical Engineering Science*, vol. 51, no. 8, p. 1231 – 1240, 1996.
[4] C. Ruyer-Quil and P. Manneville, *Eur. Phys. J. B*, vol. 15, pp. 357–369, May 2000.
[5] N. Cellier and C. Ruyer-Quil, *Int. J. Heat Mass Transf.*, vol. 154, p. 119700, June 2020.

PARTIAL WETTING ON NON-IDEAL SOLID SUBSTRATES AND LARGE BOND NUMBERS

Marc Medale[1] & Roudy Issa[1]
[1] *Aix-Marseille University, CNRS, IUSTI Marseille, France*

Abstract This work presents results at macroscopic scale of partial wetting on non-ideal solid substrates and large Bond numbers.

A macroscopic sessile drop in contact with a horizontal solid substrate is considered. When its size is much smaller than the capillary length (tiny Bond numbers) the vertical gradient in mean curvature of liquid-fluid interface is negligible, and the sessile drop shape looks like a spherical cap. The macroscopic contact angle (MCA) is given by Young-Dupré equation (YDe) for ideal solid substrate [1]. Once the size of the problem is on the scale of its capillary length or above it (moderate to large Bond numbers), the sessile drop shape strongly departs from a spherical cap. Almost all works solve for Laplace's equation [2] along the liquid-fluid interface together with YDe as a boundary condition at contact line. Despite a widespread practice one can wonder how legitimate is this approach to model real-life experiments, for which many conditions deviate from those involved in the derivation of YDe. So, the question we have addressed in this work is: does the MCA depend on the Bond number?

Experiments have been conducted to investigate the volume dependency (from 1 μl up to 1 ml) of sessile drops spanning a wide range of Bond numbers. The liquid was continuously injected into the sessile drop from below by a motorized syringe through a tiny hole drilled in the substrate to result in a monotonously advancing contact line. Distilled water lying on different substrates (PMMA, Aluminum with and without coatings) were considered. To better interpret our experimental results we have also derived the equations governing the static equilibrium of such sessile drop from the conservation of total energy. Although it is assumed at thermodynamical equilibrium, the sessile drop is not an isolated system, so it exchanges mechanical work with the substrate and surrounding fluid until equilibrium satisfies the conservation of total energy. While most of the mechanical work is reversible, that associated with the contact line displacement on non-ideal substrate is not and induces dissipation. This irreversibility along with the pinning at contact line are both responsible for the differential behavior observed when contact line advances or recedes, causing a hysteresis in MCA.

The main results of this work are: i) the equilibrium shape of a sessile drop on a horizontal solid wall results from two competing effects: the vertical gradient in mean curvature of the liquid-fluid interface leads to the drop flattening and spreading on the substrate, which induces a decrease in MCA; this spreading in turn induces the contact line to advance, which on a non-ideal substrate increases the MCA; ii) the greater the ratio between the sessile drop height and mean curvature of its liquid-fluid interface, the greater its deformation under the effect of gravity compared to weightlessness; iii) parametric studies reveal that the MCA depends on the Bond number over a wide range of values, cf. fig. 1 (left). For moderate to large Bond number values ($0.1 \ll \mathrm{Bo}$), YDe which predicts a unique value of the MCA, provides only an approximation of the MCA. Thus, in these cases, it is advisable to avoid combining the sessile drop method and YDe to correctly identify the solid-liquid and solid-fluid interfacial free energies.

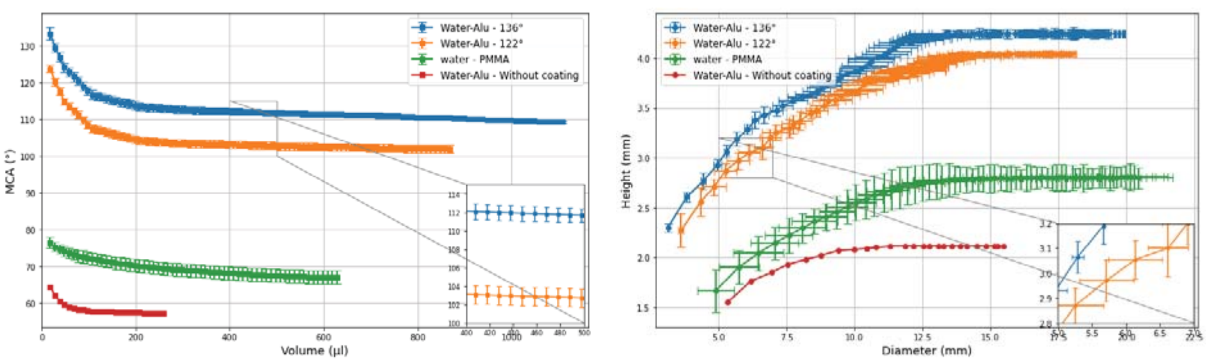

Figure 1. Experimental results. Left: macroscopic contact angle vs drop volume. Right: drop height vs drop diameter.

References

[1] de Gennes P. G., Brochard-Wyart F. & Quéré D., *Capillarity and Wetting Phenomena.* Drops, Bubbles, Pearls, Waves. Springer New York, NY (2004).

[2] Laplace P. S., *Supplément au livre X du Traité de Mécanique Céleste. Sur l'action capillaire.* Gauthier- Villars, Paris (1806).

RIGOROUS VALIDATION OF CONTACT-LINE SIMUALTIONS USING OPENFOAM

Conor Quigley[1], Lennon Ó Náraigh [1]
[1] *School of Mathematics and Statistics, University College Dublin, Belfield, Dublin 4, Ireland*

Abstract We propose a rigorous examination of existing open-source dynamic contact-angle models in OpenFOAM. We correct their defects and validate the resulting model with respect to benchmark contact-angle flows, in particular the well-studied droplet-impact problem.

We consider the problem of modelling moving contact lines using the OpenFOAM computational modelling framework. OpenFOAM is an attractive option for computational modelling as it is a well supported open-source framework, allows for complex mesh generation, and provides the user with a range of pre-defined solvers for simulating fluid-flow problems. The framework also provides for multiphase flow simulations using a finite-volume method called `interFOAM`. However, the framework only comes equipped with very simplistic methods for solving problems involving a moving contact line. In this work, we investigate existing open-source contact-line models freely available in the OpenFOAM ecosystem (e.g. via online repositories) which allow for a dynamic contact angle through the Kistler–Hoffman contact-angle model. Many of these open-source solutions are not rigorously validated with respect to experimental works. For this reason, we rigorously examine the open-source Kistler–Hoffman models, correct their defects, and validate the resulting simulations against benchmark contact-angle flows, in particular, the droplet-impact study by Roisman *et al.* [1]. Our approach involves a particularly challenging validation, as we consider not only the dynamic contact angle but also, contact-angle hysteresis. Our work has implications for computational modelling of instability, as above the splash threshold, the rim-lamella regime of droplet impact (e.g. Figure 1) no longer applies, and hydrodynamic instabilities give rise to complex splashing patterns. Only by modelling the contact-line dynamics correctly can such short-timescale instabilities be properly captured.

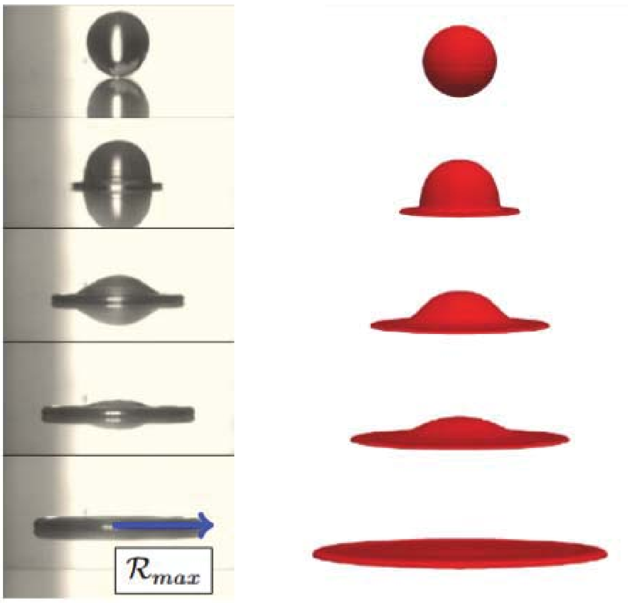

Figure 1. The concept of the validation study: shown on the left are frames from high-speed video analysis of droplet impact conducted in-house. Shown on the right are snapshots of simulation results at the same times. This work proposes a rigorous quantitative validation of simulations (right) with respect to experiments (left). Parameters: $\mathrm{We} = 20$, $\mathrm{Re} = 1700$.

References

[1] Roisman, I.V., Opfer, L., Tropea, C., Raessi, M., Mostaghimi, J. and Chandra, S., *Drop impact onto a dry surface: Role of the dynamic contact angle*, Colloids and Surfaces A: Physicochemical and Engineering Aspects, **322(1-3)**, pp.183-191 (2008).

VALIDITY OF APPROXIMATE MODELS FOR ION PERMEABILITIES IN BIOLOGICAL NANOPORES.

Blessing Nansubuga[1,2], Luca Biancofiore[1] & Mauro Chinappi[2]
[1] *Department of Industrial and Information Engineering and Economics, University of L'Aquila, L'Aquila, Italy*
[2] *Department of Industrial Engineering, University of Rome Tor Vergata, Rome, Italy*

Abstract
Analytical derivation and validation of GHK and Nernst-like formulations for ionic transport in nanoscale biosystems, with Poisson–Nernst–Planck–Stokes simulations.
Keywords: nanoscale biosystems; ionic transport; GHK equation; Nernst-like equation; Poisson–Nernst–Planck; computational fluid dynamics.

Recent studies have questioned the validity and range of applicability of simplified continuum and constant-field models for nanoscale ionic transport, highlighting the need for more physically consistent formulations that account for coupled electro-diffusive and hydrodynamic effects [1, 2]. As shown in Figure 1A, nanoscale ionic transport is typically investigated by considering ion flow through a nanopore membrane under an applied electrochemical potential difference. In this work, we critically reassessed two widely adopted theoretical frameworks for nanoscale ion transport: the Goldman-Hodgkin-Katz (GHK) [3, 4] and Nernst-like [5] models. As illustrated in Figure 1B, both frameworks relate the measured current-voltage response to the reversal voltage V_r, from which the permeability ratio and the transference-number ratio can be explicitly extracted. These quantities offer physically interpretable measures of ionic selectivity under electrochemical gradients. We evaluate them against published experimental data to assess their consistency and interpretability. We further test the two relations against a computational fluid dynamics (CFD) framework built on the coupled Poisson-Nernst-Planck (PNP) and Stokes equations. This enables high-fidelity simulations of electro-hydrodynamic ion transport in nanoscale biosystems and allows systematic exploration of the interplay between electric fields, concentration gradients, and fluid flow. Overall, this approach connects analytical modelling, experimental validation, and CFD-based simulation, contributing to the modelling of nanoscale biosystems.

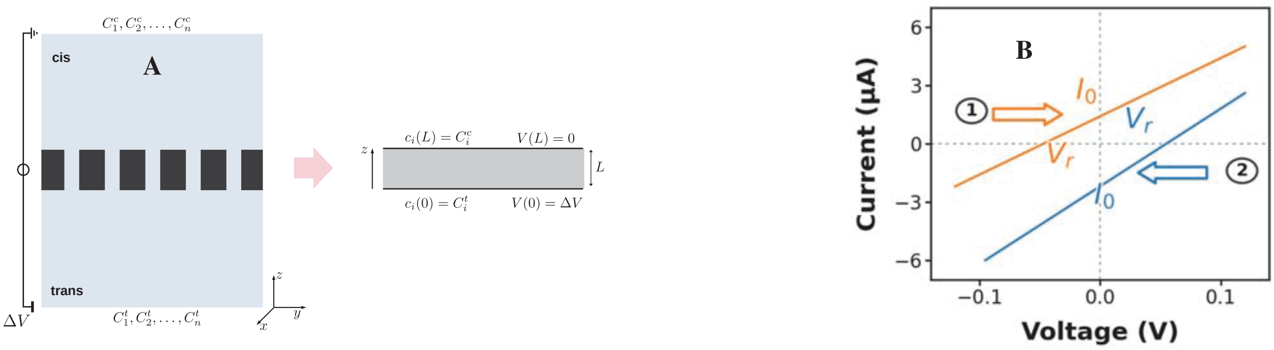

Figure 1. Schematic representation of the nanopore membrane system and associated current-voltage characteristics. Figure 1A shows the membrane geometry and applied electrochemical conditions. Figure 1B shows a representative current–voltage curve highlighting the reversal voltage V_r. From the measured value of V_r, GHK and Nernst-like formulations allow the extraction of the ionic permeability ratio and transference-number ratio.

References

[1] Y. Green, *Goldman–Hodgkin–Katz equation, reverse electrodialysis, and everything in between*, Phys. Rev. E **111**(6), 064408 (2025).
[2] M. Baldelli, G. Di Muccio, F. Viola, A. Giacomello, F. Cecconi, S. Balme, and M. Chinappi, *Performance of single nanopore and multi-pore membranes for blue energy*, Chem.Phys.Chem **25**(23), e202400395 (2024).
[3] D. E. Goldman, *Potential, impedance, and rectification in membranes*, J. Gen. Physiol. **27**, (1943).
[4] A. L. Hodgkin and B. Katz, *The effect of sodium ions on the electrical activity of the giant axon of the squid*, J. Physiol. **108**, (1949).
[5] S. Zhang, J. Wang, A. Yaroshchuk, Q. Du, P. Xin, M. L. Bruening, and F. Xia, *Addressing challenges in ion-selectivity characterization in nanopores*, J. Am. Chem. Soc. **146**(16), 11036–11042 (2024).

CONTACT ANGLE HYSTERESIS ON SLIPPERY MICROPATTERNED BIPHILIC LIQUID-LIKE SURFACES

Ruiheng Hu[1], Glen McHale[2], Hernán Barrio-Zhang[3], Chiara Neto[4], Gary G. Wells[1]
Institute for Multiscale Thermofluids, University of Edinburgh,
EH10 5HF, Edinburgh, United Kingdom

Keywords: Contact angle, Defects, Hydrophobicity, Hysteresis, Liquids

Abstract

Droplet and bubble shedding is essential to applications such as self-cleaning, anti-icing, and boiling heat transfer, yet is often limited by contact-line pinning. We study pinning on slippery biphilic surfaces composed of hydrophilic microdomains patterned within a hydrophobic SCALS background, where both materials exhibit ultralow contact angle hysteresis (~3°). Roll-off experiments show that pinning follows a strong dilute-defect model at low (<35%) and high (>65%) Cassie-area fractions, while intermediate fractions lead to contact-line faceting and more variable roll-off angles. A single parameter, a = 0.54 ± 0.04, captures the pinning behaviour for both hydrophilic-in-hydrophobic and hydrophobic-in-hydrophilic configurations. We also provide an expression for the pinning force per defect based on contact angles and defect geometry. These results clarify how microscale heterogeneity governs liquid mobility on slippery surfaces.

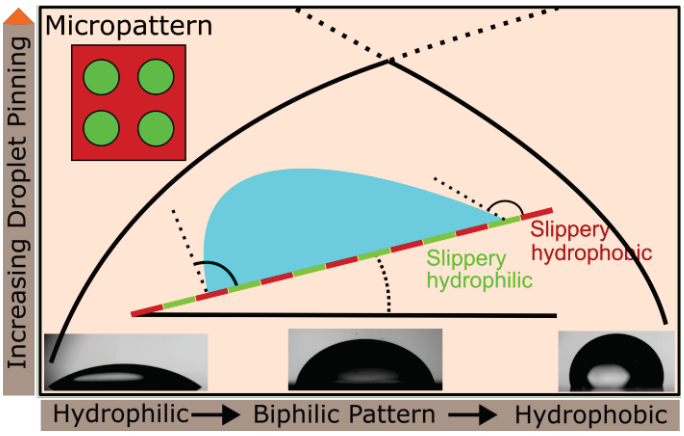

Figure 1. Change in Droplet Pinning as Surface Wettability Shifts from Hydrophilic to Hydrophobic

References

[1] Ruiheng Hu, Glen McHale, Hernán Barrio-Zhang, Chiara Neto, and Gary G. Wells, Langmuir 2025 41 (42), 28579-28591, DOI: 10.1021/acs.langmuir.5c03793

NONLINEAR DYNAMICS OF FARADAY WAVES AT THE SURFACTANT-COVERED FREE SURFACE OF THE VERTICALLY VIBRATED NON-ISOTHERMAL LIQUID

Alexander B. Mikishev[1] & Alexander A. Nepomnyashchy[2]
[1]*Department of Engineering Technology, Sam Houston State University, Huntsville, TX 77341, USA*
[2]*Department of Mathematics, Technion – Israel Institute of Technology, Haifa 32000, Israel*

Keywords: Marangoni convection, Faraday waves, amplitude equation

Abstract

We consider a deep-water container that is vibrated vertically and subjected to a vertical temperature gradient (see Figure 1). Parametric excitation induced by the vibration leads to the appearance of Faraday ripples on the liquid's free surface. Vertical heating of the liquid, as well as the presence of an insoluble surfactant spread over the free surface, act as two additional factors that influence stability.

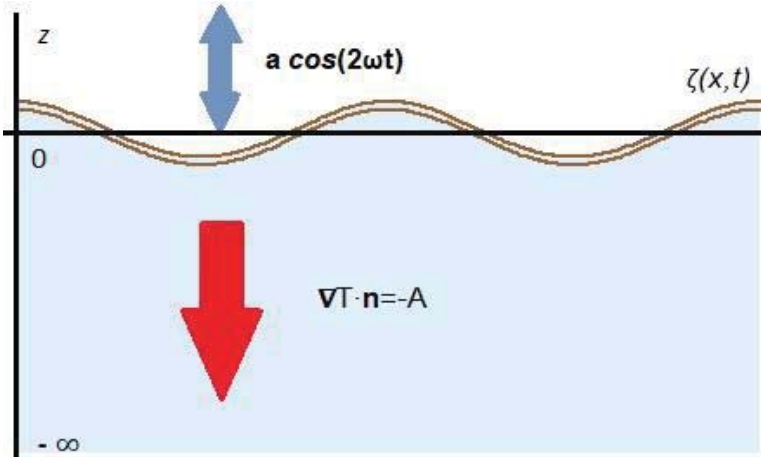

Figure 1. Schematic of the problem

To simplify the complexity of the problem, we consider a two-dimensional configuration and adopt the semi-infinite approximation, meaning that the liquid layer thickness H and the typical disturbance wavenumbers k satisfy $kH \gg 1$. Consequently, lateral boundary effects are neglected, and the nonlinear interactions of growing capillary waves determine the symmetry and wavelengths of the resulting regular patterns.

The linear theory of this process was developed earlier in [1], predicting that the parametric resonance occurs for arbitrarily small driving amplitudes. In the nonlinear regime, we employ a multi-scale approach. All variables in the problem are expanded into series of a small parameter ε, defined as the ratio of the viscous skin layer thickness to the capillary length. This procedure yields an amplitude equation, which is then analyzed.

References

[1] A.B. Mikishev & A. A. Nepomnyashchy, Faraday waves at the surfactant-covered free surface of the vertically vibrated non-isothermal liquid, Phys. Fluids 37, 064102 (2025).

Cold Droplet Impact on a Heated Liquid Film: Coupled Cavity Dynamics and Thermal Mixing

Jemimah Magit[1], Rajab Omar[1], Wigdan Kisha[1] & David Hann[1]
[1] *Faculty of Engineering, University of Nottingham, Nottingham, UK*

Keywords: Droplet impact; Droplet breakup; Heated liquid film; Thermal mixing; Surface tension effects

Abstract
Understanding droplet impact on liquid films is central to predicting the efficiency of spray cooling, aeroengine lubrication, and thermal management systems. Although impacts on dry heated surfaces are extensively studied [1], the coupled hydrodynamic and thermal behaviour of cold droplets striking hot liquid films remains insufficiently understood, particularly regarding cavity evolution, jetting, mixing, and transient heat transfer [2]. This work experimentally investigates a cold-water droplet (D = 3.35 mm) impacting a 21 mm deep heated water film at U = 2.57 m/s under inertia-dominated conditions. Film temperatures range from 31°C to 78°C. Synchronised high-speed and infrared imaging (IR) are used to simultaneously capture cavity dynamics and surface temperature evolution.

Figure 1 demonstrates paired high-speed and IR images highlighting the key impact mechanisms. Immediately after impact, a corona forms and ejects secondary droplets that are colder than the film, confirming that the crown droplets originate from largely unmixed droplet liquid. The impact of the droplet causes an increase in surface temperature around the point of impact as the core fluid upwells around the impact location.

During cavity growth and collapse, a proportion of the cold liquid is trapped by the collapsing cavity and gradually mixes with the hot film. Some of the droplet liquid is carried upward in the jet tip, and the varying surface temperature (and so surface tension along the jet) prompts the detachment of the cold liquid as a separate drop.

These mechanisms will be explored further in the full presentation.

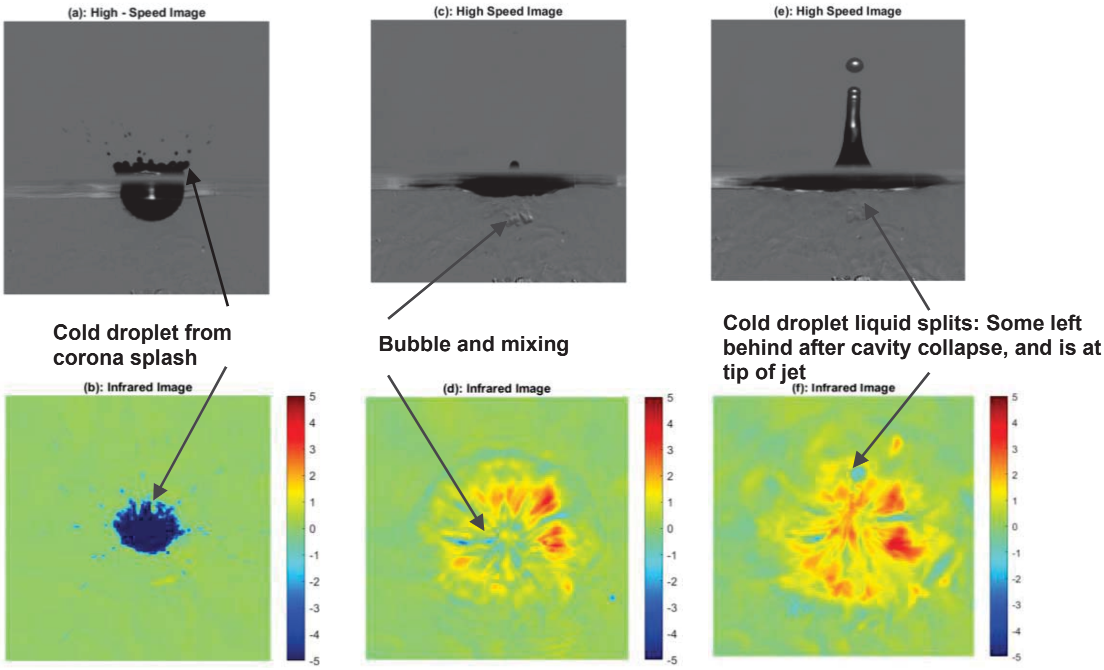

Figure 1. Sample of Sequential Images of a Cold Drop (D= 3.35mm, U= 2.57m/s, Td=22 ^{0}C) Impacting onto a Hot Film (T_f = 58 ^{0}C) and showing that the variation of temperature affects the mixing and Droplet Production.

References

[1] C. Josserand and S. T. Thoroddsen, "Drop impact on a solid surface," Annual Review of Fluid Mechanics, vol. 48, pp. 365–391, 2016.

[2] Hann, D. B., Underhill, E. R., & Mitchell, A. (2016). The Effect of Film Temperature on crater morphology during the impact of a single droplet. MATEC Web Conf., 84, 00015.

IMMERSED BOUNDARY-LATTICE BOLTZMANN METHOD FOR WETTING PROBLEMS

Elisa Bellantoni[1,2,3], Fabio Guglietta[2], Andreas Demou[1], Francesca Pelusi[4], Kiwon Um[3], Mihalis Nicolaou[1,6], Mathieu Desbrun[5], Mauro Sbragaglia[2], & Nikos Savva[1,7]

[1] *CaSToRC, The Cyprus Institute, 20 Konstantinou Kavafi Street, 2121 Nicosia, Cyprus*
[2] *Dept. of Physics & INFN, Tor Vergata University of Rome, Via della Ricerca Scientifica, 1-00133 Rome, Italy*
[3] *LTCI, Télécom Paris, IP Paris, 19 Place Marguerite Perey, 91120 Palaiseau, France*
[4] *CNR - Istituto per le Applicazioni del Calcolo, Via dei Taurini 19, 00185 Rome, Italy*
[5] *Inria and LIX (École Polytechnique), IP Paris, 1 rue Honoré d'Estienne d'Orves, 91120 Palaiseau, France*
[6] *Dept. of Computer Science, University of Cyprus, 1 Panepistimiou Avenue, 2109 Nicosia, Cyprus*
[7] *Dept. of Mathematics and Statistics, University of Cyprus, 1 Panepistimiou Avenue, 2109 Nicosia, Cyprus*

Abstract Droplets, wetting, lattice Boltzmann, immersed boundary.

The study of wetting is a captivating problem laying at the intersection between physics, chemistry and engineering. The multi-scale nature of this phenomenon makes it challenging to model, calling for advanced numerical techniques. We present an immersed boundary-lattice Boltzmann (IB-LB) method [1] to tackle this task, improving on existing work [2] in scope and applicability, in order to reproduce droplets on a horizontal, homogeneous solid substrate ranging from hydrophobic to hydrophilic wetting regimes.

The droplet's non-ideal sharp interface, modelled via the immersed boundary (IB) method, is coupled to the inner and outer fluids resolved via the lattice Boltzmann (LB) method; the wetting interaction with the substrate is achieved through a force term designed with the key computational advantage of providing a regularization of the interface profile close to the contact line, avoiding abrupt curvature changes that would cause numerical instabilities. Extensive model validations against analytical results for equilibrium droplet shape and scaling laws for droplet spreading dynamics are addressed. Furthermore, comparisons against other independent solvers are presented to investigate the hydrodynamic behaviour of the IB-LB method in relation to the implemented contact-line model [3].

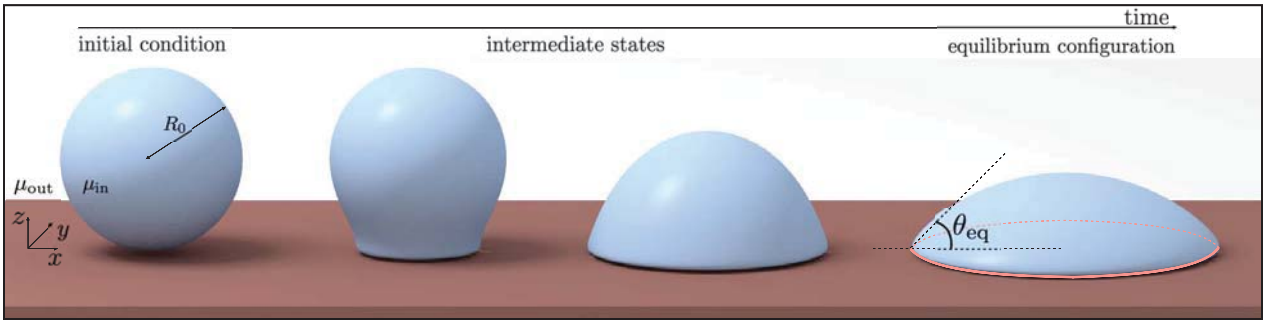

Figure 1. Numerical simulation of a droplet spreading on a flat substrate with the IB-LB method. The spreading process drives an initially spherical droplet of radius R_0 towards its equilibrium shape with contact angle $\theta_{\rm eq}$. Different viscosities $\mu_{\rm in}$ and $\mu_{\rm our}$ are used for the fluid inside and outside of the droplet respectively.

This research is supported by the European Union's HORIZON MSCA Doctoral Networks programme, under Grant Agreement No. 101072344, project AQTIVATE (Advanced computing, QuanTum algorIthms and data-driVen Approaches for science, Technology and Engineering).

References

[1] **E. Bellantoni** et al., Phys. Rev. E **112**, 025305 (2025).
[2] F. Pelusi et al., Phys. of Fluids **35**, 082126 (2023).
[3] , **E. Bellantoni** et al.,arXiv, arXiv:2604.17463 (2026).

AXIAL INSTABILITY IN INERTIAL LIQUID ENTRAINMENT BY A ROTATING DRUM

J. John Soundar Jerome, Pierre Trontin & Jean-Philippe Matas
Université Claude Bernard Lyon 1, LMFA, CNRS UMR 5509,
Boulevard du 11 novembre 1918, F–69622 Villeurbanne cedex, France

Abstract Inertial coating; surface instability; directional Saffman–Taylor; liquid entrainment.

Liquid entrainment on the outer rising wall of a rotating cylinder is a generic configuration in coating and process engineering. While ribbing and fingering instabilities are well documented in the viscous (low-Reynolds) regime [1], the mechanisms selecting patterns when inertia becomes dominant remain unclear. Here we report a robust axial "ribbing" pattern observed during high-speed rotary drag-out, where the entrained liquid organizes into an ensemble of quasi-vertical thin sheets along the drum axis.

Experiments are performed with a drum of radius $R = 19.5$ cm and width 30 cm, partially immersed in a reservoir. The working fluids are water and water–UCON mixtures (30% UCON in mass), with dynamic viscosity up to $\mathcal{O}(10^2)$ times that of water. The rib spacing is extracted from image intensity profiles across the drum width. Over the investigated parameter range, the most probable wavelength depends very weakly on the linear velocity and immersion depth, and remains in the narrow interval $\lambda \approx 3.5$–4.5 cm for all fluids.

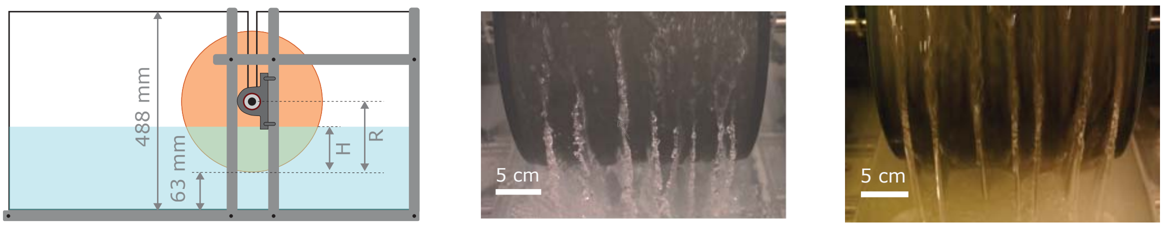

(a) (b) (c)

Figure 1. a) Side view schematics of experimental setup. Water depth can be changed to control the drum immersion b) Examples of ribbing patterns in water, linear velocity 3.8 m/s and c) water/UCON mixture of approximately 100 times the viscosity of water, 1.6 m/s. Immersion is 10% of drum radius in both cases.

We propose that the axial pattern is triggered by a primary instability driven by an adverse pressure gradient in the meniscus region of the rotary Landau–Levich–Derjaguin flow, analogous to the directional Saffman–Taylor instability [2]. A lubrication-based model yields the most probable spacing $\lambda^* = 2\pi\, l_c\sqrt{\frac{3}{\xi}}$, where $l_c = \sqrt{\sigma/(\rho g)}$ is the capillary length and ξ is the corresponding dimensionless mean adverse pressure gradient for the inclined-plate drag-out analogue. The resulting scaling $\lambda \propto l_c$ is consistent with the measured wavelengths [3].

Numerical Simulations of the two-phase incompressible Navier–Stokes equations (Basilisk, adaptive octree grid and VOF interface tracking) reproduce both the ribbing patterns and the wavelength selection. They show a pressure gradient exists in the film, as predicted by our model. In addition, simulations confirm the predicted sensitivity to surface tension and density variations (doubling or halving λ when σ or ρ are modified accordingly).

We will finally discuss the impact of viscosity on the instability, and how a Rayleigh-Taylor instability due to the centrifugal force [4] can be recovered when viscosity is further increased up to $\mathcal{O}(10^3)$ times that of water.

References

[1] D. A. Reinelt, *The primary and inverse instabilities of directional viscous fingering*, J. Fluid Mech. **285**, 303–327 (1995).
[2] P. G. Saffman & G. I. Taylor, *The penetration of a fluid into a porous medium or Hele–Shaw cell containing a more viscous liquid*, Proc. R. Soc. London A **245**, 312–329 (1958).
[3] John Soundar Jerome, P. Trontin & J.-P. Matas, *Ribbing patterns in inertial rotary drag-out*, J. Fluid Mech. **1007** A84 (2025).
[4] P. G. Saffman & G. I. Taylor, *Behaviour of a viscous film on the outer surface of a rotating cylinder*, Journal de Mécanique **16** (1977).

DYNAMICS OF BUBBLE RISE NEAR THE LIQUID-VAPOR CRITICAL POINT VIA COMPRESSIBLE PHASE-FIELD MODEL

Deewakar Sharma & Sakir Amiroudine
Université de Bordeaux, I2M, UMR CNRS 5295, Talence, F-33400, France

Keywords: Near-critical fluids, Compressible fluids, bubble rise, Two-phase flow

Abstract

The behavior of fluids near their liquid-vapor critical point is quite intriguing attributed to the various thermophysical properties showing singularity at the critical point [1], such as high isothermal compressibility even in the liquid phase. This peculiarity of these properties renders the dynamics of fluid flow quite challenging in the vicinity of critical point. As a first step of simulating complex phenomena in the near-critical region, we propose an isothermal two-phase model based on the phase-field modeling approach. The literature is abundant with studies using phase-field method for incompressible fluids while for compressible fluids, several studies have used diffuse interface method (similar to phase-field method but using density as a parameter to distinguish between the two phases). The model proposed in this work is based on using a scalar phase field parameter ϕ denoting mass fraction of phase 2 to distinguish between the two phases, as described in [2], in conjunction with the compressible model described in [3, 4]. In addition to solving the governing equations for conservation of mass and momentum, the model comprises of Cahn-Hilliard equation adapted for compressible fluid for the phase-field variable. The mobility parameter in Cahn-Hilliard equation is evaluated as described in [5] and is adapted for compressible model. The equation of state requires to evaluate the pressure in terms of state variables density (ρ) and (ϕ) and is derived in terms of isothermal compressibility (χ_T).

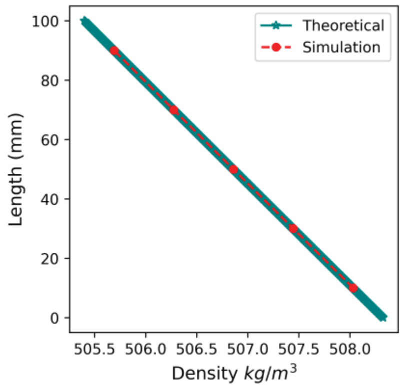

Figure 1 : Stratified density profile in 1D case

The derived model is validated for numerous cases before using it to study the vapor bubble rise near the critical point. Firstly, we validate the model in a single phase for a stratified density due to the high compressibility with the analytical expression as shown in Fig. 1. Further, we compare the rise of oxygen bubble in the liquid oxygen at 90.1 K and pressure of 1 bar with gravity being 0.4g as described in the experiment [6] and a good agreement is observed. We then compare the results obtained with the current model with those obtained from fully incompressible model [5]. To account for incompressibility of both the phases, their compressibility was set to be very small ($\chi_T = 10^{-14}\ Pa^{-1}$) rendering their behavior to be incompressible to the numerical precision. Lastly, comparison between bubble rise velocity for various proximities to the critical point is done and results for two of them is shown in the Fig. 2c. Lower velocity on approaching the critical point is attributed to a smaller difference in densities of both the phases and thus a lower buoyancy force.

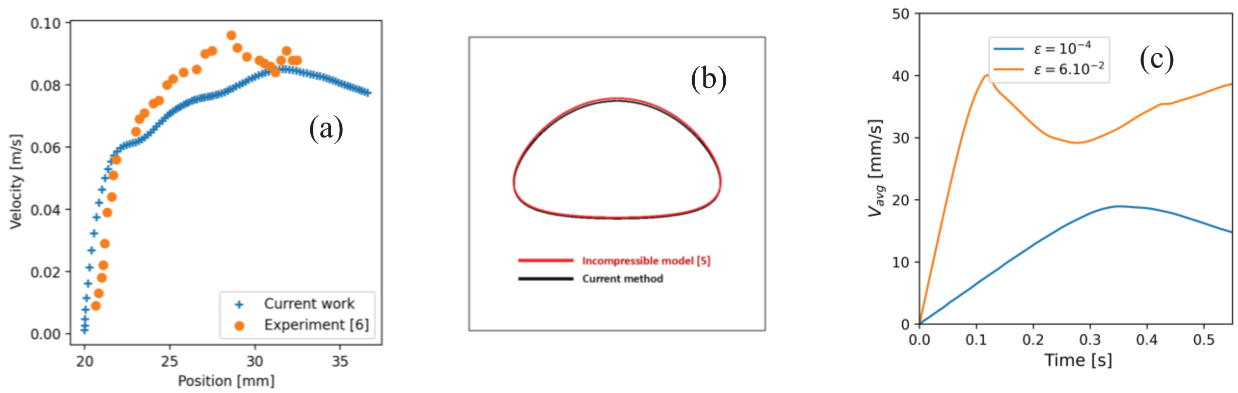

Figure 2: a) Comparison with experimental work for rise of oxygen bubble in liquid oxygen at 90.1K [6] (b) Test cases comparing the bubble rise dynamics for density ratio 10 at t = 3s in incompressible fluid c) comparison of bubble rise for different proximities to the critical point.

References

[1] B. Zappoli, D. Beysens, Y. Garrabos, Heat Transfers and Related Effects in Supercritical Fluids, 1st ed., Springer Netherlands, 2014. https://doi.org/10.1007/978-94-017-9187-8.
[2] Z. Guo, P. Lin, A thermodynamically consistent phase-field model for two-phase flows with thermocapillary effects, J. Fluid Mech. 766 (2015) 226–271. https://doi.org/10.1017/jfm.2014.696.
[3] S. Amiroudine, J.P. Caltagirone, A. Erriguible, A Lagrangian–Eulerian compressible model for the trans-critical path of near-critical fluids, Int. J. Multiph. Flow 59 (2AD) 15–23. https://doi.org/10.1016/j.ijmultiphaseflow.2013.10.008
[4] D. Sharma, A. Erriguible, S. Amiroudine, Numerical modeling of the impact pressure in a compressible liquid medium: application to the slap phase of the locomotion of a basilisk lizard, Theor. Comput. Fluid Dyn. 31 (2017) 281–293. https://doi.org/10.1007/s00162-017-0422-4.
[5] D. Sharma, M. Coquerelle, A. Erriguible, S. Amiroudine, Adaptive interface thickness based mobility—Phase-field method for incompressible fluids, Int. J. Multiph. Flow 142 (2021) 103687. https://doi.org/10.1016/j.ijmultiphaseflow.2021.103687.
[6] A. Mongruel, G. Gandikota, D. Chatain, A. Mailfert, P. Andriamananjaona, and D. Beysens, Transient Rising of Oxygen Bubbles in a Fast Varying Gravity, International Journal of Multiphase Flow 168, 104560 (2023).

Stability analysis of dense-gas/liquid annular two-phase flow with liquid entrainment

Edson O. da Silva[1], Oscar M. H. Rodriguez[2]
[1,2] *Industrial Multiphase Flow Laboratory (LEMI), Mechanical Engineering Department, São Carlos School of Engineering, University of São Paulo (USP), Brazil*

Keywords: annular two-phase flow, dense gas, interfacial shear stress, droplet entrainment, flow transition

Abstract

The hydrodynamic stability of annular two-phase flow is dictated by the shear stress exerted by the gas flowing over the interface of a wavy, thin liquid film, since the drag force is much stronger than the gravity force acting on the entire film body. Negligible liquid entrainment and low film velocity are two assumptions often included to simplify the theoretical approach. Presumably, droplet entrainment and relative velocity play a key role in the stability of annular flow when the gas phase density becomes comparable with that of the liquid phase. Large content of carbon dioxide occurs in some ultra-deepwater offshore scenarios, and sulphur hexafluoride is used in the present experiments to simulate two-phase flow conditions of low liquid/gas density ratios. In this study, one aims to investigate two transition mechanisms of annular flow: the suspension of entrained droplets by the shearing action and drag force of the gas core [1], and the film instability due to the formation of an unstable velocity profile at the wall region [2]. Upward-vertical experiments were carried out with mineral oil (867 kg/m^3, 20 mPa·s) and dense gas (100 kg/m^3) at pressures (P) of about 15 bara. Figure 1(a) displays the preliminary results obtained from the analysis of the first-mentioned mechanism by assuming two possible cases, i.e., one for fixed gas mass flux and another for fixed gas momentum flux, while Fig. 1(b) shows the total pressure drop against the superficial dense gas velocity $\langle j_g \rangle$ for low liquid superficial velocities. In Fig. 1(a), the trend of $\langle j_g \rangle$ with the rise of P at constant momentum flux of gas is, as expected, quite similar to the predicted values using the transition model [1]. Note in Fig. 1(b) that the minimum $\langle j_g \rangle$ associated with the transition to annular flow occurs between 1.5 and 2.5 m/s, which is above the predicted value of 1.25 m/s at 13.3 bara [1]. The film instability mechanism will be investigated by treating annular flow as a gas core laden with liquid droplets in the presence of a liquid film, and the interfacial shear stress is suitably defined to account for the effects of droplet entrainment and the relative velocity between the gas core and film interface velocities [3].

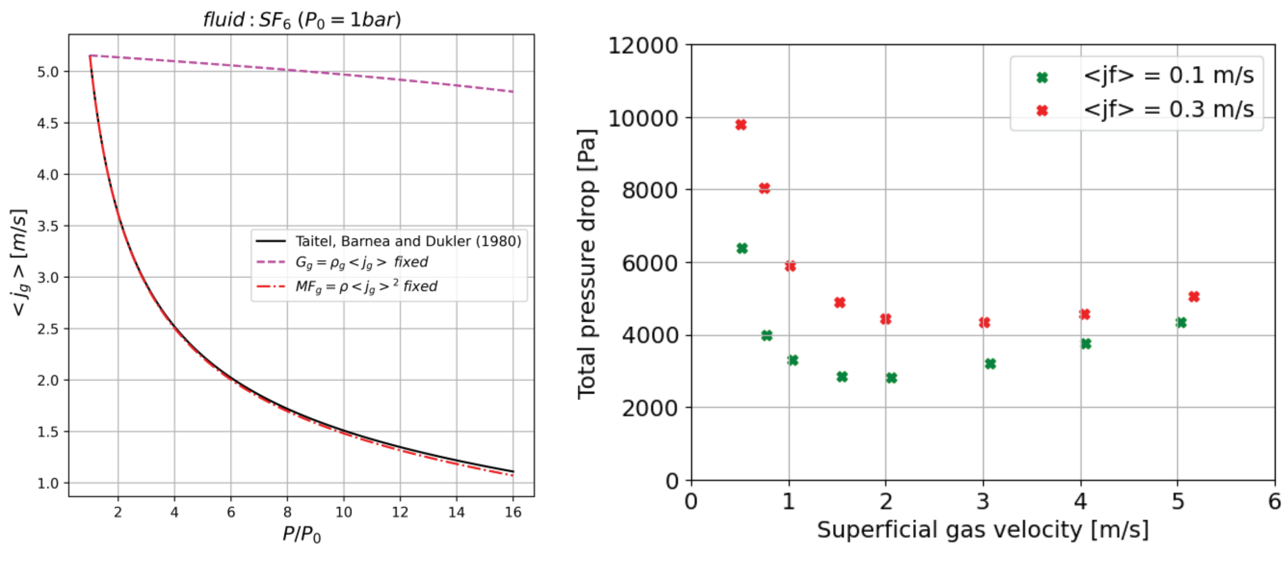

Figure 1. (a) Results obtained for fixed gas mass flux and (b) Data points collected from a 24.35 mm i.d. vertical pipe

References

[1] Y. Taitel, D. Barnea & A. E. Dukler, Modelling flow pattern transitions for steady upward gas-liquid flow in vertical tubes, AIChE Journal 26, 345-354 (1980).
[2] D. Barnea, Transition from annular flow and from dispersed bubble flow – unified models for the whole range of pipe inclinations, Int. J. Multiphase Flow 12, 733-744 (1986).
[3] R. V. A. Oliemans, B. F. M. Pots & N. Trompé, Modelling of annular dispersed two-phase flow in vertical pipes, Int. J. Multiphase Flow 12, 711-732 (1986).

PREDICTION OF DRYOUT INCEPTION FOR BOILING CO_2 IN PIPE FLOWS: TOWARD SAFER AND SUSTAINABLE PARTICLE DETECTOR COOLING

Giuseppe Arnone[1], Giulio Cantini[2], Florinda Capone[3], Mauro Carnevale[4] & Jacopo A. Gianfrani[3]

[1] *Istituto Nazionale di Alta Matematica "Francesco Severi", Rome, Italy*
[2] *Departement of Mechanical Engineering, University of Bath, United Kingdom*
[3] *Dipartimento di Matematica e Applicazioni "R. Caccioppoli", University "Federico II" of Naples, Italy*
[4] *Department of Engineering and Applied Sciences, University of Bergamo, Dalmine (BG), Italy*

Abstract Interfacial instability, Dryout inception, Annular flow, Linear stability, Liquid-vapour interface, CO_2.

Carbon dioxide is a cost-effective, reliable, and environmentally friendly refrigerant that is increasingly used in evaporator design. A thorough understanding of the underlying flow physics, along with accurate predictions of phase change through boiling, is crucial for the widespread adoption of CO_2 as a coolant. Among the various physical phenomena involved, dryout inception is particularly critical because it marks the transition from annular to mist flow. This transition associated with a sudden drop in the heat transfer coefficient, which can have potentially catastrophic consequences. Two opposing behaviors regarding the onset of dryout, from now on defined as δ^- and δ^+ regimes, have been reported in [1]. The δ^- regime is characterized by a decreasing dryout vapor quality with increasing mass flux, whereas the δ^+ regime—more relevant for CO_2 in microchannels—exhibits an increasing dryout vapor quality with mass flux. A detailed experimental campaign conducted at CERN has provided unprecedented insight into the mechanisms leading to dryout inception.

In this presentation, I will introduce a mathematical model developed to predict the instability of the smooth liquid-vapor interface characterizing annular flow. This model is motivated by the ansatz that *dryout occurs due to the disruption of the interface caused by interfacial instability*.

Within the framework of continuum mechanics, we derive the mathematical model by imposing the conservation of momentum and mass astride the interface, [2]. Heat exchange between liquid and vapor has been modelled through a density production term (Hsieh's hypothesis, [3]), while the normal component of the stress tensor at the interface was described by the Young-Laplace equation. Once the interfacial conditions were obtained along with the governing equations in dimensionless form, we have performed an instability analysis, introducing a key dimensionless group characterizing the onset of dryout. Numerical investigation show that the correlation between mass flux and dryout vapor quality is consistent with the experimental data (see Fig. 1), validating the hypothesis that dryout inception is governed by interface instabilities.

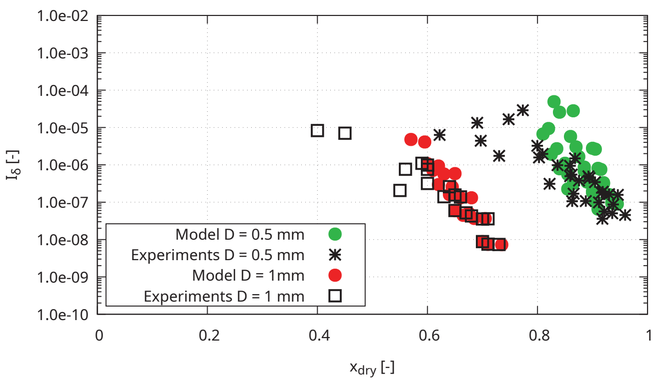

Figure 1. Comparison between results obtained via numerical investigations on the theoretical model and experimental data.

References

[1] Ducoulombier M., Colasson S., Bonjour J., Haberschill P., **Carbon dioxide flow boiling in a single microchannel–Part II: Heat transfer**, *Experimental Thermal and Fluid Science*. 2011. 35, 4. 597–611.
[2] Cantini G., Arnone G., Capone F., Gianfrani J.A., Carnevale M. **Interfacial instability as a trigger for dryout inception in two-phase CO_2 flow**, *submitted*.
[3] Hsieh D.Y., **Interfacial stability with mass and heat transfer**, *The Physics of Fluids*. 1978. 21, 5. 745–748.

DOWNWARD DENSE-GAS/LIQUID PIPE FLOW: EXPERIMENTAL CHARACTERIZATION AND LINEAR STABILITY ANALYSIS

P. J. Miranda-Lugo[1], Jorge E. Arrollo-Caballero[1], C. E. Álvarez-Pacheco[1], Freddy A. P. Morales[1], Gabriel M. B. Cruz[1], Ivan Perissini[1] & Oscar M. H. Rodriguez[1]

[1]Industrial Multiphase Flow Laboratory (LEMI), Mechanical Engineering Department, São Carlos School of Engineering (EESC), University of São Paulo (USP).

Keywords: Dense gas, Downward flow, Hydrodynamic stability, Stratified flow pattern transition, Two-phase flow.

Abstract

Downward two-phase flow is increasingly relevant in applications such as carbon capture and storage (CCS), enhanced oil recovery, and flow assurance [1, 2]. These flows exhibit hydrodynamic behaviours that differ markedly from those observed in upward configurations, which can be explained by how inertial and gravitational forces act with respect to each other and in relation to the flow direction [3, 4, 5]. Existing models still show limited accuracy in predicting void fraction and frictional pressure gradient in downward gas-liquid flow [1, 2, 6, 7]. Another challenge is predicting flow pattern transition boundaries, particularly when viscous liquids or dense gases are involved. In the latter case the high gas density makes the gas-liquid flow exhibit a hydrodynamic behaviour comparable to that of a liquid-liquid flow under certain conditions. Nevertheless, classical instability models, such as the inviscid and viscous Kelvin-Helmholtz criteria, do not accurately predict the stratified-flow region, likely due to the closure relations employed [8]. This study presents an experimental and theoretical investigation of downward two-phase flow with a low liquid-gas density ratio ($\rho_l/\rho_g \approx 8$) at multiple inclinations, conducted in a new 30 m-long stainless-steel test facility with a 52.5 mm internal diameter. Flow patterns were characterized using high-speed video recording combined with synchronized measurements of void fraction and pressure drop. Data on void fraction were obtained by gamma-ray densitometry, while frictional and total pressure gradients were determined from time-series pressure drop measurements. The results demonstrated that pipe inclination and the presence of dense gas significantly influence flow pattern transition, void fraction, and pressure gradients. The low-density ratio effect was found to affect flow-pattern transition boundaries not only in gravity-dominated operational envelopes, but also in turbulence-dominated ones. The one-dimensional two-fluid model and the hydrodynamic linear stability analysis are the chosen tools to model the stratified dense-gas/liquid flow pattern transition, which were adapted from liquid-liquid models [9, 10]. The dataset generated in this work advances the understanding of downward two-phase flow, aiding to the refinement of current models for predicting flow pattern transition, void fraction, and pressure gradients.

References

[1] A. Arabi, R. L. Höhn, J. Pallares, and Y. Stiriba, "New modeling approaches for liquid holdup and pressure drop in vertical downward gas-liquid two-phase flow," *International Journal of Multiphase Flow*, p. 105371, 2025.

[2] H. Bouyahiaoui, F. Saidj, A. Arabi, A. Al-Sarkhi, and A. Azzi, "Vertically downward gas-liquid flow: Void fraction and pressure drop," *International Journal of Multiphase Flow*, vol. 172, p. 104711, 2024.

[3] S. M. Bhagwat and A. J. Ghajar, "Similarities and differences in the flow patterns and void fraction in vertical upward and downward two phase flow," *Exp Therm Fluid Sci*, vol. 39, pp. 213–227, 2012.

[4] O. Shoham, "Mechanistic modeling of gas-liquid two-phase flow in pipes," 2005.

[5] G. B. Wallis, *One-dimensional two-phase flow*. New York: McGraw-Hill, 1969.

[6] H. Bouyahiaoui, A. Azzi, A. Zeghloul, A. H. Hasan, A. Al-Sarkhi, and M. Parsi, "Vertical upward and downward churn flow: Similarities and differences," *J Nat Gas Sci Eng*, vol. 73, p. 103080, 2020.

[7] S. M. Bhagwat and A. J. Ghajar, "Experimental investigation of non-boiling gas-liquid two phase flow in downward inclined pipes," *Exp Therm Fluid Sci*, vol. 89, pp. 219–237, 2017.

[8] A. M. Quintino, R. da Fonseca Junior, and O. M. H. Rodriguez, "Experimental study of liquid/dense-gas pipe flow," *Geoenergy Science and Engineering*, vol. 230, Nov. 2023, doi: 10.1016/j.geoen.2023.212179.

[9] O. M. H. Rodriguez and M. S. Castro, "International Journal of Multiphase Flow Interfacial-tension-force model for the wavy-stratified liquid – liquid flow pattern transition," vol. 58, pp. 114–126, 2014.

[10] P. J. Miranda-Lugo and O. M. H. Rodriguez, "Plateau–Rayleigh instability in low-viscosity ratio stratified liquid–liquid flow," *International Journal of Multiphase Flow*, vol. 189, Aug. 2025, doi: 10.1016/j.ijmultiphaseflow.2025.105253.

TWO-PHASE SIMULATION OF PARTICLE DYNAMICS IN A T-JUNCTION MICROCHANNEL FLOW

Matteo Chiatto[1], Luigi de Luca[1], Howard A. Stone[2] & Francesco Grasso[3]
[1] *Department of Industrial Engineering, University of Naples "Federico II", Naples, 80125, Italy*
[2] *Department of Mechanical and Aerospace Engineering, Princeton University, Princeton 08544, USA*
[3] *DynFluid Laboratory, CNAM-Arts et Metiers Paris Tech, Paris 75013, France*

Abstract Two-phase flows, microfluidics, particle/fluid flows.

Branching flows are common in both technological and biological transport systems, where geometric bifurcations generate coherent vortical structures that strongly affect stability, mixing, and particle transport. In square cross-section T-junctions, the curvature of streamlines induces a dominant counter-rotating vortex pair in the branch channel. As the Reynolds number increases, this structure undergoes qualitative transitions, including the onset of steady vortex breakdown and, at higher Reynolds numbers, a Hopf bifurcation leading to a helical breathing mode [1, 2]. Although the bifurcation structure of the single-phase configuration has been established, the corresponding dynamics in the presence of dispersed inertial particles remain largely unexplored.
In previous work, particle trapping was investigated using one-way coupled simulations, where Lagrangian particles were transported within a precomputed single-phase flow field calculating their trajectory by solving the Maxey-Riley equation [3]. That approach revealed transient accumulation inside the steady breakdown bubble at $Re = 500$, where the recirculation region acts as a confinement zone for finite-inertia particles. Beyond the Hopf threshold at $Re = 570$, the time-periodic breathing of the vortex core introduced injection-time-dependent trajectories and variations of the trapping region over time.
In the present study, we extend the analysis to fully coupled two-phase numerical simulations in the range $500 \leq Re \leq 570$, resolving the momentum exchange between the carrier flow and the dispersed phase. This framework enables a direct comparison between particle trajectories obtained in the previous one-way coupled formulation and those emerging from the two-way coupled simulations. At the same time, it allows us to assess how particle loading influences vortex morphology, breakdown topology, and the characteristics of the Hopf-induced oscillatory mode.
The two-phase framework indicates that dispersed particles influence the vortex structure in both the steady breakdown and post-Hopf regimes, underlining the role of phase coupling in the overall dynamics. Ongoing analyses aim to clarify how particle back-reaction interacts with the underlying instability mechanisms and affects the modal organisation of the flow.

References

[1] D. Vigolo & S. Radl & H.A. Stone, *Unexpected trapping of particles at a t junction*, Proceedings of the National Academy of Sciences of the United States of America, **111(13)**,4770–4775 (2014). doi: 10.1073/pnas.1321585111.
[2] K. K. Chen & C. W. Rowley & H. A. Stone, *Vortex breakdown, linear global instability and sensitivity of pipe bifurcation flows*, Journal of Fluid Mechanics, **815**, 257–294 (2017). doi: 10.1017/jfm.2017.49.
[3] M. R. Maxey & J.J.Riley, *Equation of motion for a small rigid sphere in a nonuniform flow*, Physics of Fluids, **26 (4)**, 883–889 (1983).

H THEOREM OF THE ENSKOG–VLASOV EQUATION: KINETIC THEORY APPROACH FOR PHASE CHANGE

Shigeru Takata[1] & Aoto Takahashi[1]
[1] *Department of Aeronautics and Astronautics, Kyoto University, Kyoto 615-8540, Japan*

Abstract The Enskog equation is a kinetic equation for dense gases that incorporates into the Boltzmann equation the effects of differences in the center positions of colliding molecules and the influence of volume fraction on the frequency of intermolecular collisions. It is one of the significant works by Enskog. Unfortunately, however, the H theorem has not been established for its original form. The H theorem was established for the so-called modified (or revised) Enskog equation, whose mathematical complexity has hindered the development of numerical methods for this variant. The same applies to the Enskog–Vlasov equation that further incorporates the long-range molecular interaction and provides the kinetic description of the phase change between the gas and liquid phases.

In this presentation, we report recent findings [1] that a slight modification of the original Enskog equation allows us to establish the H theorem. The modification is enough simple to allow direct application of existing numerical methods developed for the original Enskog equation.

References

[1] S. Takata & A. Takahashi, *Enskog and Enskog-Vlasov equations with a modified correlation factor and their H theorem*, Phys. Rev. E **111**, 065108 (2025).

SUPERCOOLING OF LIQUIDS, AS DESCRIBED BY THE ENSKOG–VLASOV KINETIC EQUATION

Eugene Benilov[1]
[1]*University of Limerick, Limerick, Ireland*

Keywords: phase transitions, kinetic equation, supercooling

Abstract

A model combining Enskog's collision integral for dense fluids with a Vlasov-style description of the van der Waals force [1] is applied to supercooling. First, the spinodal temperature T_s is calculated, at which a liquid becomes unstable to small perturbations and transitions to solid. It turns out that isochoric cooling allows one to reach a lower, or even much lower, temperature than isobaric cooling. Second, the surface tension γ of a supercooled liquid/vapor interface is shown to diverge at $T \rightarrow T_s$. The growth of γ is caused by an oscillatory region emerging on the liquid side of the interface; it develops because the liquid approaches instability, and the interface starts radiating (so far, evanescent) waves. At $T = T_s$, the waves stop being evanescent, and the width of the oscillatory region becomes infinite. Given the clear physical interpretation of this effect, it should be reproducible in any model describing liquid/vapor interfaces and the liquid–solid transition, rather than being specific to the Enskog–Vlasov theory. The general results are applied to argon and several other fluids.

References:

[1] E. S. Benilov & M. S. Benilov, Energy conservation and H theorem for the Enskog–Vlasov equation, Phys. Rev. E 97, 062115 (2018).

THERMAL BIFURCATION AND PHASE-LAG INSTABILITIES IN SOLID-SOLID PHASE CHANGE MATERIALS UNDER TRANSIENT HEAT LOADING

Mayank Maroliya[1], Sandip K. Saha[1]
[1]*Thermal Science Lab, Department of Mechanical Engineering, Indian Institute of Technology Bombay, Mumbai, 400076, India.*

Keywords: Thermal Bifurcation, Solid-Solid Phase Change Materials, Phase Lag Instabilities, Supercooling.

Abstract

Solid-solid phase change materials (SSPCMs) exhibit complex thermal instabilities during phase transitions, including supercooling, spontaneous recalescence, and phase-lag phenomena that challenge conventional thermal modeling approaches [1, 2]. Traditional Resistance-Capacitance (RC) circuit models fail to capture the inertial effects and bifurcation behavior observed during rapid phase transitions in SSPCM-based thermal management systems. This study presents a novel Thermal Inductance-Capacitance-Resistance (LCR) circuit framework that accurately models these instability phenomena under transient heat loading conditions.

The primary objective is to characterize thermal bifurcation events during solid-solid phase transitions, with emphasis on supercooling-induced instabilities and recalescence dynamics. By introducing thermal inductance, the model accounts for the delayed response of heat flux to temperature gradients, enabling prediction of critical bifurcation points where metastable supercooled states transition abruptly to equilibrium through recalescence. This approach reveals phase-lag instabilities that govern the temporal evolution of temperature profiles in high-performance computing systems and satellite avionics applications.

The numerical framework employs a lumped-parameter thermal LCR model integrated with machine learning algorithms to predict supercooling thresholds, nucleation events, and recalescence onset conditions. Validation against experimental data from SSPCM-integrated honeycomb heat sinks demonstrates superior predictive accuracy compared to conventional RC models, particularly during rapid thermal transients. The model successfully captures hysteresis behavior and thermal oscillations characteristic of phase transition bifurcations.

Results indicate that thermal inductance plays a critical role in determining stability boundaries during phase change. The framework identifies distinct bifurcation regimes where small perturbations in heat load trigger dramatic shifts in thermal response, offering insights for robust thermal management design. Applications include passive cooling of electronics, and battery thermal management systems where understanding bifurcation phenomena is essential for preventing thermal runaway and optimizing phase change timing.

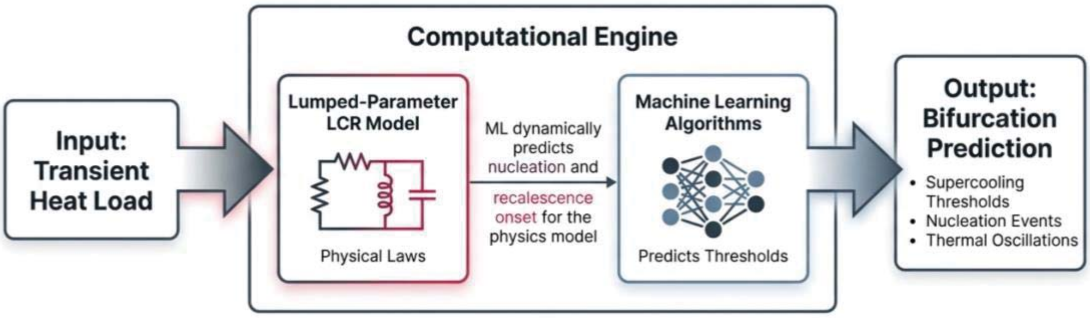

Figure 1. The Integrated Numerical Framework

References

[1] N. Bianco, A. Fragnito, M. Iasiello, G. M. Mauro & L. Mongibello, Subcooling Effect on PCM Solidification: A Thermostat-like Approach to Thermal Energy Storage. Energies 16, 4834 (2023).
[2] I. Shamseddine, F. Pennec, P. Biwole & F. Fardoun, Supercooling of phase change materials: A review, Renewable and Sustainable Energy Reviews 158,112172 (2022).

COLLECTIVE EFFECTS IN THE PHASE CHANGE OF FALLING RAINDROPS

Lucile Bisquert[1], Debarshi Debnath[1], David Scott[2], Rama Govindarajan[3] & Prashant Valluri[1]

[1] *Institute for Multiscale Thermofluids, School of Engineering, University of Edinburgh, Edinburgh, United Kingdom*

[2] *Edinburgh Parallel Computing Centre, University of Edinburgh, Edinburgh, United Kingdom*

[3] *International Centre for Theoretical Science, Tata Institute of Fundamental Research, Bengaluru, India*

Keywords: Falling raindrops, Evaporation, Condensation, Diffuse interface, Heat and Mass transfert

Abstract

Rainfall results from a succession of processes including droplet formation within clouds, gravitational descent through the atmosphere, and impact at the surface. As raindrops fall under gravity, they interact with the surrounding air, deform under aerodynamic forces, and exchange heat and mass with the environment through evaporation or condensation.

The phase change depends strongly on ambient conditions, and in particular on the local relative humidity. In slightly supersaturated environments, with relative humidity of order 105%, water vapour is available in excess and droplets may experience condensation while descending. Such conditions can be found locally inside moist convective clouds, for example within cumulus or cumulonimbus systems, such as those often observed during the monsoon season. In contrast, when droplets fall through subsaturated air with relative humidity around 95%, the surrounding environment favours evaporation, leading to a reduction of droplet volume during descent.

When many droplets fall together, they interact, so that the volume evolution of a droplet depends not only on the ambient conditions but also on the presence and spacing of neighbouring droplets. In the present work we explore how these interactions can modify the local humidity and convective flow experienced by each droplet, affecting the rate of evaporation or condensation. To investigate these collective effects, we perform three-dimensional simulations using a numerical framework based on a diffuse-interface approach. With our in-house finite volume solver (https://sourceforge.net/projects/tpls/)[1], we capture the dynamics of droplet deformation, evaporation or condensation, and interactions with the surrounding gas phase by coupling the Cahn–Hilliard equation with the conservation equations for mass, momentum, and energy, while phase change is treated using a diffusion-limited formulation.

References

[1] Sáenz, P. J., Sefiane, K., Kim, J., Matar, O. K., and Valluri, P. (2015). Evaporation of sessile drops: a three-dimensional approach. Journal of Fluid Mechanics, 772, 705-739.

NANODROPLET CONDENSATION ON SOLID SURFACES

Matteo Teodori[1], Dario Abbondanza[1], Mirko Gallo[1], & Carlo Massimo Casciola[1]
[1] *Dipartimento di Ingegneria Meccanica e Aerospaziale, Sapienza Università di Roma, Via Eudossiana 18, 00184 Roma, Italy*

Abstract A stochastic mesoscale model based on the theory of fluctuating hydrodynamics and the thermodynamics of a diffuse interface approach shows how direct simulation of the vapor-liquid phase transition from nucleation to hydrodynamics can be achieved.

Condensation is of central interest due to the innumerable conditions where vapour/liquid phase change takes place, from a planetary scale (e.g., clouds), to human (e.g., water harvesting) and micro/nano scales (e.g., electronics cooling). This talk deals with nanodroplet condensation on hydrophobic and hydrophilic surfaces. Fluid mechanics has long been involved in deciphering condensation, an effort partially hindered by the poor understanding of the onset of the phenomenon, namely the nucleation process. Most numerical techniques addressing vapour-liquid phase transition, requires that droplets are patched inside a vapour system when the simulation starts. The nucleation stage of the condensation process is basically skipped and taken as a parameter. Currently, Molecular Dynamics (MD) is the only universally-trusted tool to address nucleation, but its computational cost limits its use to rather small system (nanometer scale). Our approach for direct numerical simulations of the vapour-liquid transition is based on a mesoscale model that couples Landau-Lifshitz-Navier-Stokes equations and diffuse interface thermodynamics [1]. By properly describing thermal fluctuations, liquid nuclei spontaneously appear and temporal and spatial scale larger than MD can be explored (hundreds of nanometers) with a reduced computational burden, opening the way to physically-based condensation simulations of macroscopic systems of high technological interest. This approach has already been employed to address cavitation [1]. In the present simulation campaign, heterogeneous condensation of a metastable vapour (modified Benedict-Webb-Rubin equation of state for mimicking Lennard-Jones fluids [2]) is explored by enclosing the fluid between two parallel flat solid surfaces. Periodicity is enforced on the remaining directions. In nucleation phenomena, the crucial observable is the nucleation rate J, related to the number of droplets formed per unit time $N_d(t)$. Several simulations in identical thermodynamic conditions are typically needed in MD to obtain a proper statistic. In our case, multiple nucleation events occur at nearly-constant thermodynamic states and a single simulation is enough. The evolution of the number of droplets over time is illustrated in the left panel of Fig. 1. The two typical condensation regimes can be seen depending on the enforced contact angle: filmwise condensation, at low contact angles ϕ the surface is completely cover by the liquid phase (top-right panel) and dropwise condensation for high contact angle ϕ, where individual droplets grow separately (bottom-right).

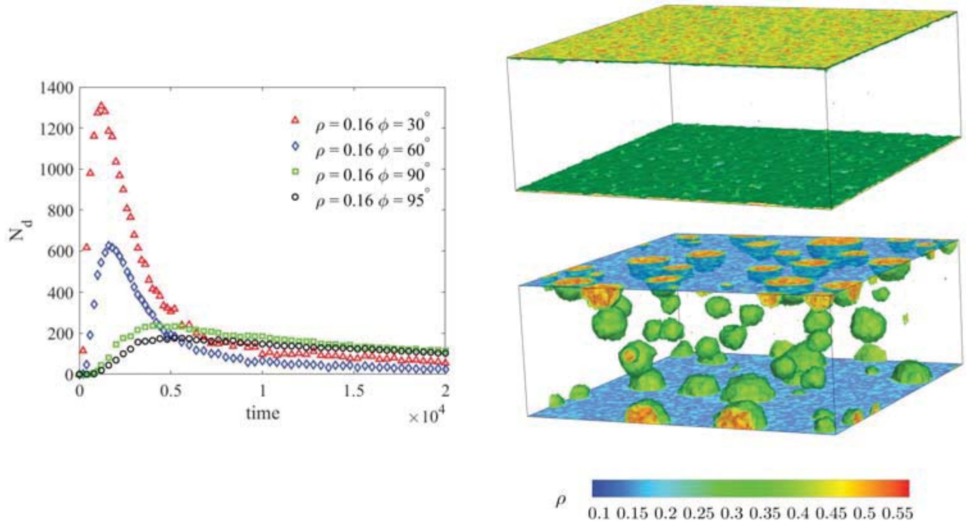

Figure 1. Number of supercritical droplets over time at different wall wettabilities ϕ and initial vapour densities ρ. On the right panel, snapshots showing the density isosurfaces for two different ϕ, 30° at the top and 90° at the bottom. The interface appears in green.

References

[1] Gallo, Mirko, Francesco Magaletti, and Carlo Massimo Casciola. *Fluctuating hydrodynamics as a tool to investigate nucleation of cavitation bubbles*, Multiphase Flow: Theory and Applications 347 (2018).
[2] Johnson, J. Karl, John A. Zollweg, and Keith E. Gubbins. *The Lennard-Jones equation of state revisited.* Molecular Physics 78.3 (1993).

FLUCTUATING THIN FILMS WITH ORIENTABLE SURFACTANTS: MICROSCOPIC ORIGINS, STABILITY AND RUPTURE

Toby Kay[1] & Serafim Kalliadasis[1]

[1] *Complex Multiscale Systems Group, Department of Chemical Engineering, Imperial College, London, SW7 2AZ, United Kingdom*

Abstract Fluctuating thin films derived from microscopics, with orientable surfactants, and stochastic amplitude equations for rupture.

Thin liquid films are found across countless natural and engineering systems, from the tear film in the eye to industrial coating processes. In very thin films that are at the nanoscale in height, rupture and thus dewetting are not purely mechanical but also impacted by thermal fluctuations originating at the molecular scale. This requires the extension of classical thin film models by introducing stochastic noise which accounts for the thermal fluctuations. In this talk, we present a unified theoretical framework for fluctuating thin films with surface active agents (surfactants), incorporating both thermal noise and surfactant orientational structure, and use it to study stability and rupture times.

We begin by deriving stochastic thin film equations from the exact underlying Hamiltonian dynamics using a coarse-grained mesoscopic description based on fluctuating dynamic density functional theory (DDFT) [1]. Within this framework, we incorporate surface-active molecules directly at the microscopic level, treating surfactants as polar uniaxial particles rather than symmetric point-like species. By confining the fluctuating DDFT dynamics to a deformable interface [2] and performing a long-wave approximation [3], we obtain a set of stochastic thin film equations governing the coupled evolution of the film height, surfactant concentration, and surfactant polarization field. The resulting model preserves a gradient dynamics structure and yields a generalized surface tension that depends on both concentration and orientational order in a thermodynamically consistent way. The same framework also allows for straightforward extensions to non-conserved dynamics, such as evaporation, leading to additional stochastic terms not present in standard thin film models.

Building on this microscopic derivation, we investigate the rupture of surfactant-laden fluctuating thin films. Focusing on unstable films close to criticality, we perform a multiple-scales weakly nonlinear analysis of the stochastic thin film equations, deriving a stochastic Stuart–Landau equation governing the amplitude of the critical mode [4]. In this regime, the rapid growth of this mode leads to the onset of rupture. By further reducing the dynamics to an effective stochastic equation for the amplitude magnitude, rupture is characterized as a first-passage event, allowing analytical expressions for the mean rupture time to be obtained. To confirm the validity of our approach we compare these analytical results to fully nonlinear simulations of the stochastic thin film equation, where we see good agreement.

Finally, we use this reduced description to quantify how surfactants modify film stability and rupture statistics. We compare rupture times and stability thresholds between bare fluctuating thin films and surfactant-laden films, and examine how these properties depend on surfactant concentration and orientational degrees of freedom. In particular, we demonstrate how surfactant shape and polarization alter the effective surface tension, and in turn rupture times, providing new insight into the microscopic mechanisms by which complex interfacial physics influences phase change in thin liquid films.

References

[1] M. A. Durán-Olivencia, P. Yatsyshin, B. D. Goddard, and S. Kalliadasis, "General framework for fluctuating dynamic density functional theory," *New J. Phys.*, vol. 19, no. 12, p. 123022, 2017.

[2] A. Pereira and S. Kalliadasis, "On the transport equation for an interfacial quantity," *Eur. Phys. J. Appl. Phys.*, vol. 44, no. 2, pp. 211–214, 2008.

[3] M. A. Durán-Olivencia, R. S. Gvalani, S. Kalliadasis, and G. A. Pavliotis, "Instability, rupture and fluctuations in thin liquid films: Theory and computations," *J. Stat. Phys.*, vol. 174, no. 3, pp. 579–604, 2019.

[4] M. Pradas, D. Tseluiko, S. Kalliadasis, D. T. Papageorgiou, and G. A. Pavliotis, "Noise induced state transitions, intermittency, and universality in the noisy Kuramoto–Sivashinsky equation," *Phys. Rev. Lett.*, vol. 106, no. 6, p. 060602, 2011.

FLUCTUATING HYDRODYNAMICS AND RARE-EVENT TECHNIQUES UNVEIL THE MESOSCALE PHYSICS OF BOILING

Andrea Bonanno[1], Filippo Occhioni[1], Marco Bussoletti[1] & Mirko Gallo[1]
[1] *Department of Mechanical and Aerospace Engineering, Sapienza University of Rome, Italy*

Abstract Non-equilibrium phase change from nucleation to macroscopic multiphase flow.

Deciphering the incipient stages of phase change in superheated fluids — and their subsequent evolution — remains a major challenge, as it requires bridging microscopic nucleation with macroscopic bubble dynamics and heat transfer. This gap has long hindered predictive boiling models and limited progress in emerging thermal technologies. Here, we leverage large-scale high-performance simulations of fluctuating hydrodynamics [2], combined with a rare-event technique [3, 1], to rationalise liquid–vapour transformation from nucleation to bubble growth. We quantify the statistics of nucleated bubbles and hydrodynamic fields, onset temperatures, and non trivial wettability effects on the nucleation pathways. The results reveal previously inaccessible physics of boiling, recovering microscopic features for nucleation and macroscopic scaling laws in line with experiments.

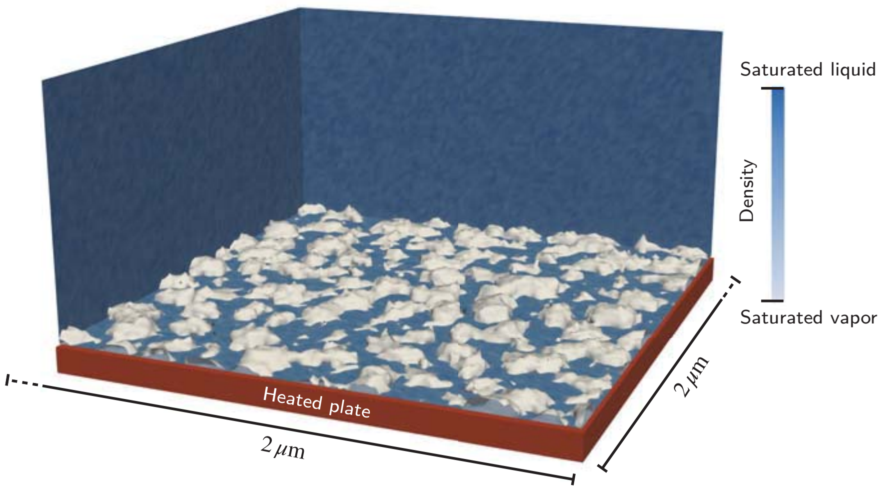

Figure 1. Snapshot from a Fluctuating Hydrodynamics simulation of boiling water under intense heat injection.

References

[1] Weinan E, Weiqing Ren, and Eric Vanden-Eijnden. Simplified and improved string method for computing the minimum energy paths in barrier-crossing events. *Journal of Chemical Physics*, 126(16):164103, 2007.

[2] Mirko Gallo, Francesco Magaletti, Anastasios Georgoulas, Marco Marengo, Joel De Coninck, and Carlo Massimo Casciola. A nanoscale view of the origin of boiling and its dynamics. *Nature Communications*, 14(1):6428, 2023.

[3] Francesco Magaletti, Mirko Gallo, and Carlo Massimo Casciola. Water cavitation from ambient to high temperatures. *Scientific reports*, 11(1):20801, 2021.

RARE EVENTS IN PHASE CHANGE DYNAMICS

Mirko Gallo[1], Filippo Occhioni [1], Riccardo Daniele[1], Carlo Massimo Casciola[1]
Department of Mechanical and Aerospace Engineering Sapienza University of Rome

Abstract Characterise phase change in fluids as a rare event.

Phase-change phenomena such as boiling and cavitation are ultimately controlled by rare microscopic fluctuations. Even under strongly stretched or superheated conditions, liquids may remain metastable for extremely long times, until an improbable fluctuation initiates the formation of a vapour nucleus large enough to trigger the transition. Nucleation is therefore not a deterministic event, but the outcome of rare stochastic processes governed by free-energy barriers. At the microscopic level, the emergence of a new phase results from the probabilistic aggregation and dispersion of molecules into transient clusters. Most of these clusters dissolve rapidly, but with vanishing probability, a critical nucleus is formed, allowing the system to escape the metastable basin. This intrinsically statistical-mechanical nature of nucleation implies that understanding phase-change inception requires explicit access to rare-event dynamics. A major challenge stems from the enormous separation of time scales involved. The mean nucleation time $\langle\tau\rangle$ scales exponentially with the nucleation barrier, $\langle\tau\rangle \sim \exp(\Delta F^{\dagger}/k_B T)$, and can range from nanoseconds near spinodal conditions to geological times close to saturation. While molecular dynamics can faithfully capture microscopic fluctuations, its computational cost confines it to short times and small systems, preventing a consistent coupling with hydrodynamics and heat transport.

In this talk, I will show how rare-event techniques grounded in Large Deviation Theory overcome these limitations. When coupled with multiphase fluctuating hydrodynamics and diffuse-interface thermodynamics, they make it possible to identify the most likely nucleation pathways and quantify their probabilities. This unified framework yields predictive estimates of boiling temperatures and cavitation pressures for several real fluids, together with the associated hydrodynamic fields, in quantitative agreement with experimental observations.

References

[1] Gallo, Mirko, et al. "Heterogeneous Bubble Nucleation dynamics." Journal of Fluid Mechanics 2021.
[2] Gallo, Mirko, et al. "A nanoscale view of the origin of boiling and its dynamics." Nature Communications 2023.
[3] Gallo, Mirko et al. "Complex Transition Pathways in Boiling and Cavitation" Journal of Fluid Mechanics 2025.
[4] Gallo, Mirko, et al. "Hydrodynamical pathways in the phase change of real uids" Research Square 2025.

SCALE-DEPENDENT HYDRODYNAMIC MECHANISMS GOVERNING NUCLEATION STABILITY AND VAPOR REMOVAL IN NUCLEATE BOILING

Rameez Iqbal[1], Gautier Rouaze[1], Gio Bellone[1], Francesco Minola[1], Lenan Zhang[2] & Zhengmao Lu[1*]
[1]*Energy Transport Advances Laboratory, Institute of Mechanical Engineering, EPFL, 1015 Lausanne, Switzerland*
[2]*Sibley School of Mechanical and Aerospace Engineering, Cornell University, Ithaca, NY 14853, USA*
**Corresponding author: zhengmao.lu@epfl.ch*

Keywords: multiscale nucleate boiling, bubble interactions, nucleation stability, hydrodynamic shielding

Abstract

Nucleate boiling underpins technologies from power generation to electronics cooling, yet nominally identical micro-engineered surfaces often exhibit large variability in nucleation onset, persistence, and hysteresis. This variability is typically attributed to differences in individual cavity geometry or thermal history, while interactions between neighboring sites are discussed mainly in the context of bubble departure rather than nucleation itself. Here, we demonstrate that hydrodynamic interactions between neighboring nucleation sites operate across two distinct length scales and play fundamentally different roles. eWe design micro-engineered surfaces with cylindrical cavities arranged into discrete pairs, defining two independent geometric parameters (Figure 1): an intra-pair spacing (L_{in}), and an inter-pair separation (L_D). Pool-boiling experiments reveal that when L_{in} approaches hydrodynamic boundary layer thickness (δ_H), nucleation activates more readily, persists over a wider range of conditions, and exhibits markedly reduced hysteresis. Flow-field analysis suggests a hydrodynamic shielding mechanism: closely spaced bubbles create a low-velocity region along the wall that suppresses convective heat removal and stabilizes vapor embryos. Once all sites are active, heat transfer becomes insensitive to L_{in} and is instead governed by macroscopic coalescence and entrainment patterns set by L_D/D_b, exhibiting a non-monotonic dependence reflecting competing vapor-removal regimes. Here, D_b represents the buoyancy-driven departure diameter. These results establish a clear scale separation between mechanisms governing nucleation stability and those controlling vapor removal, providing a framework for designing boiling surfaces that are both robust and high-performing.

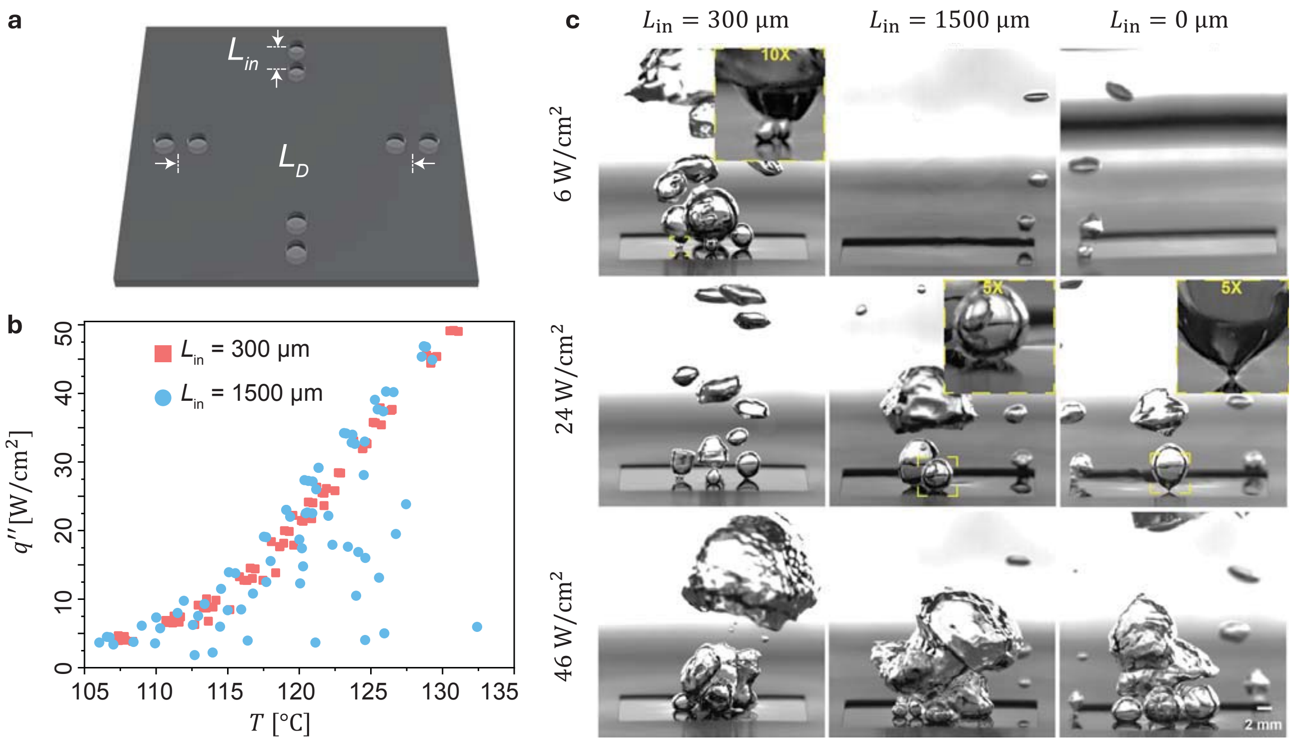

Figure 1. Dual-scale nucleation-site layout and representative boiling behavior across heat flux. (a) Schematic of the micro-engineered surface consisting of eight identical cylindrical cavities arranged into four discrete pairs. (b) Boiling curves (heat flux vs temperature) for L_{in} = 300 µm (red) and L_{in} = 1500 µm (blue). Closely spaced cavity pairs exhibit sharply defined and reproducible deactivation behavior, whereas widely spaced pairs show pronounced run-to-run and sample-to-sample variability. (c) Side-view high-speed images showing representative bubble behavior at three applied heat fluxes, $q'' \approx 6$, 24, and 46 W/cm^2, for L_{in} = 300 µm, 1500 µm, and 0 µm.

MODELING AND SIMULATION OF BUBBLE NUCLEATION IN MAGMA

Matteo Bottacchiari[1], James E Gardner[2], Mizuki Nishiwaki[4], Dork Sahagian[3], Patrick Sullivan[5], Fabian Wadsworth[6] and Mirko Gallo[1]

[1] *Department of Mechanical and Aerospace Engineering, Sapienza University of Rome, Rome, Italy*
[2] *Department of Earth and Planetary Sciences, Jackson School of Geosciences, The University of Texas at Austin, Austin, Texas, USA*
[3] *Department of Earth and Environmental Sciences, Lehigh University, Bethlehem, Pennsylvania, USA*
[4] *Center for Glass Science and Technology, School of Engineering, The University of Shiga Prefecture, Hikone, Shiga, Japan*
[5] *Department of Earth Sciences, Durham University, Science Labs, Durham DH1 3LE, United Kingdom*
[6] *Earth and Environmental Science, Ludwig-Maximilians-Universität, Munich, Germany*

Abstract Magma, Bubble nucleation, Diffuse interface, Nucleation rate, Surface tension

Volcanic eruptions are triggered by magma degassing, whose critical first step is the nucleation of bubbles. The pressure decrease during magma ascent makes the melt supersaturated in volatiles such as water, leading to the nucleation of supercritical fluid bubbles that subsequently grow and coalesce [1].
The mechanism is not yet fully understood, not only because bubbles nucleate at depth and therefore cannot be directly observed, but also because their critical radii can be as small as a few nanometers, making experimental studies of bubble nucleation extremely difficult. Another major challenge is the determination of surface tension, since comparisons between experimental measurements of the nucleation rate and predictions of classical nucleation theory reveal discrepancies spanning several orders of magnitude [2].
Here, we develop an asymmetric free energy model for a binary mixture of silicate melt and water, following the same ideas that recently led to a symmetric model [3]. We calibrate the model parameters by fitting experimental phase diagrams[4]. We then augment the free energy using square-gradient theory, thereby introducing a diffuse interface [5]. The capillary coefficient is calibrated to reproduce the (planar) surface tension measured in experiments [6]. The model allows us to calculate curvature corrections to the planar surface tension, such as the Tolman length, as well as the thickness of the melt-water interface. Finally, we couple the free energy with a rare-event technique and carry out simulations of water-bubble nucleation under different thermodynamic conditions. We measure critical radii, the nucleation energy barriers, and the associated nucleation rates.

References

[1] James E. Gardner et al., *Bubble formation in magma*, Annual Review of Earth and Planetary Sciences, Vol. 51, pp. 131–154, 2023.
[2] Sahand Hajimirza et al., *Predicting homogeneous bubble nucleation in rhyolite*, Journal of Geophysical Research: Solid Earth, Vol. 124, No. 3, pp. 2395–2416, 2019.
[3] Mizuki Nishiwaki, *Can spinodal decomposition occur during decompression-induced vesiculation of magma?*, Earth and Planetary Science Letters, Vol. 671, 119655, 2024.
[4] Yang Liu, Youxue Zhang, and Harald Behrens, *Solubility of H_2O in rhyolitic melts at low pressures and a new empirical model for mixed H_2O–CO_2 solubility in rhyolitic melts*, Journal of Volcanology and Geothermal Research, Vol. 143, No. 1–3, pp. 219–235, 2005.
[5] Francesco Magaletti, Mirko Gallo, and Carlo Massimo Casciola, *Water cavitation from ambient to high temperatures*, Scientific Reports, Vol. 11, No. 1, 20801, 2021.
[6] Nikolai Bagdassarov, Alexander Dorfman, and Donald B. Dingwell, *Effect of alkalis, phosphorus, and water on the surface tension of haplogranite melt*, American Mineralogist, Vol. 85, No. 1, pp. 33–40, 2000.

DIRECT NUMERICAL SIMULATIONS EXPLORING THE INFLUENCE OF WETTABILITY AND NUCLEATION SITE DENSITY ON THE TRANSITION TO FILM BOILING

Daiman Somerville[1], David Scott[1], Omar Matar[2], Tassos Karayiannis[3], Dani Orejon[1], Khellil Sefiane[1] & Prashant Valluri[1]

[1]*School of Engineering, The University of Edinburgh, United Kingdom*

[2]*Department of Chemical Engineering, Imperial College London, United Kingdom*

[3]*Department of Mechanical and Aerospace Engineering, Brunel University London, United Kingdom*

Keywords: Boiling, Wettability, Cahn-Hilliard

Abstract

The transition from nucleate boiling to vapour-film formation depends sensitively on surface wettability and the spatial density of active nucleation sites [2], yet the underlying contact-line and coalescence mechanisms remain difficult to isolate experimentally . We investigate the transition from nucleate to film boiling through direct numerical simulations (DNS) using an in-house TPLS solver based on the incompressible Navier-Stokes equations coupled with a diffuse interface Cahn-Hilliard phase-field formulation in order to alleviate stress discontinuities at the three-phase contact line. To accurately capture contact line mechanics, the model incorporates the geometric dynamic boundary condition proposed by Ding and Spelt 2007 [1] which imposes a specified microcontact angle within a hysteresis window. Additionally, a reformulated mass source term is employed to enforce saturation conditions at the liquid-vapour interface.

The numerical framework is validated against the experimental data of Liu et al. 2024 [3] for single nucleation site configurations, demonstrating strong agreement (within experimental uncertainty) regarding the bubble growth rate and departure dynamics. The investigation extends to multiple nucleation sites to characterise the physical mechanisms driving bubble coalescence and the subsequent formation of vapour films. Parametric analyses quantify contact line velocity as a function of substrate wettability and initial nucleation site distance, revealing non-monotonic velocity profiles. These results elucidate the critical role of contact line dynamics and increasing nucleation site density in determining the departure from nucleate boiling, providing a robust framework for optimising heat transfer in applications ranging from microelectronic cooling to high-temperature surface protection.

References

[1] Hang Ding and Peter D. M. Spelt. "Wetting condition in diffuse interface simulations of contact line motion". In: Physical Review E 75.4 (Apr. 2007). Publisher: American Physical Society, p. 046708. doi: 10.1103/PhysRevE.75.046708. url: https://link.aps.org/doi/10.1103/PhysRevE.75.046708 (visited on 09/30/2024).
[2] Mahyar Ghazivini et al. "A review on correlations of bubble growth mechanisms and bubble dynamics parameters in nucleate boiling". en. In: Journal of Thermal Analysis and Calorimetry 147.11 (June 2022), pp. 6035–6071. issn: 1588-2926. doi: 10.1007/s10973-021-10876-2. url: https://doi.org/10.1007/ s10973-021-10876-2 (visited on 10/30/2025).
[3] Jionghui Liu et al. "Bubble Coalescence During Pool Boiling with Different Surface Characteristics". In: Heat Transfer Engineering 45.4-5 (Mar. 2024). Publisher: Taylor & Francis eprint: https://doi.org/10.1080/01457632.202pp. 360–380. issn: 0145-7632. doi: 10.1080/01457632.2023.2191438. url: https://doi.org/10.1080/ 01457632.2023.2191438 (visited on 08/13/2025).

ICE-WATER MORPHODYNAMICS IN TURBULENT SHEAR FLOWS

Diego Perissutti[1], Cristian Marchioli[2] & Alfredo Soldati[1]
[1] *Institute of Fluid Mechanics and Heat Transfer, TU-Wien, 1060 Vienna, Austria*
[2] *Department of Engineering and Architecture, University of Udine, 33100 Udine, Italy*

Abstract The morphodynamics of a melting ice–water interface driven by a subsurface turbulent shear flow is controlled by two distinct regimes. At early stages of the melting, the surface develops streamwise-oriented ice streaks. As melting progresses, a morphological instability sets in, and spanwise wavy ice ripples spontaneously emerge, migrating slowly downstream while growing in amplitude.

The interaction between deep oceanic currents and the ice base of glaciers is a critical factor in accurately predicting global ice melting rates. However, current predictive models are frequently hindered by inaccuracies stemming from inadequate dynamical representations of the ice–water interface morphology. Large-scale turbulent shear-dominated flows induce complex interface evolutions that significantly alter local heat transfer and hydrodynamic drag. Because experimental data in these extreme oceanic conditions are difficult to obtain, high-fidelity numerical investigations are essential to uncover the scaling laws that govern ice roughness evolution and to bridge the gap between geophysical models and observations. The investigation presented in this paper is based on interface-resolved direct numerical simulations aimed at characterizing the dynamical evolution of the ice–water interface morphology. The simulation data were generated using a pseudo-spectral, parallel, GPU-accelerated solver that couples the incompressible Navier–Stokes equations with a phase-field formulation and a volume-penalization immersed boundary method to resolve melting and freezing processes. The simulations capture the melting of a horizontal layer of ice subjected to a fully developed turbulent shear flow at $Re_\tau = 636$ and a unitary Stefan number (ratio between the typical latent heat and sensible heat in the system). To simulate a deep-water stream, a free-shear condition is imposed on the bottom boundary of the water layer, which is maintained at a bulk temperature above the melting point, while the top of the ice layer is kept below freezing. Results show that to two distinct morphodynamical regimes exist: initially, the interface consists solely of streamwise streaky patterns. As the simulation progresses, a morphodynamical instability occurs, leading to the formation of a wavy pattern known as ice ripples. In a previous work [1] we demonstrated that this instability emerges only at high shear Reynolds numbers, later showing also that the morphodynamics and their characteristic scales are influenced by latent heat [2]. Ongoing research is investigating these phenomena at even higher shear rates (Re_τ up to 1600), with a specific focus on the downstream migration velocity (celerity) of the ice ripples.

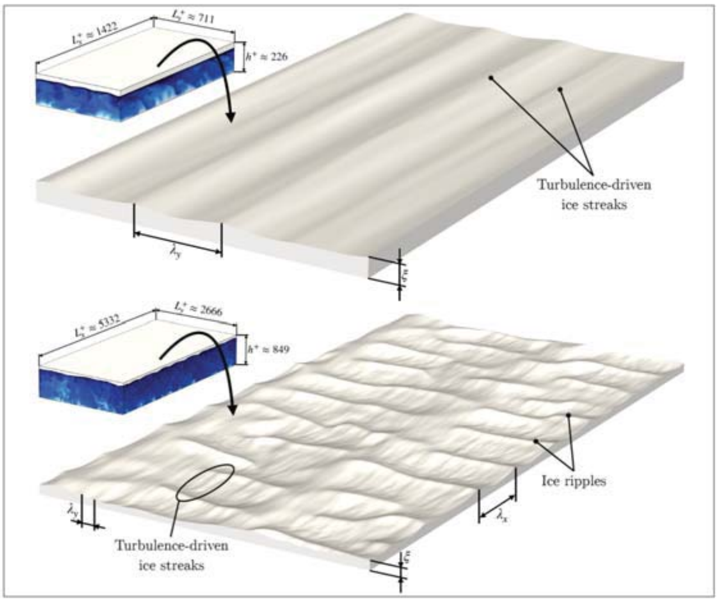

Figure 1. Streamwise streaks and spanwise ripples control the morphodynamics of an ice–water interface melted by shear turbulence.

References

[1] D. Perissutti, C. Marchioli, C. & A. Soldati, *Morphodynamics of melting ice over turbulent warm water streams.* Int. J. Multiphase Flow, **181**, 105007 (2024).
[2] D. Perissutti, C. Marchioli, C. & A. Soldati, *Time and length scales of ice morphodynamics driven by subsurface shear turbulence.* J. Fluid Mech., **1019**, A34 (2025).

CHAOTIC ORBITS OF MULTIPLE IMMERSED ELLIPSOIDS

Andrew Boyd[1,2], Mark Sawyer[2], David Scott[2], Rama Govindarajan[3] & Prashant Valluri[1]
[1]Institute of Multiscale Thermofluids, School of Engineering, University of Edinburgh, Edinburgh, United Kingdom
[2]EPCC, University of Edinburgh, Edinburgh, United Kingdom
[3]International Centre for Theoretical Sciences, TIFR Bengaluru, Bangalore, India

Keywords: multi-body hydrodynamic interaction; chaotic dynamics; immersed ellipsoids; potential flow; vortex-induced motion; recurrence quantification analysis

Abstract

Building on prior investigations of the complex dynamics of a single immersed ellipsoid (Essmann et al., 2020), this work examines the coupled translational and rotational dynamics of multiple immersed ellipsoids in both inviscid and viscous flow regimes. While it is established that a single rigid body may exhibit chaotic motion under viscous conditions due to vortex shedding, the extension to interacting multi-body systems introduces fundamentally new nonlinear coupling mechanisms mediated by hydrodynamic interactions.
In the inviscid limit, Kirchhoff's equations are generalised to multi-body configurations following the classical formulation of Lamb (1932). Unlike the single-body case, analytical expressions for added mass and inertia tensors are no longer available. The governing potential flow is therefore solved numerically via boundary integral equations, from which hydrodynamic forces and moments are obtained through surface interpolation. The resulting fully coupled six-degree-of-freedom equations of motion are integrated numerically, with rotational kinematics represented using quaternions to ensure robustness. The computational framework is implemented in Rust and parallelised for high efficiency.
The emergent dynamics are analysed using recurrence quantification analysis and cross-correlation techniques (Marwan et al., 2007) to characterise the onset, structure, and modulation of chaotic motion, as well as inter-body synchronisation and phase relationships. Inviscid predictions are systematically compared with fully resolved viscous simulations performed using the Xcompact3D solver (Laizet & Lamballais, 2009).
The results demonstrate that multi-body hydrodynamic coupling significantly alters the bifurcation structure and routes to chaos relative to the single-body case. These findings provide new insight into the role of fluid-mediated interactions in shaping complex solid–fluid dynamical systems and contribute to a broader understanding of instabilities in particulate and multi-body flows.

References

Essmann, E., Zuriguel, I. & Magnaudet, J. (2020) Chaotic dynamics of an immersed ellipsoidal body in viscous flow. Journal of Fluid Mechanics, 899, A12.
Lamb, H. (1932) Hydrodynamics, 6th ed. Cambridge University Press.
Marwan, N., Romano, M. C., Thiel, M. & Kurths, J. (2007) Recurrence plots for the analysis of complex systems. Physics Reports, 438, 237–329.

NONLINEAR PARTICLE DYNAMICS IN VORTICAL FLOWS

Alok Kumar, & Yuval Dagan
Fluid Dynamics and Stability Laboratory,
The Stephen B. Klein Faculty of Aerospace Engineering,
Technion-Israel Institute of Technology, Haifa, 3200003, Israel

Abstract
The transport and aggregation of inertial particles in vortical flows underpin a wide range of environmental and engineering processes, including aerosol clustering in the atmosphere, microplastic dispersion in the ocean, and particle separation in industrial mixing devices. Despite its importance, a predictive understanding of particle dynamics remains challenging due to the strongly nonlinear coupling between drag, buoyancy, virtual mass, Coriolis, and rotational lift forces. In this study, we investigate the motion of spherical inertial particles in an analytically prescribed three-dimensional rotating cylindrical vortex, serving as an idealized model of geophysical flow structures such as oceanic eddies. The analytical formulation enables systematic isolation of the physical mechanisms governing particle transport and stability. Using Lagrangian particle tracking combined with bifurcation theory and time-series analysis, we explore particle dynamics across a broad range of Stokes numbers, density ratios, and vortex rotation rates [1]. Particle trajectories at different (St, $\bar{\rho}$) in a cylindrical domain are shown in Figure 1 (a&b). We identify equilibrium states, periodic orbits, and escape dynamics arising from the balance of hydrodynamic and inertial forces. Neutrally buoyant particles undergo a transition from stable to unstable equilibrium via a limit point bifurcation, whereas slightly negatively buoyant particles remain stable over a wide parameter range. Magnus lift force is shown to be essentially included in the model for accurately capturing the system dynamics; neglecting this force changes the equilibrium profile. The onset of time-periodic motion is governed by a Hopf bifurcation, with codimension-two analysis revealing a Generalised Hopf point that delineates supercritical and subcritical regimes. In the supercritical regime, particles exhibit pronounced axial oscillations at low Stokes numbers, reflecting the enhanced influence of rotational lift and vortex forcing (shown by limit cycle behavior in Figure 1(c&d)). In contrast, the subcritical regime is confined to a parameter range, where perturbations beyond a critical threshold of the amplitude lead to immediate particle escape. These findings provide a mechanistic framework linking force balance, bifurcation structure, and particle fate in rotating flows, and offer insights relevant to modeling dispersed-phase transport in environmental vortices.

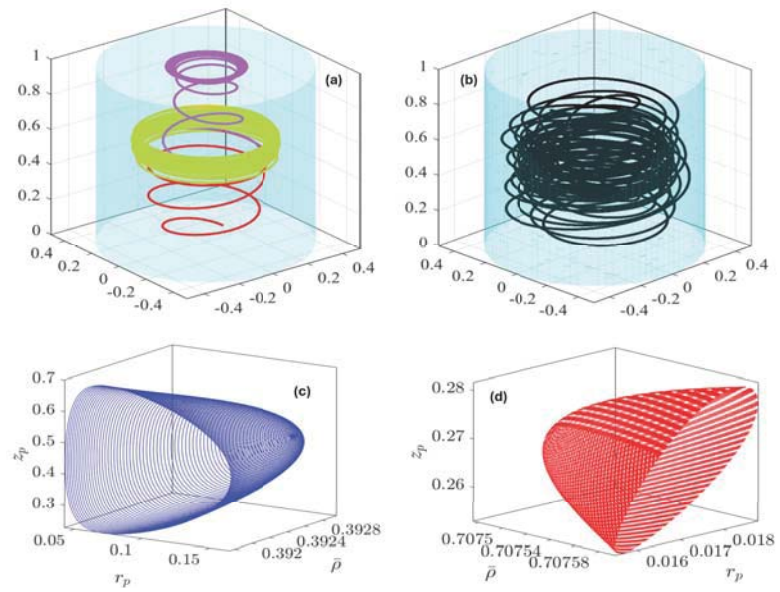

Figure 1. Particle trajectories showing stable trapping at bottom, migration to the top and the oscillatory behavior at different inertia and density ratio and the stable and unstable limit cycle continuation in the obtained supercritical and subcritical Hopf regions, respectively.

References

[1] Orr Avni, Alok Kumar & Yuval dagan, *Heavy Particle Motion in Rotational Vortices*, https://arxiv.org/abs/2506.09821, (2025).

EMPTYING BOTTLES FILLED WITH SUSPENSIONS

Sasha Perez[1], Valérie Vidal[1] & Sylvain Joubaud[1]
[1] *ENS de Lyon, CNRS, Laboratoire de Physique, F-69342 Lyon, France*

Abstract Multiphase flow, Suspension, Drainage.

Emptying a bottle filled with a suspension is a model system for studying multiphase flows. A simple everyday experiment shows that emptying a bottle filled only with water involves alternating between jets of liquid and rising air bubbles [1, 2]. However, the case of a suspension remains little or unstudied, despite its crucial importance in geophysical processes and in the optimisation of industrial processes.

We study this phenomenon experimentally. A cylindrical tank is filled with different isodense suspensions: hydrogel beads in a water/UCON mixture or polyamide beads in salt water. A force sensor allows to assess the mass flow rate. A pressure sensor at the top of the bottle quantifies the pressure variations above the suspension. Finally, a camera allows for direct visualisation of the suspension drainage including the position of the free surface, the particles exiting the bottle, the liquid jet and the bubbles rising. The draining behaviour is explored depending on the particle-to-hole ratio and the beads packing fraction.

Similarly to the emptying of a viscous fluid [3], the volume flow rate remains constant throughout the emptying process and its value is mainly determined by the size of the outlet hole. The flow rate decreases slightly as the initial volume fraction of particles increases. Revisiting the model developed by Clanet and Searby [1], we find that this change in flow rate is linked to the dynamics of bubble rise.

Furthermore, during the emptying, the suspension leaving the bottle contains fewer particles than the initial suspension, leading to an accumulation of particles in the bottle (see figure 1). When the volume fraction reaches a certain threshold, close to the particle random close packing, the particles emerge above the free surface of the liquid. Our measurements allow us to calculate the average particle volume fraction in the bottle. We also propose a model describing this transition.

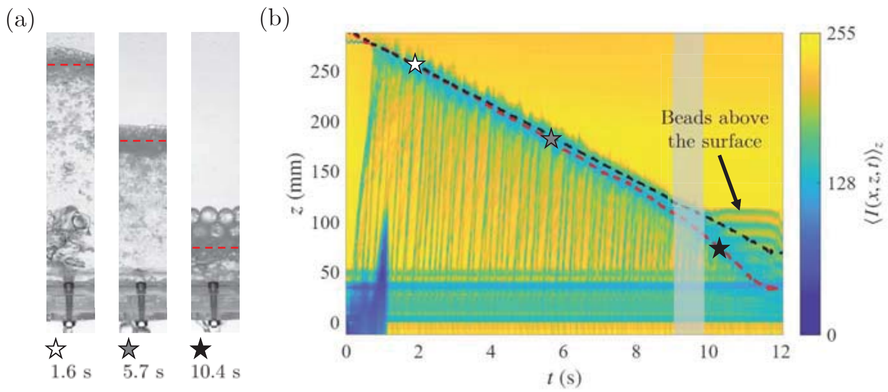

Figure 1. Example of suspension drainage of hydrogel breads. (a) Chronophotography of the experiment. (b) Intensity averaged along the horizontal axis, $\langle I(x, z, t)\rangle_x$, as a function of time t. The color bar is in grey level, with yellow indicating light and blue indicating dark. The stars identify the time corresponding to each picture in (a). The black dashed line shows the position of the free surface if no particles accumulation occurs. The grey zone indicates approximately the time when particles start to emerge above the liquid surface, from visual observations. In both (a) and (b), the red dashed line denotes the position of the free surface obtained from the pressure signal.

More recent work has made it possible to study the local dynamics of particles during the emptying by adjusting the optical index of the beads and the liquid, and using a laser sheet. This makes it possible to measure, in particular, the local volume fraction and particle velocities in order to refine previous models.

References

[1] C. Clanet & G. Searby , *On the glug-glug of ideal bottles*, Journal of Fluid Mechanics **510**, 145-168 (2004).
[2] S. Mer et al., *The emptying of a bottle as a test case for assessing interfacial momentum exchange models for Euler–Euler simulations of multi-scale gas-liquid flows*, International Journal of Multiphase Flow **106**, 109-124 (2018).
[3] B. Monnet, *Fluides newtoniens et suspensions : bulle unique et vidange*, Ecole normale supérieure de lyon - ENS LYON, PhD Thesis (2024).

COLLECTIVE DIFFUSION OF A QUASI-2D COLLOIDAL MONOLAYER ABOVE A WALL

Adam Carter[1], Eleanor K. R. Mackay[2], Ryker Fish[3], Brennan Sprinkle[3], Alice L. Thorneywork[2], & Sophie Marbach[1]
[1] *CNRS, Sorbonne Universite, Physicochimie des Electrolytes et Nanosystemes Interfaciaux, Paris, France*
[2]*Physical and Theoretical Chemistry Laboratory, Oxford, UK*
[3]*Applied Math and Statistics, Colorado School of Mines, Golden, CO, USA*

Abstract We describe the collective diffusion coefficient of a colloidal monolayer above a wall with theory, experiment, and simulation.

It is known that the collective diffusion coefficient, which governs the relaxation of macroscopic density fluctuations in a quasi-2D colloidal monolayer (where the colloids are restricted to two dimensions but the fluid extends in three) is divergent due to long-ranged hydrodynamic interactions between the colloids [1, 2]. We demonstrate, though theory, experiment, and numerical simulations, that in the presence of a wall below (or above) the colloidal monolayer, the collective diffusion coefficient no longer diverges. We discuss the impact of hydrodynamic interactions in this geometry, connect our results to the problem of collective sedimentation, and consider the case of a slit channel with walls above and below the colloids.

References

[1] Pesché, Raphaël, and Gerhard Nägele. 'Stokesian Dynamics Study of Quasi-Two-Dimensional Suspensions Confined between Two Parallel Walls'. Physical Review E 62, no. 4 (2000): 5432–43.
[2] Bleibel, J., A. Domínguez, F. Günther, J. Harting, and M. Oettel. 'Hydrodynamic Interactions Induce Anomalous Diffusion under Partial Confinement'. Soft Matter 10, no. 17 (2014): 2945–48.

EMERGENCE OF FLUIDIZATION INSTABILITIES AT GRANULAR INTERFACES

Camille Porceillon[1, 2], Aurélien Gay[1], Alfredo Taboada[1] & Valérie Vidal[2]
[1] *Géosciences Montpellier, Univ. Montpellier, Univ. Antilles, CNRS, 34 095 Montpellier, France*
[2] *Laboratoire de Physique, ENS de Lyon, CNRS, 69 364 Lyon Cedex 07, France*

Keywords : instabilities, interfaces, multiphase flows, fluidization, geological applications.

Abstract Injection of liquid in immersed granular systems can lead, under certain conditions, to the formation of instabilities, such as a quasi-periodic fluidization pattern emerging at the interface between coarse and fine grains, or at the free surface of the grains.

Liquid injection in an immersed granular medium (two-phase system) can lead to several invasion dynamics. At low injection flow rate the liquid percolates through the granular matrix without significant grain displacement. At higher flow rate the fluid drags the particles along with it, resulting in the fluidization of the granular bed. Such behaviors can arise both from homogeneous and local injection of liquid at the base of an immersed granular medium [1].

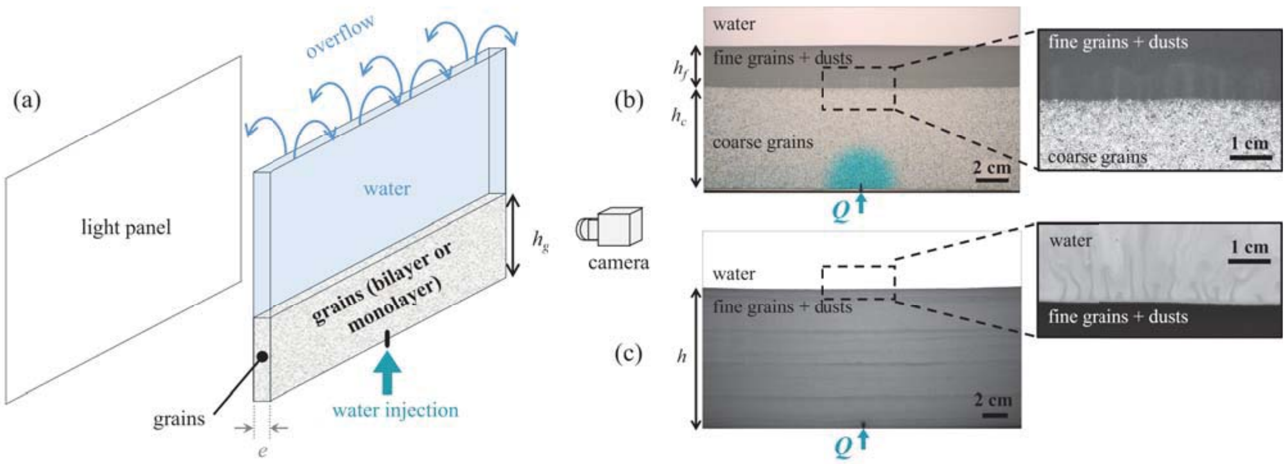

Figure 1. (a) Sketch of the experimental setup. Water is locally injected at constant flowrate Q at the bottom of a Hele-Shaw cell initially filled with a monolayer or bilayer of immersed grains (total height h_g). (b, c) Snapshots of the initial condition for (b) a bilayer [h_c and h_f are respectively the height of coarse and fine grains] or (c) a monolayer. The magnified pictures on the right-hand-side of the figure show examples of the instabilities appearing for both configurations.

Based on laboratory experiments, we investigate the emergence of instabilities at the interface between two immersed granular layers. The experiment consists of a Hele-Shaw cell (height 30 cm, width 35 cm, gap $e = 2.35$ mm) filled with grains deposited by sedimentation in water. Water is locally injected at the bottom center of the cell through a cylindrical nozzle, at a constant flow rate Q (see Fig. 1a). In a given range of parameters, a quasi-periodic fluidization pattern arises at the coarse-fine grains interface (chimneys are visible in the picture on the right-hand-side of Fig. 1b). Interestingly, this instability also appears at the free surface of the granular bed when considering a monolayer of particles, provided that the liquid percolates through the layer (Fig. 1c). We demonstrate the crucial role of the presence of very fine small particles (*dusts*) which are responsible for the instability pattern due to an elutriation process [3].
This work has direct implications in several geological fields, *e.g.* fluid escape structures in sedimentary basins, hydrothermal vents or volcanic processes [2]. Indeed, layered sediments contain numerous interfaces susceptible to initiating such instabilities. This study shows that a single injection point at depth can be the source of multiple pipes, challenging conventional interpretations of fluid migration pathways [3].

References

[1] P. Philippe & M. Badiane , *Localized fluidization in a granular medium*, Phys. Rev. E **87**, 042206 (2013).
[2] A. Nermoen, O. Galland, E. Jettestuen, K. Fristad, Y. Podladchikov, H. Svensen & A. Malthe-Sørenssen, *Experimental and analytic modeling of piercement structures*, J. Geophys. Res. **115**, B10202 (2010).
[3] C. Porceillon & A. Gay, A. Taboada, V. Vidal *Emergence of periodic chimneys during fluidization at a coarse-fine grains interface*,Phys. Rev. E **113**, 015414 (2026).

QUANTIFYING FRAGMENTATION EVENTS OF FLEXIBLE FIBERS IN WALL-BOUNDED TURBULENCE

Harishankar Muppirala[1], Darish Jeswin Dhas[1] & Cristian Marchioli[1]
[1] *Dept. of Engineering and Architecture, University of Udine, Italy*

Abstract (Key words: wall turbulence, flexible fibers, DNS).

Long, slender fiber-like particles are ubiquitous, most notably encountered in the form of microplastic pollutants. These pollutants originate from the breakdown of larger plastic debris, and subsequently undergo continuous deformation by hydrodynamic stresses in natural flows leading to further fragmentation. To this end, we perform large scale Euler-Lagrange direct numerical simulations of flexible fibers in a channel. These fibers are constructed by constraining sub-Kolmogorov rods using a rod-chain model. Through these simulations, we show how turbulent structures and intermittent shear fluctuations generate large deformations along the fiber, promoting conditions conducive to breakage. We identify such breakage events by monitoring the cumulative strain experienced along the fiber over time, using it as a physically motivated indicator for their fragmentation. We subsequently quantify the resulting breakage statistics as a function of the fiber and fluid flow properties without explicitly modeling physical fracture.

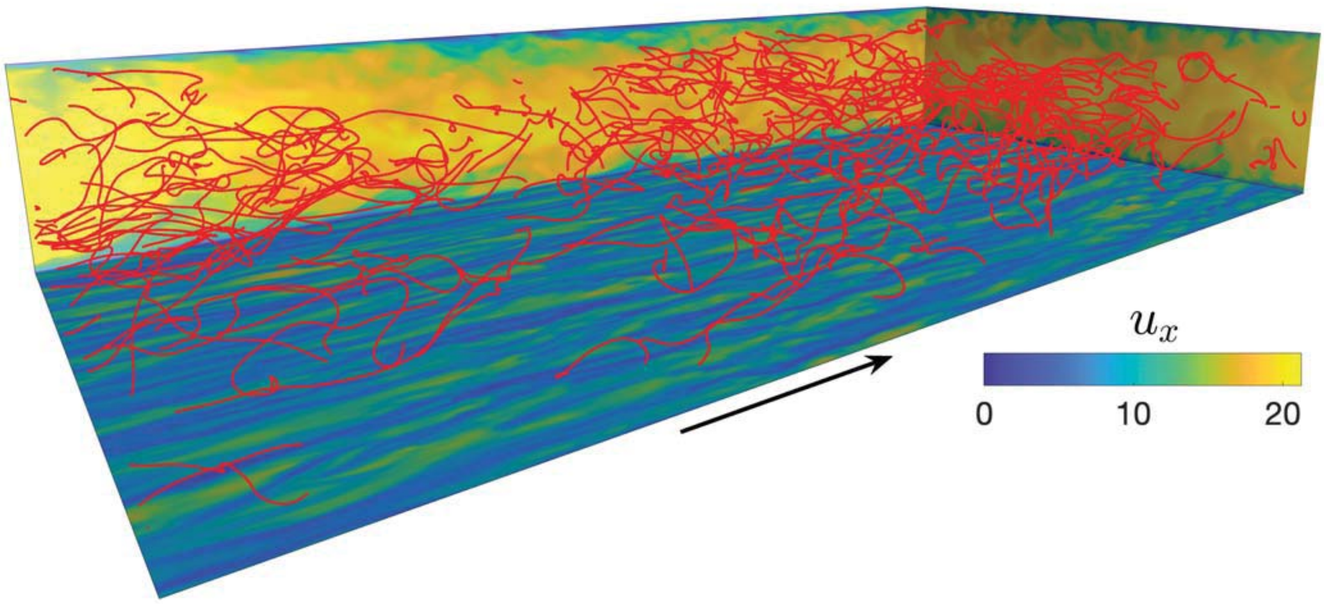

Figure 1. Instantaneous distribution of a random collection of flexible fibers of length $L_0^+ = 380$ in a turbulent channel flow with shear Reynolds number 300. The side and bottom panels display the stream-wise component of the velocity (u_x), with the bottom cut at $z^+ = 10$. The fiber thickness is magnified for better visualization.

THE TAMED CHAOS OF LONG FLEXIBLE FIBERS IN WALL TURBULENCE

Darish Jeswin Dhas[1], Davide Di Guisto[1] & Cristian Marchioli[1]
[1] *Dept. of Engineering and Architecture, University of Udine, Italy*

Abstract Key words: wall turbulence, flexible fibers, DNS

We investigate the chaotic regime of flexible fibers of varying lengths and rigidity, suspended in a turbulent channel flow at shear Reynolds numbers of 300 & 1200. We do this by performing direct numerical simulations in the Euler-Lagrange framework of a turbulent channel flow laden with long flexible fibers. Using recurrence quantification analysis, we show that increasing fiber length progressively suppresses chaotic deformation dynamics, signaling a transition toward more organized, flow-mediated motion. Through persistent homology analysis, we identify long-lived topological features in the fiber geometry and demonstrate that their maximum lifetime scales with the characteristic timescale of the largest turbulent eddies. These findings show that sufficiently long fibers sample flow structures in a manner that mitigates the intrinsic chaos of turbulence.

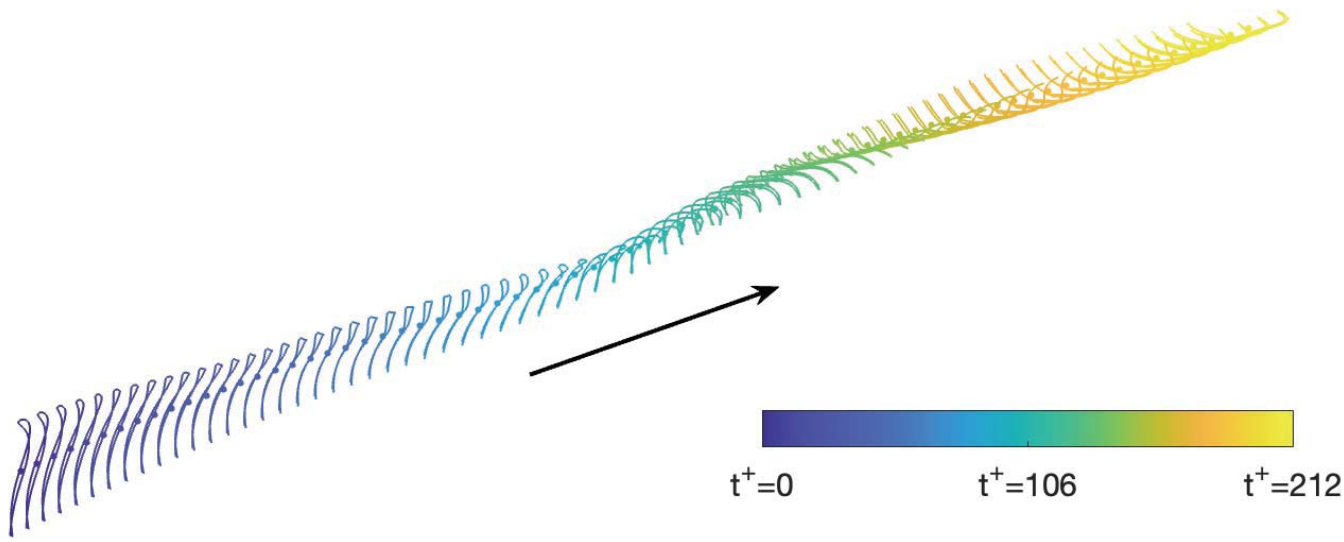

Figure 1. Persistent geometry preserved up to $t^+ \approx 212$ by a fiber of length $L_0^+ = 260$ while traveling within the central region of a turbulent channel flow at shear Reynolds number 300. The dots denote the centroid of the preserved geometric feature. The fiber thickness is magnified for clarity.

COLLECTIVE DYNAMICS OF ACTIVE FILAMENT ARRAYS

Ilteber R. Ozdemir[1], Yongyun Hwang[2] & Eric E. Keaveny[1]
[1] *Department of Mathematics, Imperial College London, SW7 2AZ, UK*
[2] *Department of Aeronautics, Imperial College London, SW7 2AZ, UK*

Abstract Active filaments, cytoplasmic streaming, linear stability analysis, Stokes flow.

Active filaments, such as biofilament-motor protein complexes, are central components of cellular flows. In cellular systems, these slender structures facilitate processes such as cytoplasmic streaming in plant cells and oocytes, leading to intracellular mixing and nutrient transport. In cases where the filaments protrude into the cell from the cell cortex to which they are attached, the nonzero curvature of the cell surface is suspected to play a role in the filament organisation, hence affecting the streaming state.

Theoretical and numerical descriptions of such systems often rely on active filament models, where internal motor activity is represented by a compressional force on the filament accompanied by an opposite force on the fluid. For a single filament in an unbounded domain, the filament begins to whirl above a critical forcing, and at even higher forcing values, transitions to planar beating [1].

Building from single-filament dynamics, we extend this perspective to arrays of active filaments distributed on a doubly-periodic surface (see Figure 1). In agreement with previous studies, our analysis reveals that collective interactions lead to oscillatory states at low filament density, while at high density the system shifts to a self-organised steady state with a net flow, corresponding to cytoplasmic streaming. We show that this change in behaviour is linked to the merger of two real eigenvalues when their associated modes are either still stable, or have already become unstable. Further, we explore the role of surface geometry on the organisation of streaming state. In particular, we will discuss the effect of surface curvature on this solution, including the selection of the streaming direction, as well as changes in filament deformation.

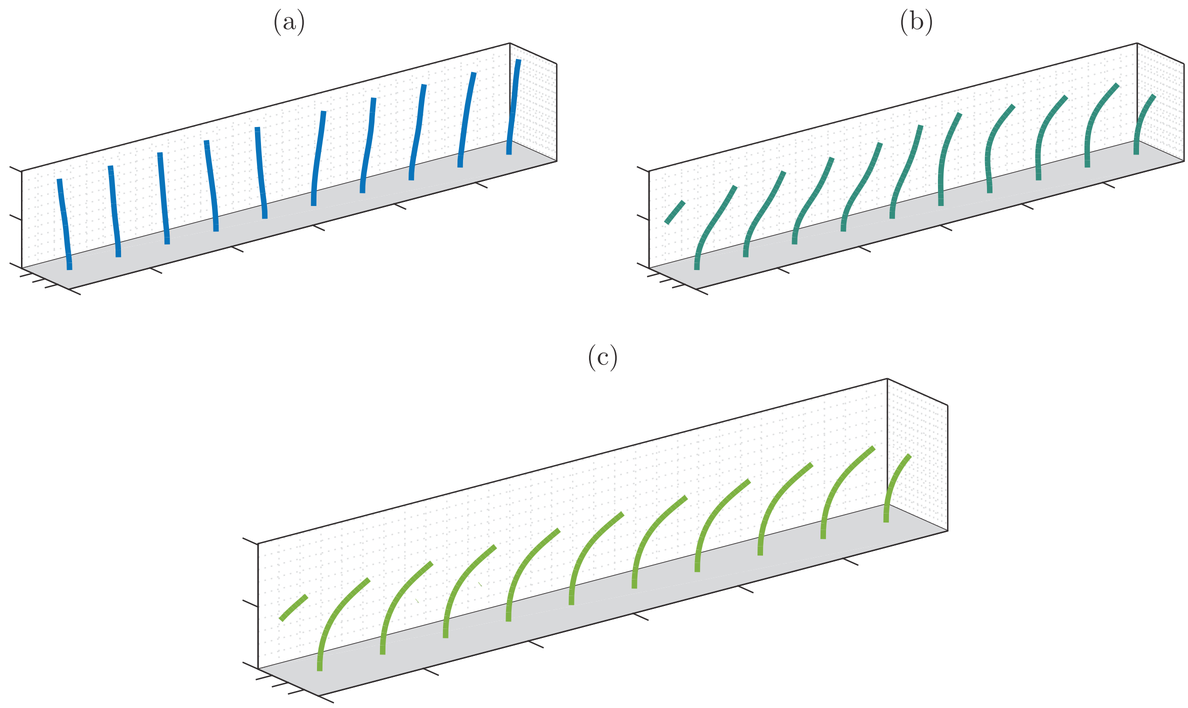

Figure 1. A filament array on a flat wall (coloured in grey) in a periodic domain in both directions. Above a critical density and forcing, filaments starting from random initial conditions quickly converge to a streaming state. Time advances as (a)→(b)→(c).

References

[1] Ozdemir, I. R., Clarke, B., Hwang, Y. & Keaveny, E. E., *A comparison of instabilities and dynamic states in active filament models*, to appear in Journal of Fluid Mechanics. https://arxiv.org/abs/2508.12831 (2026).

PARAMETRIC DESTABILIZATION OF AN ACOUSTICALLY FORCED RIVULET

Grégoire Le Lay[1,2], Adrian Daerr[1]
[1] *Laboratoire Matière et Systèmes Complexes, UMR 7057, Université Paris Cité / CNRS, 75013 Paris, France*
[2] *Laboratory of Fluid Mechanics and Instabilities, Ecole Polytechnique Fédérale de Lausanne, CH-1015 Lausanne, Switzerland*

Keywords Rivulet, Dynamics, Parametric Coupling, Pattern Generation, Weakly Nonlinear Expansion, Triadic Resonance

When studying dynamical systems, one usually considers either *external* (additive) or *parametric* forcing, each having its distinct characteristics. We investigate an original and intriguing hydrodynamic instability, where imposing an external forcing results in a parametric destabilization.
We study the behaviour of a fluid filament (a *rivulet*) flowing in an air-filled Hele-Shaw cell. In this seemingly simple system, reciprocal interactions between the flow inside the rivulet and the geometry of its free surface can lead to complex behaviour [1]. Two kind of perturbations are observable: transverse waves correspond to deformations of the rivulet path, and longitudinal waves correspond to modulations of its width (Figure 1). In the parameter range we adopt, both of these perturbations are linearly damped and the rivulet usually follows a straight path, flowing down with constant width.

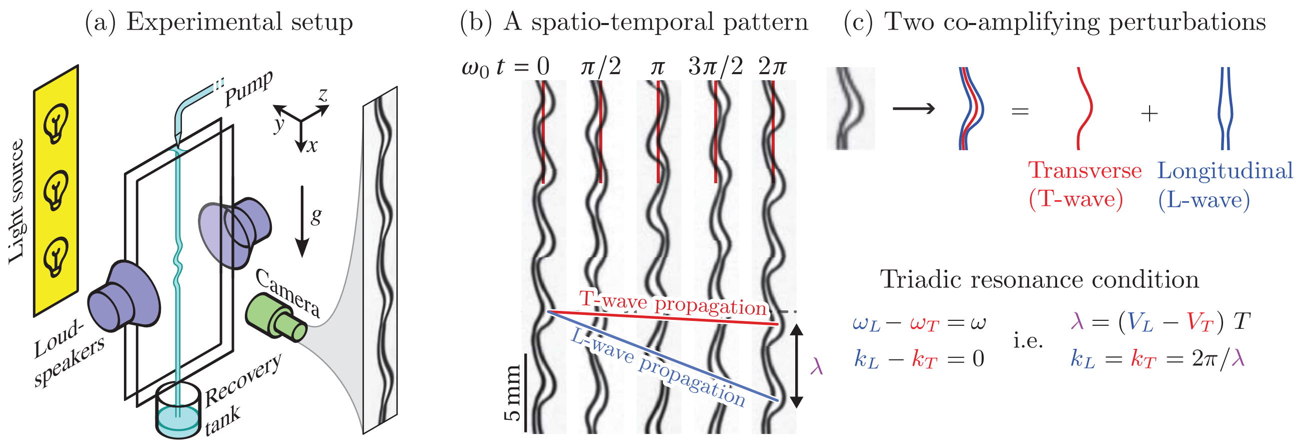

Figure 1. (a) Experimental apparatus. he speakers are used to provide a spatially homogeneous, temporally harmonic transverse forcing at frequency ω (b) The pattern exhibited by the rivulet. We observe strong transverse and longitudinal deformations, which propagate at different phase velocities V_T and V_L. (c) The instability results from a parametric coupling between the waves, which must obey a triadic resonance condition.

We impose an external, homogeneous, harmonic forcing to the rivulet. When the forcing amplitude exceeds a given threshold, the rivulet responds nonlinearly, adopting a peculiar pattern shown on Figure 1. We show that this behaviour results from a parametric co-amplification due to resonant interactions between transverse and longitudinal waves on the rivulet [2]. This is reminiscent of the interaction between counterpropagative waves in the Faraday instability [3]. The amplified waves satisfy a resonance condition, which selects a precise wavelength. We explain the observed wavelength through a resonance condition involving a weakly nonlinear triadic interaction. We then build a detailed theoretical model based on depth-averaged Navier-Stokes equations, which allows us to quantitatively describe the synchronous co-amplification, in perfect agreement with experiments. This allows us to explain the physical origin of the phenomenon and quantitatively describe its spatio-temporal features. This same model allows us to explain the experimentally observed nonlinear frequency detuning and the saturation of the phenomenon in amplitude [4]. We present extensive experimental evidence confirming the relevance of our model.

References

[1] A. DAERR, J. EGGERS, L. LIMAT & N. VALADE, *General Mechanism for the Meandering Instability of Rivulets of Newtonian Fluids*, *Phys. Rev. Lett.*, **106**, 184501 (2011).
[2] G. LE LAY & A. DAERR, *Phase-Locking Parametric Instability Coupling Longitudinal and Transverse Waves on Rivulets in a Hele-Shaw Cell*, *Phys. Rev. Lett.*, **134**, 014001 (2025).
[3] S. DOUADY, S. FAUVE & O. THUAL, *Oscillatory Phase Modulation of Parametrically Forced Surface Waves*, *EPL*, **10**, 309 (1989).
[4] G. LE LAY & A. DAERR, *Dancing rivulets in an air-filled Hele-Shaw cell*, *J. Fluid Mech.*, **1028**, A13 (2026).

SURFACE WAVES IN A CIRCULAR CHANNEL: GENERATION, PROPAGATION, COLLISION, RESONANCE AND MEAN FLOW.

Ion Dan Borcia[1], Ilke Kaykanat[1] Uwe Harlander[2] Rodica Borcia[1] & Michael Bestehorn[1]
[1]*Institute of Physics, BTU Cottbus–Senftenberg, 03046, Cottbus, Germany*
[2]*Department of Fluid Mechanics, BTU Cottbus–Senftenberg, 03044, Cottbus, Germany*

Abstract Keywords: Surface waves, Topography interaction, Mean flow.

We are studying fluid waves in a circular channel with a length of 4.7 m and a width of 8 cm, which is placed on a rotating table. The symmetry axis of the channel and the rotating axis coincide. The table can remain stationary, oscillate harmonically in the azimuthal direction, or undergo non-symmetrical (ratchet) oscillations. Firstly, we studied the wave generation and propagation using pure water as a working fluid, employing retractable barriers [1] and then bottom elevations [2]. For more viscous fluids, wave generation is also possible with periodic boundaries and a flat bottom through the horizontal Faraday instability [3]. The interaction of two waves [1] is used as a starting point for studying more complex phenomena such as resonance, or in the case of non-symmetrical channel oscillation [4, 5] or non-symmetrical surface elevation [5], the generation of a mean flow. We discuss the mechanism of flow generation based on combined experimental observations and simulations.

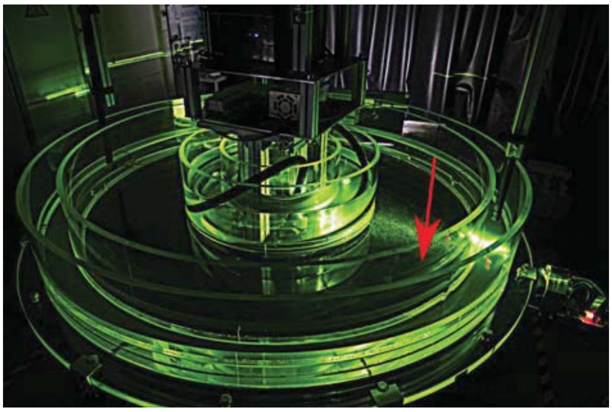

Figure 1. Rotating tank. The outer circular channel is used to produce surface waves.

References

[1] I. D. Borcia, R. Borcia, W. Xu, M. Bestehorn, S. Richter, & U. Harlander, *Undular bores in a large circular channel*, Eur. J. of Mec. B/Fluids, 79 (2020).
[2] F.-T. Schön, I. D. Borcia, U. Harlander, R. Borcia, S. Richter, &, M. Bestehorn, *Resonant surface waves in an oscillating periodic tank with a submerged hill*, J. Fluid Mech. (2024).
[3] I. D. Borcia, S. Richter, W. Xu, M. Bestehorn, & U. Harlander, *Horizontal Faraday instability in a circular channel*, PAMM, 19(1) (2019).
[4] I. D. Borcia, F.-T. Schön, U. Harlander, R. Borcia, & M. Bestehorn, *Mean flow generated by asymmetric periodic excitation in an annular channel*, Eur. Phys. J. Special Topics 233 (2024).
[5] F.T. Schön, U. Harlander, I. D. Borcia, R. Borcia, & M. Bestehorn. *Mean fluid transport in an oscillating circular channel with asymmetric forcing*, Water Waves (2025).

PERFECT ACTIVE ABSORPTION OF WATER WAVES IN A CHANNEL BY A DIPOLE SOURCE

P. Petitjeans[1], L-P. Euvé[1], K. Pham[2], V. Pagneux[3], A. Maurel[4]

(1) PMMH, ESPCI-Paris, France,
(2) LMI, ENSTA Paris, Institut Polytechnique de Paris, Palaiseau, France
(3) Laboratoire d'Acoustique de l'Université du Mans (LAUM), Le Mans, France
(4) Institut Langevin, ESPCI Paris, Paris, France

Keywords: Surface waves, Water waves, Total absorption

Abstract

We present a study on the perfect active absorption of water waves in a channel using a dipole source. The results are detailed in [1]. This study combines theoretical modeling, numerical simulations, and experimental validation to demonstrate the effectiveness of the proposed approach. Our research investigates the feasibility of employing an active device composed of two closely spaced sources operating in quasi-opposition of phase to achieve complete wave absorption through interference phenomena. The goal is to cancel both reflection and transmission of incident waves (Figure 1a).

To achieve this, we initially focus on analyzing the waves generated by the dipole source to optimize the absorption of specific incident waves. A theoretical model is developed to establish the governing law of these outgoing waves. The model is then validated numerically and experimentally by varying all geometrical parameters across a wide frequency range.

In our experimental setup, we create the dipole source by creating two side cavities connected to the wave channel through openings in the vertical walls. Independent linear motors are placed in these cavities to generate the dipole source (Figure 1a). Using Fourier transform profilometry, we measure the waves and confirm that by carefully tuning the source parameters, we achieve near-total absorption of an incident wave (99.9% over a wide range of frequencies).

We also investigate the performance of the dipole source under transient conditions, where varying wave signals are introduced (Figure 1b). Our results demonstrate that the system achieves an absorption exceeding 99%.

Our study highlights the advantages of active absorption over traditional passive methods, which require large structures and lack adaptability. The active dipole source offers a compact and flexible solution for wave energy management and coastal protection.

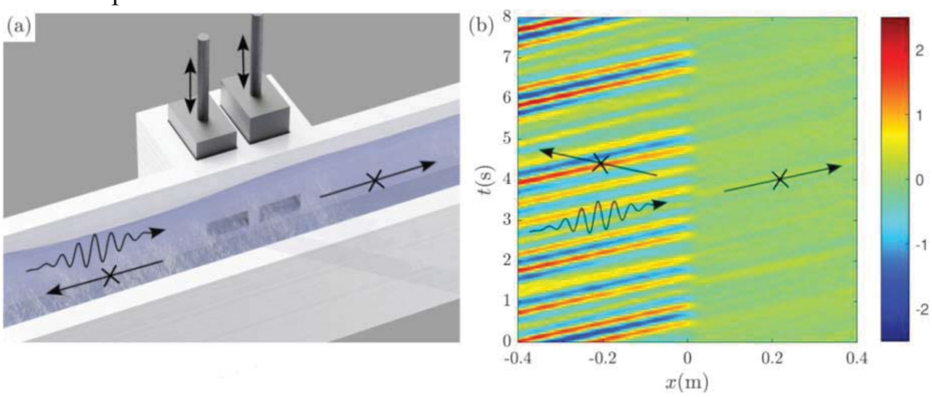

Figure 1: Perfect absorption by a dipole source. (a) Schematic view of the experimental set-up. (b) Space–time diagram η(x, t) reporting the perfect absorption of an transient incident wave by the dipole source placed in x = 0

References

[1] L.-P. Euvé, K. Pham, P. Petitjeans, V. Pagneux, A. Maurel, J. Fluid Mech, 990, (2024) A9.

WAVE PATTERN FORMATION IN A DISPERSIVE SYSTEM: DEVELOPMENT OF WIND WAVES

Evgeny Mogilevskiy[1] & Lev Shemer[1]
[1] *School of Mechanical Engineering, Tel Aviv University, Tel Aviv, Israel*

Abstract A theoretical model is proposed to account for the coexistence of multiple unstable dispersive wave modes under given initial and boundary conditions. The model is applied to the development of a water-gravity wave field that appears under impulsively applied wind forcing and is modulated in time and space. (Wind waves, Linear stability, Dispersive systems, Spatio-temporal evolution).

Conventional analysis of linear instability of 2D shear flow deals with either temporal or spatial evolution of small disturbances, implying spatial or temporal homogeneity, respectively. In reality, the flow domain is usually bounded in space and in time: the boundary conditions are specified at $x = 0$, while the flow development initiates at $t = 0$. The proposed model analyzes evolution of a wave system excited by impulsively applied forcing in a spatially semi-infinite domain. The investigation is guided by experiments on young wind waves carried out in a coupled wind/water wave facility at Tel Aviv University [1]. The model assumes that water and air are initially at rest; at $t = 0$ uniform wind is applied in the test section at $x > 0$. The lin-log velocity profile [2] with constant friction velocity u_* is adopted. The wind immediately induces water current with the surface drift velocity $U_d = 0.5u_*$ that decays exponentially with depth. The temporal linear stability analysis [4] performed for surface elevation due to each harmonic $\eta(k, x, t)$ that is based on the coupled at air/water interface Orr – Sommerfeld equations (OSE) shows that the flow is unstable in the range of wavenumbers $k_{min} < k < k_{max}$; the growth rate $\gamma(k)$ depends on the velocity profiles in air and water. Extending the approach adopted in [3] in which a superposition of multiple random coexisting harmonics is considered, and using the transport equation for each harmonic separately, the model describes the spatio-temporal modulation of the water surface elevation represented by $\eta_{rms}(x, t)$ and the peak frequency $f_p(x, t)$. The uniform power spectral distribution over a wide range is applied at $x > 0$ for $t = 0$ and at $x = 0$ for $t > 0$.

The model employs a quasi-linear approach: different wave modes do not interact; the evolution of the power spectral density represents growth in time with the rate $\gamma(k)$ and the spatial propagation with the group velocity $c_g(k)$, provided by OSE. The growth of each harmonic is limited by the finite propagation duration $x/c_g(k)$. In addition, a limit of the order of 10^{-1} is imposed on maximum possible local steepness. The model suggests that once this critical value is attained, all waves with frequencies $f > f_p$ decay, being sheltered from the wind by higher coexisting modes. The interplay between these constraints produces a complex spatiotemporal pattern in $\eta_{rms}(x, t)$ and $f_p(x, t)$, which can be decomposed into several stages exhibiting qualitatively different spectral shapes. At each fetch x, the model predicts the temporal variation of $\eta_{rms}(t)$ and the simultaneous decrease of $f_p(t)$ in general accordance with the experimental results [1] (fig. 1). The quantitative comparison of the model results with the experiments is challenging due to multiple factors as discussed in [4]. Nonetheless, the results are important as the proposed model can be applied to flows that are subject to similar spatial and temporal inhomogeneity, mechanisms of growth limitations, and the dependencies $\gamma(k)$ and $c_g(k)$.

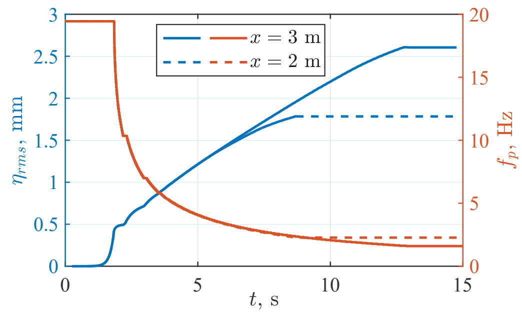

Figure 1. Evolution of the surface elevation η_{rms} and the peak frequency f_p in time for different fetches, $u_* = 0.3$ m/s.

References

[1] A. Zavadsky & L. Shemer, *Water waves excited by near-impulsive wind forcing*, J. Fluid Mech. **828**, 459–495 (2017).
[2] J. Miles, *On the velocity profile for turbulent flow near a smooth wall*, J. Aero. Sci., **24**, 704. (1957)
[3] M. Geva & L. Shemer, *Excitation of initial waves by wind: A theoretical model and its experimental verification*, Phys. Rev. Lett. **128**, 124501 (2022).
[4] K. Kumar & L. Shemer, *Shear flow instability analysis of young wind waves: coupled air–water Orr-Sommerfeld framework guided by experiment*, J. Fluid Mech. *In press* (2026).

FINITE-AMPLITUDE VISCOUS GRAVITY-CAPILLARY WATER WAVES WITH WIND-FORCING.

Nikhil Yewale[1], Vinod Kumar Kadari[1] & Ratul Dasgupta[1]
[1] *Department of Chemical Engineering, Indian Institute of Technology, Powai, 400076, India*

Abstract Parasitic capillary ripples are observed on the forward face of finite amplitude travelling, surface wave trains, both in the lab and in the sea. Steady-state permanent form solutions are calculated for viscous gravity-capillary water waves, with wind-forcing. The critical wave-steepness(ak_{cr}) is calculated beyond which the parasitic-capillary ripples start appearing in the steady-state solutions. The parasitic capillary ripples appearing beyond the critical steepness, become increasingly more asymmetric and appears on the front face of the travelling wave with the increase in Reynolds number.

The steady-state solutions are calculated based on work the time-dependent conformal mapping methodology proposed by Shelton et.al. [1]. It is to be noted that although the work by Shelton et.al. [1] establishes the method, the calculations realistic to water-waves, relevant to the ocean surface waves are not highlighted. For a particular Reynolds number (Re) and energy (ϵ) , we find permanent form travelling wave solution corresponding to an inverse Bond-number (B) (based on same length-scale as that of Reynolds number i.e. wavelength(λ) of the finite-amplitude wave) , a *Reynolds-number dependent* Froude number (F), wind-forcing (P) and wave-steepness (ak). It is evident from Figure 1 that the critical

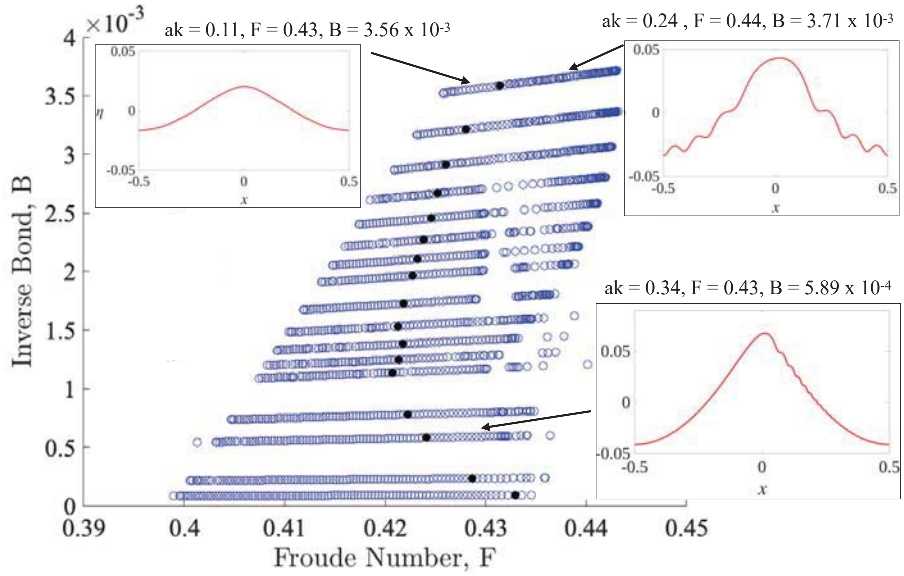

Figure 1. Steady-state solution for viscous gravity-capillary water waves, with wind-forcing. The physical properties of air-water are used for density, surface-tension coefficient and viscosity. Each data-point in the figure corresponds to a steady-state solution on an inverse Bond (B) vs Froude number (F) plane for a particular Reynolds number (Re) , wave-steepness (ak) and wind-forcing (P). Each black-dot marked on data-set corresponding to a particular Re corresponds to a critical wave-steepness (ak_{cr}) below which the parasitic capillary ripples do not appear in a steady-state solution. See the inset figures with arrows pointed to the colored data-points.

steepness beyond which the parasitic capillary ripples start appearing first is dependent on (Re) for a particular energy (ϵ). This critical steepness also increases as one approaches the inviscid limit at very high Reynolds number (see $Re = 10^5$ and $Re = 2 \times 10^5$ data-set in figure 1). Moreover, these ripples become more asymmetric (i.e. appear predominantly on the forward face of travelling waves) as calculated by *pseudo-steady* model by Longuet-Higgins (1995) [2].

References

[1] Shelton, Josh and Milewski, Paul and Trinh, Philippe H. , *Time-dependent nonlinear gravity–capillary surface waves with viscous dissipation and wind forcing*, Journal of Fluid Mechanics. **1003**, A13 (2025).
[2] M. S. Longuet-Higgins, *M. S. Longuet-Higgins, Parasitic capillary waves : a direct calculation*, , Journal of Fluid Mechanics. **301**, 79-107 (1995).

UNDULATORY LOCOMOTION OF ELASTIC PROPULSORS WITH STANDING AND TRAVELING WAVES

Andrew C. Lenart[1], Christopher L. Jawetz[1] & Alexander Alexeev [1]
[1] *George W. Woodruff School of Mechanical Engineering, Georgia Institute of Technology, Atlanta, USA*

Abstract Undulatory swimming, bifurcating wake, fluid-structure interactions

Bending kinematics have a profound effect on the hydrodynamic performance of undulatory swimmers. Traveling waves are widely associated with higher propulsive efficiency, whereas standing waves are generally linked to enhanced thrust production. In this work, we employ a three-dimensional, fully coupled fluid–structure interaction (FSI) computational model to investigate how standing and traveling wave patterns affect the undulatory propulsion of an elastic plate oscillating at different Reynolds numbers [1]. To systematically control the bending pattern, we harness thickness tapering that modifies the local flexural stiffness. As flexular waves propagate along a tapered plate they slows down which suppresses their reflection at the free end. This phenomenon, known as the acoustic black hole effect [2], leads in the formation of traveling flexular waves propagating along tapered elastic propulsor.

Our results demonstrate that varying the actuation frequency allows continuous tuning of the ratio between traveling and standing waves in the bending pattern. The oscillations can be changed from predominantly standing-wave motion at resonance to traveling-wave motion at post-resonance frequencies. We find that the maximum thrust is produced by standing-wave oscillations, and that this peak thrust increases with Re. In contrast, traveling waves yield substantially higher hydrodynamic efficiency, an advantage that is more pronounced as higher Re. At $Re = 2000$, traveling waves increase the efficiency by about 50% relative to standing-wave oscillations.

Flow field analysis reveals that standing and traveling wave oscillations produce distinctly different wake structures. In particular, traveling waves generate a characteristic bifurcating wake, with two vortex jets extending downstream at an acute angle from the plate plane. This wake bifurcation arises from the longitudinal advection of side-edge vortices by the traveling wave, which strengthens vorticity near the trailing edge. The bifurcating wake is more prominent at higher Re: it forms at $Re = 1000$ and fully develops at $Re = 2000$. Pairs of oppositely rotating vortices in bifurcating wake assist the thrust generation. At lower Re, however, increased viscous dissipation suppresses vorticity and prevents wake bifurcation, which results in the reduced thrust.

Thus, our findings support the notion that thunniform and ostraciiform locomotion that rely on standing wave oscillations is advantageous for generating greater thrust and faster swimming. However, this comes at the cost of reduced hydrodynamic efficiency. In contrast, traveling wave locomotion, characteristic of anguilliform swimming, produces somewhat weaker thrust but offers significantly greater efficiency. In addition to providing new insights into the hydrodynamics of fish locomotion, our results show that thickness tapering provides a simple, cost-effective, and highly effective strategy for enhancing the hydrodynamic performance of bio-inspired swimming robots.

References

[1] A. C. Lenart & C. L. Jawetz & A. Alexeev, *Undulatory hydrodynamics of tapered elastic plates in viscous fluid*, Journal of Fluid Mechanics. vol. 1028, A37, 2026.
[2] M. Mironov, *Propagation of a flexural wave in a plate whose thickness decreases smoothly to zero in a finite interval*, Sov. Phys. Acoust. vol. 34, 318, 1988.

A COMBINED SHARP- AND DIFFUSE-INTERFACE MODEL FOR SIMULATION OF DROPLETS WETTING MEMBRANES

Sebastian Aland[1,2]
[1]*HTW Dresden, Germany*
[2]*TU Freiberg, Germany*

Keywords: membrane dynamics, wetting, phase-field model,

Abstract

Biological cells use membranes and liquid-like droplets (called condensates) to organize their interior [1]. As every structure within a cell is either enclosed by a membrane or by a liquid interface it is fundamental to understand what happens if these two interfaces come into contact. Recent studies suggest that membrane-droplet interactions are involved in various key biological processes [2]. As experimental image resolution is limited at the corresponding length and time scales, numerical methods are essential to shed light on the dynamics of the process.

Using a combination of sharp and diffuse interface models, we derive a mathematical model to describe the interplay of a thin elastic membrane with a two-phase fluid [2,3]. Our numerical method employs adaptive, fitted finite element meshes with arbitrary Lagrangian–Eulerian (ALE) mesh motion, ensuring robustness and geometric flexibility. We validate the method through benchmark tests and demonstrate its accuracy and versatility. Finally, we showcase droplet-mediated remodeling of biological membranes, revealing capillarity-driven phenomena such as droplet wrapping (Fig.1), endocytosis-like invagination, and an inverted Cheerios effect.

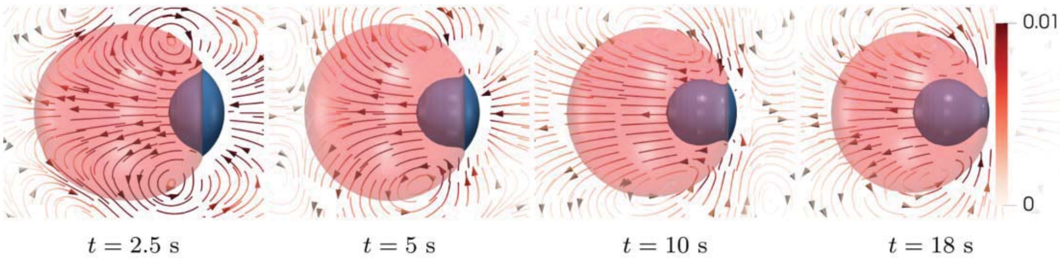

Figure 1. A membrane (pink) is largely deformed by surface tension of a droplet (blue)

References

[1] Aierken, D., Aland, S., Bo, S., Boeynaems, S., Cai, D., Carra, S., ... & Zwicker, D. (2026). Roadmap for Condensates in Cell Biology. arXiv preprint arXiv:2601.03677.

[2] Wang, Y., Li, S., Mokbel, M., May, A. I., Liang, Z., Zeng, Y., ... & Fang, X. (2024). Biomolecular condensates mediate bending and scission of endosome membranes. *Nature*, *634*(8036), 1204-1210.

[3] Mokbel, M., Mokbel, D., Liese, S., Weber, C., & Aland, S. (2024). A simulation method for the wetting dynamics of liquid droplets on deformable membranes. *SIAM journal on scientific computing*, *46*(6), B806-B829.

Emergence of natural convection beneath a fluid-supported sheet

Abstract

Understanding the interplay between thermal, elastic and hydrodynamic effects is crucial for a variety of applications, including the design of soft materials and microfluidic systems. Motivated by these applications, we investigate the emergence of natural convection in a fluid layer that is supported from below by a rigid surface, and covered from above by a thin elastic sheet. The sheet is laterally compressed and is maintained at a constant temperature lower than that of the rigid surface(See, Fig.1). We show that for very stiff sheets, and below a certain magnitude of the lateral compression, the system behaves as if the fluid were confined between two rigid walls, where the emergent flow exhibits a periodic structure of vortices with a typical length scale proportional to the depth of the fluid, similar to patterns observed in Rayleigh–Bénard convection. However, for more compliant sheets, and above a certain threshold of the lateral compression, a new local minimum appears in the stability diagram, with a corresponding wavenumber that depends solely on the bending modulus of the sheet and the specific weight of the fluid, as in wrinkling instability of thin sheets. The emergent flow field in this region synchronises with the wrinkle pattern(See, Fig.1). We investigate the exchange of stabilities between these two solutions, and construct a stability diagram of the system.

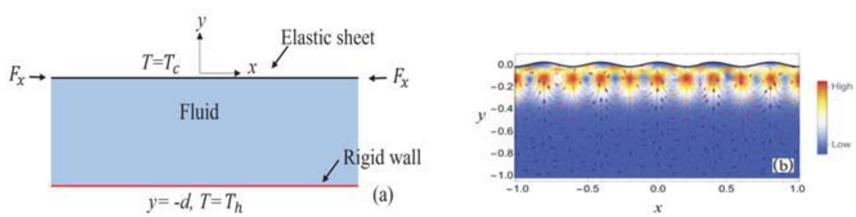

Figure 1: (a). Schematics of the setup. (b). The flow field at the new (elastic) minimum in the stability diagram.

Reference: Emergence of natural convection beneath a fluid-supported sheet, Saichand Chowkampally, Oz Oshri, *J. Fluid Mech*, ***1018***, *A 50., (2025).*

SNAP-INDUCED FLOW IN A CLOSED CHANNEL

Oz Oshri[1,] Kirill Goncharuk[1] & Yuri Feldman[1]
[1]*Department of Mechanical Engineering, Ben-Gurion University of the Negev, Beer-Sheva 84105, Israel*

Keywords: fluid-structure interaction, buckling, thin sheets.

Abstract

Snap-through is a buckling instability that allows slender objects, including those in plant and biological systems, to generate rapid motion that would be impossible if they were to use their internal forces exclusively. In microfluidic devices, such as micromechanical switches and pumps, this phenomenon has practical applications for manipulating fluids at small scales. The onset of this elastic instability often drives the surrounding fluid into motion – a process known as snap-induced flow. To analyse the complex dynamics resulting from the interaction between a sheet and a fluid, we develop a prototypical model of a thin sheet that is compressed between the two sides of a closed channel filled with an inviscid fluid. At first, the sheet bends towards the upstream direction and the system is at rest. However, once the pressure difference in the channel exceeds a critical value, the sheet snaps to the opposite side and drives the fluid dynamics. We formulate an analytical model that combines the elasticity of thin sheets with the hydrodynamics of inviscid fluids to explore how external pressure differences, material properties and geometric factors influence the system's behaviour. To analyse the early stages of the evolution, we perform a linear stability analysis and obtain the growth rate and the critical pressure difference for the onset of the instability. A weakly nonlinear analysis suggests that the system can exhibit a pressure spike in the vicinity of the inverted configuration [1].

References

[1] Oshri O, Goncharuk K, Feldman Y. Snap-induced flow in a closed channel. *Journal of Fluid Mechanics*. 2024; 986: A12.

CAPILLARY SURFERS: WAVE-DRIVEN PARTICLES ON A VIBRATING FLUID INTERFACE

Giuseppe Pucci[1,2,3]
[1] *Consiglio Nazionale delle Ricerche (CNR Nanotec), Via P. Bucci 33C, 87036 Rende, Italy.*
[2] *Dipartimento di Fisica, Università della Calabria, Via P. Bucci 31C, 87036 Rende, Italy.*
[3] *INFN, Sezione di Lecce, Via per Monteroni, 73100 Lecce, Italy.*

Abstract Capillary surfers; wave-mediated interactions; interfacial hydrodynamics.

A small solid particle resting atop a vibrating fluid interface generates outwardly propagating capillary waves owing to its vertical motion relative to the interface. Capillary surfers are wave-driven particles at a fluid interface that we have recently introduced [1] and described theoretically [2].

A capillary surfer is a hydrophobic, millimetric solid particle whose lower surface is pinned to the air–water interface of a vertically vibrating bath. When the particle's mass is unevenly distributed, it generates an asymmetric field of capillary waves and self-propels along the interface at constant speed in a straight line. The speed of the surfers, and their interactions with the environment, can be tuned broadly through the particle, fluid, and vibration parameters. More recently, we have characterized the wave field of capillary surfers and further elucidated the propulsion mechanism [3]. Capillary surfers also interact with one another through their mutual capillary wave field and exhibit collective modes characterized by a discrete set of equilibrium spacings for a given set of experimental parameters.

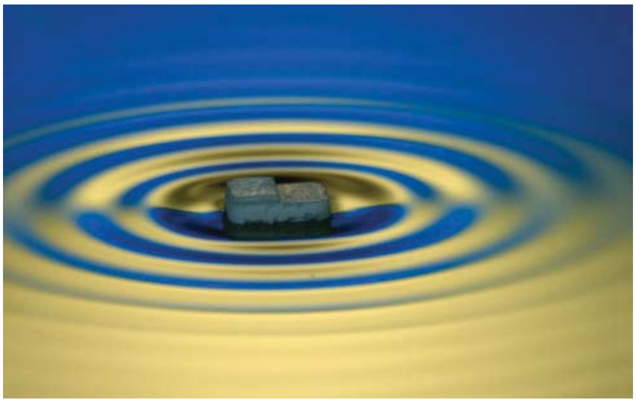

(a) A single capillary surfer.

(b) Two interacting surfers.

Figure 1. Capillary surfers on a vibrating liquid bath: single-particle propulsion and wave-mediated interactions.

References

[1] I. Ho, G. Pucci, A. U. Oza and D. M. Harris, *Capillary surfers: wave-driven particles at a vibrating fluid interface*, Phys. Rev. Fluids **8**, L112001 (2023).
[2] A. U. Oza, G. Pucci, I. Ho and D. M. Harris, *Theoretical modeling of capillary surfer interactions on a vibrating fluid bath*, Phys. Rev. Fluids **8**, 114001 (2023).
[3] W. Reino, *Ph.D. thesis*, Università della Calabria, Italy (2025).

A Revisit of Edge Effects on the Free Fall of Non-circular Plates Under Controlled Initial Conditions

Che-Kai Yang[1],Ping-Hung Yen[1], Rahul Kumar Mondal[1], Symphony Chakraborty[1] & An-Bang Wang[1]
[1]*Institute of Applied Mechanics, National Taiwan University, Taipei, 106319 Taiwan (R.O.C.)*

Keywords: freely falling bodies, fluttering instability, edge effect, planar particles, $\theta_f - I^*$ phase diagram.

Abstract

Freely falling objects are ubiquitous in nature, such as snowflakes, seeds and leaves, and they often exhibit irregular descent paths. In this study, we experimentally investigated the free-fall dynamics of non-circular flat plates to compare with that of the circular disk. The former is commonly considered as more sensitive to the surrounding disturbances. We demonstrated that the mixed zigzag and spiral patterns of a falling square plate can be effectively suppressed to be a fully repeatable sliding and then zigzag motion by a initial release control for different release angle (α) as shown in Figure 1 (a)-(c). The trajectory, fluttering period, and phase diagram of both circular and non-circular plates have been systematically analyzed and compared. To quantify the edge effects for the comparison, three characteristic length scales, i.e., the circumscribed-circle diameter, the equivalent (equal area) diameter, and the inscribed-circle diameter, are used to classify the falling patterns by the averaged extreme angle at the turning points (θ_f) in terms of dimensionless moment of inertia defined as I_i*, I_e* and I*. Based on the suitable choice of the characteric length, Figure 1(d) can reveal the common similarity trend for all tested plates in the $\theta_f - I^*$diagram and Figure 1(e) may effectively show the edge character in the $\theta_f - I_e{}^*$ diagram. The present work is expected to shed new insight for the analysis of the free-fall dynamics.

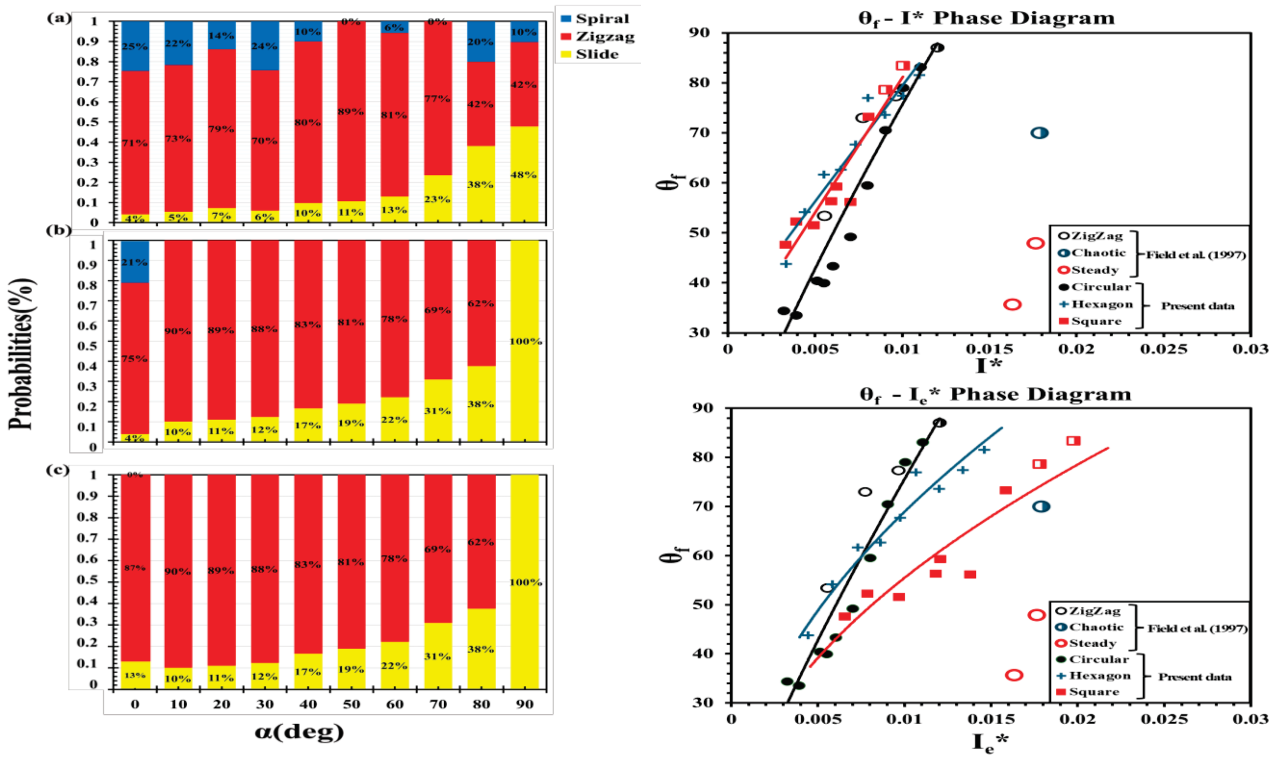

Figure 1. Falling patterns of square plates (a) without control and with (b) passive (c) active initial-condition control; and edge effects on the (d) $\theta_f - I^*$ and (e) $\theta_f - I_e{}^*$ phase diagram. (semi-hollow symbol: ZigZag-Tumbling)

References

[1] S. B. Field, M. Klaus, M. Moore & F. Nori, Chaotic dynamics of falling disks, Nature 388 (6639), 252–254 (1997).
[2] H. Zhong, S. Chen & C. Lee, Experimental study of freely falling thin disks: Transition from planar zigzag to spiral, Phys. Fluids, 23 (1), 011702 (2011).

FLUID-STRUCTURE INSTABILITIES NEEDS ACCURATE NUMERICS: A FAST AND CONSISTENT SHARP-INTERFACE IMMERSED BOUNDARY METHOD FOR MOVING BODIES

Giovanni Vagnoli[1], Martino Andrea Scarpolini[1], Roberto Verzicco[1,2] and Francesco Viola[1]
[1] *Department of Mathematics, Gran Sasso Science Institute, L'Aquila, Italy*
[2] *University of Twente, AE Enschede, Twente, 7500, the Netherlands*

Abstract Fluid-structure interaction, Immersed boundary method, fluid-structure instabilities
Immersed boundary methods (IBMs) have proven to be valuable tools for the numerical investigation of complex flow configurations and fluid–structure interaction (FSI). However, accurately predicting the onset and subsequent evolution of fluid–structure instabilities—such as those occurring in freely falling or rising bodies—requires high numerical precision. Among them, Eulerian methods [1] enforce the no-slip condition on non-conforming walls through flow reconstruction near the body, but are not adequate for moving walls and FSI due to the presence of emerging fluid nodes, the difficulties in treating zero-thickness bodies and the presence of non-smooth stresses over the wet surface. On the other hand, Lagrangian methods [2] are well suited for moving bodies thanks to the diffusion of the interface, but are known to suffer from large slip errors. Furthermore, when the IBM is implemented within a fractional-step method, the no-slip condition is modified during the projection step [3]. To avoid this, a boundary condition on the walls should be enforced on the elliptic equation, preventing the use of fast Fourier transform (FFT) methods in favour of less efficient solvers. Therefore, most IBMs lacks accuracy on the imposition of the no-slip condition at the solid wall and the evaluation of the hydrodynamics loads, key aspects for addressing correctly the onset of hydrodynamic instabilities in presence of solid wall, particularly when the bodies are moving.
In our work, we propose a novel Eulerian sharp-interface IBM suitable for FSI and zero-thickness walls. In particular, the immersed boundary forcing step is performed before the evaluation of the provisional velocity, and the no-slip condition is enforced on the closest fluid points to the surface through an interpolation of the flow between the bulk and the (possibly) moving wall. The resulting method can treat sharp interfaces (also with zero thickness), satisfying the no-slip condition on the walls up to the precision of the chosen interpolator. To reduce the projection error, the forcing term of the solenoidal projection step is modified consistently with the conservation of mass to take into account the presence of solid walls. However, the discrete Laplace operator is left unchanged, allowing the use of fast Poisson solvers based on FFT algorithms. The hydrodynamic loads are evaluated using a high order flow reconstruction near the walls, using smooth MLS interpolation, leading to an accurate prediction of the traction acting on the body. The novel method is tested against classical benchmarks, such as the flow around a fixed sphere, the FSI of a flapping flag, and highly pressurized bubbles, and the performance is compared with existing IBMs.

References

[1] E. A. Fadlun, R. Verzicco, P. Orlandi, J. Mohd-Yusof, *Combined Immersed-Boundary Finite-Difference Methods for Three-Dimensional Complex Flow Simulations*, Journal of Computational Physics, 161, 35–60, 2000.
[2] M. Vanella, E. Balaras, *A moving-least-squares reconstruction for embedded-boundary formulations*, Journal of Computational Physics, 228, 2009.
[3] G. Vagnoli, M. A. Scarpolini, R. Verzicco, F. Viola, *A local and explicit forcing correction for Lagrangian immersed boundary methods*, Computer Physics Communications, 315, 2025.

From In-House Immersed Boundary Solvers to OpenFOAM: An Implicit Framework for FSI

Yuri Feldman[1]
[1]*Department of Mechanical Engineering, Ben-Gurion University of the Negev, Beer-Sheva 84105, Israel.*

Keywords: Immersed Boundary Method, FSI, OpenFOAM

Abstract

Advanced immersed boundary and fluid-structure interaction algorithms are often developed and validated within highly specialized in-house research codes, where they can achieve excellent accuracy, robustness, and flexibility. However, their broader reuse is frequently limited by the lack of standardization: extending such solvers to new boundary conditions, improving scalability, or introducing further physical models often requires substantial code-level effort and a full understanding of the original implementation. In this talk, we address this gap in the context of direct-forcing immersed boundary methods by showing how algorithmic ideas previously developed in a custom finite-volume framework (the implicit coupling of pressure and Lagrangian forces within a SIMPLE-based formulation [1] and its efficient preconditioned solution strategy [2]) can be transferred into a widely used open-source CFD environment.

Our goal is not merely to reproduce immersed boundary capabilities in an existing solver. Instead, we embed them implicitly while preserving the formal structure and functionality of the original methodology. This approach also benefits from the mature parallelization, linear algebra, and preconditioning infrastructure already available in OpenFOAM. In contrast to implementations based mainly on explicit source-term additions, relying mostly on internal iterations to enforce the no-slip constraint, the proposed method implicitly incorporates the immersed boundary functionality directly into the solver framework. It enables efficient simulations of fully three-dimensional flows hosting stationary and moving immersed bodies. The potential extension of the methodology to a broader range of FSI problems will also be briefly outlined.

References

[1] K. Goncharuk, O. Oshri, Y. Feldman, *The immersed boundary method: A SIMPLE approach*, Journal of Computational Physics 487 (2023) 112148.

[2] R. Yovel, E. Treister, Y. Feldman, *A SIMPLE-based preconditioned solver for the direct-forcing immersed boundary method*, Computer Methods in Applied Mechanics and Engineering 453 (2026) 118833.

ON BIFURCATIONS AND TRACTION FORCES ON AN OBSTACLE IN INCOMPRESSIBLE FLOW

J. Cach[1], K. Tůma[1], J. Blechta[1] & S. Schwarzacher[1,2]
[1] *Charles University, Faculty of Mathematics and Physics, Sokolovská 83, 186 75 Prague, Czechia*
[2] *Uppsala Universitet, Ångströmlaboratoriet, Lägerhyddsvägen 1, 751 06 Uppsala, Sweden*

Keywords: Navier-Stokes flow, pointwise traction, flow around cylinder, bifurcation, multiple steady solutions, vortex street, periodic solutions.

Abstract
We present a systematic numerical investigation of bifurcations in the two-dimensional incompressible Navier-Stokes flow past a confined circular cylinder [1]. The results indicate that there is a qualitative correspondence between changes in the traction profiles of the steady Navier-Stokes equations and bifurcations in flows driven by the unsteady Navier-Stokes equations. The bifurcations include the appearance of symmetry breaking, oscillations, and multiple steady solutions.

In particular, we consider the Schäfer-Turek benchmark [2] with Reynolds numbers up to 1000. For the analysis of bifurcations and traction profiles, several numerical strategies are applied, including a duality method for computing traction profiles [3], deflation methods, and linear stability analysis. The relations presented here indicate the possibility of a computationally inexpensive strategy to detect critical Reynolds numbers.

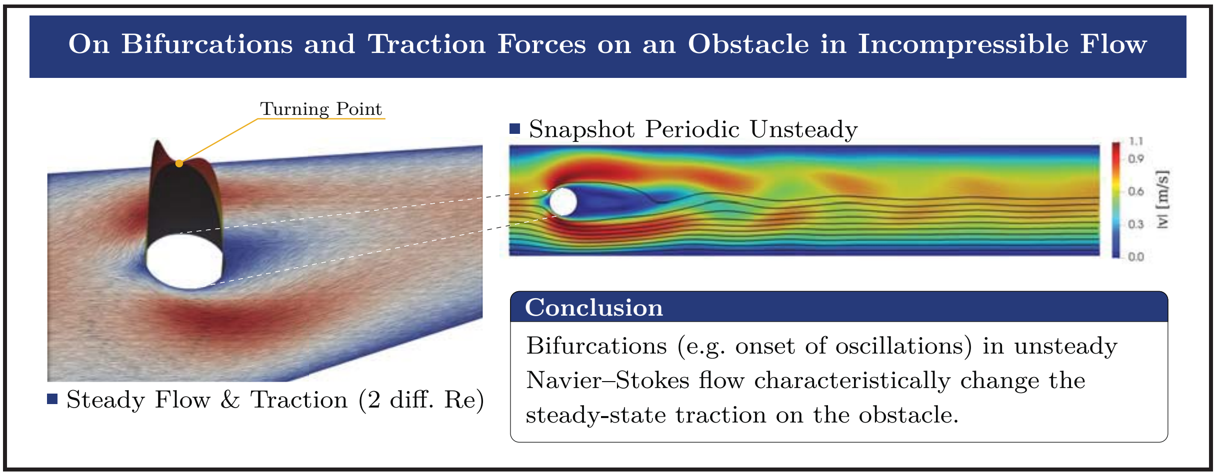

Figure 1. Graphical abstract

References

[1] Jakub Cach, Karel Tůma, Jan Blechta, & Sebastian Schwarzacher, *On bifurcations and traction forces on an obstacle in incompressible flow*, arXiv:2512.15424 [physics.flu-dyn] (2025)

[2] M. Schäfer, S. Turek, F. Durst, E. Krause & R. Rannacher, *Benchmark computations of laminar flow around a cylinder*, in *Flow Simulation with High-Performance Computers II: DFG Priority Research Programme Results 1993–1995*, Vieweg+Teubner Verlag, Wiesbaden, pp. 547–566 (1996).

[3] M. Giles, M. G. Larson, J. M. Levenstam & E. Süli, *Adaptive error control for finite element approximations of the lift and drag coefficients in viscous flow*, Oxford University Research Archive (1997).

FLOW-INDUCED VIBRATIONS OF AN ELASTICALLY-MOUNTED SQUARE CYLINDER WITH RIGID SPLITTER PLATE

Umesh Kumar Patel*, Shubham Giri & Rajneesh Bhardwaj
*email: 22D0871@iitb.ac.in

Abstract

Flow-induced vibrations (FIV) of elastically-mounted square cylinder are primarily governed by galloping instability, which can lead to large vibration amplitudes and structural damage. Passive control using splitter plates is widely employed to modify wake dynamics and suppress flow-induced vibrations (FIV); however, to the best of our knowledge, the effect of splitter-plate length on the vibration response of square cylinders has not yet been experimentally investigated. To this end, the present study experimentally examines the effect of rigid splitter plates of various length, attached on lee side of the cylinder (side length, $D = 60$ mm) in uniform flow for reduced velocity in range of $5 - 36$.
The experimental setup (Fig. 1(a)) consists of four air bearings (two on top and two on bottom) of load capacity 20 N each and eight linear springs (four on top and four on bottom) of stiffness 16 N/m each. Fig. 1(b) and 1(c) show the arrangement of bearings, springs, and cylinder-plate model. The test model is connected to a mounting plate which is fixed on air bearings allows transverse motion with nearly zero damping. Springs are connected to the mounting plate to provide elasticity to the system. The model is tested in a low speed wind tunnel with various measurement techniques such as laser displacement sensor, hot-wire anemometer, and flow visualization, detailed in our previous study [1].

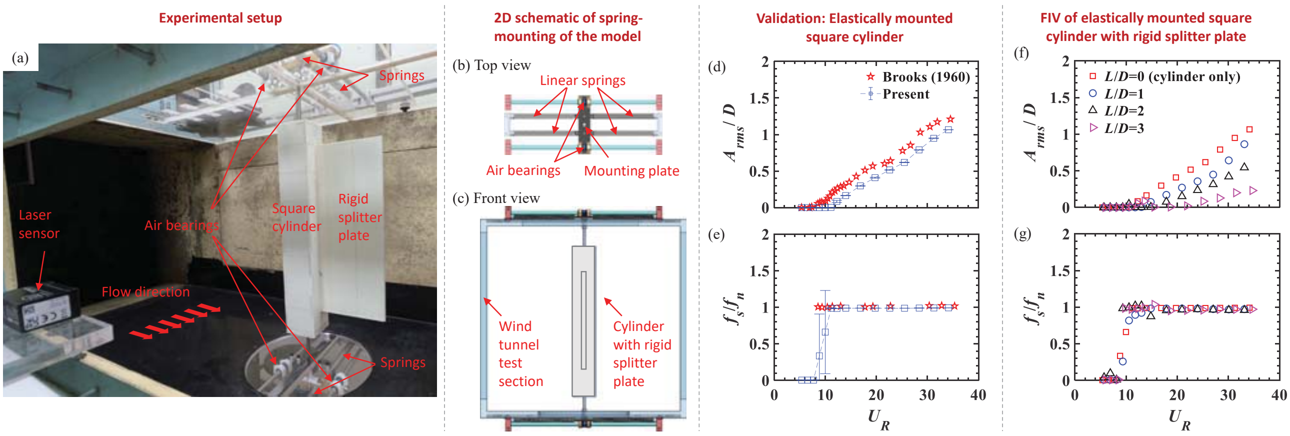

Figure 1. (a) Experimental setup, (b, c) top view and front view schematic showing the arrangement of air bearings, linear springs, and the square cylinder-plate model, (d, e) validation: amplitude (A_{rms}/D) and frequency (f_s/f_n) of square cylinder are validated with study by Brooks [2], (f, g) FIV of a square cylinder-plate model: A_{rms}/D and f_s/f_n variation with reduced velocity (U_R).

First we validate galloping of square cylinder reported earlier [2]. The validation shows good agreement in terms of amplitude, frequency, and critical reduced velocity (Fig. 1(d) and 1(e)), confirming experimental setup reliability. Next, rigid splitter plates of length ratios (plate-to-square side length ratio) $L/D = 1$, $L/D = 2$, and $L/D = 3$ are tested and compared with only cylinder case. Results in Fig. 1(f) and 1(g)) show that the presence of a splitter plate reduces the vibration amplitude significantly and delays the onset of large-amplitude oscillations. Increasing plate length leads to further reduction in vibration amplitude and the longest plate ($L/D = 3$) exhibits the strongest suppression effect. This is due to the effective wake stabilization through shear-layer separation and reduced vortex interaction with the body. Frequency measurements indicate that oscillations remain close to the natural frequency across cases, consistent with galloping-dominated behavior. Currently, we are testing the influence of plate span and flexibility. The present findings provide valuable insights into the influence of splitter plate in controlling FIV of bluff bodies.

References

[1] U. K. Patel, S. Giri, & R. Bhardwaj, *Fluid–structure interaction of an inverted flexible panel in the wake of a cylinder*, Physics of Fluids, **37(1)**, (2025).
[2] P. N. H. Brooks, *Galloping of Square and Rectangular Cylinders*, PhD Thesis, University of British Columbia, **294**, 116793 (1960).

FLUTTER INSTABILITIES OF A HORIZONTAL FLEXIBLE PLATE ELASTICALLY SUPPORTED AT ITS LEADING EDGE: EFFECTS OF FLEXIBILITY AND GRAVITY

Ramon Fernandez-Feria
Fluid Mechanics Group, University of Málaga, Dr Ortiz Ramos s/n, 29071 Málaga, Spain

Abstract Fluid-structure interactions. Flutter. Analytical formulation.

A flutter stability analysis of a two-dimenssional flexible foil elastically mounted on springs and dampers at its leading edge is presented, based on a new analytical formulation of the fluid-estructure interaction valid for oscillations and deformations of small amplitude and inviscid flow. It extends a previous analysis [1] by including the effect of gravity and a second flexural mode, thus increasing its validity range to much smaller rigidities. Gravity affects the equilibrium forms, depending on the mass ratio R and the Froude number, but not to the flutter stability. The analytical equilibrium deformations are nonetheless useful to trigger numerical stability analyses. The most relevant results are related to the extension of the flutter stability analysis to much higher flexibilities. For a clamped foil, the analytical results are validated with previous numerical results [2], capturing almost exactly the first two natural flexural modes down to values of the stiffness parameter S below unity (see figure). One of the modes is stable, whereas the other one is unstable for all S above a threshold value of R that depends on the stiffness, the unstable mode not covered by the previous analytical formulation. When only passive heave, or only passive pitch, is allowed, an upper stiffness bound for the flexural instabilities is found as the linear, or torsional, spring constant decreases from infinity. (As it is well known, flutter instabilities are not possible for a rigid ($S \to \infty$) foil with only passive heave or only passive pitch.) For small enough values of the spring constant, the flexural instability mode becomes coupled with the spring instability mode, increasing the growth rate substantially. These coupled spring (linear or torsional) and flexural instability modes occur below a threshold value of S and above a threshold value of R, both depending on the corresponding spring constant. The thresholds are lower and higher, respectively, for a passive pitch-only than for a passive heave-only configuration. Finally, the effect of flexibility on the well-known coupled pitch-heave flutter instability of a rigid foil is analyzed. These instabilities for a rigid foil are possible in a region below a curve of the parametric plane of the two springs constants that depends on R, a region of instability that shrinks to zero as R decreases. For a flexible foil, the flexural unstable mode becomes coupled with both springs unstable modes as S decreases from infinity, enlarging the mass ratio range for flutter instability and increasing the growth rate, the more so the smaller the springs constants. All these parametric regions for flutter instabilities are easily characterized with the present analytical formulation, providing the corresponding critical flutter fluid velocities for the different possible configurations. Thus, the present analytical results can be very useful in several applications, particularly as a guide in the preliminary design and sizing of future turbines based on flexible oscillating foils.
Work supported by the MCIyU/AEI grant PID2023-150588NB-I00.

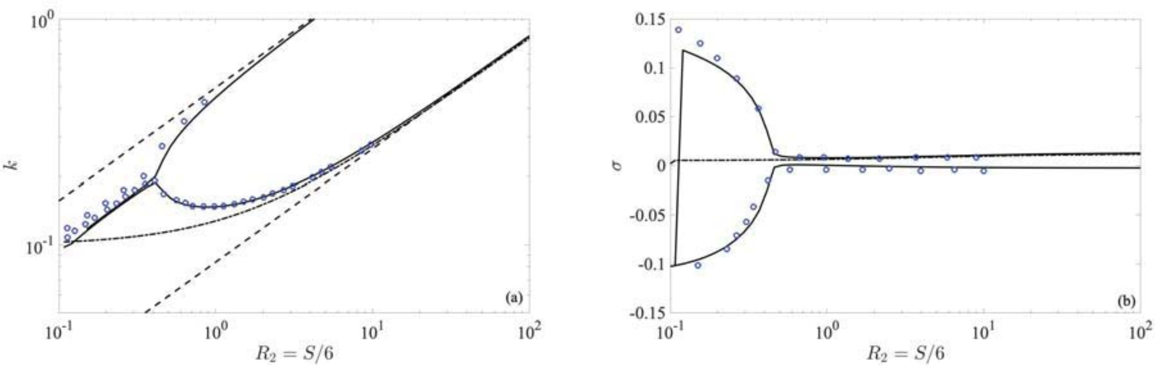

Figure 1. Comparison of the present analytical results (continuous lines) for the natural frequency (a) and minus the growth rate (b) with numerical results by Alben [2] (circles) for a clamped foil as the stiffness (S) increases for a fixed mass ratio $R = 2R_1 = 219.4$.

References

[1] R. Fernandez-Feria, *Flutter stability analysis of an elastically supported flexible foil. Application to the energy harvesting of a fully-passive flexible flapping-foil of small amplitude*, J. Fluids Structures. **109**, 103454 (2022).
[2] S. Alben, *The flapping-flag instability as a nonlinear eigenvalue problem*, Phys. Fluids. **20**, 104106 (2008).

SPREADING OF A LIQUID METAL COATING IN THE PRESENCE OF ADHESION, LORENTZ FORCES & HEAT TRANSFER

Nikos Pelekasis[1], Sotiris Rosios[1], Alkmini Lytra[1] & M. Vlachomitrou[1]
[1]*Department of Mechanical Engineering, University of Thessaly, Volos, GREECE*

Keywords: Capillary Porous System, Liquid Metals, MHD, Saturated oscillations, Drop ejection, Wetting

Abstract

We simulate the flow of a liquid lithium layer through a pore of a capillary porous system (CPS) and study the stability of the spreading process along the pore walls, in the presence of an azimuthal magnetic field. Complete wetting is assumed on the wall and the interplay with Lorentz forces is investigated when electric current enters the layer from the surrounding plasma, Fig. 1a. We initially assume isothermal conditions, low magnetic Reynolds and neglect plasma density. The Navier-Stokes equations coupled with Lorentz forces are solved for the flow and induced magnetic and electric fields, using the finite element method with spine and elliptic mesh generation techniques. A thin protective coating is formed along the wall, where the intermolecular forces between the liquid metal and the substrate are described via the disjoining pressure. We consider a long-range-attractive, short-range-repulsive (LRA-SRR) interaction [1]. Lithium is pumped out of a reservoir due to the magnetic pressure generated by the irrotational part of the Lorentz force. For given strength of adhesion with respect to surface tension, $W_0=w/\sigma$, there is a threshold value in the magnetic Bond, $Bom=B\ J\ R_0/\sigma$ based on the external electric current, under which a steady state is reached, Fig 1. Simulations above this threshold show the formation of a dynamic contact angle that conforms with the algebraic law, $O(Ca^{1/3})$, of spreading which is halted by a pulsatory motion triggered by the induced electric current. Global stability analysis is underway to identify the nature of the instability. When the magnetic Bond is raised above a threshold value a Rayleigh-Taylor instability eventually emerges due to acceleration of the interface leading to drop éjection [2], Fig. 1b. The value of the critical magnetic pressure for instability and drop ejection is inversely proportional to the pore radius while increasing with the square root of surface tension and strength of interaction potential. Upon relaxing the isothermal condition while assuming a fixed contact point on the pore mouth, simulations reveal that excessive evaporation tends to suppress drop éjection in agreement with previous experimental observations and theoretical studies [3,4]. The impact of the above effects on the stable operation of fusion reactors by protecting the divertor from extreme heat loads and runaway currents during off-normal events in the core plasma, is discussed.

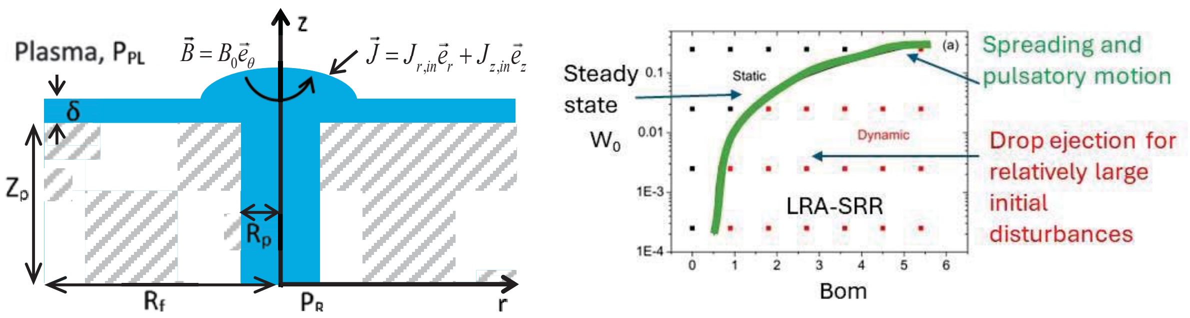

Figure 1. (a) Schematic and (b) phase diagrams of the flow arrangement

References

[1] Pelekasis, N. & Benos, L. Fusion Engineering and Design 117 (2017) 180–187.
[2] Vlachomitrou M & Pelekasis N. (2020). Fluids, 5, 12.
[3] Morgan T.W. et al, Nuclear Materials and Energy, 1–6, (2017)
[4] van Eden, G.G. et al. PRL 116, 135002 (2016).

INSTABILITY OF TWO-PHASE STRATIFIED MHD FLOWS

Arseniy Parfenov, Alexander Gelfgat & Neima Brauner
School of Mechanical Engineering, Tel Aviv University, Tel Aviv 6997801, Israel

Keywords: stability ; two-phase stratified flows ; Hartmann flow ; interfacial instability

__Abstract__

A well-known problem of stability of stratified gas–liquid flows was never examined for presence of an externally imposed magnetic field, assuming one or both liquids are electrically conducting. In the present work, we conduct a linear stability analysis of two-phase stratified magneto hydrodynamic (MHD) flows between two horizontal plates, subjected to a constant externally imposed constant vertical magnetic field. A heavier and electrically conducting liquid (e.g., mercury) occupies the lower layer beneath a lighter electrically non-conducting fluid (e.g., air). The base flow is defined by prescribed volume fluxes of both phases. The prescribed fluxes define not only the base velocity profile, but also the thickness of the two layers, rendering the base-flow problem inherently non-linear. The corresponding linear stability problem, which includes also infinitesimal deformations of the liquid-liquid interface, is governed by the Orr-Sommerfeld equations in each phase, which are coupled via continuity of velocities and viscous stresses at the interface. The problem is solved analytically in the long-wave approximation, and numerically for a full range of wavenumbers. The results are validated by comparison with the published solutions for a single-phase MHD flow [1] and two-phase stratified flows in the absence of magnetic field [2].

Unlike the single-phase Hartmann flow, conductivities of the channel walls affect the base flow velocity profile and its stability properties. In this work, we consider two limiting cases of perfectly conductive and perfectly insulating walls. We show that the strength of the imposed magnetic field has a non-monotonic effect on the flow stability, so that increasing magnetic field can stabilize or destabilize the flow. An example of the latter is shown in Fig. 1. Other results for a test case of mercury-air flow are presented as stability maps accompanied with the profiles of the most unstable (critical) disturbance.

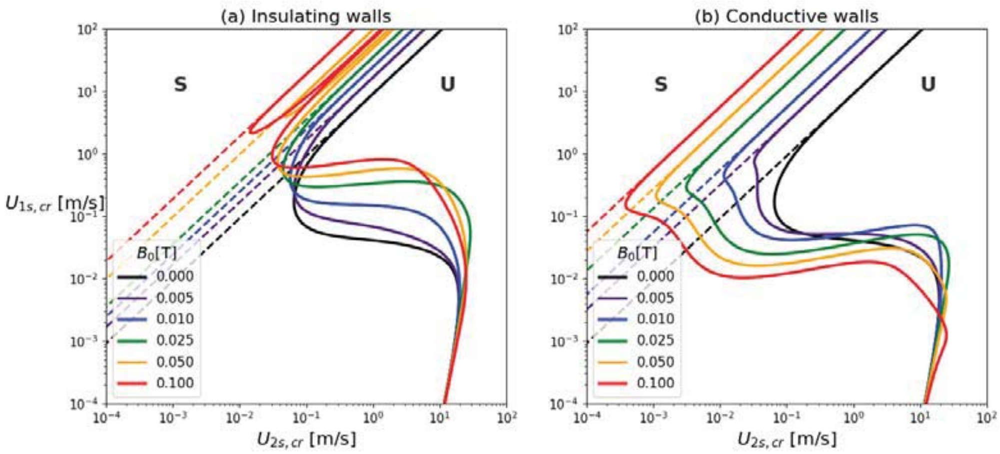

Figure 1. Long-wave stability maps of mercury-air flow ($H = 0.02$m) for fixed values of magnetic field B_0 in a channel with insulating (a) and perfectly conducting (b) walls; zero-gravity boundaries are denoted with dashed lines. U_{1s} and U_{2s} are the critical volume flux of mercury and air, respectively.

Acknowledgment
This research was supported by Israel Science Foundation (ISF), grant No 2979/23 .

References

[1] S. Takashima, The stability of the modified plane Poiseuille flow in the presence of a transverse magnetic field, Fluid Dyn. Res. 17, 293-310 (1996).
[2] I. Barmak, A. Gelfgat, H. Vitoshkin, A. Ullmann, N. Brauner, Stability of stratified two-phase flows in horizontal channels, Phys. Fluids. 28, 044101 (2016).
[3] A. Parfenov, A. Gelfgat, N. Brauner, Long-wave instability of stratified two-phase MHD channel flow, International Journal of Multiphase Flow, submitted.

DYNAMICS AND INSTABILITIES OF FLOATING DROPLETS

Alexander Nepomnyashchy[1] & Ilya Simanovskii[1]
[1] *Department of Mathematics, Technion - Israel Institute of Technology, Haifa, 3200003, Israel*

Abstract Droplets, Interfacial instabilities.

Droplets on a liquid substrate (“liquid lenses") play an important role in various branches of engineering, including microfluidics, chemical engineering, environment protection, etc. The dynamics and instabilities of non-isothermal floating droplets are of a special interest.

In applications, it can be necessary to change the shape of floating droplets or move them in a controllable way (e.g., in microfluidic devices). The simplest way to influence a liquid droplet is heating which creates Marangoni convection in the droplet and in the liquid substrate.

In the present talk, we consider a droplet of a liquid that floats on the layer of another liquid when being in contact with the gas phase. The substrate bottom and the gas are kept at different values of temperature. Assuming that the liquid droplet is slender because of a small (negative) spreading coefficient or because of the action of gravity, we apply the long-wave approximation that allows to reduce the problem to a closed system of equations that govern the evolution of the shapes of interfaces. In the framework of the precursor model, we describe the droplet on the liquid substrate as a two-layer film. In the region of the droplet, the top layer has a macroscopic thickness, and it is described by standard thin-film equations. Outside the droplet, the equations are amended by corresponding disjoining pressures.

We have analyzed the development of the longwave deformational instability of a floating droplet under the action of an inclined temperature gradient in the presence of the spatial modulation of the transverse temperature gradient. The evolution equations were discretized by central differences for spatial derivatives and solved using an explicit scheme. Periodic boundary conditions have been applied on the boundaries of the computational region.

It is shown that the spatial modulation of the transverse Marangoni number is accompanied by the change of the droplet shape and can lead to development of periodic oscillations. The period of oscillations coincides with the time of passing by the droplet the distance L, equal to the spatial period of the temperature modulation. At the definite region of parameters, the quasi-periodic oscillations accompanied by the creation of the pulsating satellites have been obtained.

EXPERIMENTAL AND NUMERICAL STUDY OF STABILITY OF STRATIFIED TWO-PHASE FLOWS IN HORIZONTAL AND INCLINED CHANNELS OF SAME HYDRAULIC DIAMETERS

Yakov Nezihovski[1], Ilya Barmak[1,2], Alexander Gelfgat[1] & Neima Brauner[1]
[1]*School of Mechanical Engineering, Tel Aviv University, Israel*
[2]*Soreq NRC, Yavne, Israel*

Keywords: Two-phase stratified flow, non-intrusive measurement, interfacial waves, stability boundary

Abstract

The study investigates the effect of the channel geometry on the onset of primary instability in laminar stratified gas–liquid flows in horizontal and slightly inclined channels. To this aim, we compare experimental and numerical results obtained for air-water flow in pipes and ducts of the same hydraulic diameter of 14 mm. The measurements and calculations are carried out by the methods described in our previous studies [1-5]. The numerical results are computed for horizontal and inclined flows (i) in ducts with square cross-section of 14 mm side length [1], (ii) in circular pipe of 14 mm diameter [2] and (iii) between two infinite plates [3] distanced at 7 mm and 14 mm, to examine whether the hydraulic diameter or the channel height is the relevant scale for comparison of the stability characteristics of two-phase flow in the different geometries. The experiments are conducted in a 2m long test section of (i) square duct of 14 mm side length [4], and (ii) circular pipe of 14 mm diameter [5]. Both the experiments and computations were conducted for horizontal and inclined ducts with shallow inclination of 0.3° and 0.6°. The main objective is to examine whether for the same water holdup and inclination, the primary instability in all configurations sets in owing to the same instability mechanism, and to compare the critical superficial velocities of the phases and the characteristics of the critical disturbances. An example is shown in Fig. 1, where the base flow and the velocity components of the most unstable disturbances in the square duct and circular pipe are compared. The close similarity between the flow fields and the disturbance patterns is evident.

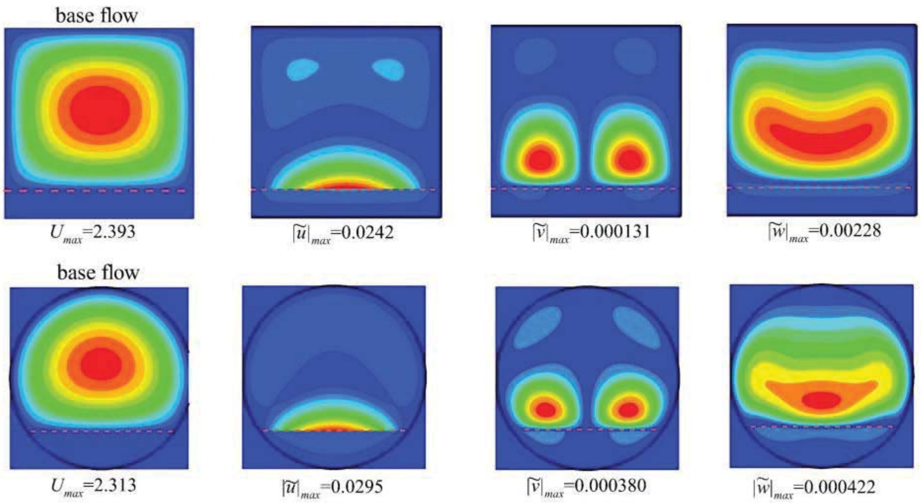

Figure 1. Contours of the base flow and velocity components of the critical short-wave disturbance in downward inclined rectangular (upper frames) and circular (lower frames) ducts. Water holdup 0.15 and β=0.3° inclination. Orange dash line indicates the position of the air-water interface.

References

[1] A. Gelfgat, I. Barmak, N. Brauner, Instability of stratified two-phase flows in inclined rectangular ducts, Int. J. Multiphase Flow 138, 103586 (2021).

[2] I. Barmak, A. Gelfgat, N. Brauner, Instability of stratified air-water flows in circular pipes, Phys. Rev. Fluids, 2024, 093901 (2024).

[3] I. Barmak, A. Gelfgat, A. Ullmann, N. Brauner, Stability of stratified two-phase flows in inclined channels, Phys. Fluids, 28, 084101 (2016).

[4] Y. Nezihovski, A. Gelfgat, A. Ullmann, N. Brauner, Experimental measurements versus linear stability analysis for primary instability of stratified two-phase flows in a square rectangular duct, Int. J. Multiphase Flows, 153, 104061 (2022).

[5] Y. Nezihovski, I. Barmak, A. Gelfgat, G. M. Horstmann, A. Ullmann, N. Brauner, Experimental and numerical study of primary instability of a two-phase stratified flow in a circular pipe. Int. J. Multiphase Flows, 185, 105130 (2025).

FROM HOLMBOE INSTABILITY TO FINITE-AMPLITUDE OCEAN WAVES: NONLINEAR EVOLUTION OF SHEAR-DRIVEN CAPILLARY–GRAVITY WAVES

Sayali N. Jadhav[1], S. Ravichandran[2] & Ratul Dasgupta[1]
[1] *Chemical Engineering, Indian Institute of Technology Bombay, India 400 076*
[2] *Centre for Climate Studies, Indian Institute of Technology Bombay, India 400 076*

Keywords: Ocean waves, shear layer instability, Holmboe instability, Stokes-like waves, permanent-form waves, finite amplitude waves

Oceanic wind-wave generation through linear instability of the flat air-water interface and breaking of resultant, finite-amplitude waves are typically investigated as separate problems [1, 2]; a clear connection between these two regimes, while crucial, has remained largely unexplored in literature [3, 4]. Here, we study the generation of ocean waves arising from an inviscid drift-layer instability resulting in sheared, finite-amplitude waves. The base flow (see figure 1) is a piecewise linear profile, comprising a uniform flow in the air and a finite-thickness drift layer of constant vorticity located below the sharp density interface. This drift layer overlies a semi-infinite quiescent water region, separated from it by a second interface (the vorticity interface) [1] in water. For a fixed Bond number, this configuration supports Holmboe-unstable modes when the Froude number exceeds a critical value. The most unstable eigenmode from linear stability analysis is used to initialize fully nonlinear simulations performed with *Basilisk* [5]. This solves the incompressible Euler's equations including gravity and surface tension. The disturbance grows exponentially initially, consistent with linear theory, and then transitions into a saturated nonlinear wave before ultimately breaking. Figure 2 shows a spatio-temporal Fourier analysis of the evolving (density) interface, revealing that the saturated state comprises bound harmonics associated with the primary unstable mode, which acts as a carrier wave, together with free-wave components that satisfy the linear dispersion relation. This demonstrates how a single unstable linear mode can evolve into a sheared nonlinear wave of approximately permanent form. Analytical permanent-form traveling wave solutions (sheared Stokes wave) for coupled density and vorticity interfaces, obtained from the fully nonlinear inviscid theory, for the aforementioned piecewise linear profile in air and water [6], show excellent agreement with the simulated interface shapes, compared at the same wave steepness. These results establish a direct pathway linking the growth of infinitesimal linear perturbations on a flat interface to the formation of finite-amplitude, (sheared) Stokes-like waves, with important implications for ocean and coastal engineering as well as wave forecasting.

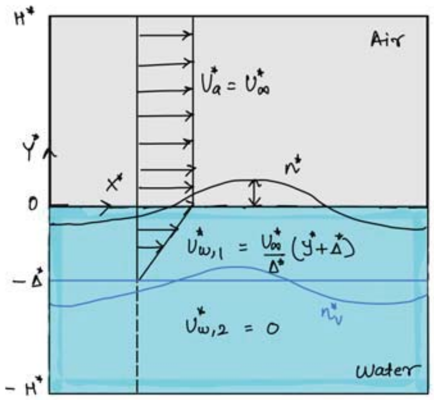

Figure 1. Piecewise linear base state velocity profile. The configuration consists of uniform flow in air and a finite shear layer of depth Δ^* with constant vorticity, overlaying quiescent water.

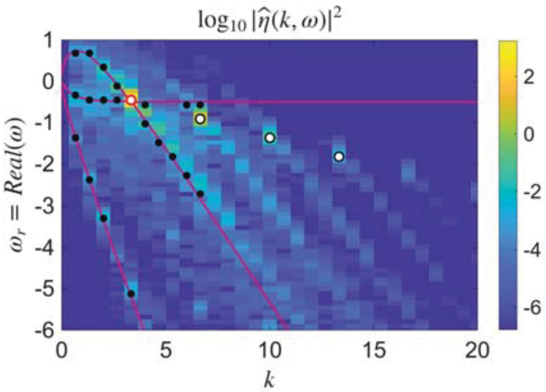

Figure 2. Non dimensional power spectrum contour $\log_{10}|\hat{\eta}(k,\omega)|^2$, of density interface profiles $\eta(x,t)$, as a function of real frequency ω_r and wavenumber k. The carrier wave is located at $(k_0, |\omega_{r,0}|) = (3.334, 0.455)$. White symbols denote bound components propagating at the primary phase speed $c_p = |\omega_{r,0}|/k_0 \approx 0.136$, while black symbols indicate free-wave components overlaid on the theoretical dispersion curves (red lines).

References

[1] L.C. Morland, P. G. Saffman & H. C. Yuen, *Waves generated by shear layer instabilities*, Proceedings of the Royal Society of London. Series A: Mathematical and Physical Sciences **433**, 441–450 (1991).
[2] L. Deike, W. K. Melville & S. Popinet, *Air entrainment and bubble statistics in breaking waves*, Journal of Fluid Mechanics. **801**, 91–129 (2016).
[3] B. M. Lake & H. C. Yuen, *A new model for nonlinear wind waves. Part 1. Physical model and experimental evidence*, Journal of Fluid Mechanics. **88(1)**, 33–62 (1978).
[4] H. C. Yuen & B. M. Lake, *A new model for nonlinear wind waves. Part 2. Theoretical model*, Studies in Applied Mathematics. **60(3)**, 261–270 (1979).
[5] Stéphane Popinet & Collaborators, *An adaptive mesh refinement algorithm for the incompressible navier–stokes equations using vof method*, https://basilisk.fr/.
[6] F. A. Milinazzo & P. G. Saffman, *Effect of a surface shear layer on gravity and gravity–capillary waves of permanent form*, Journal of Fluid Mechanics, **216**, 93–101 (1990).

MODELLING SNOWFLAKES USING 3D LATTICE-BOLTZMANN

Kaj Pettersson[1], Dario Maggiolo[1] & Gaetano Sardina[1]
[1]*Dpt. Mechanics & Maritime Sciences, Chalmers University of Technology, 41296 Göteborg, Sweden*

Keywords: lattice Boltzmann, snowflake, phase-field, atmosphere, crystallization, dendrite

Abstract
The mechanism of ice crystal growth remains a challenge for the scientific community, relying upon complex interactions at the atomic scale to facet kinetics at the macro-scale. In addition, morphology is a particular interest to the meteorological community as well as for aircraft safety regulators, as ice crystal content in clouds affects equipment performance and prediction capabilities. Current wisdom dictates variations in supersaturation and temperature lead to differing growth patterns, ranging from solid plates to fern-like dendrites, to columns and needles. These patterns are summarized in the Nakaya diagram as a function of temperature and vapor saturation. This diagram shows that from 0℃ to -15℃, primarily plates and fern-like dendrites (horizontal growth) form as the supersaturation (humidity) varies nonlinearly. Needles and columnar crystals (vertical growth) tend to form at -5℃, but also appear at lower humidities at much colder temperatures around -30℃ to -35℃. What the diagram shows is that both temperature and humidity play a pivotal role in the morphology of atmospheric ice crystal growth, even without flow. In 2022, Tan et al. [1] showed that with a diffuse-interface approach using the lattice Boltzmann method, it is possible to accurately capture ice crystal morphology corresponding to the Nakaya diagram conditions for two-dimensional flows. Furthermore, when the particle is subjected to flow ventilation, asymmetric shapes can emerge. This work expands upon that methodology by applying a 3-dimensional lattice Boltzmann model capable of fully capturing the non-isotropic growth under realistic atmospheric conditions. This model includes the saturation, temperature, and flow equations, in addition to the phase-field equation which determines the vapor-solid interface. An anisotropic growth function is also used to determine the growth characteristics of the crystal seed. This detailed growth dynamics model can be employed to generate and validate novel Lagrangian particle size equations that account for supersaturation, moving beyond the standard assumptions of purely spherical crystal shapes. Additionally, the numerical method can be more generally used in a variety of industrial applications influenced by dendritic growth, such as metal alloy solidification, additive manufacturing, and phase change materials.

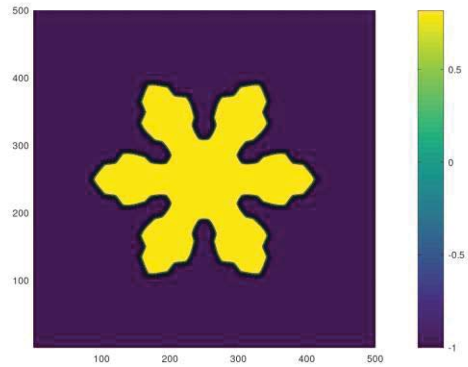

Figure 1. Phase-field representation of a growing snowflake with 6-point symmetry.

References

[1] Q. Tan, S. A. Hosseini, A. Seidel-Morgenstern, D. Thévenin, H. Lorenz; Modeling ice crystal growth using the lattice Boltzmann method. *Physics of Fluids* 1 January 2022; 34 (1): 013311.

HOW INJECTED PARTICLES MODIFY THE ONSET OF RAYLEIGH-BÉNARD CONVECTION

Silvia C. Hirata[1], Saad Raza[1], Romulo B. Freitas[2], Leonardo S. B. Alves[3] & Enrico Calzavarini[1]
[1]*Univ. Lille, Unité de Mécanique de Lille - J. Boussinesq (UML) ULR 7512, F-59000 Lille, France*
[2]*Federal Center for Technological Education Celso Suckow da Fonseca, Nova Iguaçu-RJ 26041-271, Brazil*
[3]*PGMEC, Univ. Federal Fluminense, Rua Passo da Patria 156, Niteroi, Rio de Janeiro 24210-240, Brazil*

Abstract particulate Rayleigh-Bénard convection, linear stability analysis

The coupling between thermal convection and suspended particles plays a fundamental role in a wide range of geophysical and industrial systems, including magmatic suspensions, sediment-laden flows, and bubble-driven reactors. Even at very low volume fractions, dispersed particles can strongly modify the onset of convection through combined mechanical and thermal interactions with the carrier fluid.

In this work, we examine the linear stability of thermally stratified fluid layers containing dilute suspensions of non-Brownian thermal particles that are continuously injected through the boundaries - from above for particles denser than the fluid and from below for particles lighter than the fluid. Particular emphasis is placed on the interplay between particle properties - such as density, heat capacity, and size - and boundary injection conditions in determining convective stability.

We first consider configurations in which particles are continuously injected at their terminal velocity with a prescribed temperature. In this regime, both heavy and light particles are found to systematically stabilize the system with respect to the single-phase Rayleigh-Bénard threshold, leading to substantial increases in the critical Rayleigh number. This universal stabilization arises because terminal-velocity injection renders the particle velocity field divergence-free across the entire layer. As a result, particle concentrations remain uniform and clustering is suppressed. The stabilizing effect is governed by a combination of mechanical coupling, which damps fluid motion, and particle thermal inertia, which alters interphase heat transfer.

We then examine the case of inlet velocities differing from the terminal one. In this case, particle accumulation becomes possible and introduces a marked asymmetry in the system's response. Decreasing the injection velocity stabilizes the flow when heavy particles are introduced from above, but destabilizes it when light particles are injected from below. Conversely, increasing the injection velocity has a destabilizing effect for heavy particles, while progressively stabilizing the system for light ones. For extremely light particles, such as bubbles, sufficiently low injection velocities can even trigger convection under stable thermal stratification, corresponding to negative Rayleigh numbers.

Away from terminal-velocity injection, particle concentrations become strongly heterogeneous, with accumulation near the extraction boundary and within regions of intense vertical motion. The location of accumulation depends on the injection regime: particles preferentially cluster in downwelling regions for sub-terminal injection and in upwelling regions for super-terminal injection. Our results confirm that clustering is a key ingredient in the modulation of convective instability [1, 2].

References

[1] S. Raza, S. C. Hirata & E. Calzavarini, *Stabilization of the Rayleigh-Bénard system by injection of thermal inertial particles and bubbles*, Physics of Fluids **36** (12): 124141 (2024).
[2] S. Raza, R. B. Freitas, L. S. B. Alves, E. Calzavarini & S. C. Hirata, *Impact of particle injection velocity on the stability of the particulate Rayleigh-Bénard system*, Journal of Fluid Mechanics **1015:R2** (2025).

DIRECT NUMERICAL SIMULATION OF SKIN-FRICTION REDUCTION USING STEADY BLOWING THROUGH SPANWISE SLITS

Lingchu Xi[1] Zhanying Zheng[2] & Yu Zhou[2]
[1]*Centre for Turbulence Control, Harbin Institute of Technology, Shenzhen, China*
[2]*School of Mechanical Engineering and Mechanics, Eastern Institute of Technology, Ningbo, China*

Keywords: turbulent channel flow, drag reduction, DNS

Abstract

Skin-friction drag reduction (DR) in turbulent channel flows and turbulent boundary layer has been extensively studied since the late 1970s due to its potential benefits in various engineering applications. A recent experimental study has demonstrated that an array of blowing microjets through spanwise slits was highly effective for skin-friction reduction in high Reynolds number turbulent boundary layers, and the resulted spatially averaged DR over the control area exceeded 70%, even with a net energy saving up to 26%[1]. However, due to limitations in experimental measurements, several important questions remain to be answered, such as the modification of near-wall turbulence structures and energy cascade due to control, as well as the propagation of DR effect further downstream. Previous direct numerical simulation (DNS) studies have successfully investigated the DR mechanisms of steady blowing through streamwise slits [2]. In this study, a similar DNS approach has been adopted to investigate the DR performance and flow characteristics of a channel flow under a steady blowing through an array of spanwise slits at $Re_\tau = 200$. The computational domain consists of an upstream, control and downstream regions, where 43 spanwise slits are placed, with identical center-to-center spacing, on the bottom wall of the control region along the streamwise direction, as shown in Figure 1(a). Periodic boundary conditions are applied on both side walls and a velocity inlet condition with a fully-developed turbulent channel flow velocity profile is specified in the upstream plane. The simulation results indicated that an averaged DR of 59.8% was achieved in the control region, where a substantial suppression of the near-wall streaky structures was evident, as shown in Figure 1(b). Also, the recovered turbulent boundary layer tended to be fragmented throughout the entire downstream region, indicating a prolonged influence of the blowing control downstream. The FIK identity decomposition [3] has been employed to find out various contributors to the skin-friction DR, and variations in turbulent kinetic energy budgets due to the control have been investigated. Above detailed flow results are crucial for obtaining fundamental understandings to the flow control physics and would offer direct guidance for the fine tuning of the blowing control.

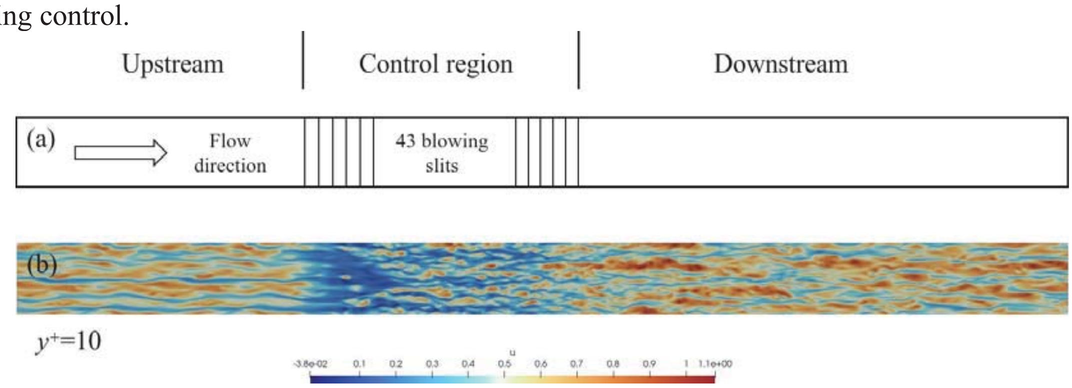

Figure 1. Schematic of the DNS computational domain (a) and the streamwise velocity contour at $y^+ = 10$ (b)

References

[1] X. Zhang, X. H. Wei, H. F. Wang & Y. Zhou, Skin Friction Reduction in a High Reynolds Number Turbulent Boundary Layer Using Spanwise Blowing Microjets. In Proceedings of the 6th Symposium on Fluid-Structure-Sound Interactions and Control (Eds. Daegyoum Kim, Kyung Chun Kim, Yu Zhou, Lixi Huang). Singapore: Springer Nature Singapore, 53-58 (2023).
[2] L. Xi, M. Quadrio & Y. Zhou, Direct Numerical Simulation of Skin-Friction Reduction Using Steady and Periodic Blowing Through Streamwise Slits. In Proceedings of the 6th Symposium on Fluid-Structure-Sound Interactions and Control (Eds. Daegyoum Kim, Kyung Chun Kim, Yu Zhou, Lixi Huang). Singapore: Springer Nature Singapore, 85-90 (2023).
[3] K. Fukagata, K. Iwamoto & N. Kasagi, Contribution of Reynolds stress distribution to the skin friction in wall-bounded flows, Phys. Fluids, 14(11), L73-L76 (2002).

MECHANICS OF PUMP FOILING

Eunok Yim[1] & Francois Gallaire[2]
[1] *HEAD-Lab, EPFL, Lausanne, Switzerland*
[2] *LFMI, EPFL, Lausanne, Switzerland*

Abstract Physics of sports, pump foil, foil propulsion, quasi-steady lift and drag, airfoil dynamics

On a calm lake, a surf foil board (Figure 1a) can glide forward without waves or wind, driven only by the rider's rhythmic leg pumping and the resulting vertical oscillations. Pump foiling enables sustained forward motion without external power by converting this periodic pumping into hydrodynamic lift and thrust. Here we present a minimal physical model for pump foil propulsion, formulated as a coupled second-order ODE system for horizontal/vertical translation and pitch in an inertial frame. The system is represented by a point mass rider and two wings (front and rear), with equations written about a pivot (**O**) at the mast-linker junction (Figure 1b). Hydrodynamic loading includes quasi-steady lift and drag, buoyancy, rotational lift, and a nonlinear rotational drag term [2, 3, 4]:

$$m\ddot{x} = \sum F_x, \quad m\ddot{y} = \sum F_y, \quad I\ddot{\theta} = \sum \tau, \tag{1}$$

where m is the effective mass and I the effective moment of inertia. The forces F_x and F_y act in the inertial frame, and τ denotes torques about the pivot point **O**.

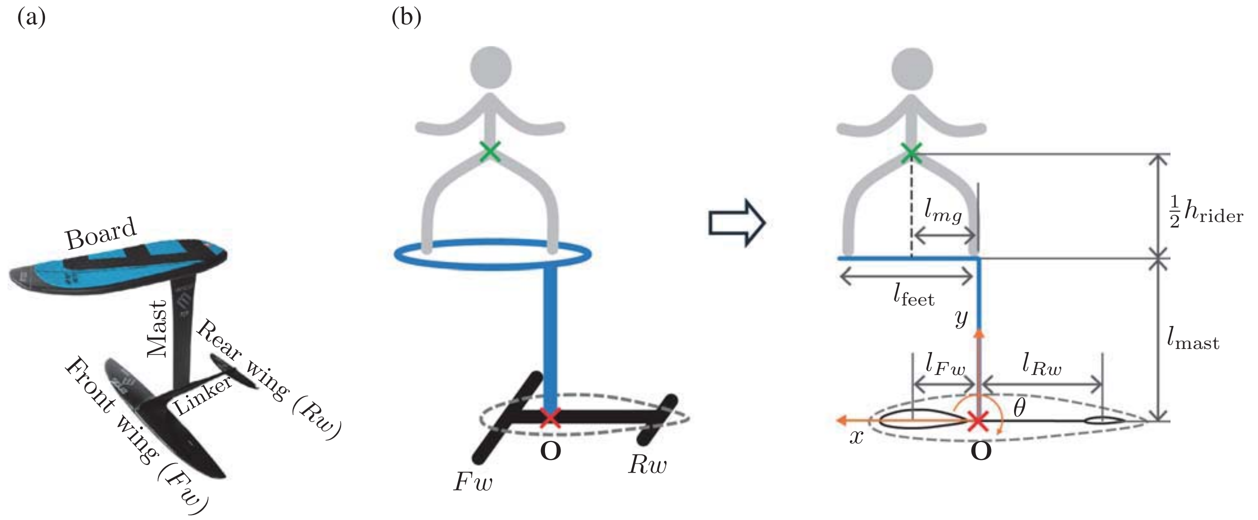

Figure 1. (a) Typical pump foil shape and the names of components (image source [1]). (b) Schematic representation of pump foil and rider and relevant dimensions. The pivot point, the rotation center (**O**), is marked with red cross. The positive directions are chosen as x from right to left, y from bottom to top and θ the nose up direction.

Under simplified control assumptions, the dominant control parameter is the total pumping force amplitude $A_{\text{pump,tot}}$, with pumping frequency fixed at 1.65 Hz for a 70 kg rider (based on observations). For this representative setup, we find that $A_{\text{pump,tot}} \approx 0.45mg$ sustains stable forward motion while maintaining a small pitch angle in the stabilized regime ($\theta \simeq 2°$). Force and moment balances show that the front wing provides most of the vertical support, while the rear wing contributes only ~ 22 % of the lift yet strongly stabilizes pitch due to its larger moment arm (about $4\times$ that of the front wing). The model provides a mechanistic picture of pump foil propulsion and motivates targeted field and laboratory measurements to refine ride control and hydrodynamic assumptions.

References

[1] Hawaiian Surfing srl, *Foil board EnSiS Hip Hop 98*, Hawaiian Surfing online shop (2025). `https://hawaiiansurfing.com/prodotto/ensis-hip-hop/`.
[2] J. G. Leishman, *Principles of Helicopter Aerodynamics*, 2nd ed., Cambridge Aerospace Series (Cambridge University Press, Cambridge, 2016).
[3] H. Li, T. Goodwill, Z. Jane Wang, & L. Ristroph, *Centre of mass location, flight modes, stability and dynamic modelling of gliders*, J. Fluid Mech. **937**, A6 (2022).
[4] O. Pomerenk & L. Ristroph, *Aerodynamic equilibria and flight stability of plates at intermediate Reynolds numbers*, J. Fluid Mech. **1014**, A24 (2025).

DYNAMICS OF A FLUTTERING PLATE IN DECAYING ISOTROPIC TURBULENCE

Bálint Nagy[1], Stefano Olivieri[2,3], Roberto Verzicco[1,4] & Francesco Viola[1]
[1] *Gran Sasso Science Institute, viale Francesco Crispi, 7 - 67100 L'Aquila (AQ), Italy*
[2]*Department of Civil, Chemical and Environmental Engineering, Università di Genova, Via Montallegro 1, Genoa, 16145, Italy*
[3]*Istituto Nazionale di Fisica Nucleare, Sezione di Genova, Via Dodecaneso 33, Genoa, 16146, Italy*
[4]*Physics of Fluids Group, University of Twente, Faculty of Science and Technology, 7500AE Enschede, the Netherlands*

Abstract fluid-structure interaction (FSI), direct numerical simulation (DNS), flutter, energy harvesting, isotropic turbulence
Self-sustained, flow-induced oscillations of a flexible plate is a viable mechanism for energy harvesting. Although computational studies of the *plate-in-the-wind* problem are well established [1, 2], they are largely confined to laminar incident flows, despite the fact that realistic conditions are typically turbulent. The present study investigates how turbulence, which can play a decisive role in triggering or suppressing flow-induced instabilities, modifies the dynamics of flow-induced oscillations, with direct implications for energy-harvesting performance.
A fully resolved direct numerical simulation (DNS) framework is employed to examine the flutter of a three-dimensional flexible plate subjected to a turbulent incoming flow. Our *in-house* finite-difference numerical solver [3] is used to solve the fluid-structure interaction problem: the flexible body is represented using an immersed boundary method [4], while turbulence is generated following the random forcing method of Eswaran and Pope [5], in which the complex Fourier coefficients of the forcing are evolved via six independent Ornstein–Uhlenbeck processes in spectral space, projected onto the divergence−free subspace to enforce incompressibility, and subsequently transformed to physical space.
The forced turbulent flow is first validated against canonical results for decaying isotropic turbulence [6]. Subsequently, the plate-in-the-wind problem is revisited by examining the effect of turbulence intensity and integral lengthscale−which is modulated by forcing different wavenumber bands−on the onset and dynamics of self-sustained flapping.
Specifically, we consider three turbulence intensities, TI $= 0\%,\ 15\%$ and 30%, and integral lengthscales $L_i/L = 0.5,\ 1.0$ and 1.5. We select representative cases of structure-to-mass ratio (M_s) and then bending rigidity of the plate (K_B), corresponding to the regular, weakly irregular, and chaotic regimes. For each case, we investigate the flapping dynamics in terms of peak-to-peak amplitude A/L and Strouhal number $St_L = \frac{fL}{U}$. In particular, we investigate how the linear relationship between A/L and the peak-to-peak amplitude-based Strouhal number $St_A = \frac{fA}{U}$ found for TI $= 0\%$ is modified by increasing the turbulence intensity. The power spectral density of the transverse displacement of the trailing-edge (TE) midpoint is computed for both laminar and turbulent conditions. For the turbulent cases, the spectra are also analyzed using scaling laws predicted by the model of Jin, Ji, and Chamorro [7].
Lastly, we assess the energy-harvesting performance of the plate by measuring the elastic strain energy and calculating the energy conversion ratio. Hence, the optimal flow configurations for energy harvesting are identified and rationalized by monitoring the effect of turbulence intensity and integral lengthscale on the corresponding flapping dynamics.

References

[1] Huang, W. X., and Sung, H. J., *Three-dimensional simulation of a flapping flag in a uniform flow*, Journal of Fluid Mechanics **653**, 301-336 (2010).
[2] Olivieri, S., Viola, F., Mazzino, A. and Rosti, M.E., *Direct numerical simulation of flapping flags in grid-induced turbulence*, Physics of Fluids **33(8)**, (2021).
[3] Viola, F., Spandan, V., Meschini, V., Romero, J., Fatica, M., De Tullio, M. D. & Verzicco, R., *FSEI-GPU: GPU accelerated simulations of the fluid–structure–electrophysiology interaction in the left heart*, Computer physics communications **273**, 108248 (2022).
[4] Verzicco, R., de Tullio, M. D., & Viola, F., *An Introduction to Immersed Boundary Methods*, Cambridge University Press (2025).
[5] Eswaran, V. & Pope, S. B., *An examination of forcing in direct numerical simulations of turbulence*, Computers & Fluids **16(3)**, 257-278 (1988).
[6] McComb, W. D., *Homogeneous, isotropic turbulence: Phenomenology, renormalization and statistical closures (Vol. 162)*, OUP Oxford (2014).
[7] Jin, Yaqing and Ji, Sheng and Chamorro, Leonardo P, *Spectral energy cascade of body rotations and oscillations under turbulence*, Physical Review E, **94(6)**, 063105, (2016).

INERTIALESS SEDIMENTATION OF POROUS DISKS

Edouard Boujo[1], Mathurin Froment[1], Pier Giuseppe Ledda[2] & François Gallaire[1]
[1]*École Polytechnique Fédérale de Lausanne, CH-1015 Lausanne, Switzerland*
[2]*DICAAR, Università degli Studi di Cagliari, Cagliari, Italy*

Abstract Low-Reynolds-number flows, Porous media, Fluid-particle interactions, Nonlinear dynamics

Sedimentation at the microscale happens at vanishing Reynolds number and is relevant to many natural and engineering processes [1]. Bodies falling freely under gravity can display non-trivial trajectories even without inertia (Stokes flow), provided they have strictly less than three planes of symmetry [1, 2]. Planar symmetry breaking induces force-rotation couplings, the relative signs of which depend on the shape of the body and lead to either settling (vertical fall), drifing (oblique fall) or fluttering (curved fall).

In this study, we design settlers, drifters and flutterers from flat disks whose nominal *macroscopic* geometry has three planar symmetries. Force-rotation couplings are generated via a *microscopic* symmetry breaking: a non-uniform distribution of porosity. The microscopic holes affect the macroscopic behavior of the fluid near the disk, which we describe rigorously via an effective stress-jump condition derived from homogenization theory [3]. We show how the shape and orientation of the holes modify the effective slip and filtrability, which in turn allows us to predict the mobility matrix of our porous disks, and therefore their trajectories.

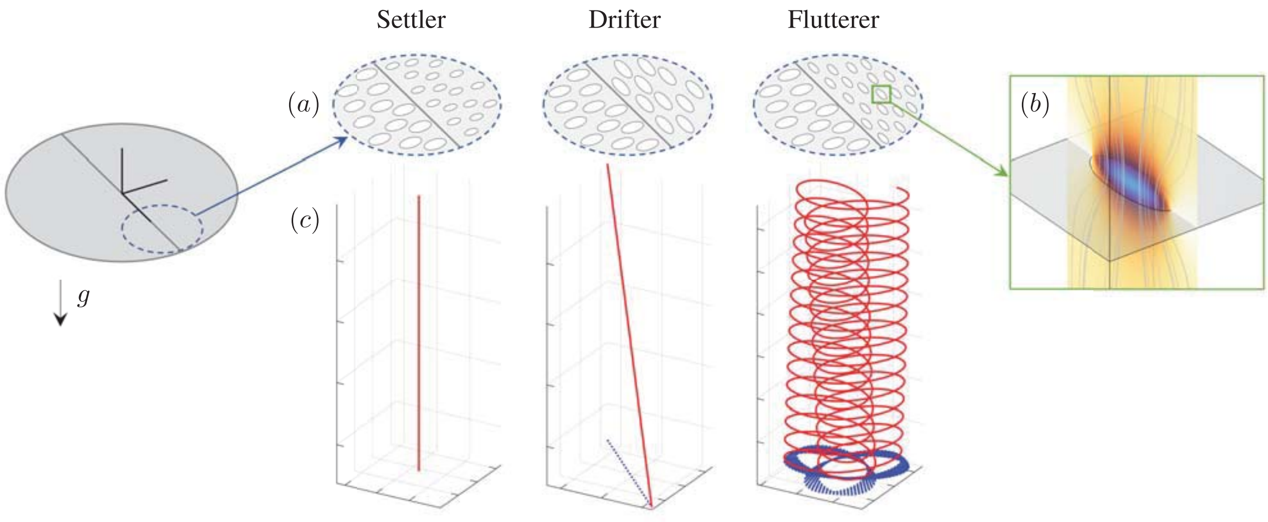

Figure 1. Design of settlers, drifters and flutterers from flat disks with a simple porous microstructure. (a) Here, we use a piecewise-uniform distribution of elliptic holes, differing in size and orientation in two halves of the disk. (b) Microscopic flow through one hole under imposed normal stress. (c) Examples of trajectories (not to scale).

References

[1] T. Miara, C. Vaquero-Stainer, D. Pihler-Puzović, D., M. Heil & A. Juel, *Dynamics of inertialess sedimentation of a rigid U-shaped disk*, Commun. Phys. **7**, 47 (2024).
[2] H. Joshi & R. Govindarajan, *Sedimentation dynamics of bodies with two planes of symmetry*, Phys. Rev. Lett. **134**, 014002 (2025).
[3] P.G. Ledda, E. Boujo, S. Camarri, F. Gallaire & G.A. Zampogna, *Homogenization-based design of microstructured membranes: wake flows past permeable shells*, J. Fluid Mech. **927**, A31 (2021).

UNDERSTANDING THE LONG-STANDING PUZZLE OF THEORY–EXPERIMENT DISCREPANCY IN PRESSURE DROP OF DILUTE VISCOELASTIC FLUIDS IN CHANNEL FLOWS

Evgeniy Boyko[1]

[1] *Faculty of Mechanical Engineering, Technion – Israel Institute of Technology, Haifa 3200003, Israel*

Abstract flow in contraction, non-Newtonian flows, viscoelastic fluids, low-Reynolds-number flows, theory–experiment discrepancy

Pressure-driven flows of viscoelastic fluids in narrow non-uniform geometries are common in physiological flows and various industrial applications. For such channel flows, one of the main interests is understanding the relationship between the flow rate q and the pressure drop Δp under steady-state conditions. For decades, researchers have experimentally observed that the flow of viscoelastic fluids through contraction channels yields results at odds with theory and simulations. In particular, while experiments show an increase in the flow resistance $\Delta p/q$, theory and simulations using Oldroyd-B and FENE-P models predict its decrease under creeping flow conditions and stable flow at small Weissenberg or Deborah numbers. This apparent contradiction between experiments and theory has been a long-standing puzzle in non-Newtonian fluid mechanics [1].

In this talk, I will discuss our approach for understanding and potentially resolving this contradiction. First, I will present a theoretical framework for calculating the flow rate–pressure drop relation of viscoelastic fluids in arbitrarily shaped, narrow geometries using the Oldroyd-B constitutive model [2, 3, 4, 5]. Since the Oldroyd-B model represents the simplest combination of viscous and elastic stresses, it is important to find the response of the simplest model before investigating more complicated constitutive equations. Our theory, based on the lubrication approximation, applies to both low and high Deborah numbers and is in excellent agreement with numerical simulations. We reveal that for the flow-rate-controlled situation, the dimensionless pressure drop of the Oldroyd-B fluid in the contraction channel monotonically decreases with the Deborah number and identify two physical mechanisms for such pressure drop reduction.

Furthermore, I will present our experimental measurements of the pressure drop in dilute viscoelastic fluids within contracting geometries, using two different types of pressure-sensing systems: conventional recessed pressure taps and flush-mounted diaphragm sensors [6]. These measurements yield qualitative agreement with theoretical predictions when the largest relaxation time is adopted for the analysis of the flow. Our results indicate that the apparent discrepancy mentioned above can be attributed to improper interpretation of the measurements and to mismatches between experimental conditions and assumptions made in the theoretical and numerical works, which include hole pressure effects, the choice of relaxation time, and the presence of experimental flow instabilities.

References

[1] E. Boyko, *Pressure-driven fully developed flow of a viscoelastic fluid in narrow channels: the role of different microscopic features in an elastic dumbbell model*, Rheol. Acta **64**, 517–530 (2025).

[2] E. Boyko & H. A. Stone, *Pressure-driven flow of the viscoelastic Oldroyd-B fluid in narrow non-uniform geometries: analytical results and comparison with simulations*, J. Fluid Mech. **936**, A23 (2022).

[3] E. Boyko, J. Hinch & H. A. Stone, *Flow of an Oldroyd-B fluid in a slowly varying contraction: theoretical results for arbitrary values of Deborah number in the ultra-dilute limit*, J. Fluid Mech. **988**, A10 (2024).

[4] J. Hinch, E. Boyko & H. A. Stone, *Fast flow of an Oldroyd-B model fluid through a narrow slowly varying contraction*, J. Fluid Mech. **988**, A11 (2024).

[5] B. Mahapatra, T. Ruangkriengsin, H. A. Stone & E. Boyko, *Viscoelastic fluid flow in a slowly varying planar contraction: the role of finite extensibility on the pressure drop*, J. Fluid Mech. **1009**, A12 (2025).

[6] N. Hu, J. Hwang, E. Boyko & H. A. Stone, *Understanding the theory–experiment discrepancy in pressure drop of dilute viscoelastic fluids in channel flows*, Submitted (2026).

RADIAL FLOW OF VISCOELASTIC FLUIDS BETWEEN PARALLEL PLATES

Ron Lottem[1] & Evgeniy Boyko[1]
[1] *Faculty of Mechanical Engineering, Technion – Israel Institute of Technology, Haifa 3200003, Israel*

Abstract radial flows, non-Newtonian flows, viscoelasticity, low-Reynolds-number flows, lubrication theory

Pressure-driven radial flows of non-Newtonian fluids are commonly encountered in industrial processes, such as injection molding and extrusion [1, 2]. It is well known that the complex rheology of these fluids can significantly impact the hydrodynamic features of non-Newtonian flows. However, these hydrodynamic features remain not fully understood compared to those observed in Newtonian flows. In this work, we analyze the pressure-driven radial flow of a viscoelastic fluid between two parallel disk-shaped plates. We describe viscoelastic behavior using the Oldroyd-B model [3] and present a theoretical framework along with finite-element numerical simulations for calculating the spatial relaxation of elastic stresses and the pressure drop between the plates. Applying the lubrication approximation and employing a perturbation expansion in powers of the Deborah number (De), we provide analytical expressions for the elastic stresses and the dimensionless pressure drop in the weakly viscoelastic limit. We show that, at low Deborah numbers, the pressure drop monotonically increases with De, and the main physical mechanism behind this increase is the higher elastic normal stresses upstream. These normal stresses must be overcome, requiring higher pressures to push the flow between the plates. Our finite-element numerical simulations reveal that entrance effects strongly depend on the Deborah number and significantly deteriorate the agreement between theoretical predictions and numerical results as De increases. Nevertheless, once the entrance effects relax, we find excellent agreement between the low-De theoretical predictions and numerical results for the elastic stresses and pressure drop [4].

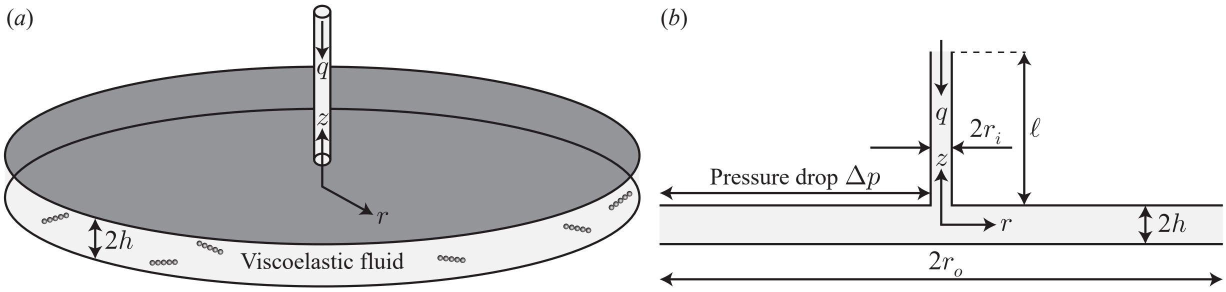

Figure 1. Schematic illustration of the flow configuration. (a) The radial flow of a viscoelastic fluid between two disk-shaped, parallel plates of radius r_o. Two plates are separated by a small gap $2h$ ($h \ll r_o$) and contain a viscoelastic fluid steadily driven by the imposed flow rate q through a narrow tube of radius r_i and length ℓ at the center of the top plate. (b) Cross-section view of the geometry. Our interest is to find the pressure drop Δp between the inlet ($r = r_i$) and outlet ($r = r_o$) and the spatial relaxation of pressure and elastic stresses.

References

[1] M. C. H. Lee & M. C. Williams, *Radial flow of viscoelastic liquids: part I: theoretical*, J. Non-Newtonian Fluid Mech. **1**, 323–341 (1976).
[2] M. C. H. Lee & M. C. Williams, *Radial flow of viscoelastic liquids: part II: experimental*, J. Non-Newtonian Fluid Mech. **1**, 343–355 (1976).
[3] J. G. Oldroyd, *On the formulation of rheological equations of state*, Proc. R. Soc. A **200**, 523–541 (1950).
[4] R. Lottem & E. Boyko, *Radial flow of an Oldroyd-B fluid*, In preparation (2026).

VISCOELASTIC FLOW IN A TEXTURED PLANE SLIDER CHANNEL

Deniz Kaplan[1], & Humayun Ahmed[2], & Luca Biancofiore[3]
Mechanical Engineering Department, Bilkent University, 06800, Ankara, Turkey [1]
International Iberian Nanotechnology Laboratory, Braga, Portugal[2]
Department of Industrial and Information Engineering and Economics, University of L'Aquila, L'Aquila, Italy[3]

Abstract Fluid viscoelasticity, textured geometries, lubrication, thin films.

The purpose of this study is to investigate the influence of sinusoidal surface roughness on the pressure distribution and load-carrying capacity of a plane slider bearing lubricated with a viscoelastic fluid modelled using the Oldroyd-B constitutive equation. The surface roughness is represented as a periodic sinusoidal variation superimposed on the nominal slider geometry (Fig. 1a). Parametric simulations are performed to examine the effects of roughness wavenumber, roughness amplitude, slider slope, and Deborah number (i.e. the ratio of the fluid relaxation time to the flow time scale) on the pressure characteristics and load response.

An initial analysis is carried out using linear perturbation theory, showing that the load-carrying capacity increases with increasing roughness amplitude. To account for non-linear effects, the VR$^{(1)}$ (first-order viscoelastic Reynolds) equation [1] is subsequently employed, in which the first-order velocity perturbation obtained from the linear analysis is incorporated into the Oldroyd-B constitutive relation. The resulting model agrees with the linear (LIN) model at low Deborah numbers, low roughness wavenumbers, and low roughness amplitudes, as expected.

As at least one of these parameters increases, the VR$^{(1)}$ model predicts an enhancement in load-carrying capacity at lower Deborah numbers than those predicted by the linear model. This behaviour is illustrated in Fig. 1b, where the load–Deborah number relationship is shown. While the linear model predicts a monotonic decrease in load with increasing Deborah number, the VR$^{(1)}$ model predicts an initial decrease followed by an increase, indicating a positive contribution to the load arising from surface roughness.

The present work demonstrates that textured surfaces can mitigate the reduced load-carrying capacity typically associated with polymer-based or viscoelastic lubricants. The results suggest that appropriately designed surface roughness may serve as a passive design strategy to compensate for viscoelastic losses. This newly identified behaviour has potential implications for the design of textured slider bearings and lubricated contacts operating with non-Newtonian fluids, particularly in applications where tuning lubricant rheology alone is insufficient or undesirable.

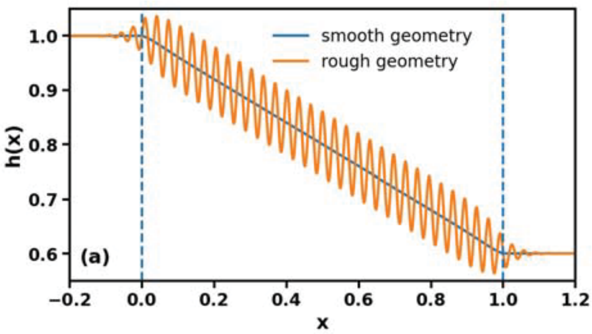

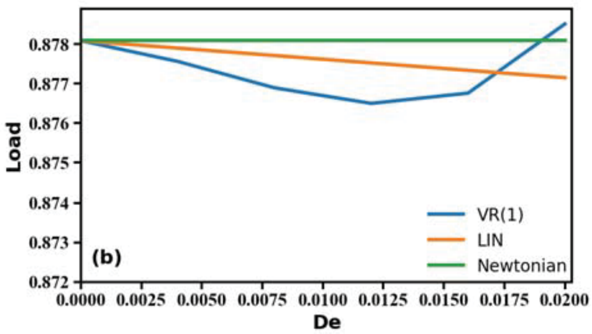

Figure 1: (a) Slider geometry for smooth and rough cases (amplitude $A = 0.1$, wavenumber $k = 30$). (b) Corresponding load as a function of the Deborah number for the same roughness parameters.

References

[1] H. Ahmed and L. Biancofiore, "Modeling polymeric lubricants with non-linear stress constitutive relations," Journal of Non-Newtonian Fluid Mechanics, vol. 321, p. 105123, 2023.

VISCOELASTICITY IN CONFINED THIN FILM SQUEEZE FLOW

Humayun Ahmed[1], Lorenzo Lombardi[2], Gaetano D'Avino[2], Pier Luca Maffetone[2] & Luca Biancofiore[3]
[1] *International Iberian Nanotechnology Laboratory, Braga, Portugal*
[2] *Department of Chemical, Materials and Production Engineering, University of Naples Federico II, Italy*
[3] *University of L'Aquila, L'Aquila, Italy*

Abstract We analyze experimentally and numerically the effect of viscoelasticity in a thin squeezed film. (viscoelasticity, thin films, squeeze film motion, lubrication theory)

Many practical applications involve a thin viscous film confined between two approaching surfaces, such as in bearings, gears, and biological joints. For Newtonian fluids, the normal forces generated by squeeze motion are well understood within classical lubrication theory. However, when the ratio of the fluid relaxation time to the characteristic flow time, i.e., the Deborah number (De), viscoelastic effects become important. In this regime, elastic stresses contribute directly to the normal force balance and can significantly modify the transmitted load. This study examines how viscoelasticity influences the force response of a thin film subjected to vertical squeeze motion. We combine a reduced-order viscoelastic Reynolds (VR) model [1], derived within the lubrication approximation, with direct numerical simulations (DNS) of the full governing equations and controlled experiments.

The VR model is first validated against DNS results. As shown in Fig. 1(a), the temporal evolution of the load-carrying capacity predicted by the VR model closely matches the DNS for different values of De. The model accurately captures the rapid pressure growth as the film thickness decreases, as well as the systematic reduction in load support with increasing De. The agreement confirms that the lubrication-based VR formulation retains the essential viscoelastic dynamics.

Experimental validation is presented in Fig. 1(b). Polyvinyl alcohol–borax solutions are used as model viscoelastic fluids, while silicone oil serves as the Newtonian reference. The fluid is confined between two parallel cylindrical plates, with the upper plate moving downward at constant speed. Viscoelastic behavior is described using the Modified Phan-Thien-Tanner (MPTT) constitutive model, incorporating shear thinning (via a Carreau approximation), finite polymer extensibility, and stress overshoot.

As shown in Fig. 1(b), the VR predictions agree well with the experimental measurements across time and Deborah numbers, capturing both the transient evolution and the peak load. The results reveal a clear physical trend: while viscous effects increase pressure as the film thins, increasing viscoelasticity reduces the load-carrying capacity. This reduction becomes more pronounced at higher De, where elastic stresses partially relax the pressure build-up generated by viscous resistance. Shear thinning further lowers the effective viscosity and therefore decreases the maximum pressure, with the highest load observed in the Newtonian case.

Overall, the combined reduced modeling, DNS, and experimental results demonstrate that the VR framework provides an accurate and computationally efficient description of confined viscoelastic thin film dynamics. The study highlights the fundamental role of elasticity in squeeze flows and clarifies how increasing Deborah number alters load transmission in lubrication-type configurations relevant to both biological and engineering systems.

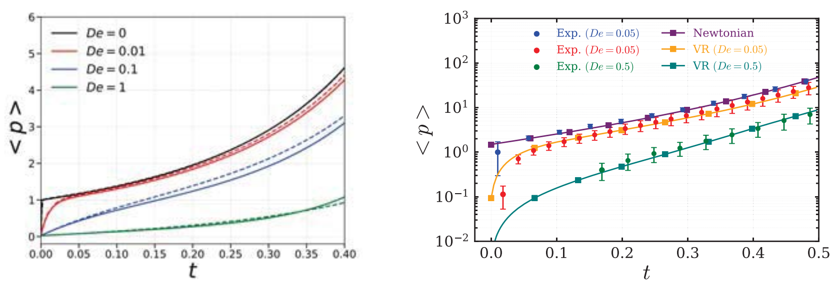

Figure 1. Comparison of load-carrying capacity as a function of time for different Deborah numbers. (a) Direct numerical simulations (DNS, dashed lines) versus the VR model. (b) Experimental measurements versus VR predictions (solid lines).

References

[1] Ahmed, H., & Biancofiore, L. (2023). Modeling polymeric lubricants with non-linear stress constitutive relations. Journal of Non-Newtonian Fluid Mechanics, 321, 105123.

ANALYSIS OF VISCOELASTIC FLUID EFFECTS OVER TRENCHED TEXTURED SURFACE

Christian A. Utreras-Silva[1,2,3], Humayun Ahmed[4], Shreyas Jalikop[3], Bernhard Scheichl[2] & Luca Biancofiore[1]
[1] *University of L'Aquila, L'Aquila, Italy*
[2] *TU Wien, Vienna, Austria*
[3]*AC^{2}T research GmbH, Wiener Neustadt, Austria*
[4] *International Iberian Nanotechnology Laboratory, Braga, Portugal*

Abstract Viscoelastic fluids, Deborah number, sharply textured surface.

Tribological contacts account for around 23% global energy consumption due to wear-related losses [1]. The present work adapts an existing simulation framework [2] that describes the viscoelastic behavior of polymer-enriched lubricants under thin-film approximation [3] in the limits of small Deborah number (*De*) and ultra-dilute polymer additivation. The tested configuration is motivated by parallel-plate setup in rheometers used to study fluid-mediated tribological contacts. The current analysis recreates a textured lower stationary plate with sharp trenches (as shown in fig. 1a) of 15 mm depth, with a rotating upper plate. The simulations were carried out in a representative domain of the full plate (a section depending on the number of trenches) within the range $0 \leq De \leq 0.2$. Preliminary results in fig. 1b indicate a reduction in torque with increasing *De*, while the predicted load increases with *De*. This is consistent with the suggestion that viscoelasticity can improve the performance of textured lubricated systems [4, 5]. The results of this study will also allow one to make *ad hoc* selection of surface texture designs and polymer content for follow-up rheological and tribological experiments. Although perfect agreement between simulations and experiments is not expected, trends convergence could help understand the interaction between these two approaches better, which is crucial for both academic and industrial design of advanced lubricated systems.

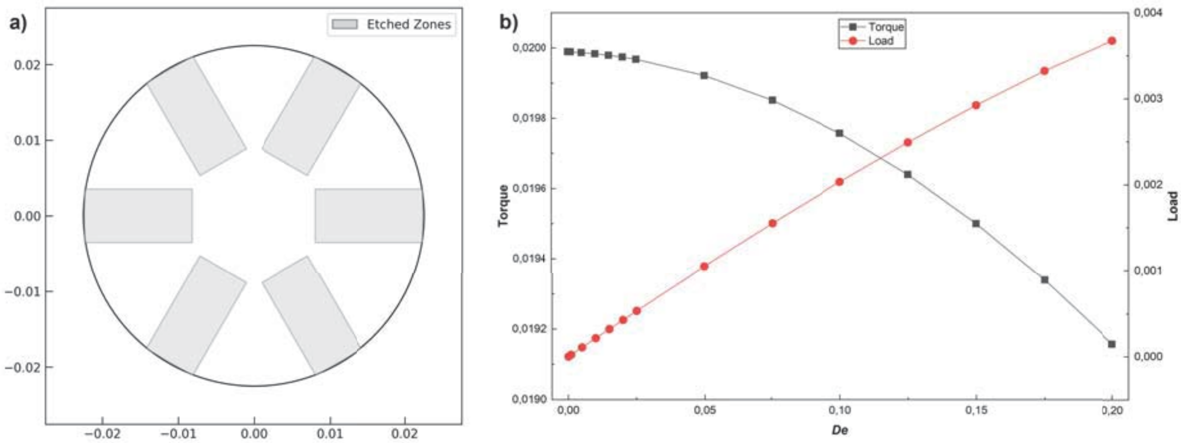

Figure 1. **a)** Target textured surface scheme; **b)** torque and load dependence on Deborah number for a sector of the full plate.

References

1. Holmberg K and Erdemir A. Friction 2017 Sep; 5:263–84
2. Ahmed H and Biancofiore L. Rheologica Acta 2025 Dec; 64:729–43
3. Szeri AZ. Vol. 9780521898232. Cambridge University Press, 2010 Jan :1–547
4. Hamrock BJ, Schmid SR, and Jacobson BO. Marcel Dekker, 2004 :699
5. Schuh JK and Ewoldt RH. Journal of Non-Newtonian Fluid Mechanics 2019 Nov; 273

INSTABILTY AND TRANSITION MECHANISMS IN VISCOELASTIC SHEAR FLOWS

Aashay Harshit[1], G. Subramanium[2] & V. Shankar[3]
[1]*Department of Chemical Engineering, Indian Institute of Technology, Kanpur 208016, Uttar Pradesh, India*
[2]*Department of Chemical Engineering and Materials Science, University of Minnesota, Minneapolis, MN 55455, USA*
[3]*Department of Chemical Engineering, Indian Institute of Technology, Kanpur 208016, Uttar Pradesh, India*

Keywords: Viscoelastic flow, Elastic Instability, Reynolds number, Shear thinning

Abstract

Viscoelastic fluid flows exhibit complex instability and transition phenomena that are fundamentally different from their Newtonian counterparts due to the presence of elastic stresses arising from polymer microstructure dynamics. Over the past decades, significant progress has been made in understanding elastic turbulence and elasto-inertial instabilities, primarily using simplified constitutive models such as Oldroyd-B and Upper-Convected Maxwell models. Although these models successfully capture essential elastic mechanisms, they fail to represent important nonlinear rheological effects such as shear thinning and stress-dependent relaxation observed in real polymer solutions and melts. Linear stability and spectral analysis are performed for canonical shear flows to investigate the influence of nonlinear constitutive behavior on the onset of elastic and elasto-inertial instabilities. The effects of key dimensionless parameters, including the Weissenberg number, Reynolds number, viscosity ratio, and extensibility parameter, are systematically examined.

The results aim to provide improved physical insight into viscoelastic transition mechanisms and enhance agreement with experimental observations. This study contributes toward developing a more realistic modeling framework for predicting flow instabilities in industrial polymer processing and microfluidic applications.

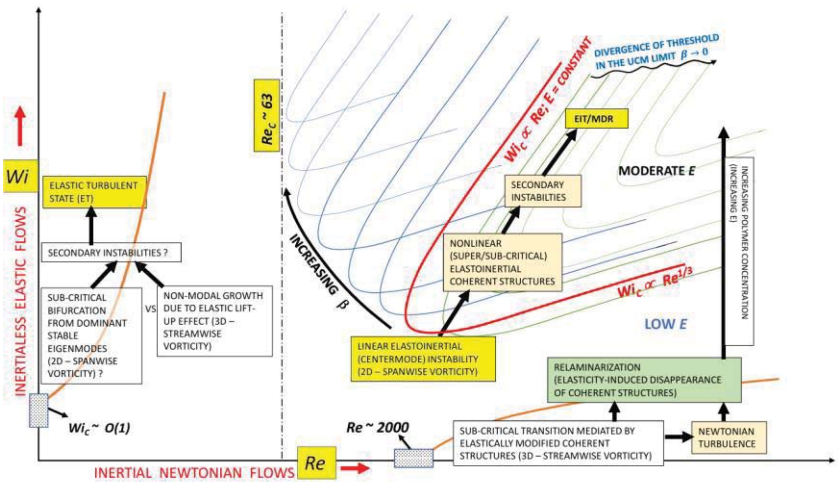

Figure 1. Schematic representation of various transition scenarios in viscoelastic pipe flow in the Wi–Re plane.

References

[1] Mohammad Khalid, V. Shankar, and Ganesh Subramanian, Continuous pathway between the elasto-inertial and elastic turbulent states in viscoelastic channel flow, Physical Review Letters, 127, 134502 (2021).

[2] Castillo-Sanchez et al., Understanding viscoelastic flow instabilities: Oldroyd-B and beyond, Journal of non-Newtonian Fluid Mechanics, 301, 104742 (2022)

SCALING THE TRANSITION THRESHOLD OF EIT

Shoaib kamil[1], Bjoern Hof[1]
[1] *Institute of Science and Technology Austria (ISTA), 3400, Klosterneuburg, Austria*

Abstract viscoelasticity, tranistion threshold.

A sufficiently elastic fluid, such as a long-chain polymer solution, can induce a new type of turbulence known as elasto-inertial turbulence (EIT) in pipe and channel flows, which typically occurs at much lower Reynolds numbers than inertial turbulence. The exact onset of this transition, however, is not solely governed by the Reynolds number, but it equally depends on the fluid properties, such as the solvent viscosity and the polymer relaxation time. To complicate matters, in experiments, the transition threshold varies with pipe diameter due to the instability's dependence on the shear rate.

The goal of the present study is to determine the scaling of the transition threshold as a function of Re and fluid parameters. In our experiments, we detect the transition onset by measuring pressure fluctuations in pipes of varying diameters. The polymer relaxation time and the shear-dependent fluid viscosity are measured using an Anton Paar (MCR 102) rheometer, allowing us to compute the viscosity ratio (β) and the elasticity number (E, Weissenberg number divided by the Reynolds number). Data sets are obtained for three different polymer concentrations and two different pipe diameters. For each data set, the elasticity number is varied by an increase in the solvent viscosity (i.e., increasing the glycerol concentration). As done in previous studies [1, 2, 3], we plot the critical Reynolds number (Re_c) for the onset of EIT as a function of $E(1-\beta)$, shown in Figure 1.

For these chosen parameters, the curves for different polymer concentrations and pipe diameters collapse. Overall, we cover five orders of magnitude in Re and $E(1-\beta)$. For not too low Re, the transition threshold scales with a power law close to -0.7, which changes to -1 for higher values of $E(1-\beta)$. However, the decrease is not monotonic, and eventually, at some minimum elasticity number, the instability is lost, and the curves diverge. The point of divergence is found to decrease with decreasing pipe diameter or with increasing polymer concentration.

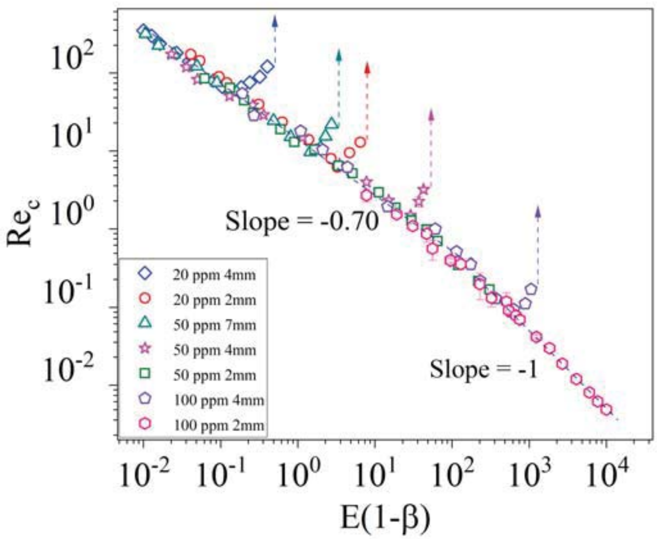

Figure 1. The critical Reynolds number at the onset of EIT as a function of $E(1-\beta)$. Here, the vertical dashed arrow lines demarcate the divergence of the instability threshold.

References

[1] B. Chandra, V. Shankar & D. Das, *Early transition, relaminarization and drag reduction in the flow of polymer solutions through microtubes*, J. Fluid Mech. **885**, A47 (2020).
[2] I. Chaudhary, P. Garg, G Subramanian & V. Shankar, *Linear instability of viscoelastic pipe flow*, J. Fluid Mech. **908**, A11 (2021).
[3] M. Khalid, V. Shankar & G Subramanian, *Continuous Pathway between the Elasto-Inertial and Elastic Turbulent States in Viscoelastic Channel Flow*, Phys. Rev. lett. **127**, 134502 (2021).

ELASTIC INSTABILITY IN A MICRO-SERPENTINE CHANNEL AT LOW REYNOLDS NUMBERS

Yusuf Alperen Degirmenci[1], Kevin Nolan[2], Luca Biancofiore[3]
[1]*M.Sc. Simulation Sciences, RWTH Aachen University, Aachen, Germany*
[2]*School of Mechanical and Materials Engineering, University College Dublin, D04 C1P1, Dublin, Ireland*
[4]*Department of Industrial and Information Engineering and Economics, University of L'Aquila, L'Aquila,Italy*

Abstract In this study, we performed direct numerical simulations (DNS) to investigate viscoelastic fluids in micro serpentine channels, comparing the results with previous experimental findings [1]. Utilizing the open-source rheoTool package in OpenFOAM, known for its stability due to the log-confirmation representation (LCR) algorithm, we employed the Oldroyd-B viscoelastic model in our simulations [2, 3]. We maintained constant values for the ratio of solvent viscosity to total viscosity ($\beta = 0.2$) and the Reynolds number ($Re = 1$) while varying the Weissenberg number (Wi).

The simulations demonstrated qualitative agreement with the experimental findings, showing that as the Weissenberg number increased, the velocity fluctuations became more pronounced throughout the domain, as shown in Fig. 1. At a relatively low Weissenberg number ($Wi = 5$), the fluctuations became apparent and increased significantly at higher Wi values, with fluctuation magnitudes reaching up to 8% of the mean velocity at $Wi = 20$. Consequently, a corresponding increase in thermal efficiency is observed at higher Wi, as illustrated in Fig. 1b.

In addition, we propose a new constitutive model combining the FENE-CR and Carreau-Yasuda formulations. This approach accounts for shear-thinning effects by making polymeric viscosity a function of the shear rate, providing a more accurate description of the fluid's viscoelastic behavior. These findings suggest that elastic instabilities induced by viscoelastic effects could potentially enhance heat transfer in microelectronics by disrupting the predominantly laminar flow at low Reynolds numbers.

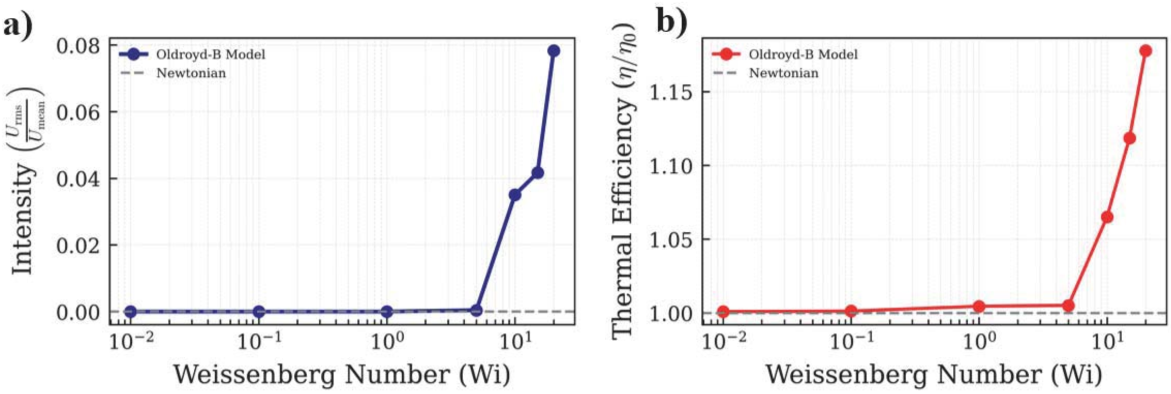

Figure 1. Effect of Weissenberg number on (a) velocity fluctuation intensity and (b) thermal efficiency (η/η_0) in a micro-serpentine channel. The dashed line represents the Newtonian baseline.

References

[1] K. P. Nolan, A. Agarwal, S. Lei and E. Dalton, Mixing enhancement due to viscoelastic instability in serpentine microchannels at very large Weissenberg numbers, 15th IEEE ITherm Conf. 301-306, 2016.
[2] R. Fattal and R. Kupferman, Constitutive laws for the matrix-logarithm of the conformation tensor, J. Non-Newtonian Fluid Mech. 123, 281–285, 2004.
[3] F. Pimenta and M. A. Alves, Stabilization of an open-source finite-volume solver for viscoelastic fluid flows, J. Non-Newtonian Fluid Mech. 239, 85–104, 2017.

Electrohydrodynamics of Viscoelastic Sessile Droplets: Subcritical Deformation and Critical CaE Thresholds

Igino Foglia[1], Giuseppe Fontanarosa[1], Giancarlo Esposito[1], Gaetano D'Avino[1], Pier Luca Maffettone[1]
[1]*Dipartimento di Ingegneria Chimica, dei Materiali e della Produzione Industriale, Universit`a di Napoli Federico II, P.le Tecchio 80, 80125 Napoli, Italy*

Keywords: Electrohydrodynamics, Droplet deformation, Subcritical regime, Supercritical regime, Instability threshold, Viscoelastic fluids, Charge relaxation, Numerical simulation

Abstract

The precise manipulation of liquids at the micro- and nano-scale is central to microfluidics and biomedical technologies. Electrohydrodynamics (EHD) enables controlled deformation of fluid interfaces via electric-field–induced charge accumulation. While most EHD studies consider Newtonian liquids, many biological fluids are viscoelastic and display strong extensional responses, which can modify droplet dynamics under electric forcing.
We numerically investigate a viscoelastic sessile droplet using a Volume-of-Fluid framework under constant electric fields. We first focus on the subcritical regime (no jetting/breakup) and quantify how deformation amplitude and transient dynamics depend on the Ohnesorge number (Oh), electric capillary number (CaE), Deborah number (De), and polymeric ratio (β), highlighting the role of extensional stresses in interface elongation. We also determine how Oh shifts the critical electric capillary number, associated with the transition to jetting/breakup. These results clarify the coupled effects of viscous-capillary and viscoelastic stresses and support the design of EHD-based microfluidic handling strategies for biological liquids. [1, 2]

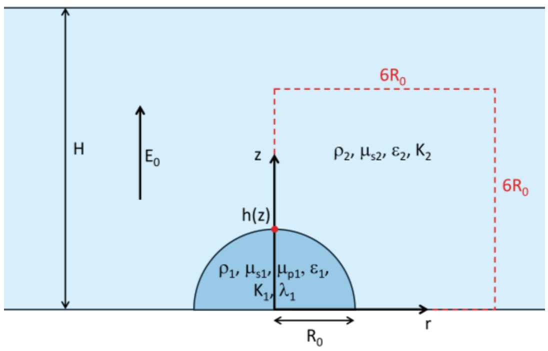

Figure 1. Schematic of the problem investigated in this work. The red dashed lines denote the computational domain.

References

[1] Taylor, Geoffrey Ingram. "Studies in electrohydrodynamics. I. The circulation produced in a drop by an electric field." Proceedings of the Royal Society of London. Series A. Mathematical and Physical Sciences 291.1425 (1966): 159-166.
[2] Beroz et al. Stability limit of electrified droplets. Phys Rev Lett. 2019;122 (24) .

IONIC-STRENGTH-DEPENDENT HYDRODYNAMIC RESISTANCE IN NON-NEWTONIAN FLUIDS: IMPLICATIONS FOR CO_2 BUBBLE DISSOLUTION DYNAMICS

Salvatore Cito[1], Nada Bouffaghar[1], Jordi Pallarès[1]
[1]*Departament d'Enginyeria Mecànica, Universitat Rovira i Virgili, Tarragona, Spain*

Abstract Key words: CO_2 dissolution; non-Newtonian fluids; ionic strength; wake dynamics; xanthan gum; settling.

Predicting CO_2 dissolution in non-Newtonian water–ionic liquid systems requires understanding how ionic environments modify hydrodynamic resistance and wake dynamics around rising bubbles. In semi-rigid polyelectrolyte solutions such as xanthan gum, ionic strength alters chain conformation and intermolecular interactions, producing measurable changes in structure and viscoelastic response [1, 2]. Yet, how these salt-activated structural effects translate into bubble-scale hydrodynamics and transport remains unclear.

In the context of a project on CO_2 bubble dissolution in structured fluids, we analyze particle settling across salinity and polymer concentration ranges using the publicly available dataset of Mrokowska & Krztoń-Maziopa [3]. Spheres and disks (1.5–3 mm) are used as controlled analogues of bubbles of comparable size, which may transition from spherical to ellipsoidal shapes depending on their position in the Galileo–Bond (Ga–Bo) space. The investigated conditions correspond to low-to-moderate Reynolds numbers ($Re \approx 0.5$–3); we also track the Weissenberg number ($Wi = \lambda U/d$) using relaxation times from oscillatory rheology.

Terminal velocities are extracted from trajectories and drag coefficients normalized against Newtonian expectations to isolate non-Newtonian contributions. Preliminary analysis indicates that drag can be highly sensitive to ionic strength even when Re and Wi vary smoothly, suggesting flow-mode-dependent structural resistance affecting wake development. Since wake topology and near-wake stresses control boundary-layer renewal, such modifications may alter the mass transfer coefficient governing CO_2 dissolution. This work positions settling as a hydrodynamic probe to inform predictive modeling of bubble dynamics and gas–liquid mass transfer in non-Newtonian water–ionic liquid systems.

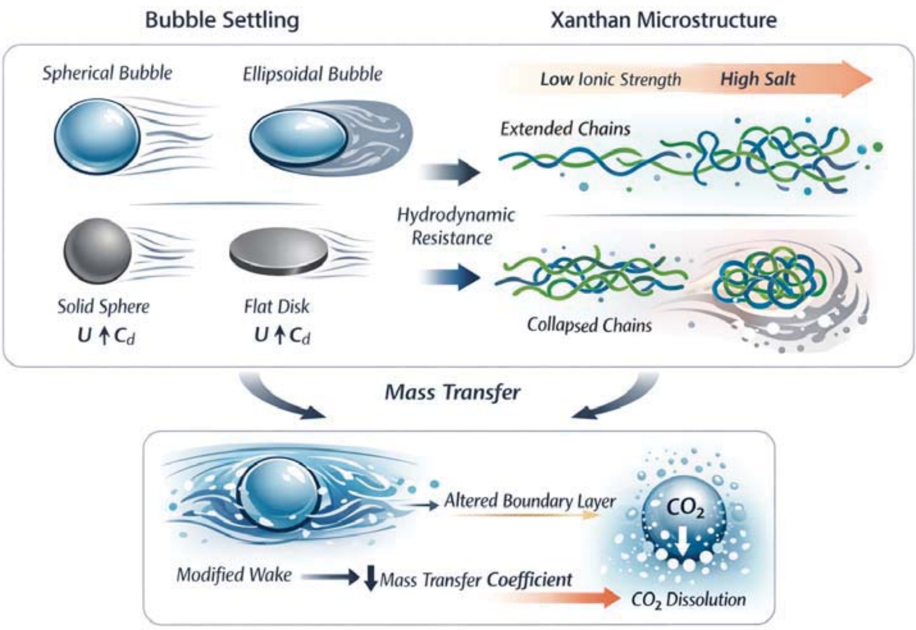

Figure 1. Schematic: ionic-strength-dependent microstructure modifies wake topology and boundary-layer renewal around bubble-scale inclusions, impacting hydrodynamic resistance and the mass transfer coefficient for CO_2 dissolution.

References

[1] C. E. Brunchi, S. Morariu, M. Bercea, *Intrinsic viscosity and conformational changes of xanthan in salt solutions*, Carbohydrate Polymers **136**, 1096–1104 (2016).

[2] J. A. Casas, V. E. Santos, F. García-Ochoa, *The effect of salts on the rheological properties of xanthan gum solutions*, Food Hydrocolloids **14**, 357–364 (2000).

[3] M. M. Mrokowska, A. Krztoń-Maziopa, *Dataset: Viscoelastic and shear-thinning effects of aqueous exopolymer solution on disk and sphere settling*, Mendeley Data (2019), DOI: 10.17632/ntgfb38k69.4.

VISCOELASTIC SUB-DIFFUSIVE CHANNEL FLOW IN A TRANSVERSE MAGNETIC FIELD

Yudhvir Singh Yadav[1], Mahesh Kumar[2], Sarthok Sircar[2] & Priyanka Shukla[1]
[1] *Department of Mathematics, Indian Institute of Technology, Madras, Chennai 600036, India*
[2] *Department of Mathematics, IIIT Delhi, Delhi 110020, India*

Keywords: Anomalous diffusion, Viscoelasticity, Linear stability analysis, Nonlinear simulations.

Abstract The linear stability and dynamics of viscoelastic, sub-diffusive plane Poiseuille flow in the presence of an external magnetic field. Viscoelastic effects are modeled using the fractional upper-convected Maxwell model. Neutral stability curves are obtained for different values of the sub-diffusive exponent, elasticity, magnetic field strength, viscosity ratio, and Reynolds number. It is found that changing the order of the sub-diffusive exponent significantly shifts the most unstable mode. To support the linear stability findings, direct numerical simulations are also performed. The evolution of the polymer conformation tensor, which remains symmetric and positive-definite, is studied using a Riemannian metric and characterized through its three scalar invariants. The results provide new insights in the formation of microstructures in sub-diffusive viscoelastic flows, which is important in various engineering problems.

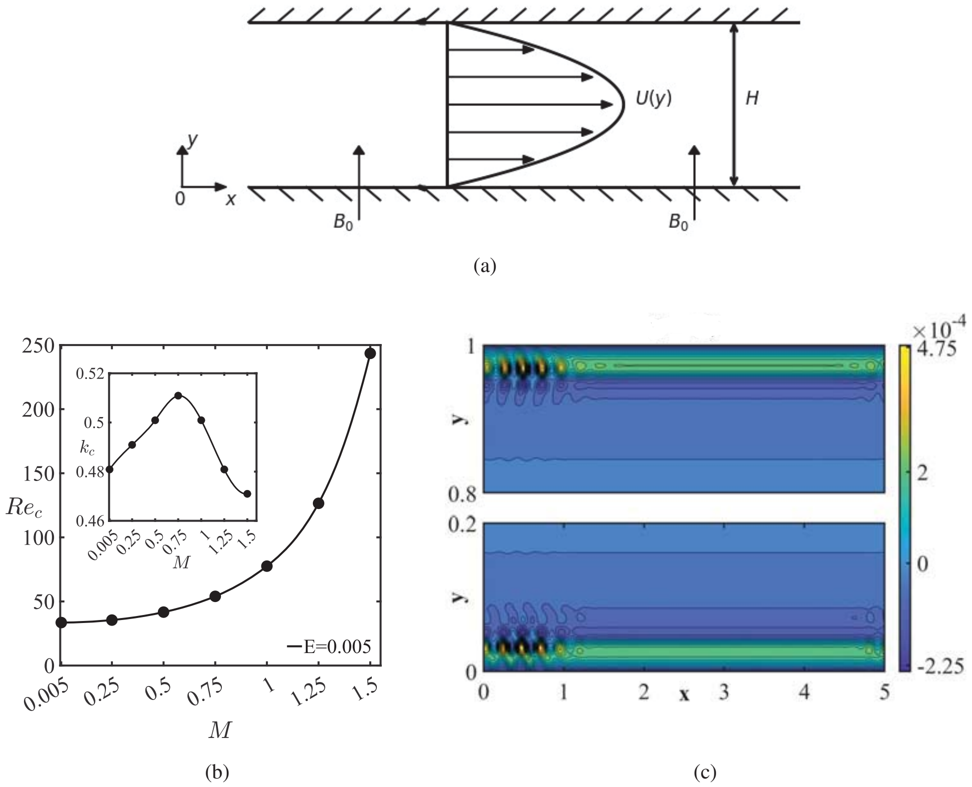

Figure 1. (a) Schematic of the plane Poiseuille flow in a rigid channel under external magnetic field B_0. (b) Variation of the critical Reynolds number Re_c and critical wavenumber k_c (inset) with Hartmann number M for elastisity number $E = 0.005$. The stabilizing influence of the Hartmann number is evident from the monotonic increase in the critical Reynolds number with increasing M. (c) Contours of instantaneous volume ratio in (x, y)-plane at simulation time $T = 19$. The other parameters are : sub-diffusive exponent $\alpha = 0.8$, dimensionless solvent viscosity $\nu = 0.5$, and elasticity number $E = 0.005$. Panel c displays the formation of symmetric microstructures along the channel walls in the presence of weak magnetic field.

References

[1] B.S. Ng & W.H. Reid, *The compound matrix method for ordinary differential systems*, J. Comput. Phys. **58**, (1985).
[2] Y.S. Yadav, M. Kumar, S. Sircar, & P. Shukla, *Viscoelastic sub-diffusive channel flow in a transverse magnetic field*, Phys. Fluids **37**, (2025).

SYMMETRY BREAKING IN VISCOELASTIC FLOWS PAST CYLINDER ARRAYS

Henry M. Broadley[1], Jack R. C. King[1], & Miguel Beneitez[1]
[1] *Department of Mechanical & Aerospace Engineering, The University of Manchester, Manchester, UK*

Abstract Key Words: Viscoelastic Flow; Elasto-Inertial Turbulence; Complex Geometry; High-order Direct Numerical Simulation.
Enhanced mixing caused by turbulence in viscoelastic flows is desirable in many manufacturing processes. In addition to classical Newtonian turbulence observed in strongly inertial flows, elastic effects in polymer flows can lead to purely elastic or elasto-inertial turbulence. We investigate transition to elasto-inertial turbulence (EIT) in polymer flows through a representative, hexagonal array of cylinders as in the experiments of [1], but across a wide region of the Reynolds number (Re) and Weissenberg number (Wi) parameter space. By performing high-order direct numerical simulation (DNS) in 2D using the SUNSET-code, a mesh-free code developed for viscoelastic flows [2], we map and categorise the transition boundaries in the $Re \in [10, 500], Wi \in [0, 320]$ parameter space. Unlike previous numerical studies in similar geometries [3], our discretisation enables high-order approximation everywhere in the flow field including at boundaries. At $Re = 100$, there is periodic vortex shedding in the Newtonian case ($Wi = 0$). As Wi increases, elasto-intertial instabilities begin to develop as the solution branch disappears through a subcritical saddle-node bifurcation. Continuing this branch back down to lower Wi, we observe a separate stable branch of solutions in which wake oscillations are suppressed, mean kinetic energy is larger and mean elastic energy is reduced. Increasing Wi beyond the saddle-node bifurcation point we observe a seemingly supercritical transition to a fully chaotic EIT state. In the EIT regime, the dynamics appear to be controlled by the interaction between vortex shedding in the wake of cylinders and the motion of streaks of stretched polymers in the channels above and below cylinders. In contrast, for simulations performed at much lower Re (e.g. $Re = 10$) arrowhead structures emerge at relatively low Wi, however transition to fully developed EIT never takes place. At $Re = 50$, we see periodic vortex shedding above a critical $Wi \approx 3$, with increasing frequencies present up to $Wi \approx 10$, but at higher Wi this unsteady behaviour is suppressed, suggesting that arrowheads do not play a role in the transition to EIT in this geometry. Our simulations therefore demonstrate that in the current setting the onset of EIT is not driven by purely elastic effects, but that inertial vortex shedding plays a key role in the transition process. At $Re = 100$, in the Newtonian limit the flow is two-dimensional. We show that our two-dimensional EIT solutions at $Re = 100, Wi = 10$ develop three-dimensional structure, highlighting a symmetry breaking induced by elasticity. These insights into the transition pathway may support strategies to control or exploit EIT in these geometries, with important implications to many industrial processes.

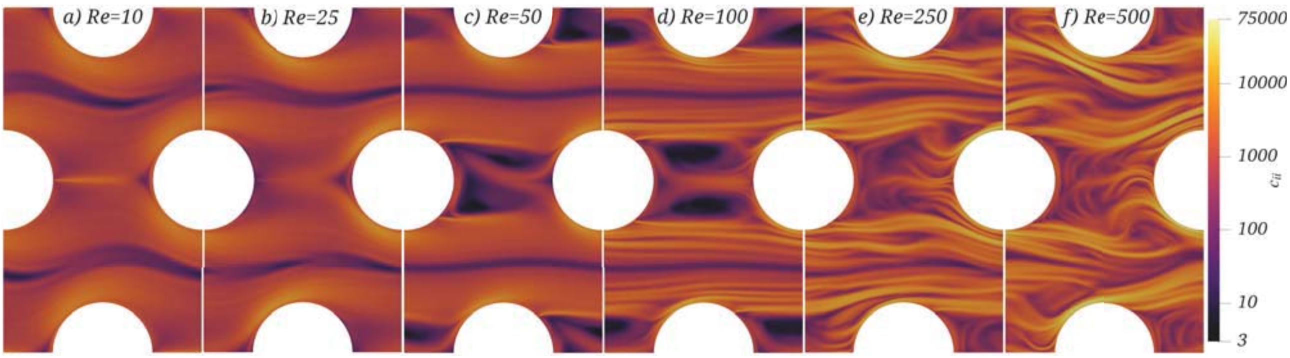

Figure 1. Snapshots of the trace of the conformation tensor c_{ii} in fully developed 2D flow when $Wi = 10$ for increasing values of Re. Note the arrowhead structure formed in both channels when $Re = 10$ and $Re = 25$ which is not present at $Re \geq 50$.

References

[1] S. J. Haward, C. Cameron, & A. Q. Shen *Stagnation points control chaotic fluctuations in viscoelastic porous media flow* Proc. Natl. Acad. Sci. **118**, (38) e2111651118 (2021).
[2] J. R. C. King & S. J. Lind *A mesh-free framework for high-order simulations of viscoelastic flows in complex geometries* JN-NFM **330**, 105278 (2024).
[3] L. Zhu & R. R. Kerswell *Early turbulence in viscoelastic flow past a periodic cylinder array* arXiv: 2410.12033 (2025).

ON THE STREAKY INSTABILITY OF SHEAR-THINNING FLOW IN A CORRUGATED TUBE

Xuerao He[1], Kengo Deguchi[1] & Hugh M. Blackburn[2]
[1] *School of Mathematics, Monash University, Clayton, VIC 3800, Australia*
[2] *Department of Mechanical and Aerospace Engineering, Monash University, Clayton, VIC 3800, Australia*

Abstract Shear-thinning fluids; Corrugated pipe flow; Shear-flow instability; CarreauYasuda model

Shear-thinning fluids flowing near rough or wavy walls are common in engineering and biological applications, yet their behaviour remains poorly understood. Direct numerical simulation of highly shear-thinning flows is computationally demanding, so convenient methods for assessing the stability of the base flow are highly sought after. We partially overcome this challenge for the classical test case of corrugated pipe flow by employing a large-Reynolds-number asymptotic analysis. First we obtain the analytic neutral curve for power law fluids using only the leading order terms. To improve predictive accuracy and to handle more general Carreau–Yasuda fluids, we then develop an asymptotic preserving reduction (APR) that retains several higher order terms. Both approaches show good agreement with full system results computed using a spectral element solver for moderately shear-thinning fluids, including the streaky characteristics of the perturbation flow fields. Furthermore, we extend the stability predictions to strongly shear-thinning fluids. Using APR with Carreau–Yasuda parameters relevant to the experiments, we find that under certain conditions, the instability can arise even for very small wall undulations.

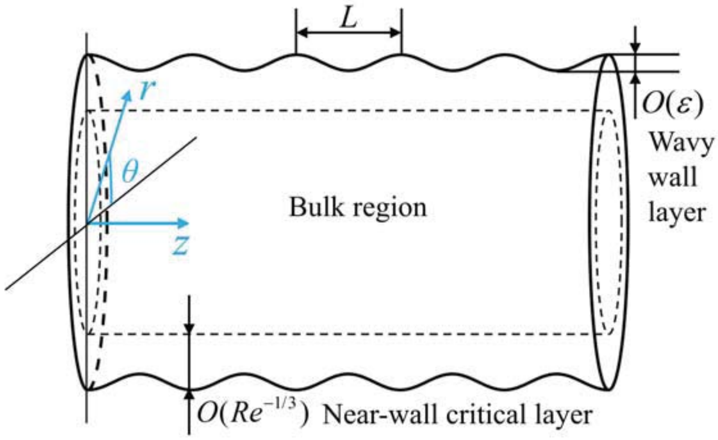

Figure 1. Sketch of the flow configuration in the non-dimensional cylindrical coordinates (r, θ, z).

SPH-BASED ANALYSIS OF INTEGRAL FRACTIONAL K-BKZ VISCOELASTIC MODELS

Luca Santelli[1], Adolfo Vazquez-Quesada[2] & Marco Ellero[3,4]
[1]*Department of Mathematics, University of Padua, Padua, Italy*
[2]*Departamento de Física Fundamental, UNED, Madrid, Spain*
[3]*Basque Center for Applied Mathematics, Bilbao, Spain*
[4]*IKERBASQUE, Basque Foundation for Science, Bilbao, Spain.*

Keywords: Fractional viscoelasticity, Large amplitude oscillatory shear, K-BKZ equation, Smoothed particle hydrodynamics

Abstract

Fractional constitutive models have gained attention in recent years for their ability to capture specific characteristics of non-Newtonian fluids [1]. These models provide a simple yet effective framework for describing complex viscoelastic behaviour, particularly in materials with power-law relaxation processes, such as polymer melts [2]. However, implementing these models requires numerical frameworks for integral constitutive equations [3]. A Lagrangian Framework simplifies integration along streamlines compared to the Eulerian approach, which reconstructs flow history and is computationally expensive. Using a Lagrangian Smoothed Particle Hydrodynamics (SPH) method, we can efficiently track particle history, enabling innovative solutions for integral constitutive models while avoiding complex computations. Our SPH-based integral fractional viscoelastic method has been validated using classical frameworks under benchmark flows such as Small Amplitude Oscillatory Shear (SAOS), Kolmogorov, and Poiseuille [4]. Building on this, we have extended our analysis to non-linear flow scenarios, focusing on Large Amplitude Oscillatory Shear (LAOS), implemented with a fractional K-BKZ integral model and compared with experimental data for isotactic polypropylene. Unlike SAOS, LAOS cannot be fully characterised by elastic and loss moduli. Therefore, we integrate our study with an analysis of the Chebyshev coefficients [5]. Ongoing developments extend this framework to more complex flows, including viscoelastic benchmarks like flow around obstacles, planar and axisymmetric contractions, and heterogeneous systems with rigid particle suspensions.

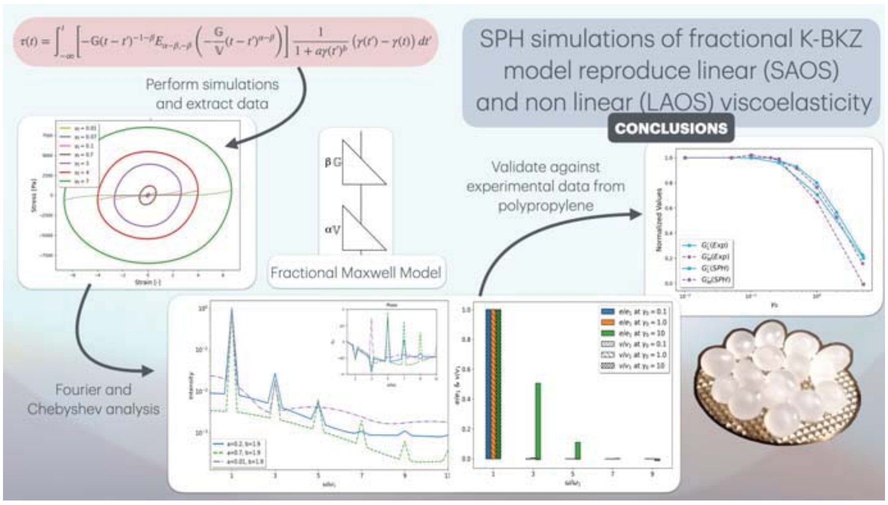

Figure 1. Graphical Abstract

References

[1] Jaishankar A, McKinley GH. J. Rheo 58-2014
[2] Yang P, Lam YC, Zhu KQ. J. of Non-Newtonian Fluid Mech 165-2010
[3] Luo XL, Tanner RI. International J. Num Meth in Engineering 25-1988
[4] Santelli L, Vázquez-Quesada A, Ellero M. J. of Non-Newtonian Fluid Mech 329-2024
[5] Santelli L, Vázquez-Quesada A, Burgoa A, Arriaga A, Hernandez R, Ellero M. Rheologica Acta 1-17-2026

STOCHASTIC TRANSIENT FORMATION OF TURBULENT BAND IN CHANNEL FLOW

Ryoko Ono[1], Yuki Matsukawa[1], Kazuki Kohyama & Takahiro Tsukahara[1]
[1] *Department of Mechanical & Aerospace Engineering, Tokyo University of Science, Japan*

Keywords: subcritical transition, transient process, turbulent band, plane Poiseuille flow, DNS

Abstract Wall-bounded shear flows in the subcritical transition regime exhibit spatio-temporal intermittency, where turbulent and laminar regions coexist with characteristic lengths $L \approx 10^1$–10^2 (normalized by the channel width or pipe diameter). In a pipe flow, turbulent puffs undergo stochastic splitting and decay [1]—phenomena that was proposed to relate to directed percolation (DP), a universality class in non-equilibrium statistical physics, though this connection remains a subject of ongoing debate [2]. A high-aspect-ratio channel experiment reported DP-like scaling for turbulent bands [3], but concerns remain that finite length and imposed inflow condition, i.e., a homogeneously disturbed inflow, may capture only a transient stage of band formation [2].

This study aims to assess the characteristic time scales associated with the formation and sustenance of the turbulent band in the channel, through direct numerical simulations (DNSs) of plane Poiseuille flow in a periodic domain of $102.4\delta \times 102.4\delta$ with channel width 2δ. From fully-turbulent states as initial fields, the friction Reynolds number Re_τ was decreased linearly in time. The time length ΔT to reduce from $Re_\tau = 150$ to 54 was set as a control parameter in this study. The onset timing of the Re_τ-reduction was arbitrarily chosen, and for each condition, 10 trials were performed with different instant. The time when ΔT had elapsed was set as $t = 0$, after which Re_τ was fixed at 54. Given a sufficiently long ΔT, turbulent bands should form and persist quasi-permanently at $Re_\tau = 54$. In fact, for $\Delta T^* \equiv \Delta T u_\tau/\delta = 1600$ (u_τ: the friction velocity), the flow during Re_τ-reduction has been indistinguishable from the steady-state field at the corresponding Re_τ at each instant (figure not shown). If ΔT is shorter than the characteristic time required for the formation of turbulent bands, they may decay before fully forming, resulting in relaminarization. Thus, a parametric investigation with respect to ΔT allows us to estimate the formation time of turbulent bands and assess the validity of prior experimental results [3].

Figure 1(a) shows the results of ten trials for $\Delta T^* = 16$. Here, the turbulent kinetic energy K' is based on the fluctuations from the laminar base flow. At the end of Re_τ-reduction phase ($t = 0$), K' is still decreasing in all trials until $tu_\tau/\delta \approx 5$. In five out of ten trials, K' continued to decrease and eventually remained at zero, indicating that the flow had fully laminarized. However, the other five trials exhibited the formation of turbulent bands. From a dynamics perspective, the ten trials stochastically bifurcate into laminarization or turbulent band formation during the transient, as shown in Figs. 1(b,c) and (d,e), respectively. From the snapshots of panels (b) and (d), it is evident that the flow field contains sparsely distributed turbulent spots that serve as seeds for turbulent bands, and stochastic dynamics determine whether these spots grow or decay. Based on the parametric study, the formation timescale of turbulent bands can be considered comparable to $\Delta T^* = 16$ that exhibited the aforementioned stochastic characteristics. Such a finite Re_τ-reduction rate yields fluctuation localization and triggers stochastic turbulent formation, implying a stochastic scenario consistent with DP.

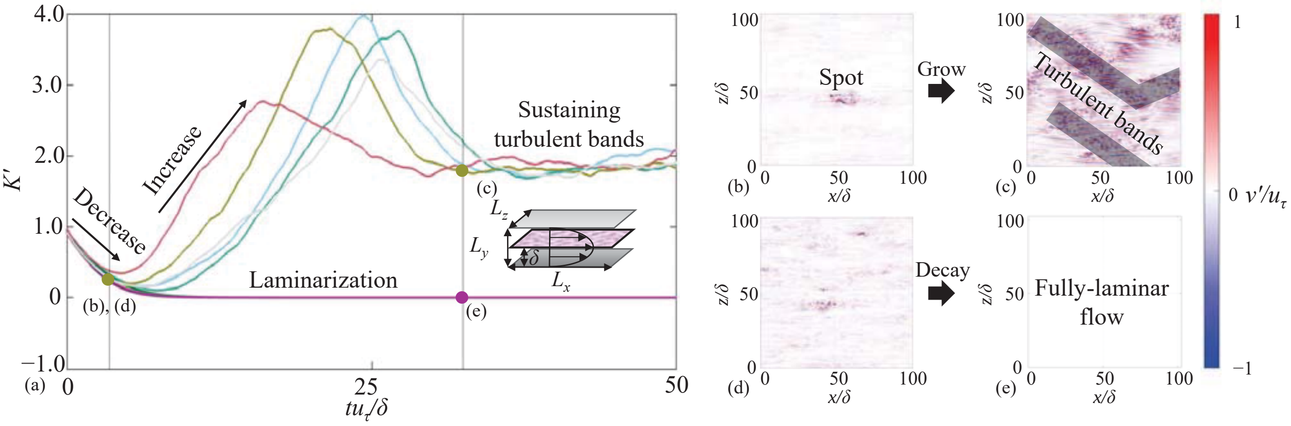

Figure 1. (a) Time evolution of turbulent kinetic energy K' from the end of Re_τ-reduction phase ($t = 0$) to the statistically steady state at $Re_\tau = 54$. Ten trials for $\Delta T^* = 16$ are shown; five trials maintain turbulence, while the remaining five decay to fully-laminar flow, despite similar initial states with turbulent spots as in (b,d). (b–e) Instantaneous wall-normal velocity fields at the channel center: (b) turbulent spot before the formation of turbulent bands at $tu_\tau/\delta = 3.5$, (c) developed turbulent bands at $tu_\tau/\delta = 32.5$, (d) a turbulent spot before the laminarization at $tu_\tau/\delta = 3.0$, and (e) a fully-laminar flow after decaying from the turbulent spot at $tu_\tau/\delta = 32.5$.

References

[1] K. Avila, D. Moxey, A. de Lozar, M. Avila, D. Barkley, & B, Hof, The onset of turbulence in pipe flow, Science, 333, 192–196, (2011).
[2] B. Hof, Directed percolation and the transition to turbulence, Nat. Rev. Phys., 5, 67–72, (2023).
[3] M. Sano & K. Tamai, A universal transition to turbulence in channel flow, Nat. Phys., 12, 249–53, (2016).

UPPER EDGE BISECTION AND EDGE STATE IN PIPE FLOW

Robert Bennett[1], Yohann Duguet[2], Ashley P. Willis[3] & Elena Marensi[1]
[1]*School of Mechanical, Aerospace and Civil Engineering, University of Sheffield, Sheffield S1 3JD, UK.*
[2]*Laboratoire Interdisciplinaire des Sciences du Numérique–LISN-CNRS, Université Paris-Saclay, F-91400 Orsay, France.*
[3]*School of Mathematical and Physical Sciences, University of Sheffield, Sheffield S3 7RH, United Kingdom.*

Abstract (Nonlinear dynamics, turbulent pipe flow, edge of chaos, relaminarisation).

Recent experimental studies [1, 2] have suggested several large-scale control strategies for completely relaminarising turbulent flows in pipe flow. Counter-intuitively, many of these strategies involve initially increasing the turbulent kinetic energy of the flow before it fully decays. This points to the dynamical systems concept of the 'upper edge' [3], separating turbulent flows from high energy initial conditions that relaminarise, and which stands in contrast to the well-studied 'lower edge' that separates initial conditions energetic enough to reach turbulence from those that are not.

We adapt the classical bisection algorithm to the upper edge in order to investigate the upper edge state, which governs the long-term asymptotic behaviour of trajectories on the upper edge. We find that not only do upper edge trajectories rapidly decay in energy, but that the upper edge state precisely coincides with the previously well-studied (lower) edge state. Furthermore, we provide evidence that the decay of edge trajectories from the upper edge is too rapid to be memoryless.

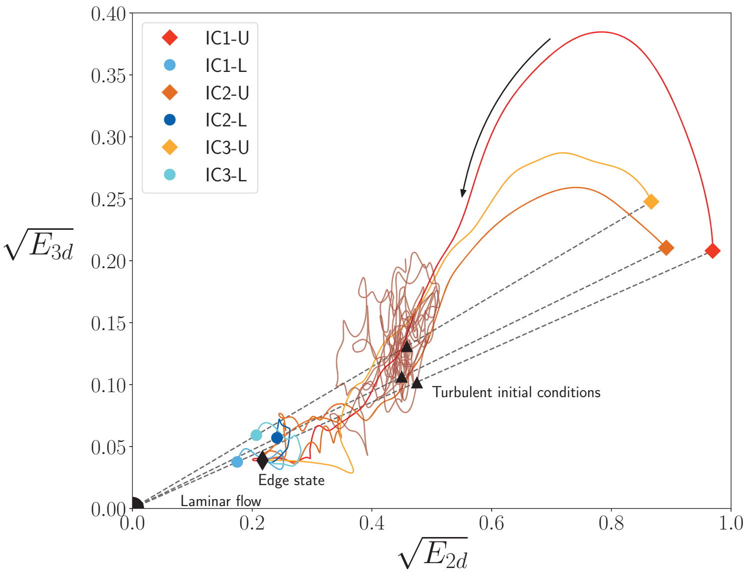

Figure 1. State space portrait of upper and lower edge trajectories, based on the energy of the streamwise average (E_{2d}) and streamwise dependent component (E_{3d}) of the flow. Each pair of upper/lower edge trajectories start from specific initial conditions (circles/diamonds respectively) obtained by rescaling total perturbation energy E from a turbulent initial condition (brown). The arrow indicates the direction of time. All trajectories asymptotically reach the same edge state, the travelling wave solution N2 found in Duguet et al. (2008) [4].

References

[1] J. Kühnen, B. Song, D. Scarselli, N. B. Budanur, M. Riedl, A. P. Willis, M. Avila & B. Hof , *Destabilizing turbulence in pipe flow*, Nat. Phys. **14**, 386–390, (2018).
[2] J. Kühnen, D. Scarselli, M. Schaner & B. Hof , *Relaminarization by steady modification of the streamwise velocity profile in a pipe*, Flow Turbul. Combust., (2018).
[3] N. B. Budanur, E. Marensi, A. P. Willis & B. Hof , *Upper edge of chaos and the energetics of transition in pipe flow*, Physical Review Fluids **5**(2), 023903, (2020).
[4] Y. Duguet, A. P. Willis & R. R. Kerswell , *Transition in pipe flow: the saddle structure on the boundary of turbulence*, J. Fluid Mech., 255–274, (2008).

SIMULATION OF COUNTER-ROTATING SPHERICAL COUETTE FLOW BETWEEN VERY LARGE SPHERES

Juan Cruz Gonzalez Sembla[1], Laurette S. Tuckerman[1]
[1] *PMMH, CNRS, ESPCI Paris, Univ. PSL, Sorbonne Univ., Univ. de Paris, 75005 Paris, France*

Abstract We study counter-rotating spherical Couette flow with a very large radius-to-gap aspect ratio.
Key words: spherical Couette flow, transition to turbulence, wall-bounded shear flows, rotating fluids, geophysical flows

Spheres and spherical shells are the natural domains of geophysics and astrophysics, but simulations in these geometries are more complex and computationally expensive than in planar Cartesian domains. We have formulated a set of equations and a numerical code to study flows in large-radius spherical shells. Our approach retains spherical topology but neglects weak curvature, and uses reduced radial resolution in order to cover a large spherical surface at low computational cost:

a) Fields are expanded in spherical harmonics using the SHTns library [1]. Further savings are obtained by restricting the domain to a longitudinal sector, suppressing large-scale longitudinal variations but retaining the crucial latitudinal ones.
b) We adopt the narrow-gap approximation, neglecting curvature terms.
c) Free-slip boundary conditions are imposed on the spheres. These avoid boundary layers, reducing both radial and angular resolution requirements, but require an imposed azimuthal forcing to generate rotation.
d) Under assumptions (b) and (c), the radial dependence is represented using trigonometric expansions with a drastic radial truncation.

In plane Couette flow, a similar reduced model has successfully reproduced turbulent–laminar banded patterns, including their wavelengths and angles [2]. Such patterns are expected to occur between counter-rotating spheres, since they are observed both between counter-rotating cylinders [3], which resemble the equatorial regions, and between differentially rotating disks [4] which resemble the polar regions, when the horizontal dimensions greatly exceed the gap thickness. Using this approach, we have observed a rich sequence of flows, from axisymmetric vortices to waves and then to turbulence.

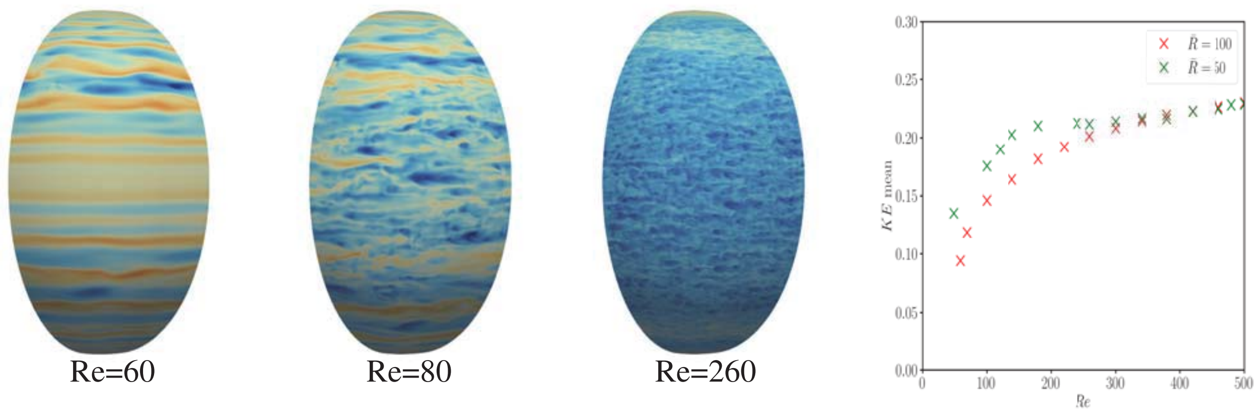

Figure 1. Left: Azimuthal velocity between exactly counter-rotating spheres with $d \equiv r_{\rm out} - r_{\rm in} = 2$ and $\bar{R} \equiv (r_{\rm out} + r_{\rm in})/2 = 100$ using narrow-gap approximation and free-slip radial boundaries. $Re \equiv \bar{R}\Omega d/\nu$.
Right: Total kinetic energy as a function of Re. Values for $\bar{R} = 100$ and $\bar{R} = 50$ agree for $Re \geq 350$ and differ for $Re < 350$.

References

[1] N. Schaeffer, *Efficient spherical harmonic transforms aimed at pseudospectral numerical simulations*, Geochem. Geophys. Geosyst.**14**, 751–758 (2013).
[2] M. Chantry, L.S. Tuckerman & D. Barkley, *Turbulent–laminar patterns in shear flows without walls*, J. Fluid Mech. **791**, R8 (2016).
[3] A. Prigent, G. Grégoire, H. Chaté, O. Dauchot & W. van Saarloos, *Large-scale finite-wavelength modulation within turbulent shear flows*, Phys. Rev. Lett. **89**, 014501 (2002).
[4] A. Cros & P. Le Gal, *Spatiotemporal intermittency in the torsional Couette flow between a rotating and a stationary disk*, Phys. Fluids **14**, 3755–3765 (2002).

COMPETING INSTABILITIES IN CURVED PIPE FLOWS

Ritwik Das[1], Stefano Brizzolara[2] & Björn Hof[1]
[1] *Institute of Science and Technology, Austria*
[2] *Mechanical and Aerospace Engineering, Princeton University*

Keywords: Curved pipe flow, Laminar-turbulent transition, Turbulent puffs, Supercritical instability

Abstract

Flows through curved pipes exhibit a uniquely complex transitional behavior that fundamentally diverges from straight pipe flow dynamics. In a straight pipe, the laminar Hagen–Poiseuille flow remains linearly stable across all Reynolds numbers (Re), with turbulence arising exclusively via subcritical transitions triggered by finite-amplitude perturbations[1]. Conversely, introducing pipe curvature fundamentally alters the base state: centrifugal forces induce secondary circulations, known as Dean vortices , and establish entirely new instability mechanisms[2]. Depending on the degree of curvature, the transition to turbulence in these systems is governed by either a subcritical or a supercritical route [3]. In the supercritical case, the laminar flow becomes linearly unstable to a traveling wave (see Fig. 1, top) and, through a sequence of bifurcations, becomes chaotic [4]. Here, we investigate flows at a curvature above the critical threshold and report a surprising phenomenon within the supercritical regime: the intermittent emergence of localized turbulent bursts (fig 1 bottom). Strikingly, these structures strongly resemble the turbulent "puffs" that are familiar from the subcritical transition in straight pipes. We present a comprehensive characterization of these bursts, detailing their global properties—including size, generation frequency, lifetime, birth, and decay rates—alongside their local structural features, quantified through energy content and spectral analysis. Our findings demonstrate that as Re increases, these subcritical-like structures rapidly proliferate, effectively overriding and completely erasing the preceding supercritical wave motions. Consequently, despite the flow's initial linear instability and a seemingly straightforward supercritical transition route, the fully developed flow is eventually dominated by turbulent motions strictly akin to the subcritical straight pipe case, revealing an unexpected universality in the ultimate fate of transitional pipe flows.

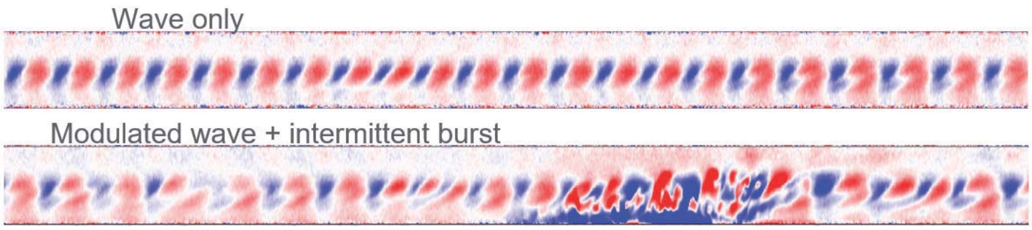

Figure 1. Particle image velocimetry (PIV) measurements reveal intermittent turbulent bursts disrupting supercritical traveling waves. Spacetime diagrams of the outer wall region flow dynamics contrast the initial supercritical 'wave-only' state with the emergence of a 'modulated wave + intermittent burst' state at elevated Reynolds numbers.

References

[1] Avila, Marc, Dwight Barkley, and Björn Hof. "Transition to turbulence in pipe flow." Annual Review of Fluid Mechanics 55.1 (2023): 575-602.
[2] Sreenivasan, K. R., and P. J. Strykowski. "Stabilization effects in flow through helically coiled pipes." Experiments in Fluids 1.1 (1983): 31-36.
[3] Kühnen J, Braunshier P, Schwegel M, Kuhlmann HC, Hof B. Subcritical versus supercritical transition to turbulence in curved pipes. Journal of Fluid Mechanics. 2015;770:R3. doi:10.1017/jfm.2015.184.
[4] Kühnen, Jakob, et al. "Experimental investigation of transitional flow in a toroidal pipe." Journal of fluid mechanics 738 (2014): 463-491.

STUDY OF THE LINEAR INSTABILITY OF THE FEATURLESS TURBULENT FLOW

Arthur Viallefont[1], Grégoire Lemoult[1] & Arnaud Prigent[1]
[1]*LOMC, Université Le Havre Normandie-CNRS,53 rue prony ,Le Havre , France*

Keywords: Taylor-Couette flow, linear instability, transition to turbulence

Abstract

In Taylor-Couette flow (TCF), the transition to turbulence can take different forms. When the cylinders rotate in opposite directions, the transition is characterized by the emergence of the intermittency (INT) and the spiral turbulence (SPT) regimes, two laminar-turbulent coexistence regimes, in which regions of laminar and fully turbulent flow coexist. Spiral turbulence, a turbulent helix within laminar flow produces a periodic pattern in space and time whereas the INT regime, turbulent spots surrounded by laminar flow, is spatio-temporally intermittent. These regimes have been studied since the 1960s [1-3] and have been reproduced numerically using direct numerical simulations (DNS) since 2009 [4-5]. They are a characteristic feature of the transition to turbulence in wall-bounded shear flows. Recently, it has been shown that the transition from laminar flow to the INT regime is well described as a continuous transition belonging to the directed percolation class [6]. The transition from the SPT regime to the homogeneous turbulence has traditionally been studied starting from the fully turbulent state. It has been shown that this regime can be understood as a long-wavelength instability of the turbulent flow [7]. More recently, Kashyap et al. [8-9] have investigated the linear stability of turbulent plane channel flow. Their numerical studies provide evidence that the regular laminar-turbulent coexistence regime indeed results from a linear instability of the fully turbulent regime. However, this result has not yet been confirmed by theoretical and experimental studies. The objective of this work is to determine whether the coexistence regimes come from a linear instability of the turbulent flow and to verify that numerical and experimental way are consistent. Firstly, we conducted our experimental study using a double-axis rheometer with a Couette geometry characterized by a radius ratio of η=0.977 and an aspect ratio of Γ=132. Taking advantage of this configuration, we explored the state diagram while simultaneously measuring the torque. This allowed us to introduce a new order parameter based on torque measurements and to study its variation as a function of the system control parameters. We found that its variation behaves as a supercritical transition for different value of speed ratio. Additionally, we present the results of the linear stability analysis of the flow by performing quenches from the fully turbulent state. We measured the growth rates of the modes associated with the observed patterns by visualizing the flow. Secondly, we perform the numerical work by using the DNS open source code NsCouette [10-11]. We follow the same approach as in [8]: the featureless turbulent state is perturbed using divergence-free white noise, and we analyze the modulus of the Fourier modes at large scales corresponding to the oblique turbulent band.

References

[1] Coles, D. (1965). Transition in circular Couette flow. J. Fluid Mech. **21**(3), 385-425.
[2] Van Atta, C. (1966). Exploratory measurements in spiral turbulence. J. Fluid Mech. **25**(3), 495-512.
[3] Andereck, C. D., Liu, S. S., & Swinney, H. L. (1986). Flow regimes in a circular Couette system with independently rotating cylinders. J. Fluid Mech. **164**, 155-183.
[4] Meseguer, A., Mellibovsky, F., Avila, M., & Marques, F. (2009). Instability mechanisms and transition scenarios of spiral turbulence in Taylor-Couette flow. Phys. Rev. E **80**(4), 046315.
[5] Dong, S. (2007). Direct numerical simulation of turbulent Taylor–Couette flow. J. Fluid Mech. **587**, 373-393.
[6] Lemoult, G., Shi, L., Avila, K., Jalikop, S. V., Avila, M., & Hof, B. (2016). Directed percolation phase transition to sustained turbulence in Couette flow. Nature Physics **12**(3), 254-258.
[7] Prigent, A., Grégoire, G., Chaté, H., Dauchot, O., & van Saarloos, W. (2002). Large-scale finite-wavelength modulation within turbulent shear flows. Phys. Rev. Lett. **89**(1), 014501.
[8] Kashyap, P. V., Duguet, Y. & Dauchot, O. (2022). Linear instability of turbulent channel flow. Phys. Rev. Lett. **129**(24), 244501.
[9] Kashyap, P. V., Duguet, Y., & Dauchot, O. (2024). Linear stability of turbulent channel flow with one-point closure. Phys. Rev. Fluids **9**(6), 063906
[10] Jose Manuel Lopez, Daniel Feldmann, Markus Rampp, Alberto Vela-Martin, Liang Shi & Marc Avila. nsCouette -- A high-performance code for direct numerical simulations of turbulent Taylor-Couette flow. arXiv:1908.00587
[11] Liang Shi, Markus Rampp, Bjoern Hof & Marc Avila. A hybrid MPI-OpenMP parallel implementation for pseudospectral simulations with application to Taylor-Couette flow. Computers & Fluids, 106, p. 1-11, 2015.

MODELING OF HIGH-SPEED LAMINAR-TURBULENT TRANSITION BASED ON FIELD INVERSION AND SYMBOLIC REGRESSION

Lei Wu & Zuoli Xiao
State Key Laboratory for Turbulence and Complex Systems, School of Mechanics and Engineering Science, Peking University, China

Abstract High-speed flow, Overshoot, Reynolds-averaged Navier-Stokes, Field inversion, symbolic regression, White-box expression.

The laminar-turbulent transition is ubiquitous across a wide variety of aero- and hydrodynamic vehicles. When shifting towards high-speed transitional flows, local peaks in wall skin friction and heat transfer coefficients frequently occur near the end of transition region [1, 2]. The inability to resolve the overshoot phenomena of wall skin friction and heat transfer remains a longstanding deficiency in transition-turbulence modeling for Reynolds-averaged Navier-Stokes (RANS) simulations. Field inversion (FI) and symbolic regression (SR) techniques are employed to explore a generalizable and interpretable augmentation, and thus resolve the missing overshoot behavior. To be specific, ensemble Kalman filter (EnKF) method is first used to infer the overshoot-resolved RANS field, and then SR strategy is employed to discover a white-box overshoot-predictive correction expression over original transition model. The multiplicative correction field $\beta(\mathbf{x})$ is introduced in the production term of the intermittency factor equation for the high-speed k-ω-γ-$\widetilde{Re}_{\theta t}$ transition-turbulence model [3] to depict the model-form uncertainty in overshoot phenomenon, which can be inferred directly from the overshoot-resolved EnKF field. Results for flate plate and sharp cone manifest that the learned expression faithfully reproduces the overshoot magnitudes in transition region while avoiding spurious behavior in other regions. Shown in figure 1 are several representative predictions of heat transfer coefficient of a sharp cone with different transition-turbulence models. It turns out that the model with correction term $\beta(\mathbf{x})$ yields a significant improvement over the previously improved model for high-speed flows ([3]), accurately capturing the overshoot behavior in wall skin friction (not shown here) and heat transfer during the late transition phase. More importantly, this augmentation does not corrupt the precision of high-speed model (i.e., legend "Improved mode" in figure 1) in transition onset and length, which have been well worked out by our previous modifications ([3]). To the best of the authors' knowledge, this work represents the first interpretable, data-driven correction for overshoot prediction of the RANS transition model. The resultant expression not only breaks through the long-missing physical feature but also is generalizable to other transition model frameworks, offering a principled pathway toward overshoot-resolved transition modeling.

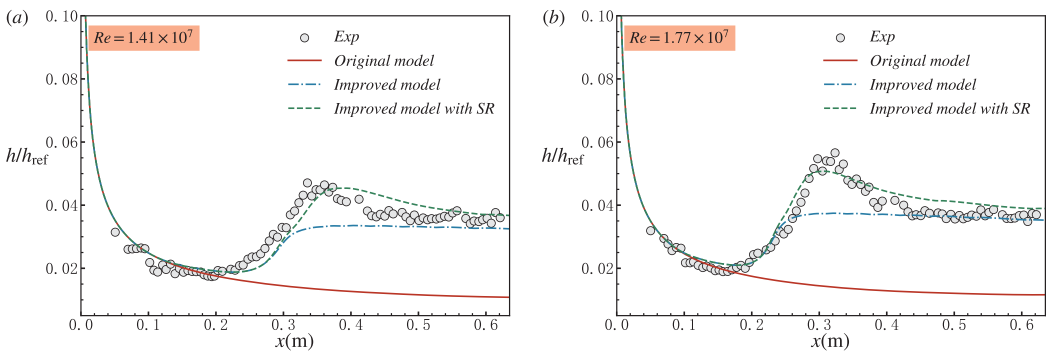

Figure 1. Distributions of heat transfer coefficient $h/h_{\rm ref}$ for sharp cone at (a) $Ma = 6.00, Re = 1.41 \times 10^7$ and (b) $Ma = 6.00, Re = 1.77 \times 10^7$. Here, the legend "DNS" refers to the high-fidelity observation data, legends "Original model" and "Improved model" denote the low-speed transition-turbulence model and its high-speed-corrected counterpart, respectively, and the legend "Improved model with SR" represents the high-speed k-ω-γ-$\widetilde{Re}_{\theta t}$ transition-turbulence model with correction term $\beta(\mathbf{x})$.

References

[1] Kenneth J. Franko & Sanjiva K. Lele, *Breakdown mechanisms and heat transfer overshoot in hypersonic zero pressure gradient boundary layers*, J. Fluid Mech. **730**, 491–532 (2013).
[2] N. D. Sandham, E. Schülein, A. Wagner, S. Willems & J. Steelant, *Transitional shock-wave/boundary-layer interactions in hypersonic flow*, J. Fluid Mech. **752**, 349–382 (2014).
[3] L. Wu & Z. Xiao, *An improved four-equation transition-turbulence model for high-speed flows: Transition prediction and physical insight*, Int. J. Heat Mass Transf. **255**, 127798 (2026).

SEEDLESS VELOCIMETRY OF TURBULENT FLOWS

Franz-Theo Schön[1], Sebastian Merbold[1] & Stefanie de Graaf[1]
[1] *Department of Architecture and Integration of Propulsion System, Institute of Electrified Aero Engines, German Aerospace Centre (DLR), Cottbus, Germany*

Abstract Optical Flow, Background Orientated Schlieren, Karman Vortex Street, Image Velocimetry, Flow Measurement

Background Orientated Schlieren (BOS) is a common method in the study of fluid flows. Hereby, local variations of a transparent flow's refraction index are measured, based on a correlative evaluation of perspective shifts in a background pattern. When all boundary conditions and optical parameters are known, these perspective shifts can be integrated to the local density field $\tilde{c}\langle n\rangle_z$, which is averaged in the direction z - orthogonal to the background plane. The advantage of this method is that it achieves results without manipulating the flow, the disadvantage is that often only relative or qualitative statements are possible. In the present study, a method that extracts the 2D-velocity fields from the Schlieren patterns of a turbulent non-isothermal flow is developed, tackling the weaknesses of BOS. This method is based on an optical flow algorithm, which was already successfully applied to cloud data e.g. of Saturn's Northern Vortex [1]. This seedless velocimetry provides a complete non-invasive measurement technique, which makes it especially useful for flow measurements in aerospace research and applications.
To evaluate the method, the flow around a heated cylinder is observed, which is illustrated in Figure 1. Furthermore, the optical flow velocity fields are compared with a state-of-the-art particle tracking velocimetry.

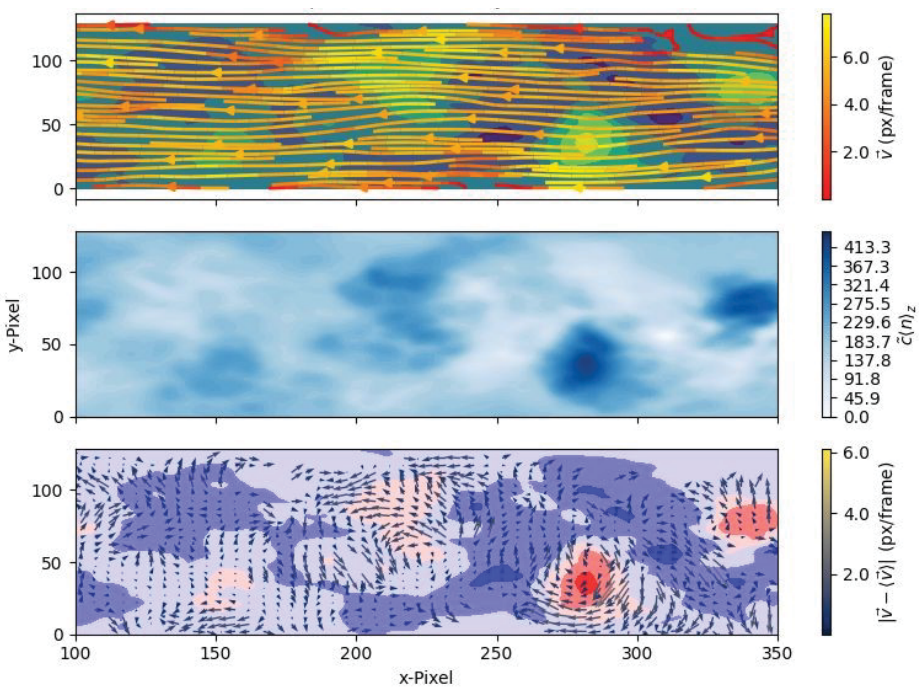

Figure 1. Results of BOS optical flow algorithm used on the flow inside a von-Karman-Vortex Street in turbulent transition regime. Top: streamlines of velocity field $\vec{v}$. Mid: local refraction index variations $\tilde{c}\langle n\rangle_z$. Bottom: velocity field with subtracted mean velocity $\vec{v} - \langle\vec{v}\rangle$.

References

[1] Liu, T., Sayanagi, K. M., Brueshaber, S. R., Blalock, J. J., Ingersoll, A. P., Dyudina, U. A. & Ewald, S. P., *Saturn's North Polar Vortex Structure Extracted From Cloud Images by the Optical Flow Method*, Journal of Geophysical Research: Planets **124**, 3041–3062 (2019).

NEURAL MODEL PREDICTIVE CONTROL FOR PRECISION HISTOTRIPSY

Paolo Guida[1] & William L. Roberts[1]
[1]*Clean Energy Research Center (CERP), King Abdullah University of Science and Technology (KAUST), Thuwal 23955, Saudi Arabia*

Abstract This work focuses on histotripsy and cavitation control using neural model predictive control driven by Fourier Neural Operators for brain-focused high intensity focused ultrasounds.

Histotripsy is a non-thermal high-intensity focused ultrasound technique that mechanically fragments tissue through the rapid nucleation, growth, and collapse of dense microbubble clouds. For brain applications, therapeutic benefit depends on initiating cavitation only at the intended focal target while suppressing off-target activity near sensitive vasculature and critical structures. This is difficult because the governing physics span extreme length and time scales, from micrometer bubbles and nanosecond collapses to centimeter anatomy and millisecond motion, and because tissue and cavitating media exhibit metastable behavior under strong negative pressures. In this work we develop a predictive and control-oriented framework that combines a physics-based compressible diffuse-interface model with fast operator-learning surrogates to enable neural model predictive control (NMPC) of histotripsy.

Our high-fidelity numerical model is based on the compressible Navier–Stokes–Korteweg formulation, where capillary (Korteweg) stresses arising from strong density gradients provide a diffuse-interface representation of phase boundaries and non-local pressure effects. Thermodynamic closure is introduced through free-energy-based modeling in the spirit of density-gradient theory to describe non-homogeneous regions and support cavitation-relevant metastable and unstable regimes. Anatomical variability is represented through two-dimensional brain MRI slices embedded in a computational domain and subjected to focused pressure waves representative of histotripsy-relevant conditions, including MHz-range excitation and high peak negative pressures that promote cavitation. To make this physics accessible for real-time control, we train Fourier Neural Operators (FNOs) [1], a resolution-flexible surrogate models that learn mappings from input fields and protocol parameters to pressure-field and cavitation-relevant outputs. The spectral structure of the FNOs enables efficient capture of long-range dependencies that arise from wave propagation and focusing. The resulting surrogate is then integrated into a neural model predictive control loop, where candidate ultrasound actions can be evaluated rapidly over a planning horizon to steer cavitation toward the target while respecting safety constraints.

The learned surrogate reproduces key trends of the high-fidelity simulations across variations in anatomy pose and forcing, and it reduces evaluation time sufficiently to support control-oriented what-if testing. Overall, the combined diffuse-interface physics and operator-learning approach provides a practical pathway to closed-loop, patient-specific histotripsy, with the potential to improve targeting accuracy and safety.

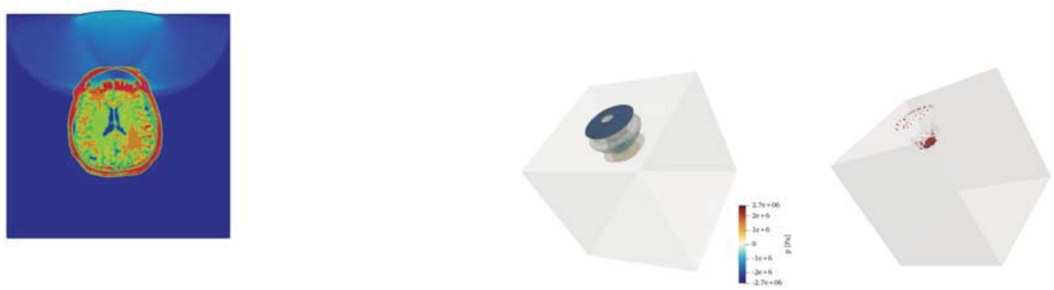

Figure 1. Representative numerical fields and setup visualizations used for histotripsy modeling and control.

Acknowledgement. This work was supported by King Abdullah University of Science and Technology (KAUST). The authors acknowledge KAUST and the Clean Energy Research Center (CERP) for research funding, facilities, and computational resources.

References

[1] Z. Li, N. Kovachki, K. Azizzadenesheli, B. Liu, K. Bhattacharya, A. Stuart, and A. Anandkumar, *Fourier Neural Operator for Parametric Partial Differential Equations*, arXiv:2010.08895 (2020).

ATTRACTOR SORTING ALGORITHM FOR POST PROCESSING BISTABLE HYDRODYNAMIC SYSTEMS WITH INTERMITTENT SWITCHING

Didzis Berenis
Institute of Physics, University of Latvia,
Jelgavas iela 3, LV-1004 Riga, Latvia

Abstract An algorithm for finding states of a bistable chaotic system is presented and tested on a parametric numerical calculation of a three-dimensional hydrodynamic system (bistability, intermittency, chaotic attractor, large scale fluctuations).

A chaotic process, sometimes called two-state intermittent bistability (TSIB), if present in a fluid system could lead to large scale mixing. This study focuses on employing an algorithm [1] to extract relevant transient data from the simulation results and convert the data into useful information about the regimes of the system. A rotating permanent magnet generated flow in a rectangular container filled with liquid GaInSn eutectic is considered, since it is a simple system that is known to exhibit TSIB or become fixed onto a single state depending on the system's parameters [2]. The fact that onset of TSIB and the switching intervals can be much longer than the turbulent fluctuations makes it difficult to describe this type of system. Firstly, Reynolds-averaged Navier-Stokes (RANS) equations struggle to converge to a steady solution [2]. In addition to that, even performing unsteady RANS to collect switching statistics for a single set of system's parameters is a computationally costly process. Nevertheless, unsteady RANS is a reasonable option for a parametric study. The minimum pressure coordinate in the side-wise direction, the difference between two velocity probes and the maximum/minimum curl of the velocity, weighed by the respective area of the container, were used as the initial state-indicating signal, $s_0(t)$. First, the signal is prepared to be symmetric $s_1(t) = s_0(t) - \frac{1}{T}\int s_0(t)\mathrm{d}t$, where T is the total calculation time. Next, threshold values $s_{th+} = 0.05\max(s_1(t))$, $s_{th-} = 0.05\min(s_1(t))$ can be set and flow states can be estimated with

$$s_2(t) = \begin{cases} 0, & s_1(t) < s_{th-} \\ s_1(t-\Delta t), & s_{th-} \leq s_1(t) \leq s_{th+} \\ 1, & s_1(t) > s_{th+} \end{cases} \tag{1}$$

The flow kinetic energy of each state can then be calculated $e_i(t) = \frac{1}{V}\int 0.5||\mathbf{v}_i(\mathbf{x}) - \mathbf{v}(\mathbf{x},t)||^2\mathrm{d}V, i = 0, 1$, where V is the liquid volume and the time-averaged velocity for each state is found from $\mathbf{v}_i(\mathbf{x}) = \frac{\int |s_2(t)-i|\mathbf{v}(\mathbf{x},t)\mathrm{d}t}{\int |s_2(t)-i|\mathrm{d}t}, i = 0, 1$. The process is repeated by iterating with $s_1(t) = e_0(t) - e_1(t)$ for the next iteration until the error $\frac{1}{T}\int |\Delta s_2(t)|\mathrm{d}t < 0.1\%$, where Δ denotes the difference between the last two iterations. The post-processed results are shown in Fig. 1.

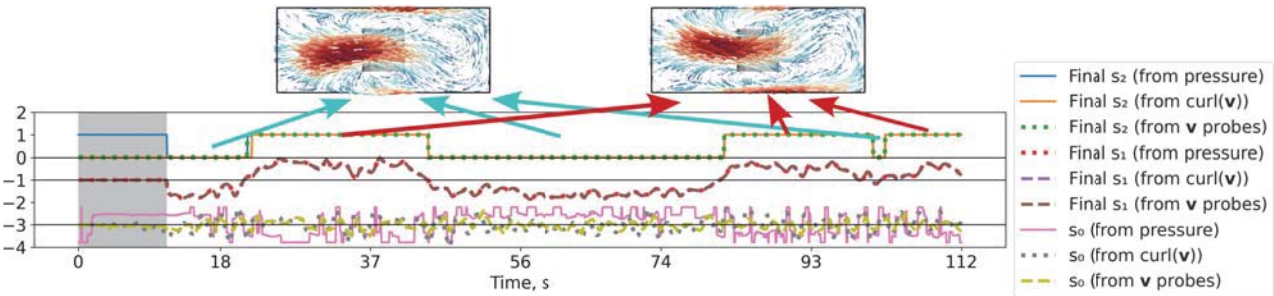

Figure 1. Selected time series from the numerical simulation output and the post-processed results. The gray area shows the disregarded data to account for spin-up. The final time averaged velocities, calculated from the sorted states, are shown at the top.

Acknowledgments

This study has been financed by the project "Algorithm and numerical tool development and experimental validation for directly seeking solution to industrially relevant bistable hydrodynamical systems" under grant No. 1.1.1.9./LZP/1/24/182.

References

[1] D. Berenis and I. Grants, *Experimental and numerical investigation of bistability in rotating permanent magnet-generated electrolyte flow in a ring-shaped container*, POF. **34**, 1070-6631 (2022).
[2] A. Gaile et al., *Permanent Magnet Pump for Aluminum Transport in a Linear Channel*, Metals. **13**, 1160 (2023).

RAYLEIGH–TAYLOR INSTABILITY IN THE PRESENCE OF SURFACTANTS: A THEORETICAL AND NUMERICAL STUDY USING A COUPLED VOF/DIFFUSE INTERFACE METHOD

Ilies Haouche[1], Benjamin Reichert[1], Guillaume Lagubeau[1], Alexis Duchesne[1], Palas Kumar Faroisya[2] and Michael Baudoin[1,3]

[1] *Univ. Lille, CNRS, Centrale Lille, Univ. Polytechnique Hauts-de-France, UMR 8520, IEMN, F59000 Lille, France*

[2] *Department of Chemical Engineering, Indian Institute of Technology Roorkee, Roorkee, Uttarakhand, India*

[3] *Institut Universitaire de France, 1 rue Descartes, 75005 Paris, France*

Abstract Rayleigh-Taylor instability, Numerical methods, Soluble surfactants, Basilisk.

The Rayleigh–Taylor (RT) instability, which arises at the interface between two fluids of different densities under acceleration, plays a central role in many interfacial flow phenomena. The presence of surfactants can significantly alter the growth and nonlinear evolution of the instability due to Marangoni stresses induced by interfacial concentration gradients. In this work, we investigate the influence of both insoluble and soluble surfactants on the dynamics of the Rayleigh–Taylor instability through a combined theoretical and numerical approach.

We first derive the linear dispersion relation governing the growth rate of infinitesimal perturbations, accounting for adsorption/desorption kinetics, interfacial elasticity, and surfactant diffusion in both the bulk and along the interface. The analytical results highlight the stabilizing effect of surfactants, which depends on the solubility, elasticity, and diffusivity parameters.

To investigate the nonlinear regime, we introduce a novel hybrid numerical framework coupling the Volume-of-Fluid (VoF) and Phase-Field methods. This open-source solver, integrated within the Basilisk platform, allows accurate treatment of soluble surfactant transport through a coupled advection–diffusion system in both bulk and interfacial phases, including Marangoni stresses and adsorption/desorption dynamics.

Beyond Rayleigh Taylor instability, this new module provides a versatile tool to investigate surfactant-driven effects in interfacial instabilities and multiphase flows.

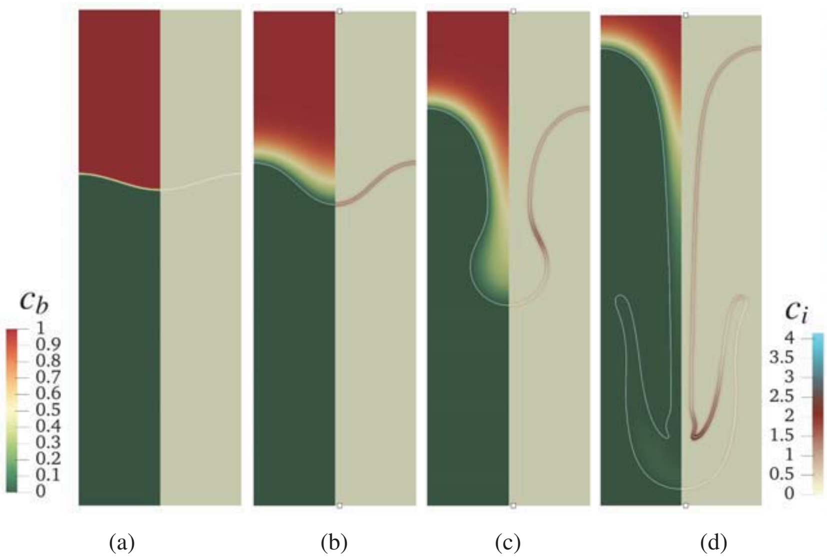

Figure 1. $c_i(\mathbf{x}, t)$: interfacial surfacant concentration, $c_b(\mathbf{x}, t)$: bulk concentration. Time evolution of the Rayleigh–Taylor instability with soluble surfactants, illustrating the interfacial dynamics and deformation.

References

[1] S. S. Jain, *Modeling soluble surfactants in two-phase flows.* (2023).

[2] Farsoiya et al., *Coupled volume of fluid and phase field method for direct numerical simulation of insoluble surfactant-laden interfacial flows and application to rising bubbles*, Phys. Fluids. (2024).

[3] Shu Yamashita et al., *Conservative transport model for surfactant on the interface based on the phase-field method*, Journal of Computational Physics (2024).

[4] D. E. Weidner, *The effect of surfactant convection and diffusion on the evolution of an axisymmetric pendant droplet*, Phys. Fluids. (2012).

A CERTIFIED REDUCED-ORDER MODEL BASED ON LEGENDRE COLLOCATION FOR A RAYLEIGH-BÉNARD PROBLEM

Henar Herrero[1], Jesús Cortés[1] & Francisco Pla[1]
[1] *Department of Mathematics-IMACI, Universidad de Castilla-La Mancha, Spain*

Abstract Reduced order model, Rayleigh-Bénard, Numerical Method.

This study presents an a posteriori error estimation of a reduced-order model for the study of bifurcations in a Rayleigh-Bard problem. The reduced method follows the reduced basis paradigm, which consists of using several low-dimensional bases to create a reduced-order problem. The high fidelity discretization underlying the reduced order method is a spectral Legendre Collocation method. This problem is formulated as a least-squares problem based on a high-fidelity discretization, avoiding the variational formulation. The resulting reduced solutions are certified by an a posteriori error estimator, which follows the standard pattern of dividing the norm of the residual by a stability factor [1]. Overall, the proposed methodology computes accurately, quickly and reliably, the bifurcation diagram [2].

References

[1] A. Quarteroni, A. Manzoni and F. Negri. Reduced Basis Methods for Partial Differential Equations: An Introduction. Springer Cham, 2016.
[2] J. Cortés, H. Herrero and F. Pla. A certified Reduced-Order Framework Based on Legendre Collocation for a Rayleigh-Bénard problem. J. of Scientific Computing, 105(1). 1-44, 2025.

EXPLORATION OF TECHNIQUES FOR FINDING CHAOTIC ATTRACTORS AND THEIR SWITCHING STATISTICS IN INTERMITTENT BISTABLE HYDRODYNAMIC SYSTEMS

Didzis Berenis
Institute of Physics, University of Latvia,
Jelgavas iela 3, LV-1004 Riga, Latvia

Abstract A repulsive force, in addition to an effective viscosity model, is explored as the means to find characteristics of a bistable system with intermittent switching between chaotic attractors (bistability, intermittency, chaotic attractor, modified Lorenz system).

A hydrodynamic system that switches between chaotic attractors or is trapped in one of them can be a difference between global mixing of the liquid and a local swirling motion. Differentiating between the two in a parametric study usually requires a long time series calculation with post-processing to extract the system characteristics, which is a computationally costly process. In this work, a cheaper alternative is sought. An effective viscosity model, based on the magnitude of the velocity fluctuations in a time interval τ_a, is proposed as a means to disable the switching between the attractors. Additionally, a repulsive force is added to trigger a switching event on demand. Initially, the consequences are studied in the low-dimensional case of the Lorenz system [1]

$$\begin{cases} X' = -(\sigma + C_f\sqrt{X_f})X + \sigma Y(t) + F_{repulsive} \\ Y' = -XZ + rX - Y \\ Z' = XY - bZ \\ X'_d = \dfrac{X - X(t-\tau_a)}{\tau_a} \\ X'_f = \dfrac{(X_d - X)^2 - (X_d(t-\tau_a) - X(t-\tau_a))^2}{\tau_a} \end{cases}, \quad F_{repulsive} = C_f \mathrm{Sign}(X_d)\exp\left(|X_d - X| - \sqrt{X_f}/C_f^2\right) \tag{1}$$

where $X = 0$ for $t < 0$. The simulation results shown in Fig. 1 confirm that the proposed method allows for the switching between the two attractors of the Lorenz system to be disabled, and with the repulsive force turned on, the times between the switching events can be predicted; thus, potentially allowing one to extract some of the system's characteristics in a computationally cheaper way. A generalization of the technique is tested on a three-dimensional electromagnetically forced flow case, which depending on geometric parameters can exhibit intermittent switching between chaotic attractors [2].

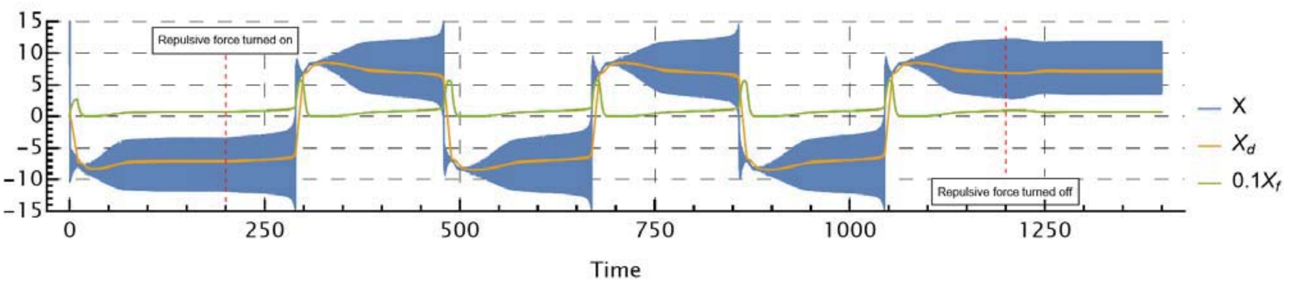

Figure 1. Simulated time series of the modified Lorenz system

Acknowledgments

This study has been financed by project "Algorithm and numerical tool development and experimental validation for directly seeking solution to industrially relevant bistable hydrodynamical systems" under grant No. 1.1.1.9./LZP/1/24/182.

References

[1] E. N. Lorenz, *Deterministic Nonperiodic Flow*, Journal of Atmospheric Sciences **20**, 130–141 (1963).
[2] A. Gaile et al., *Permanent Magnet Pump for Aluminum Transport in a Linear Channel*, Metals. **13**, 1160 (2023).

VARIATIONAL FLOW-STATE ESTIMATION AND SENSOR PLACEMENT OPTIMIZATION FROM DISCRETE MEASUREMENTS

Mathias Lemke[1] & Vincenzo Citro[2]
[1]*Institute of Fluid Dynamics and Technical Acoustics, TU/B, Müller-Breslau-Str. 8, 10623 Berlin, Germany*
[2]*DIIN, University of Salerno, Via Giovanni Paolo II, 132, 84084 Fisciano (SA), Italy*

Abstract Variational data assimilation, adjoint methods, sensor placement, observability, cylinder wake.

Reconstructing unsteady flow fields from limited experimental or numerical data remains a fundamental challenge in fluid dynamics, particularly when full-field measurements are impractical or prohibitively expensive. A powerful and physically consistent way to address this problem is to combine sparse observations with the governing equations of the flow within an optimization-based framework. In this presentation, we propose a variational assimilation methodology for the reconstruction of complete unsteady flow fields from a small number of discrete point measurements. The approach relies on the compressible Navier–Stokes equations and their continuous adjoint and is complemented by a systematic strategy for optimal sensor placement. The methodology is illustrated using a canonical configuration: the laminar vortex-shedding wake of a circular cylinder at a Reynolds number of $Re = 100$ and a Mach number of $M = 0.28$.

Flow reconstruction is achieved by introducing a localised momentum forcing that acts as the assimilation control. This forcing is distributed over a prescribed action region which is spatially separated from the sensor locations. The assimilation problem is formulated using a cost functional that measures the discrepancy between the simulated and measured velocity data, and this cost functional is localised in space using a sensor mask. Gradients of the cost functional with respect to the high-dimensional, space- and time-dependent forcing are computed by integrating the adjoint equations backwards in time, and these are then employed within an iterative optimisation procedure. The numerical framework is based on high-order finite-difference discretisation, explicit Runge–Kutta time integration, volume penalisation to represent solid boundaries and non-reflecting boundary conditions.

To ensure an efficient use of the available measurements, we propose a simple, inexpensive sensor placement strategy based on maximising sensitivity measures derived from the adjoint. We first validate this sensitivity-based approach against a Gramian-based observability analysis for a stationary flow configuration, where we use a singular value decomposition to identify the dominant observable directions of the system. Having validated the strategy, we applied it to the unsteady cylinder wake, enabling optimised sensor placement without the need for costly Gramian computations.

Results for the cylinder wake demonstrate that accurate reconstructions of the unsteady vortex-shedding dynamics can be achieved with a remarkably small number of sensors. Even a limited set of velocity probes is sufficient to recover the correct amplitude, frequency and phase of the shedding process. Additional sensors mainly enhance robustness, providing only marginal improvements in near-wake accuracy. Overall, this study demonstrates the effectiveness of combining variational data assimilation with an optimised sensor placement strategy for estimating the state of a flow from sparse measurements, and provides a flexible framework that can be readily extended to more complex geometries and flow regimes.

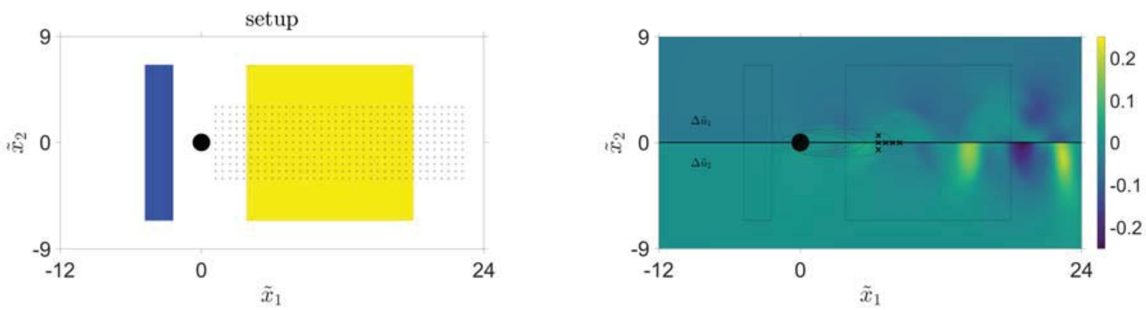

Figure 1. (Left) Numerical setup with a circular obstacle. The blue region upstream indicates the actuation domain, while the yellow region downstream denotes the evaluation domain used to assess the reconstruction. Black dots mark candidate locations for discrete sensors. (Right) Deviation of the velocity components u_1 (in x_1-direction) and u_2 (in x_2-direction) from the reference solution obtained by data assimilation using six sensors (black crosses), normalized by the inflow velocity.

References

[1] M. Lemke, V. Citro & F. Giannetti, *External acoustic control of the laminar vortex shedding past a bluff body*, Fluid Dynamics Research **53**, 015506 (2021).
[2] M. Lemke, J. Reiss & J. Sesterhenn, *Adjoint based optimisation of reactive compressible flows*, Combustion and Flame **161**, 2552–2564 (2014).
[3] M. Lemke & J. Sesterhenn, *Adjoint-based pressure determination from PIV data in compressible flows — Validation and assessment based on synthetic data*, European Journal of Mechanics – B/Fluids **58**, 29–38 (2016).

A LOW-DISSIPATIVE SOLVER FOR MULTI-SPECIES COMPRESSIBLE FLOW SIMULATIONS ON UNSTRUCTURED GRIDS

Francesco Duronio[1] & Andrea Di Mascio[1]
[1] *Dipartimento di Ingegneria Industriale Informazione e di Economia - Universitá degli studi dell'Aquila*

Abstract compressible flows; low dissipative solver; multi-specie flows

The numerical simulation of fluid flows characterized by large density gradients, shock waves, and multiple chemical species has become increasingly significant in advanced engineering applications. In such regimes, minimizing numerical diffusivity is essential to achieve accurate and predictive results, as it directly affects the stability and robustness of the spatial and temporal discretization of the governing equations.
This work presents the assessment of a low-dissipative, high order OpenFOAM solver designed for compressible, multi-species flow configurations. The solver is initially evaluated through benchmark test cases involving shock-dominated flows with species interactions under ideal-gas thermodynamic assumptions. Subsequently, its capabilities are examined through simulations of high-Reynolds-number, supercritical, multi-species flows governed by real-gas effects and strong density gradients.
Finally, leveraging OpenFOAM's support for unstructured meshes, the solver is applied to complex three-dimensional geometries. The results demonstrate that the proposed methodology provides an accurate and robust representation of a broad spectrum of compressible flow regimes, confirming its suitability for the simulation of ideal-gas, supercritical, and geometrically complex multi-species flows.

IMPLICIT SCHWARZ DOMAIN DECOMPOSITION FOR THE RAYLEIGH-BÉNARD CONVECTION

Darío Martínez, Henar Herrero & Francisco Pla
Departamento de Matemáticas, Universidad de Castilla-La Mancha, Spain

Abstract The implicit Schwarz domain decomposition method is the last improvement to Legendre collocation that allows to obtain more accurate solutions for the Rayleigh-Bénard problem, even reaching turbulence.

Spectral methods, such as Legendre collocation, provide high accuracy for solving PDEs while not being very computationally expensive. However, they suffer from ill-conditioning which leads to convergence problems for more complex and bigger approaches. In order to overcome this, Schwarz domain decomposition methods can be coupled with Legendre collocation. Even the simplest Schwarz domain decomposition method, an alternating algorithm using Dirichlet interface conditions, brings a great improvement over Legendre collocation alone [1, 2].

Nonetheless, it presents another problems, like the stagnation of the errors due to the slow transmission of the information or the necessity of an overlap between adjacent subdomains. Some researchers try to solve these inconveniences with complex interface boundary conditions or with the use of some extra steps like sparse meshes. The implicit Schwarz domain decomposition method presented in [3] allows to perfectly communicate every subdomain. This does not only eliminate completely the errors of the alternating algorithm, but also reduces the impact of using an overlap. Moreover, with its implicit version, there is no necessity to over complicate the problem with the interface boundary conditions.

The implicit Schwarz domain decomposition method makes it possible to redefine the meshes through the algorithm, making it easier to adapt to the characteristics required for each particular problem. This adaptability improves the convergence and accuracy of the method, crucial for complex problems like the transition to turbulence. A low turbulent solution of the Rayleigh-Bénard convection problem using implicit Schwarz domain decomposition coupled with Legendre collocation is shown in Figure .

The main disadvantage of the implicit Schwarz domain decomposition, compared to the alternating version, is its computational cost. However, by closely examining the matrices used in the implicit method, a specific algorithm can be developed that makes their efficiencies equivalent. Moreover, depending on the characteristics of the method, the implicit Schwarz domain decomposition may even outperform the alternating method.

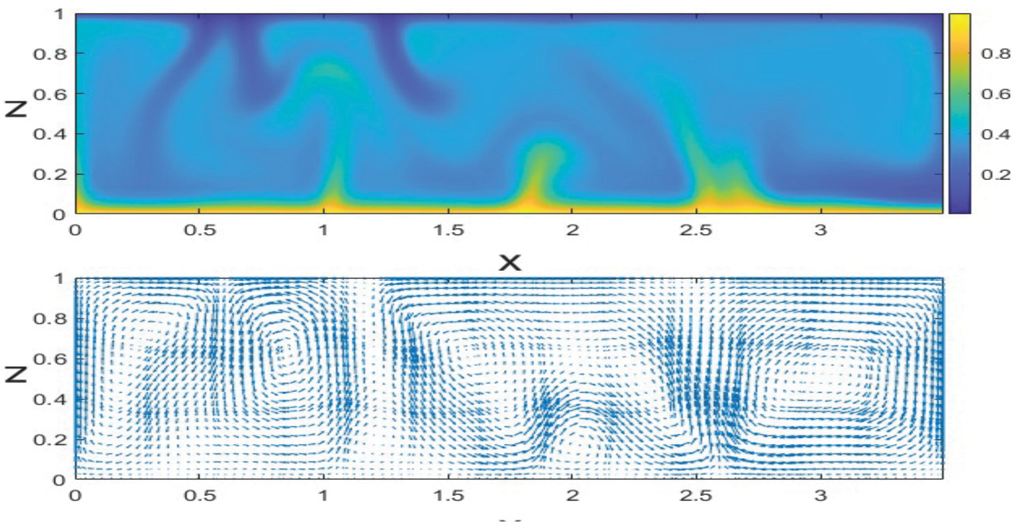

Figure 1. Isotherms and velocity field of the Ryleigh-Bénard problem with $Ra = 2.5 \cdot 10^5$

References

[1] D. Martínez; H. Herrero; and F. Pla *2D Newton Schwarz Legendre Collocation Method for a Convection Problem*, Mathematics (2022).
[2] D. Martínez; H. Herrero; and F. Pla *A Schwarz alternating method for an evolution convection problem*, Applied Numerical Mathematics (2023).
[3] D. Martínez; H. Herrero; and F. Pla *Implicit Schwarz domain decomposition method for a Rayleigh–Bénard problem*, Journal of Computational and Applied Mathematics (2025).